CHEMISTRY OF THE LANTHANIDES WITH PYRAZOLYLBORATE LIGANDS

Thesis submitted in partial fulfilment of the requirements of University College London for the degree of Doctor of Philosophy

Anna C. Hillier

Christopher Ingold Laboratories
Department of Chemistry

September 1998

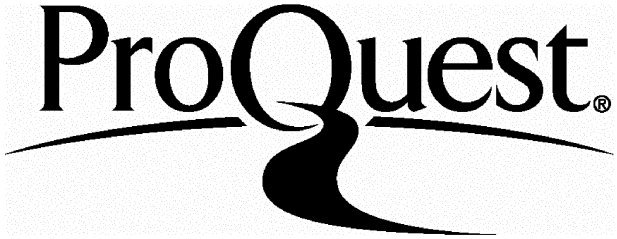

ProQuest LLC
789 East Eisenhower Parkway
P.O. Box 1346
Ann Arbor, MI 48106-1346

Summary

In this thesis we present continuing work on the synthesis of new tris(pyrazolylborate)lanthanide complexes.

Chapter 1 introduces, and offers a limited review of, the chemistry of the lanthanides with particular emphasis on sandwich and half-sandwich complexes with cyclopentadienyl ligands. The poly(pyrazolyl)borate class of ligands is introduced and their use in lanthanide chemistry reviewed.

Chapter 2 reviews the synthesis of lanthanide complexes with chalcogenolate ligands and describes the preparation of a series of compounds of formula $Sm(Tp^{Me,Me})_2EAr$ (E = O, S, Se, Te). The compounds formed by reduction of anthraquinone and tetraethylthiuram disulfide are also described. These complexes have been shown to exhibit fluxionality in solution on the NMR timescale and have been characterised by X-ray crystallography.

The work presented in **Chapter 3** details the reactivity of half-sandwich and sandwich (pyrazolylborate)lanthanide (Sm, Yb) complexes with transition metal carbonyl species. The preparation of divalent lanthanide complexes with isocarbonyl bridges to molybdenum is described. The reaction of $[Sm(Tp^{Me,Me})_2]$ with $Mn_2(CO)_{10}$ affords two products, $[Sm(Tp^{Me,Me})_2][Mn(CO)_5]$ and $[Sm(Tp^{Me,Me})_2]_2(\mu\text{-}O_2CH)$; a mechanism of formation of the latter is proposed. The X-ray structure of $[Re_4H(CO)_{17}]^-$ is described and compared with similar spiked triangular clusters.

Chapter 4 describes our attempts to prepare new sandwich and half-sandwich (pyrazolylborate)lanthanide complexes with halide, carboxylate, hydrocarbyl, amide, borohydride and aluminohydride ligands. Problems with ligand redistribution have been encountered in many of these syntheses, including the formation of $LiTp^{Me,Me}$ in reactions where lithium reagents were employed.

The work described in this thesis was carried out in the Christopher Ingold Laboratories of University College London from October 1995 to September 1998 under the supervision of Dr. A. Sella.

All the work described is my own unless stated to the contrary and it has not been submitted previously for a degree in this or any other university.

Abbreviations

acac	acetylacetonate
acacH	acetylacetone
Ar	aryl group
br	broad
BM	Bohr magneton
Bp	dihydrido-*bis*-(pyrazoly-1-yl)borate
Bu^n	*n*-Butyl
Bu^t or t-Bu	*tert*-Buryl
Bu^t_2DAB	1,4-di-*tert*-butyldiazabutadiene
COT	cyclooctatetraenyl (C_8H_8)
Cp	cyclopentadienyl (C_5H_5)
Cp*	pentamethylcyclopentadienyl (C_5Me_5)
δ	chemical shift (ppm)
d	doublet
ΔG	free energy of activation ($KJmol^{-1}$)
ΔH	enthalpy of activation ($KJmol^{-1}$)
DME	dimethoxyethane
E	group 16 element
esd	estimated standard deviation
Et	ethyl
E°	standard electrode potential
FAB	fast atom bombardment
HMPA	hexamethylphosphoramide
HOMO	highest occupied molecular orbital
J	coupling constant
J	spin-orbital angular momentum
L	ancillary ligand
Ln	lanthanide (Ln to Lu and Y)
M	metal
m/z	mass to charge ratio
μ_B	Bohr magneton (9.27408×10^{-24} J T^{-1})
Me	methyl
μ_{eff}	effective magnetic moment
MO	molecular orbital
ν_{XY}	infrared X-Y stretching frequency
OTf	trifluoromethanesulphonate (triflate, O_3SCF_3)
Ph	phenyl
Pr^i or i-Pr	*iso*-propyl
py	pyridine
pz	pyrazolyl
pzH	pyrazole
pzTp	*tetrakis*-(pyrazol-1-yl)borate
t	cone angle (°)
q	quartet
R, R', R", R'"	alkyl or aryl groups
S	solvent
s	singlet
sh	shoulder
T	temperature (K)
TCNE	tetracyanoethylene
THF	tetrahydrofuran
TMEDA	tetramethylethylenediamine

TMS	trimethylsilyl ($SiMe_3$)
Tp	hydrido-*tris*-(pyrazol-1-yl)borate
$Tp^{R,R'-4-R''}$	hydrido-*tris*-(3-R-5-R'-4-R"-pyrazol-1-yl)borate
triflate	trifluoromethanesulphonate (OTf, O_3SCF_3)
triflic acid	trifluoromethanesulphonic acid ($HOTf,HO_3SCF_3$)
ω	wedge angle
$w_{1/2}$	width at half height
X	anionic ligand

Acknowledgements

I am indebted to many people. The biggest thanks of course go to my supervisor Andrea Sella, whose knowledge in most subjects, but particularly things chemical and edible, puts mine to shame, although I do have a lot more hair than him. Nik Kaltsoyannis and Tony Deeming have provided invaluable advice and are responsible for the transformation of parts of my thesis from incomprehensible gibberish to semi-coherent writing (the semi is mine, not theirs). Without the expertise of Mark Elsegood and Derek Tocher in things crystallographic my appendices (and indeed the thesis) would be somewhat shorter. I thank them, you might not. Collaborative work with Joe Takats and Noemia Marques has been interesting. Graeme Hogarth, Steve Price, Despo Speel and Claire Carmalt have each contributed to my PhD in their own way and I thank them.

I also acknowledge everyone I have worked with in the lab: Simon Redmond, Andy Pateman, Tiz Coffey, Venus Lee, Shahbano Ali and the incomparable Maria Christofi, who has had to put up with me for the whole 3 years.

The technical staff of UCL are excellent and I thank in particular Alan Stones, Dave Knapp, Joe Nolan and Dick Waymark for their expertise and friendliness.

Outside UCL I have been well-provided with emotional and financial support by my family, Richard and Sonia (and their families), and everyone at Cats.

Thanks.

Chapter 1 - Review of the Chemistry of the Lanthanides and of Poly(pyrazolyl)borate ligands

Introduction

The lanthanides are the fourteen elements following lanthanum in the periodic table. The symbol Ln will be used in any general reaction to denote some or all of the lanthanide elements plus yttrium.

The most characteristic feature of these elements is that they have very similar chemical properties which they share with scandium, yttrium and lanthanum of Group 3. Indeed, when the mineral ceria was isolated in 1803 (independently by Klaproth and Berzelius & Hisinger) it was thought to be the oxide of a single element, and it was not until 1839 that Mosander showed that both ceria and yttria (first reported by Gadolin in 1794) were different mixtures of what turned out to be the 13 non-radioactive lanthanides, together with scandium, yttrium and lanthanum. The problems encountered in early studies of these elements were exacerbated by the difficulties involved in the separation of the elements; the almost identical chemistries of the lanthanides meant that tedious repeated fractional recrystallisations were typically required in order to obtain pure compounds.

Two events led to rapid advances in lanthanide chemistry. The first was the development in the late 19th century of the Thoria Coal Gas Mantle (99 % ThO_2 and 1 % CeO_2) by von Welsbach.[1] The ensuing large scale mining of thorium-containing ores which followed produced large quantities of lanthanide oxides as by-products, renewing interest in the chemistry and potential applications of these elements. More significantly, research into f element chemistry was an important aspect of the Manhattan Project during the Second World War. This work led to the development of ion exchange (by the groups of Cohn [2] and Spedding [3]) and solvent extraction [4] techniques, which provided the means of separating the lanthanides efficiently and economically. In addition, these elements were a major product of many of the nuclear fission processes under investigation, and the 14th lanthanide,

radioactive promethium, was identified in 1947 by Coryell and coworkers as one of the products of ^{235}U disintegration.[5]

Electronic Configuration of the Lanthanides

The neutral lanthanide atoms have electronic configuration $[Xe]4f^n6s^2$ with the 4f orbitals being filled steadily across the series. In three cases the 5d orbitals are occupied in preference to the 4f orbitals: gadolinium has electronic configuration $[Xe]4f^75d^16s^2$, reflecting the stability of the half-filled 4f shell; and lanthanum ($[Xe]5d^16s^2$) and cerium ($[Xe]4f^15d^16s^2$), for which the 5d orbitals lie below the 4f in energy.

The 4f orbitals are radially very contracted compared to the 5s and 5p orbitals, *i.e.* they are drawn into the inner core of electrons and do not protrude significantly beyond the filled $5s^25p^6$ orbitals.[6] One consequence of this is that the 4f electrons imperfectly shield the increasing positive charge of the nucleus going across the series. The effective nuclear charge therefore increases across the series with a concomitant decrease in atomic and ionic radius. This change in ionic radius is known as the lanthanide contraction and results in the ionic radius of Ho(III) being similar to that of the much lighter Y(III) (*ca.* 0.90 Å). It should be noted, however, that the lanthanide elements are, nonetheless, relatively large in size compared with the transition metals; even Lu(III), the smallest trivalent lanthanide ion, has an ionic radius of 0.85 Å, compared with 0.65 Å for Fe(III) and 0.68 Å for Ru(III). High coordination numbers are, therefore, common, especially with small, "hard" ligands. This is illustrated by $(NH_4)_2Ce(NO_3)_6$ where the coordination number of cerium is twelve.

The trivalent state, with electronic configuration $4f^n5d^06s^0$, is the most stable oxidation state for all the lanthanide elements. The first two electrons are removed from the 6s orbital and the third from the 4f valence orbitals. Although a stable divalent state might be expected from removal of only the two 6s electrons, the solvation or lattice enthalpy of the trivalent ions is usually sufficiently large to exceed the sum of the third ionisation energy and the solvation or lattice enthalpy of the divalent ions.[7] The sum of the first three ionisation energies is low, varying from 3500 - 4200 $kJmol^{-1}$, compared with, for example, 5230 $kJmol^{-1}$ for Cr (III) and 5640 $kJmol^{-1}$ for Co (III), which also have very stable +3

oxidation states. Those lanthanide elements with the highest third ionisation energy are, however, able to form divalent ions under reducing conditions. Thus europium and ytterbium, which have the highest third ionisation potentials of the lanthanide elements (the third electron is removed from the stable half-filled ($4f^7$) and filled ($4f^{14}$) electronic configurations respectively), both have chemically accessible divalent states. The fourth ionisation potential is, in general, prohibitively large, owing to the contraction of the 4f orbitals into the core with increased positive charge at the nucleus. Cerium, with ground state electronic configuration $4f^15d^16s^2$, is the only lanthanide with a well-defined tetravalent chemistry, the Ce (IV) ion possessing f^0 electronic configuration. These orbital considerations are not, however, the main factor in stabilising non-trivalent states, as evidenced by the accessible divalent state for Sm.

A number of zerovalent lanthanide compounds has been synthesised in recent years by co-condensation of the metal atoms with bulky organic ligands (*vide infra*).[8] It should, however, be emphasised that the situation for the lanthanides is not analogous to that for the transition metal elements, whose chemistry is dominated by the existence of several oxidation states of similar stability for the same metal. Despite the existence of divalent and tetravalent states there is no lanthanide for which both oxidation states are chemically accessible (although there are reports of Ce (II)[9] no convincing characterisation data have yet been presented, *vide infra*). Similarly, the lanthanides which possess a chemically accessible divalent oxidation state form the least stable complexes in the zerovalent oxidation state. Because reaction pathways involving two electron processes such as oxidative addition and reductive elimination are not available, the lanthanides often react with polar and non-polar bonds *via* acid base mechanisms involving concerted σ-bond metathesis involving a highly-ordered 4-centred transition state.

Oxidation States of the Lanthanides

Trivalent Lanthanides

The trivalent lanthanide ions are large ions with a high charge-to-radius ratio. A sterically unsaturated lanthanide metal centre in a complex will be very susceptible to attack by donor ligands, (in particular

oxygen-containing species), thereby acting as a hard Lewis acid. The lack of covalency in lanthanide complexes means that the metal-ligand bond is very highly polarised, hence the ligands are very basic and readily form bonds with a stronger Lewis acid than the Ln (III) ion. For this reason complexes of the lanthanides are often extremely air- and moisture-sensitive. In order to maximise the thermal stability of organometallic complexes of the lanthanides, particularly without coordinated solvent, a ligand must be anionic, to balance the metal charge and optimise electrostatic interaction. Bulky ligands that occupy the metal coordination sphere and sterically block decomposition, or alkyl ligands unable to undergo common decomposition routes such as β-hydrogen elimination, lend kinetic stability to these compounds. As the charge requirement must always be met, the stability of these species is generally dependent upon steric factors. Polyhapto ligands such as the cyclopentadienyl and cyclooctatetraenyl anions were among the first used to stabilise organolanthanide complexes. Chelating ligands or neutral bases are often incorporated into the metal coordination sphere, as are alkali metal halides, depending on the size of the lanthanide metal cation and the steric bulk of the ancillary ligands. The small, later lanthanides, in particular Er, Yb and Lu, are often used as steric saturation of the metal centre and isolation of products is less difficult.

Divalent Lanthanides

Although formally divalent halides of the lanthanides, such as GdF_2, are known, these materials are metallic and are best viewed as consisting of Gd^{3+} and F^- with one electron in a conduction band. Nevertheless, almost all of the lanthanide elements have been obtained in the divalent state by irradiation of Ln^{3+} ions doped into CaF_2,[10] hence their spectroscopic properties are well-understood. For practical purposes, however, most of the divalent lanthanide ions are extremely unstable, with disproportionation or electron transfer to other substrates providing facile decomposition routes. Well defined coordination chemistry, however, is restricted to the compounds of Sm, Eu and Yb. There has been one report of a formally divalent Ce complex, $\{K(DME)\}_2Ce(COT)_2$ (DME = dimethoxyethane; COT = cyclooctatetraenyl (dianion), C_8H_8), formed by the reduction of $[Ce(COT)_2]$ with an excess of K metal.[9] The only characterising data reported, however, were elemental analysis and infrared absorptions. Considering the very negative redox potential of the Ce^{3+}/Ce^{2+} couple (-2.92 V), it seems unlikely that this is a genuine Ce^{2+} compound. Furthermore, the green colour of

the complex is more consistent with it being a trivalent compound containing the $[(COT)_2Ce]^-$ anion.[11] There has also been a report of a formally divalent organoneodymium complex, $\{K(THF)_n\}_2Cp^*_2NdCl_2$ (THF = tetrahydrofuran; Cp^* = pentamethylcyclopentadienyl, C_5Me_5), although once again the characterising data are insufficient to determine whether this species contains Nd^{2+}.[12] However, the recent preparation of $TmI_2(DME)_3$ by comproportionation of thulium metal with TmI_3 suggests that the list of divalent complexes may expand as more determined efforts are made in this field. This complex was crystallographically characterised.[13] A La(II) compound has recently been detected by EPR spectroscopy in the reaction of $La(C_5H_3\{SiMe_3\}_2)_3Cl$ with potassium in DME.[14]

The aqueous reduction potentials for the Ln^{3+}/Ln^{2+} couples have been measured[15,16] and are shown in Table 1.1. The redox potentials of -0.34 V (Eu), -1.18 V (Yb) and -1.5 V (Sm) *vs.* NHE indicate that Eu(II) is the most stable and Sm(II) the most reactive of the chemically accessible divalent lanthanides in terms of reducing power. Complexes of the smaller Yb(II) ion are expected to be the most stable in terms of steric saturation of the metal coordination sphere and those of the larger Sm(II) the most reactive in this regard. Hence, for studies into the reactivity of divalent lanthanide complexes, Sm is the most desirable.

Table 1.1. Standard electrode potentials (E°) for the couple Ln^{3+}/Ln^{2+}

Couple	Potential (V)
$E°(Y^{3+}/Y^{2+})$	-
$E°(La^{3+}/La^{2+})$	-2.94
$E°(Ce^{3+}/Ce^{2+})$	-2.92
$E°(Pr^{3+}/Pr^{2+})$	-2.84
$E°(Nd^{3+}/Nd^{2+})$	-2.62
$E°(Pm^{3+}/Pm^{2+})$	-2.44
$E°(Sm^{3+}/Sm^{2+})$	-1.50
$E°(Eu^{3+}/Eu^{2+})$	-0.34

Couple	Potential (V)
$E°(Gd^{3+}/Gd^{2+})$	-2.85
$E°(Tb^{3+}/Tb^{2+})$	-2.83
$E°(Dy^{3+}/Dy^{2+})$	-2.56
$E°(Ho^{3+}/Ho^{2+})$	-2.79
$E°(Er^{3+}/Er^{2+})$	-2.87
$E°(Tm^{3+}/Tm^{2+})$	-2.22
$E°(Yb^{3+}/Yb^{2+})$	-1.18
$E°(Lu^{3+}/Lu^{2+})$	-2.72

The stability of the divalent oxidation state depends upon a number of thermodynamic parameters but broadly mirrors the ease of removal of the third electron from the Ln^{2+} ion, *i.e.* the third ionisation

potential, as shown in Figure 1.1. Thus the elements with the highest value of I_3 are observed to form the most stable divalent ions.

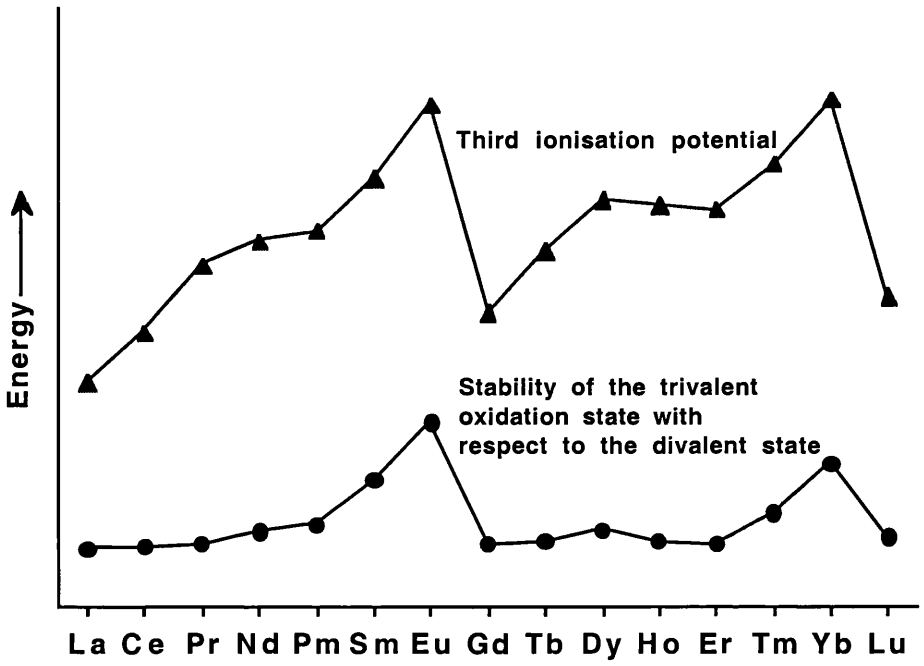

Figure 1.1 **A comparison of the third ionisation energy of the lanthanides with the relative stability of the trivalent and divalent Ions[10,17]**

Bonding Considerations in Lanthanide Complexes

The metal-ligand bonding mode for lanthanides differs from that of most transition metals. Transition metal valence d-orbitals are radially extended and allow covalent metal-ligand bonding through donation of ligand electron density into vacant metal d orbitals, or back-donation of metal electron density from the d orbitals into suitable ligand levels. In this way, respectively high and low oxidation states can be stabilised and strong, directional metal-ligand interactions result. For the lanthanides, the 4f orbitals are radially much more contracted than the transition metal d orbitals and there is no significant spatial overlap with the ligand orbitals; they are also sufficiently low in energy that the 4f

electrons are seldom ionised or shared and are largely buried in the semicore. As a result, the 4f electrons interact only very slightly with the ligands around the metal. The 5d and 5s orbitals of the lanthanides are much more extended than the 4f, but their interaction with ligand orbitals is also generaly small on account of their being high in energy. Thus the lanthanides are generally considered to form "ionic" complexes and the coordination geometry of lanthanide complexes is governed not by considerations arising from covalency or strong ligand fields as is the case for transition metals, but rather by the minimisation of repulsive steric and electrostatic terms in the metal coordination sphere. This ionic bonding is nondirectional, giving rise to non-rigid geometry. There is, furthermore, no lanthanide equivalent of the eighteen electron rule that governs the stability and reactivity of transition metal complexes.

Electronic spectroscopy of the Lanthanides

A further consequence of their spatial inaccessibility is that the 4f electrons are relatively unperturbed by the ligand field, hence the magnetic and spectroscopic properties of the trivalent lanthanide ions in complexes may be derived from those of the gaseous ions by only small perturbation and remain approximately unchanged for the same metal ion with different ligands. The states arising from a particular $4f^n$ electronic configuration are almost invariant for a given ion. As a result, the absorption bands arising from f-f transitions from one *J* state of an f^n configuration to another *J* state of the same f^n configuration are extremely sharp and similar to those observed for the free ions, in contrast with the broad bands observed for d-d transitions. The Laporte-forbidden nature of the f-f transitions and the lack of a vibronic coupling mechanism to relax the Laporte selection rules means that the colours of Ln(III) complexes are weak and do not vary with coordination environment. Most of the spectroscopy (and the weak colours) of the trivalent lanthanides arise from redistribution of electrons within the ground electronic configuration.

The divalent lanthanide ions, with smaller positive charge, have more diffuse f orbitals and more energetically accessible d orbitals. This is manifest in the intense, ligand-dependent colours observed for Ln(II) complexes, caused by Laporte-allowed f-d or charge transfer electronic transitions.

Chemistry of the Lanthanides

As the major oxidation state for the lanthanides is +3, differences in the chemistry of lanthanide complexes are largely due to variations in ionic radius. (La(III), 1.061 Å - Lu(III), 0.848 Å). Another basis for differences is found under strongly oxidising or reducing conditions with the lanthanides with chemically accessible non-trivalent oxidation states.

The systematic study of lanthanide coordination and organometallic chemistry started in the 1950s as large quantities of pure elements became available, with the separation of the lanthanides by ion-exchange methods. Early studies in organolanthanide compounds suggested that they should have limited chemistry. The complexes were assumed to be ionic and therefore viewed as trivalent versions of alkali and alkaline earth metal organometallic species, with all the lanthanide elements exhibiting very similar (if not identical) chemistry. The fact that the two-electron oxidative addition and reductive elimination processes are not possible at a single lanthanide metal centre, and the belief that many reagents of interest, such as CO, unsaturated hydrocarbons, hydrogen, phosphines and other soft or π-ligands would not exhibit any chemistry with the "hard" lanthanide(III) ionic complexes, meant that the lanthanides were considered less interesting than the transition metals. Organolanthanide chemistry is also experimentally difficult compared with many transition metal systems. The Lewis acidity of the metals, together with the extreme charge separation in the lanthanide–ligand interaction, can render the compounds very air- and moisture-sensitive and purification and isolation of products is difficult; they often decompose on chromatographic supports, ligand redistribution is common during recrystallisation, and sublimation often gives only a poor yield.

The lanthanides do, however, possess a combination of physical properties, including size, type of valence orbital, ionisation potential and electron affinity, which is not duplicated elsewhere in the periodic table; it has indeed been shown that in the proper oxidation state and coordination environment, they exhibit potential for unique chemistry, both catalytic and stoicheiometric.[18,19]

Synthetic Chemistry of the Lanthanides

Since the most studied lanthanide complexes are the cyclopentadienyl derivatives this section will provide a selective literature review of their synthesis and chemistry.

The trihalides are the starting materials for most lanthanide complexes. The sequential addition of cyclopentadienyl anions to the halides affords mono-, bis- and tris(cyclopentadienyl)lanthanide species; tris(cyclopenyadienyl)lanthanides were isolated soon after the synthesis of ferrocene.[20,21] Increasing the steric bulk of the ligand by introducing ring substituents allowed the isolation of metallocene and half-sandwich halides; these compounds are key starting materials for a range of heteroleptic complexes $Ln(Cp')X_2$ and $Ln(Cp')_2X$, (Cp' = C_5H_5, C_5Me_5, or substituted cyclopentadienyl) *via* metathesis reactions involving precipitation of metal halide. The complexes adopt monomeric, dimeric or oligomeric structures depending on the bulk of the ancillary ligand, halide used and solvent coordination.

The same structural motifs have been observed for most of the mono- and bis(cyclopentadienyl)lanthanide derivatives with "X" ligands such as alkyl, amide and chalcogenolate. Where the steric demands of the large lanthanides are not sufficiently satisfied by the combination of ancillary and "X" ligands, coordinative saturation is often achieved through dimer- or oligomerisation or through coordination of solvent or salt.

General synthetic strategies for lanthanide complexes

A variety of synthetic strategies has been employed in the preparation of lanthanide complexes.

1. Metal Vapour Synthesis

Conceptually the simplest method of preparing homoleptic complexes, this technique involves direct reaction of atomic metal with ligand, usually at low temperature in an inert matrix.

$$M + nL \rightarrow ML_n$$

The initial synthesis of $[Sm(C_5Me_5)_2(THF)_2]$ was achieved via metal vapour methods.[22,23] This route has also been used in the preparation of zerovalent lanthanide compounds, notably the series of bis(arene)lanthanide complexes synthesised by Cloke and coworkers.[8]

2. Salt Metathesis

The salt metathesis route, most commonly the reaction of lanthanide halide with alkali metal reagent has been employed extensively in the preparation of homo- and heteroleptic lanthanide compounds.

$$LnX_3 + ML \rightarrow LnX_2L + MX$$

$$LnX_2L + ML \rightarrow LnXL_2 + MX$$

$$LnXL_2 + ML \rightarrow LnL_3 + MX$$

Ligand redistribution is a common problem in lanthanide systems, depending on the relative solubilities and stability constants of the components in a given system. In this method the precipitation of insoluble main group metal halide is usually the primary driving force. The key issue in this approach is, therefore, the relative solubility of the starting materials versus that of the products.

Examples of problems associated with this method are illustrated by syntheses of borohydride and fluoride complexes. The salt metathesis route to mono(pyrazolylborate)lanthanide bis(borohydride) compounds offers the choice of lanthanide chloride or iodide starting materials, with lithium, sodium or potassium borohydrides.

$$Ln(Tp)Cl_2 + M(BH_4) \leftrightarrow Ln(Tp)(BH_4)_2 + MCl$$

$$Ln(Tp)I_2 + M(BH_4) \leftrightarrow Ln(Tp)(BH_4)_2 + MI$$

M = Li, Na, K.

The use of $Ln(Tp)I_2$ with lithium or sodium reagents would afford the corresponding alkali metal iodides, which are soluble in THF; the result is that the equilibrium is not shifted sufficiciently to the right hand side. KBH_4, on the other hand, is of comparable (in)solubility to KI, so again there is effectively no driving force for the forward reaction. The reagents of choice in this case should, therefore, be the lanthanide chloride starting material with lithium or sodium reagents.

The preparation of lanthanide fluoride drivatives is hampered by the extreme insolubility of lanthanide trifluorides; this is such that precipitation of LnF_3 often occurs, effectively terminating the reaction. Alternative routes to lanthanide fluoride complexes have therefore been necessary, such as abstraction

of fluoride from a halocarbon by a divalent lanthanide. There remain relatively few reported organolanthanide fluorides.

A further common problem with salt metathesis reactions involving lanthanides is the formation of "ate" complexes, where the Lewis acidity of the lanthanide results in the salt byproduct being incorporated into the desired complex to give either a lanthanide anion with metal cation or a ligand-bridged bimetallic complex. Salt incorporation is often accompanied by solvent coordination at the alkali metal.

$$LnL_2X + MY \rightarrow [LnL_2XY]M(S)_n$$

M = alkali metal, L = ancillary ligand, X, Y = "X" ligand, S = donor solvent.

The formation of "ate" complexes arises from the need to sterically saturate the lanthanide metal centre and tends to be a more important consideration when using larger lanthanides, less bulky ancillary ligands or lithium or sodium reagents.

Despite these inherent problems, salt metathesis reactions have been used extensively in the preparation of lanthanide complexes, with varying degrees of success. The preparation of the lanthanidocene halide complexes $Ln(C_5H_5)_2Cl$[24] and $Ln(C_5H_5)Cl_2$ by Maginn in 1963 by reaction of lanthanide trihalide with alkali metal cyclopentadienyl provided starting materials for a wide variety of heteroleptic cyclopentadienyl lanthanide derivatives.

$$LnCl_3 + 2MCp \rightarrow LnCp_2Cl + 2MCl$$

$$LnCl_3 + MCp \rightarrow LnCpCl_2 + MCl$$

$$LnCl_3 + MCp \rightarrow LnCp_2Cl_2M(S)_n$$

(Cp = C_5H_5, C_5Me_5, *etc.*; M = Li, Na, K; S = donor solvent *e.g.* THF, DME, TMEDA)

Virtually all the lanthanide halide precursor complexes $LnCp_2Cl_2ML_2$ (M = alkali metal, L = donor solvent), $[LnCp_2Cl]_2$ or $LnCp_2Cl$ are accessible *via* this route and many have been crystallographically characterised.[25] Starting from the halides, a large number of complexes has been prepared, including amides[24,26] and carboxylates.

$$ErCp_2Cl + NaNH_2 \rightarrow [ErCp_2NH_2] + NaCl$$

$$Ln(C_5Me_5)_2Cl_2K(THF) + KN(SiMe_3)_2 \rightarrow [Ln(C_5Me_5)_2N(SiMe_3)_2] + 2KCl$$

(Ln = Ce, Nd, Sm).

$$2\,[Ln(C_5H_5)_2Cl(THF)] + 2\,NaO_2CR \xrightarrow[-\,2\,NaCl]{THF} (C_5H_5)_2Ln(\mu\text{-}O_2CR)_2Ln(C_5H_5)_2$$

Examples include :

Ln = Er, R = H, Me; Ln = Yb, R = Me.[24]

Ln = Sc, R = Me.[27]

Ln = Sm, R = Me.[28]

The use of chelating ligands such as acetylacetonate (acac) and other β-diketonates, on the other hand, results in the formation of monomeric complexes.[27]

$$2\,[ScCp_2Cl(THF)] + 2\,Na(acac) \xrightarrow[reflux]{benzene} Cp_2Sc(acac) + NaCl$$

This route also allows access to half-sandwich complexes of the type $Ln(Cp')X_2$, such as the monomeric alkoxide $Ln(C_5Me_5)(O\text{-}2,6\text{-}Bu^t_2\text{-}C_6H_3)_2$ (Ln = Ce,[29,30] Y,[31] La [32])and the bulky amides $Ln(C_5Me_5)\{N(SiMe_3)_2\}_2$ (Ln = Y, La[33] Ce[29,34], Nd[35])

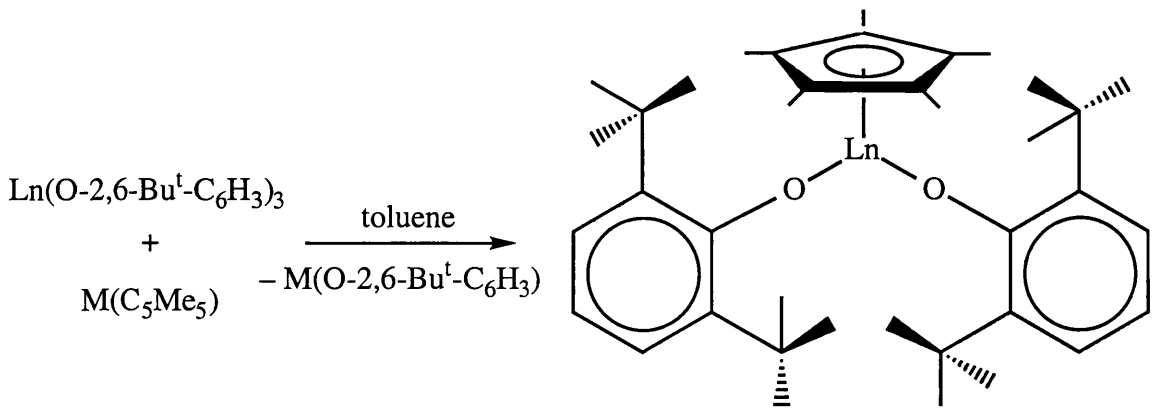

Salt metathesis is the most easily accessible and widely used synthetic method for preparing (cyclopentadienyl)lanthanide alkyl complexes. Grignard and organolithium reagents are often employed in THF solution and a large number of THF adducts of composition [$LnCp_2R(THF)$] have been prepared. [36] Potassium reagents are also used but can cause problems owing to their high reactivity.

$$LnCp_2Cl(THF) + LiR \rightarrow LnCp_2R(THF) + LiCl$$

Ln = Y, Nd, Sm, Dy, Er, Tm, Yb, Lu; R = Me, Et, Pr^i, Bu^n, Bu^t, CH_2Bu^t, CH_2SiMe_3, Bz, Ph, 4-Me-C_6H_4, 4-Cl-C_6H_4, CH_2PMe_2.

Alternative, less widely used preparative methods include treatment of lanthanide tris(cyclopentadienyl) complexes with organolithium reagents.

$$[LnCp_3(THF)] + LiR \rightarrow [LnCp_2R(THF] + LiCp$$

Ln = Nd, Lu; R = Bu^s, Bu^t.

The few known half-sandwich lanthanide hydrocarbyls have been prepared via salt metathesis reactions. For example, $LuCp\{CH_2(SiMe_3)\}_2(THF)_3$ has been prepared from $LuCp(OTf)_2$ and $Li\{CH_2(SiMe_3)\}$ and characterised by NMR spectroscopy.[37] More examples are given below.

3. Protonolysis

The predominantly ionic nature of the bonding in lanthanide complexes, *i.e.* the very high degree of charge separation across the lanthanide-ligand bond, means that the anionic negative charge in such compounds is essentially ligand based and must be stabilised by the ligand rather than by covalent

electron sharing interactions with the metal centre. The result is that the ligands in lanthanide amides, alkyls, alkoxides, *etc.* are very basic and of comparable reactivity to alkali metal reagents. It is possible to draw up a list of ligands in order of increasing basicity (when attached to a lanthanide metal):

halide ≅ carboxylate < alkoxide < thiolate < amide < phosphide < silyl < alkyl.

A more basic ligand (at the end of the series) can be replaced by the corresponding acid, lying earlier in the series; this is commonly effected by protonolysis of an acidic hydrogen.

$$LnL_2X + HY \rightarrow LnL_2Y + HX$$

The key advantage is that problems with salt residues are avoided and the products are easily separable from the volatile byproducts. Whilst this route is not useful for ligands of comparable basicity (for example a carboxylate complex can not be synthesised from a halide by protonolysis) it has been used to good effect in the preparation of complexes with ligands with a much larger difference in basicity. Thus reaction of bis(pentamethylcyclopentadienyl)(hydrocarbyl)-[38] or tris(cyclopentadienyl)-lanthanides[39] with equimolar amounts of nonchelating alcohols or β-diketones containing acidic hydrogens affords the desired products.[40]

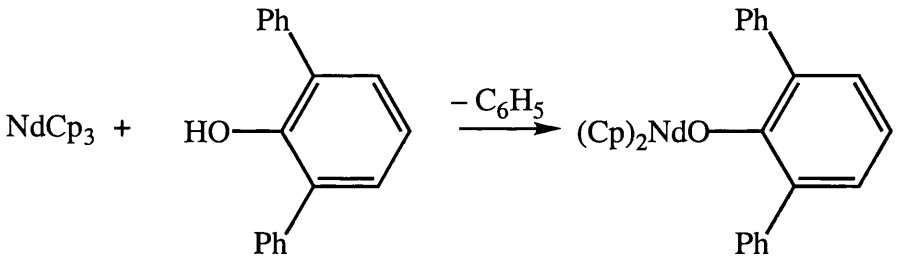

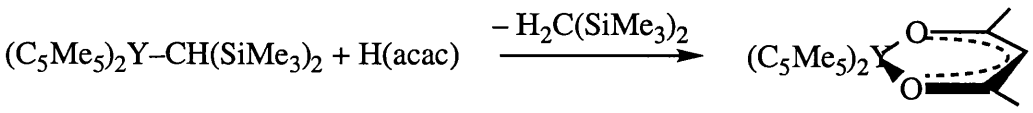

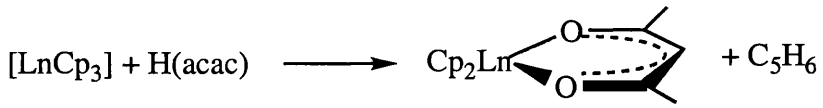

Ln = Nd, Sm, Gd, Dy, Er, Yb.

Bis(cyclopentadienyl)lanthanide alkoxide and thiolate complexes $[Ln(C_5H_5)_2X]_2$ (X = OR, SR) have been prepared from tris(cyclopentadienyl)lanthanide and alcohol or thiol in analogous fashion to the preparation of these acac and alkoxide complexes[41] and the compound where Ln = Yb and SR = n-propanethiolate crystallographically characterised, to give one example.[42]

$$Ln(C_5H_5)_3 + HX \rightarrow [Ln(C_5H_5)_2X]_2 + C_5H_6$$

The synthesis of half-sandwich complexes with acetylacetonate or other chelating ligands has been effected via protonolysis. The first such complexes were the (cyclopentadienyl)lanthanide β-amino ketone species reported by Bielang and Fischer in 1979, from reaction of bis- and tris(cyclopentadienyl)ytterbium compounds with the protonic acid 4-anilino-3-penten-2-one.[43]

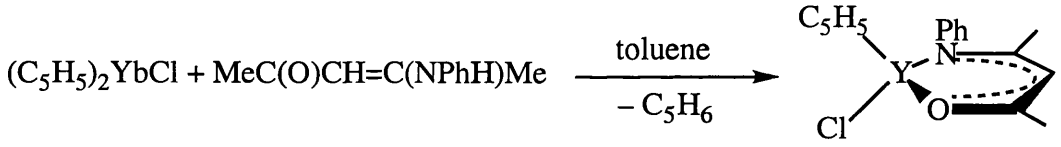

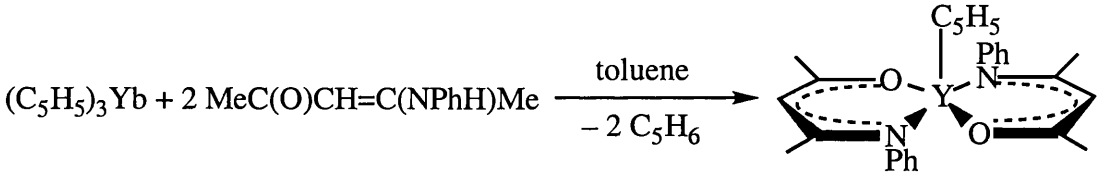

Amide complexes have been prepared via protonolysis of lanthanide-carbon bonds:

$$Ln(C_5Me_5)_2R + HNR'_2 \rightarrow [Ln(C_5Me_5)_2NR'_2] + RH$$

Ln = Sc; R = R' = Me[44]

Ln = Ce; R = $CH(SiMe_3)_2$; R' = $SiMe_3$.[45]

Ln = Nd, Sm; R = H; R' = Me.[46]

Alternatively the tris(amido)lanthanide starting material reacts with pentamethylcyclopentadiene with formation of volatile amine as driving force.[33]

$$Ln\{N(SiMe_3)_2\}_3 + 2\ C_5Me_5H \rightarrow [Ln(C_5Me_5)_2N(SiMe_3)_2] + 2\ HN(SiMe_3)_2$$

Silyl complexes have been prepared recently by protonolysis of lanthanide alkyl bonds. Reaction of $[Ln(C_5Me_5)_2(CH\{SiMe_3\}_2)]$ (Ln = Sm, Nd, Y) with a bulky silane, $H_2Si(SiMe_3)_2$, gave the monomeric proton transfer product $[Ln(C_5Me_5)_2(SiH(SiMe_3)_2)]$.[47]

$$[Ln(C_5Me_5)_2(CH\{SiMe_3\}_2)] + H_2Si(SiMe_3)_2 \rightarrow [Ln(C_5Me_5)_2(SiH(SiMe_3)_2)] + CH_2\{SiMe_3\}_2$$

The utility of the protonolysis route in the preparation of lanthanide and group 3 hydrocarbyl derivatives is restricted by the high basicity of hydrocarbyl anions and by the limited availability of suitable starting materials such as homoleptic tris(hydrocarbyl)metal compounds. Examples appear to be limited to the preparation of $[Sc(Tp^{Me,Me})_2(CH_2SiMe_3)]$ from $[Sc(CH_2SiMe_3)_3]$ and $Tp^{Me,Me}H$[48] and the synthesis of bis(cyclopentadienyl)lanthanide alkynyl complexes via elimination of C_5H_6.[19,25,49]

$$[Sc(CH_2SiMe_3)_3] + 2\ Tp^{Me,Me}H \rightarrow [Sc(Tp^{Me,Me})_2(CH_2SiMe_3)] + 2\ CH_3SiMe_3$$

$$2\ Ln(C_5H_5)_3 + 2\ HC{\equiv}CR \rightarrow [Ln(C_5H_5)_2(\mu\text{-}C{\equiv}CR)]_2 + 2\ C_5H_6$$

Ln = Nd, Yb; R = Bu^n, $C_6H_{13}{}^n$, c-C_6H_{11}, Ph, $CpFeC_5H_4$

Miscellaneous Methods

Reduction by divalent lanthanides

The reducing ability of the divalent lanthanides has been utilised in the preparation of lanthanide halides, *via* transmetallation reactions, and abstraction of halides from halocarbons. $Yb(C_5H_5)_2Cl$ has been prepared by oxidation of $Yb(C_5H_5)_2$ with "soft" metal halides such as mercury or tin in THF. Mercury dichloride was reported to give the cleanest reaction. The corresponding monobromide and iodide were also prepared from the mercury dihalides.

$$2Yb(C_5H_5)_2 + MCl_2 \rightarrow Yb(C_5H_5)_2Cl(THF)_{0.5} + M$$

(M = Hg, Pd, Cu, Zn, Sn, Pb).

$$Yb(C_5H_5)_2 + MCl \rightarrow Yb(C_5H_5)_2Cl(THF)_{0.5} + M$$

(M = Cu, Ag, Tl).

$Yb(C_5H_5)_2$ also abstracts halides from halocarbons and both solvated (monomeric) and unsolvated (dimeric) bis(cyclopentadienyl)ytterbium chlorides, bromides and iodides have been prepared in this manner.[50]

$$YbCp_2 + C_2Cl_6 \rightarrow YbCp_2Cl(THF)_{0.5}$$

$$YbCp_2 + (CH_2X)_2 \rightarrow YbCp_2X(THF)$$

X = Br, I.

The oxidation of ytterbocene with thallous, mercuric, argentic or cuprous reagents has also been employed by Deacon *et al* in the preparation of carboxylates and β-diketonates.[51,52]

The transmetallation route employing mercury reagents, HgR_2, has similarly been used in the preparation of lanthanide hydrocarbyls.[53-55]

$$2[YbCp_2(DME)] + HgR_2 \rightarrow 2[YbCp_2R] + Hg$$

R = C_6F_5, C_6Cl_5, C≡CPh.

The divalent and metallic lanthanides have also been used to reductively cleave element-element bonds in, for example, dichalcogenides and transition metal carbonyl complexes. This type of reaction forms the basis of chapters 2 and 3.

Insertion Reactions

The scandium carboxylate complex $Sc(C_5Me_5)_2(\eta^2\text{-}O_2CC_6H_4Me\text{-}4)$ has been prepared by insertion of carbon dioxide into the scandium–aryl bond of the p-tolyl species $Sc(C_5Me_5)(4\text{-}Me\text{-}C_6H_4)$.[56] The

related yttrium complexes $Y(C_5Me_5)_2(\eta^2\text{-}O_2CCH_2C_6H_3\{3,5\text{-}Me\}_2)$ and $Y(C_5Me_5)_2(\eta^2\text{-}O_2CCH\{SiMe_3\}_2)$ have also been synthesised by this route.[57]

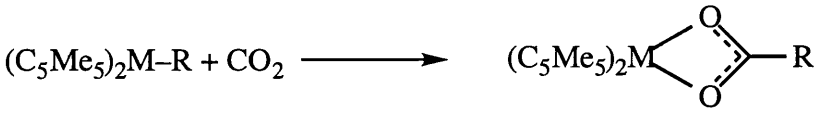

Reactions with Lewis acids

Unsolvated dimeric $[LnCp_2R]_2$ species have been prepared in a two-step process. Initial reaction of $[YbCp_2Cl]$ with lithium tetraalkyl aluminate $Li(AlR_4)$ affords the bimetallic alkyl-bridged complexes $[LnCp_2(\mu\text{-}R)_2AlR_2]$. The AlR_3 can then be abstracted by addition of pyridine, with formation of an insoluble 1:1 adduct $R_3AlNC_5H_5$ as driving force.[58]

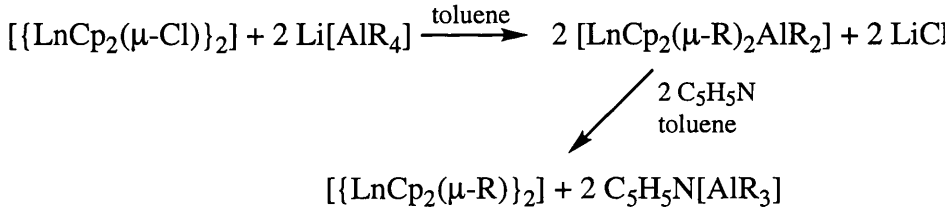

R = Me, Ln = Sc, Y, Gd, Dy, Ho, Er, Tm, Yb; R = Et, Ln = Sc, Y, Ho.

Lanthanide hydrides have been synthesised by analogous routes employing borohydride and aluminohydride ligands in the presence of base (see chapter 4).

Lanthanide Cyclopentadienyl Chemistry

An extensive organolanthanide chemistry has developed utilising the bulky cyclopentadienyl and substituted cyclopentadienyl ligands, in particular the pentamethylcyclopentadienyl anion. An important factor governing the kinetic stability of such complexes is the degree of coordinative saturation of the lanthanide metal centre.

Reactivity of (cyclopentadienyl)lanthanide(III) complexes

As expected, much of the reactivity exhibited by the trivalent (cyclopentadienyl)lanthanide complexes is associated with the most basic ligands such as hydrocarbyls. High reactivity and limited stability are associated with free coordination sites and with terminal as opposed to bridging ligands. The

monomeric hydrocarbyl complexes (and the corresponding hydrides which are readily obtained from the alkyl by hydrogenolysis) have been shown to exhibit catalytic activity in a number of processes involving unsaturated hydrocarbons.[18,19,25,41,49,59,60] The pentamethylcyclopentadienyl derivatives, $[Ln(C_5Me_5)_2R]$ (R = $CH(SiMe_3)_2$, H) in particular act as homogeneous catalysts or precatalysts for hydrogenation, oligomerisation, cyclisation, polymerisation, hydroamination, hydrosilylation and hydroboration reactions.[49] Some interesting stoicheiometric reactivity has also been observed for complexes containing the very bulky $CH(SiMe_3)_2$ ligand. For example the facile insertion of unsaturated substrates such as CO_2 and Bu^tCN into the metal-alkyl bond of $[Y(C_5Me_5)_2CH(SiMe_3)_2]$ (Figure 1.6) and the less sterically hindered $[Y(C_5Me_5)_2CH_2C_6H_3$-3,5-$(CH_3)_2]$ has been reported.[57] The less sterically hindered $[Ln(C_5H_5)_2R]$ complexes exhibit lower reactivity.

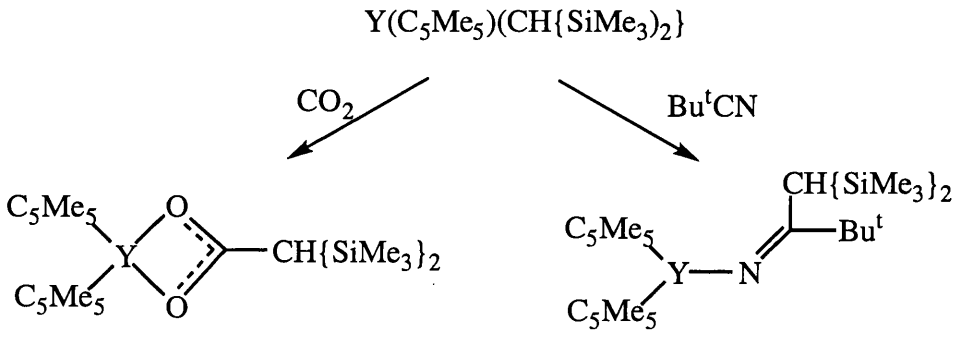

Figure 1.4 Reaction scheme for insertion into YC bonds.

An illustration of the importance in these systems of steric considerations and terminal versus bridging ligands is given by the reactivity of $[Ln(Cp')_2R]_n$ (Cp' = C_5H_5, C_5Me_5; Ln = Y, Lu; R = CH_3, Bu^t) towards hydrogenolysis and C-H activation.

$[(C_5H_5)_2Y(\mu\text{-}CH_3)]_2$ undergoes very slow hydrogenolysis in toluene, owing to the lack of coordination sites accessible for even the very small H_2 molecule. The monomeric complex $(C_5H_5)_2Ln(Bu^t)(THF)$, however, reacts rapidly with H_2 in toluene.

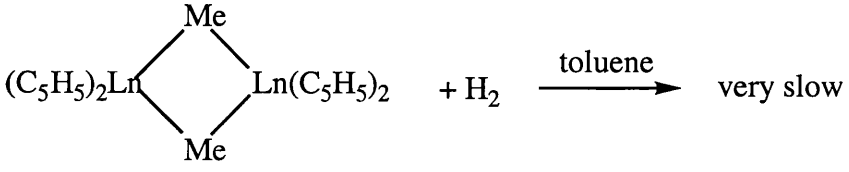

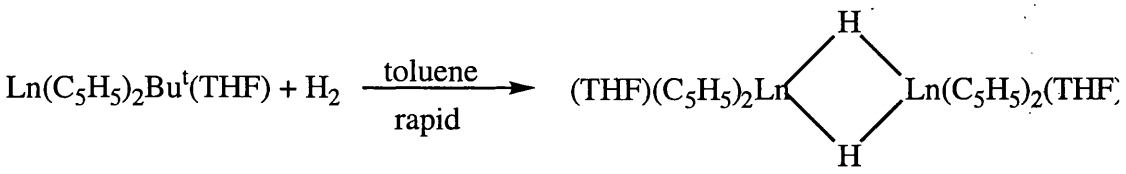

In THF, the *tert*-butyl complex is unreactive towards H_2, presumably since effectively no dissociation of the coordinated THF molecule occurs, hence there is no open site available for H_2. Even with a terminal alkyl group, therefore, a vacant coordination site is required for reactivity.[61] An example where the steric bulk of the ancillary ligands is important in determining reactivity is also given by these complexes. $[(C_5H_5)_2Ln(\mu\text{-Me})]_2$ (Ln = Y, Lu) does not activate the methane C-H bond. The use of the bulky C_5Me_5 ligand, however, inhibits the formation of the corresponding bridging alkyl dimers and the monomeric $Ln(C_5Me_5)_2CH_3$ complexes activate the C-H bonds in benzene[62] (equation 1.45) and methane.[63]

$$(C_5Me_5)_2Ln\text{–}CH_3 + C_6H_6 \rightarrow (C_5Me_5)_2Ln\text{–}C_6H_5 + CH_4$$

$$(C_5Me_5)_2Ln\text{–}^{12}CH_3 + {}^{13}CH_4 \leftrightarrow (C_5Me_5)_2Ln\text{–}^{13}CH_3 + {}^{12}CH_4$$

The absence of a facile pre-equilibrium dissociation in the very stable ground state alkyl-bridged species inhibits their kinetic activity, despite the apparent steric advantage.

Divalent Lanthanides

Ligands that will stabilise the divalent state must meet similar criteria to those for the trivalent state, *i.e.* they must be bulky and anionic, with the added stipulation that they must tolerate the fairly high reduction potentials of the Ln (II) ions. A further consideration in the investigation of these systems is characterisation of the products and starting materials. Samarium is the only Ln^{2+}-Ln^{3+} system where both oxidation states afford reasonably sharp ^1H NMR resonances, generally within ±10 ppm of the normal diamagnetic region, in spite of fairly high room temperature magnetic moments. The NMR resonances of complexes of Eu(II), Eu(III) and Yb(III) are often too broad to be reliably interpreted;

Yb(II) is diamagnetic, hence Yb(II) complexes give sharp unshifted spectra. Yb also has an NMR-active isotope, ^{171}Yb, which has been used increasingly to characterise complexes.[64]

Organolanthanide(II) complexes

Like sodium, europium and ytterbium dissolve in liquid ammonia to form highly reducing blue solutions of $[Ln(NH_3)_x]^{2+}[e^-(NH_3)_4]_2$. The first divalent organolanthanides were prepared by reaction of cyclooctatetraene or cyclopentadiene with lanthanide metal in liquid ammonia.[65]

$$Ln + 1,3,5,7\text{-}C_8H_8 \rightarrow LnC_8H_8$$

$$Eu + 3\ C_5H_6 \rightarrow Eu(C_5H_5)_2(NH_3) + C_5H_8$$

The analogous reaction between Yb and C_5H_6 gave a mixture of products, including trivalent $(C_5H_5)_3Yb(NH_3)$ despite the reducing conditions, illustrating in part a general trend in divalent lanthanide chemistry, namely that Eu (II) complexes are the least difficult to obtain pure, Yb (II) chemistry is more complex and Sm (II) the most difficult.

There are now several synthetic routes available for the synthesis of divalent organolanthanide complexes. It was not, however, until the introduction of a relatively facile preparation of the diiodide precursors $LnI_2(L)_x$ (Ln = Sm, L = THF; Ln= Yb, L = THF, NH_3; Ln = Eu, L = NH_3)[66] from the metal plus 1,2-diiodoethane that this area of organolanthanide chemistry began to be more widely investigated. Many synthetic routes now use the diiodides as divalent precursors, rather than reducing a trivalent precursor complex such as $Ln(C_5H_5)_2Cl$. These starting materials have the added advantage that the larger iodide ion impedes coordination of the alkali metal salt formed in the metathetical exchange reaction.

$$SmI_2(THF)_x + 2\ Na(C_5H_5) \rightarrow Sm(C_5H_5)_2(THF)_2 + 2\ NaI$$

The crystal structures of the solvated and the unsolvated $[Ln(C_5Me_5)_2]$ (Ln = Sm, Eu, Yb) show that both have a bent metallocenene geometry, as do the analogous solvent-free $[M(C_5Me_5)_2]$ (M = Ca, Ba)[67-70]. For a predominantly ionic complex governed by electrostatic factors a parallel ring structure should be optimal, as the anionic ligands are as far apart as possible. Similarly, on steric grounds a

parallel ring structure is preferred over a bent metallocene geometry. Molecular orbital calculations on $M(C_5H_5)_2$ (M = Ca, Ba, Sr, Sm, Eu, Yb) also suggest that a linear geometry is favoured;[71] the calculations are reconciled with the experimentally determined structures by very shallow bending potentials, *i.e.* although the linear structure is calculated to be energetically more favourable the bent metallocene structure is not significantly less stable. Small intramolecular non-bonded Van der Waals interactions between the ligands (which were not included in the calculations) are thought to cause the bent geometry.

Several divalent organolanthanide complexes with alkynyl ligands have been reported. One synthetic route is by transmetallation with mercury reagents.[72,73]

$$Yb + Hg(C{\equiv}CPh)_2 \rightarrow Yb(C{\equiv}CPh)_2 + Hg$$

Metal vapour synthesis affords divalent alkynides from terminal alkynes. Hence, reaction of Yb metal with 1-hexyne affords complexes of general formula $[HYb_2(C{\equiv}CBu^t)_3]_n$.[74] This product is highly associated in solution and oligomerisation via alkynide bridges is believed to occur. This type of bridging complex has been confirmed crystallographically using C_5Me_5 as ancillary ligand in the reaction of $[Ln(C_5Me_5)_2(OEt_2)]$ (Ln = Yb, Eu) with $HC{\equiv}CPh$.[75] In the more strongly reducing Yb system, some oxidation of the metal occurs to give a mixed valent system. In the presence of H_2, $[Sm(C_5Me_5)_2(THF)_2]$ reacts with alkynes $RC{\equiv}CR$ (*e.g.* R = Ph, Et) to form systems that are active hydrogenation catalysts.

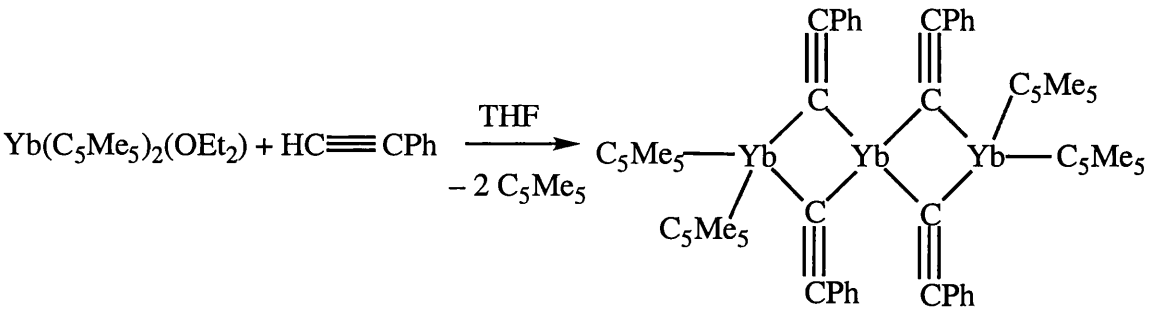

A number of synthetic routes to divalent alkyl and aryl lanthanide complexes, for example reaction of alkyl or aryl iodides with Sm, Eu or Yb metals[76] has been reported in the literature.[18] The products are often complex mixtures.

An extensive chemistry has been developed based on the $[Sm(C_5Me_5)_2]$ and $[Sm(C_5Me_5)_2(THF)_2]$ systems. The strongly reducing Ln^{3+}/Ln^{2+} couple acts as a one electron reducing agent with the metal being oxidised and forming a sterically saturated complex containing a new bond to the most electronegative ligand or ligands available in the system. This type of reactivity is particularly important for the Sm^{3+}/Sm^{2+} couple and accounts for its use in synthetic organic chemistry.

Bis(cyclopentadienyl)Yb and Sm complexes react with a variety of alkyl halides to afford the trivalent halide complexes $Ln(C_5R_5)_2X(solvent)$, some of which have been characterised crystallographically.[77] The reaction of $(C_5H_5)_2Yb$ in THF or DME with metal halides and pseudohalides, HgX_2, TlX, AgX_2, CuX (X = O_2CMe, $O_2CC_6F_5$, $O_2CC_5H_4N$, Cl, Br, I, C_6F_5, C≡CPh, $CH(OCMe)_2$) similarly gives the oxidation products.[52]

$$[Yb(C_5H_5)_2(L)] + MX \rightarrow [Yb(C_5H_5)_2X(L)] + M$$

M = Tl, Cu; L = solvent

$$2\,[Yb(C_5H_5)_2(L)] + MX_2 \rightarrow 2\,[Yb(C_5H_5)_2X(L)] + M$$

M = Hg, Ag; L = solvent

$[Sm(C_5Me_5)_2(THF)_2]$ abstracts oxygen from a variety of substrates, including CH_3CH_2CHCHO, NO, N_2O and C_5H_5NO with formation of the trivalent oxo-bridged complex $[Sm(C_5Me_5)_2]_2(\mu\text{-}O)$.[78]

This reactivity is in contrast to the reaction of $[Sm(Tp^{Me,Me})_2]$ with NO which gave $[Sm(Tp^{Me,Me})_2(NO_2)]$.[79]

Treatment of $[Yb(C_5Me_5)_2(OEt_2)]$ with chalcogenide-containing species such as R_3PE (R = Ph, n-C_4H_9; E = S, Se, Te)[80] affords the corresponding chalcogen-bridged species $[Yb(C_5Me_5)_2]_2(\mu\text{-}E)$. Reaction of $[Yb(C_5Me_5)_2(OEt_2)]$ with excess Te powder yields a product containing a bridging ditelluride.[81]

$$Yb(C_5Me_5)_2(OEt_2) + R_3PE \rightarrow (C_5Me_5)_2Yb\text{–}E\text{–}Yb(C_5Me_5)_2$$

$$Yb(C_5Me_5)_2 + Te\ (xs) \xrightarrow[2\ days]{hexane} (C_5Me_5)_2Yb\begin{array}{c}Te\\ \|\\ Te\end{array}Yb(C_5Me_5)_2$$

Divalent organosamarium and ytterbium complexes reductively cleave chalcogen-chalcogen bonds in organic dichalcogenides to give the products of the one electron transfer reaction. This type of reactivity is discussed in Chapter 2.

Lanthanide bonds to other "soft" ligands containing phosphorus and arsenic have been made by reaction with lithium reagents or by protonolysis reactions, as well as by the reductive cleavage of element-element bonds.[82-84]

The first f-element dinitrogen complex, $[Sm(C_5Me_5)_2]_2(\mu\text{-}\eta^2\text{:}\eta^2\text{-}N_2)$, containing an unusual side-bound N_2 ligand and a planar $Sm(\mu\text{-}N_2)Sm$ unit,[85] was obtained by slow crystallisation of $[Sm(C_5Me_5)_2]$ from toluene under nitrogen. The reaction of $[Sm(C_5Me_5)_2]$ with $BiPh_3$ in inert solvent afforded a structurally analogous bismuth complex,[86] but a similar reaction between $[Sm(C_5Me_5)_2]$ and $[Sb(Bu^t)_3]$ gave the complex $[Sm(C_5Me_5)_2]_3(\mu\text{-}\eta^2\text{:}\eta^2\text{:}\eta^1\text{-}Sb_3)(THF)$ containing a triantimony Zintl ion.[87]

Two equivalents of $[Sm(C_5Me_5)_2(THF)_2]$ react with one of azobenzene to form an intensely coloured product[88] which undergoes a double insertion of CO into the N=N double bond to form the fused heterocycle product shown.[89,90]

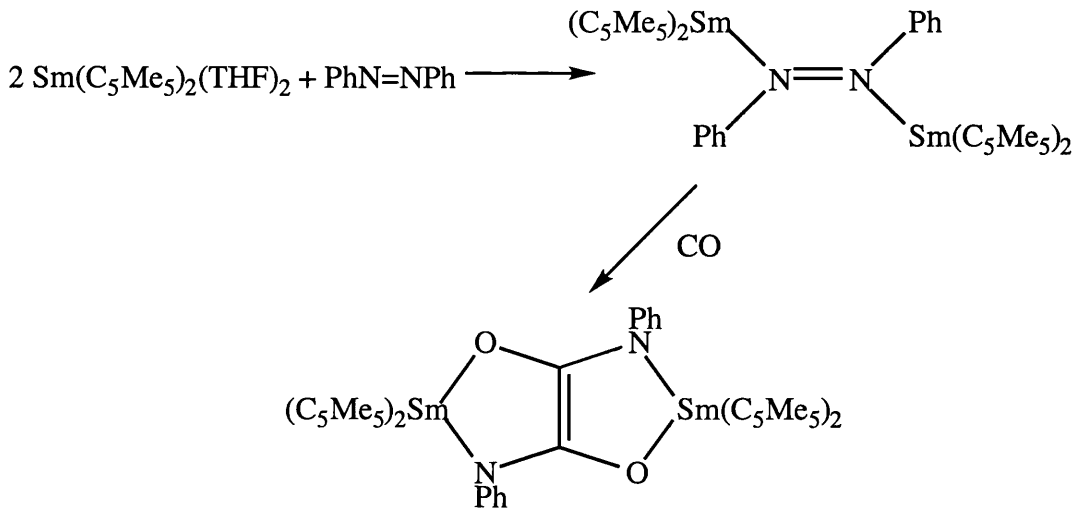

This contrasts with the product of the analogous reaction between $[Sm(C_5Me_5)_2(THF)_2]$ and $PhC{\equiv}CPh$[91] in the presence of CO.[92] This stereospecific synthesis of an indenoindene diolate is proposed to occur via CO insertion into Sm-C bonds and subsequent insertion of the carbene-like acyl carbon atoms into ortho-C-H bonds to generate the two five-membered rings.

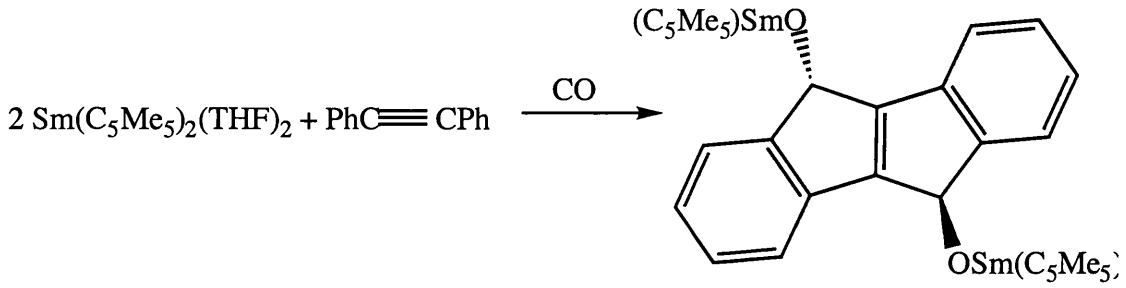

In contrast to the reaction of $(C_5Me_5)_2Sm(THF)_2$ with azobenzene, reaction with diphenylhydrazine, PhN(H)N(H)Ph, in hexane cleaves the N-N bond to form $(C_5Me_5)_2SmN(H)Ph(THF)$. [93] The reaction of $(C_5Me_5)_2Sm$ or $[(C_5Me_5)_2SmH]_2$ with hydrazine affords the bridging hydrazido complex $[(C_5Me_5)_2Sm]_2(\mu\text{-}\eta^2\text{:}\eta^2\text{-NHNH})$ with a 'butterfly' structure containing both nitrogens displaced to one side of the Sm-Sm vector, rather than a planar Sm(μ-NN)Sm unit.[94]

$(C_5Me_5)_2Sm(THF)_2$ is generally observed to react with unsaturated molecules in reductive coupling reactions. Further examples are the one electron processes involving pyridazine or PhCH=NN=CHPh where coupling occurs *via* C-C bond formation.[95]

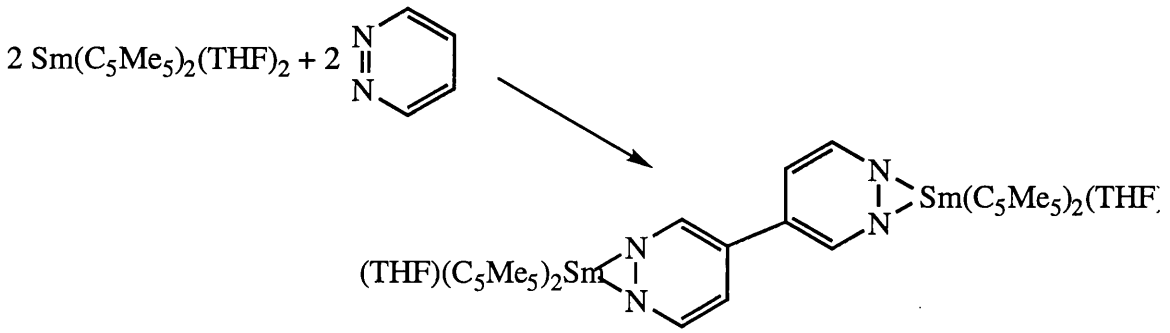

Divalent organometallic complexes of Yb and Sm are strongly reducing enough to reduce many transition metal carbonyl complexes to anionic species. Products of the reactions involving the

$Yb(C_5Me_5)_2$ moiety have proved the least difficult to characterise, hence these have been the most extensively investigated. Typically, a one electron transfer reaction occurs and M-M linkages are broken in the formation of anionic species. The mechanism is believed to entail initial interaction of a carbonyl oxygen with the Lewis acidic Ln (II) metal centre, followed by transfer of an electron from the lanthanide to the M-M anti-bonding LUMO of the dimeric transition metal carbonyl complex resulting in cleavage of the M-M links.[96] This chemistry is discussed in Chapter 3.

Zerovalent Lanthanide Complexes

A number of zerovalent lanthanide compounds has been reported, generally being synthesised by condensation of the metal vapour with the appropriate ligand. They include poorly characterised carbonyl species $Ln(CO)_n$ (n = 1 to 6) which are stable only at very low temperatures, and a series of compounds with unsaturated hydrocarbons such as hex-3-yne and butadiene.[18] Complexes in the latter class displayed very different properties from typical trivalent compounds in their colours, apparently low coordination numbers, magnetic moments and nuclear magnetic resonance (NMR) behaviour; whether this was due to the presence of a zerovalent metal or a highly reduced ligand is not clear, as no structural analysis was possible due to oligomerisation in solution.[18] Formally zerovalent lanthanide complexes have been synthesised by the condensation of lanthanide metals (Ln = Y, Nd, Sm, Eu, Gd, Ho and Yb) with 1,4-di-*tert*-butyldiazabutadiene (Bu^t_2DAB, $Bu^tN{=}CHCH{=}NBu^t$).[97] Most of these were, however, shown to be trivalent complexes of the butadiene radical anion, $[Ln^{3+}(Bu^t_2DAB^{\cdot-})_3]$. The Eu compound was reported to be better formulated as $[Eu^{2+}(Bu^t_2DAB^{\cdot-})_2(Bu^t_2DAB)]$, with the Yb analogue adopting this divalent composition at low temperatures and the trivalent one at higher temperatures.[98,99] In contrast, the condensation of lanthanide metals with bulky arenes such as 1,3,5-tri-(*tert*-butyl)benzene has given the first unquestionably zerovalent lanthanide complexes.[8,100,101] The Gd and Y species are particularly stable (being sublimable at 100 °C) and [Gd(1,3,5-tri-(*tert*-butyl)benzene$)_2$] has been characterised by X-ray crystallography and found to adopt a monomeric 'sandwich' structure in which the *tert*-butyl groups are staggered.

The first lanthanide bis(heteroelement-arene) compound, $[Ho(2,4,6\text{-}Bu^t_3\text{-}C_5H_2P)_2]$ has been structurally characterised recently.[102]

The bonding in the zerovalent lanthanide complexes [Ln(1,3,5-tri-(*tert*-butyl)benzene)$_2$] has also been addressed.[100,103,104] The stable Y complex has no available f orbitals and hence, a $5s^2 4d^1$ electron configuration was postulated as being necessary for covalent interaction with the arene rings.[100] Consistent with this, the 4f $\rightarrow$ 5d promotion energies of the elemental lanthanides correlate well with the observed stabilities of the zerovalent complexes: Gd has the ground state configuration $[Xe]4f^7 5d^1 6s^2$ and [Gd(1,3,5-tri-(*tert*-butyl)benzene)$_2$] is one of the most stable of this series, whilst Eu, Tm and Yb have the highest promotion energies and their complexes are too unstable to be isolated.

Poly(pyrazolyl)borates

Pyrazolylborate ligands were first reported by Trofimenko in 1966.[105] They are borohydride anions in which two, three or four of the hydrides have been replaced either with pyrazolyl (pz) groups alone or with a combination of pyrazolyl groups and other substituents (Figure 1.3).

The abbreviations used for these ligands are Bp for dihydrido-*bis*-(pyrazol-1-yl)borate, Tp for hydrido-*tris*-(pyrazol-1-yl)borate, and pzTp for *tetrakis*-(pyrazol-1-yl)borate. Substituents on the pyrazolyl ring are indicated by a superscript giving the nature of the group(s) and their position on the ring (the nitrogen bonded to boron being numbered 1-, the second nitrogen 2- *etc.*). Where two identical groups are indicated but no position is given (*eg* Tp^{Me_2}), the pyrazolyl ring is substituted at the 3-(R) and 5-(R") positions.

Poly(pyrazolyl)borates are monoanionic chelate ligands that, since their introduction, have found widespread application in coordination chemistry throughout the periodic table.[106] The importance of this area of coordination chemistry has grown since the introduction in 1986 of the coordination-controlling 'second generation' ligands.[107] The shape and size and therefore the stereochemical and electronic properties of the ligands may easily be modified by changing the number of pyrazolyl rings coordinated to the boron atom and the number and nature of the substituents on the pyrazolyl rings.

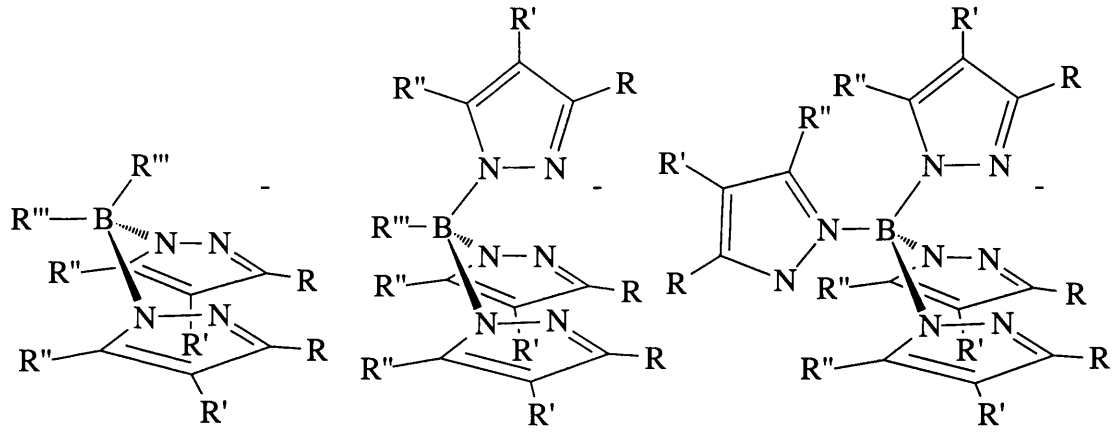

Bis-(pyrazolyl)borate *Tris*-(pyrazolyl)borate *Tetrakis*-(pyrazolyl)borate

Figure 1.3 The Poly-(pyrazolyl)borate Class of Ligands

Direct reaction of the appropriate pyrazole with alkali metal borohydride at elevated temperatures yields the poly(pyrazolyl)borate anion. The pyrazole is always in six-to-eight-fold excess, hence the formation of bis-, tris-, or tetrakis(pyrazolyl)borate is very dependent on temperature and on the size of the substituents on the pyrazole rings. $[B(pz)_4]^-$ is rarely formed with bulky substituents.

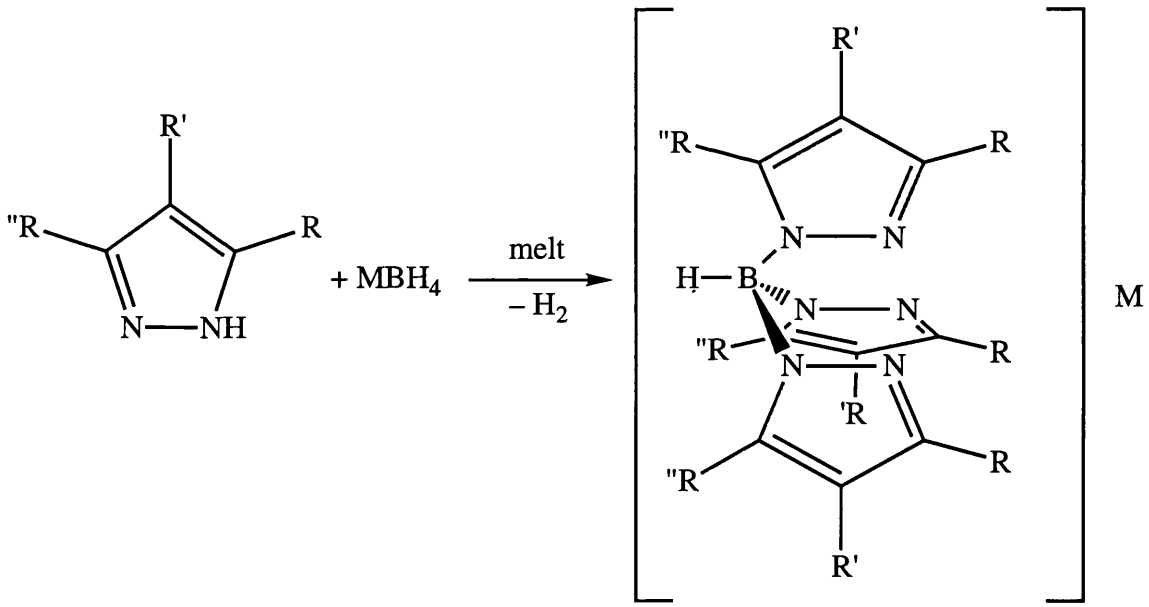

When the pyrazolylborates are synthesised, the B–N bond is usually formed adjacent to the carbon atom bearing the least sterically demanding substituent. Thus, reaction of 3-*tert*-butyl-5-

methylpyrazole with KBH_4 leads exclusively to the formation of potassium hydrido-*tris*-(3-*tert*-butyl-5-methylpyrazol-1-yl)borate, $KTp^{3\text{-}t\text{-}Bu\text{-}5\text{-}Me}$. The use of an alkyl substituent at the 5-position of the pyrazolyl ring (R") provides steric protection for the B–H bond (when R''' = H) which is susceptible to hydrolysis, and tightens the bite angle of the ligand at the metal centre; 5-Me substituted pyrazolyl groups are commonly used for this reason. On the other hand the extra steric congestion conferred on the boron atom by a substituent at the 5-position of the pyrazolyl ring probably plays a part in the greater susceptibility to hydrolysis of the B–N bond that has been observed for the $Tp^{Me,Me}$ ligand compared with the unsubstituted tris(pyrazolylborate) Tp. Pyrazolylborates in which the substituent(s) on the boron atom (R''') is neither hydrogen nor a pyrazolyl group can be synthesised by reaction of the substituted borane with the desired pyrazole or pyrazolide anion.

The tris(pyrazolyl)borate anion may be considered as comparable to the cyclopentadienyl anion in some respects. In the tridentate binding mode it is a six electron donor, coordinating through three nitrogen atoms which lie in a plane, capping one face of the metal centre. It may also coordinate to the metal in a bidentate fashion, through two nitrogen atoms, analogous to ring slippage in the cyclopentadienyl systems. The substituents in the 3-position on the pyrazolyl rings, however, form a protective "cradle" around the metal and may be varied to allow fine tuning of the steric environment at the metal centre, thereby offering steric bulk and hence a degree of stability to lanthanide complexes not possible with the planar cyclopentadienyl ligands.

In comparing the pyrazolylborate and cyclopentadienyl classes of ligands it is useful to have some standard of measurement of the steric effects of the ligand at the coordinated metal centre. The most commonly invoked measure of ligand bulk is the cone angle, θ; this is defined as the "apex angle of a cone, centred on the metal, just large enough to enclose the Van der Waals radii of the outermost atoms of the ligand" (Figure 1.4).[108] A comparison of the cone angles of common cyclopentadienyl and *tris*-(pyrazolyl)borate ligands is given in Table 1.2.

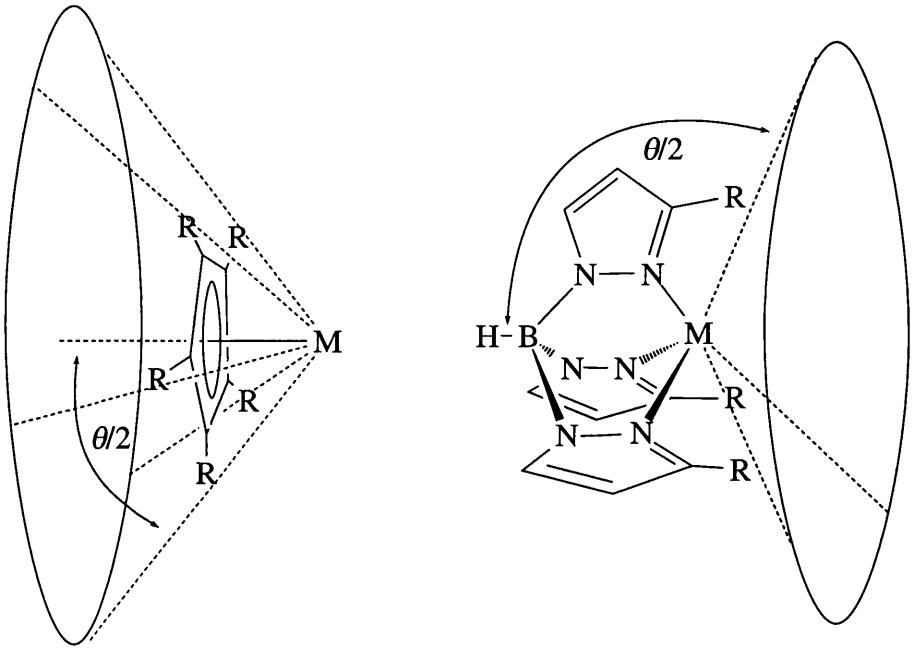

Figure 1.4 The measurement of ligand cone angles[108]

Whilst the concept of cone angles is frequently applied to considerations of ligand bulk, it should be remembered that even within a group of isostructural ligands, this parameter is somewhat unreliable since it is highly sensitive to the ligand-metal bond length. Furthermore, because the values given in Table 1.2 have all been measured in transition element complexes (for which the metal-ligand bond lengths are significantly smaller than for the lanthanides), they should be taken as overestimates for the f elements.

The cone angle of a particular *tris*-(pyrazolyl)borate ligand gives only some insight into its steric properties. In fact, it is possible for groups to coordinate in the cleft between the 3-substituents of the pyrazolyl rings. A measure of the size of this coordination site, the wedge angle, ω,[112] has been proposed, and values of ω are included in Table 1.2.

Table 1.2 **Cone and wedge angles for some cyclopentadienyl and tris-(pyrazolyl)borate ligands**

Ligand	Cone Angle $\theta°$	Wedge Angle $\omega°$
Cyclopentadienyl (Cp)[110,111]	136 to 150	-
Pentamethylcyclopentadienyl (Cp^*)[111]	*ca* 185	-
Hydrido-*tris*-(pyrazol-1-yl)borate (Tp)[112]	198.5	91
Hydrido-*tris*-(3-phenylpyrazol-1-yl)borate (Tp^{Ph})[113]	235	-
Hydrido-*tris*-(3,5-dimethylpyrazol-1-yl)borate (Tp^{Me2})[112]	236	75
Hydrido-*tris*-(3-phenyl-5-methylpyrazol-1-yl)borate ($Tp^{3\text{-Ph-5-Me}}$)[112]	250	32
Hydrido-*tris*-(3-*i*-propyl-4-bromopyrazol-1-yl)borate ($Tp^{3\text{-}i\text{-Pr-4-Br}}$)[112]	262	36
Hydrido-*tris*-(2-*H*-benz[g]-4,5-dihydroindazol-2-yl)borate (Tp^{a})[112]	262	44
Hydrido-*tris*-(3-methyl-2-*H*-benz[g]-4,5-dihydroindazol-2-yl)borate ($Tp^{3\text{-a-5-Me}}$)[112]	263	43.5
Hydrido-*tris*-(3-*tert*-butylpyrazol-1-yl)borate ($Tp^{t\text{-Bu}}$)[112]	265	35

Lanthanide pyrazolylborate complexes

The versatility of the tris(pyrazolyl)borate ligands is demonstrated by the fact that they form complexes with metals varying in size from Be^{2+} to U^{3+}.[106] Pyrazolylborates have been used as ancillary ligands for most metals in the periodic table and several reviews have been published covering the very extensive chemistry that has been developed in this field.[106,114,115] The first use of these ligands with f-elements was reported by Bagnall in 1975.[116] Since then many trivalent and divalent poly(pyrazolyl)borate lanthanide complexes have been synthesised and a review of f element pyrazolylborate chemistry[117] has been published quite recently.

All of the *tris*-(pyrazolyl)borate lanthanide chemistry reported in the literature prior to 1993 utilised the unsubstituted and sterically relatively undemanding ligand Tp. Thus, the compounds $[Ln(Tp)_3]$ (Ln = La, Ce, Pr, Sm, Gd, Er, Yb and Y) were synthesised in aqueous solution from the corresponding chlorides, [118,119] and similar routes were used to make the corresponding *tetrakis*-(pyrazolyl)borate analogues $[Ln(pzTp)_3]$.[118] The geometry of the metal centre is dependent upon the ionic radius of the metal, with 9-coordination observed for the larger, earlier lanthanides and 8-coordination for the heavier metals. In both cases the Yb complexes are eight coordinate at Yb and isostructural (Figure 1.5),[118,120] displaying bicapped trigonal prismatic coordination geometry, with two tridentate and one bidentate pyrazolylborate ligands.

Interestingly, this structure persists in solution on the NMR time scale (as shown by multinuclear studies);[121] in general, the ionic bonding in lanthanide compounds leads to highly fluxional species in solution.

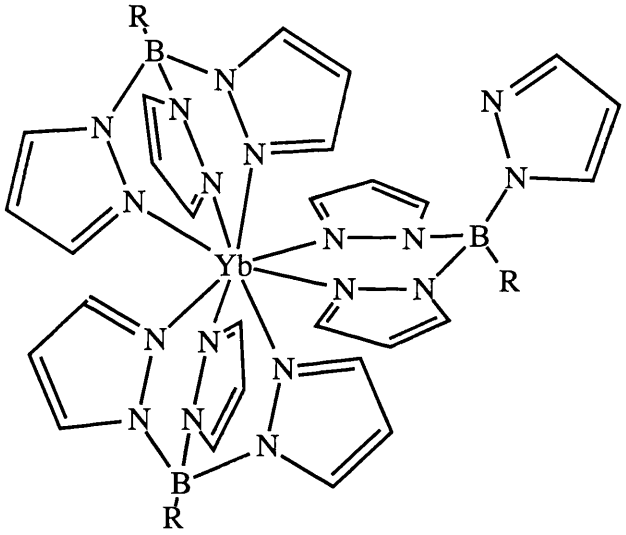

Figure 1.5. Structure of $[Yb(RTp)_3]$ (R = H, pz).

Mono- and bis(trispyrazolylborate)lanthanide halides analogous to the cyclopentadienyl complexes have not, on the whole, been studied systematically and reported syntheses tend to be incidental to the preparation of other derivatives. It might be expected that the additional bulk associated with the Tp or substituted Tp ligands would prevent dimerisation, coordination of solvent, ligand redistribution or salt incorporation. The salt metathesis synthetic route in THF is commonly utilised (Tp' = Tp or substituted Tp):

$$LnCl_3 + 2\ KTp' \rightarrow LnTp'_2Cl + 2\ KCl$$

$$LnCl_3 + KTp' \rightarrow LnTp'_2Cl + KCl$$

Reaction of lanthanide chlorides with one or two equivalents of KTp or NaTp under a variety of conditions has allowed the isolation of the following complexes: $TpLnCl_2(THF)_{1.5}$ (Ln = Er and Y),[119,125] Tp_2LnCl (Ln = Sm, Tb, Er and Y),[122-124] $Tp_2LnCl(THF)$ (Ln = Er, Yb, Lu and Y),[119,125,126] $Tp_2LnCl(pzH)$ (Ln = Tb and Y)[123,124] and $Tp_2LnCl(OH_2)$ (Ln = La and Y).[123] However, structural characterisation of these mixed chloride/*tris*-(pyrazolyl)borate compounds is limited to the water and pyrazole adducts $[Y(Tp)_2Cl(L)]$ (L = H_2O,[123] Hpz[122]) These complexes are monomeric and contain an eight coordinate yttrium centre as shown (Figure 1.6). The coordination geometry of the remaining complexes is not known.

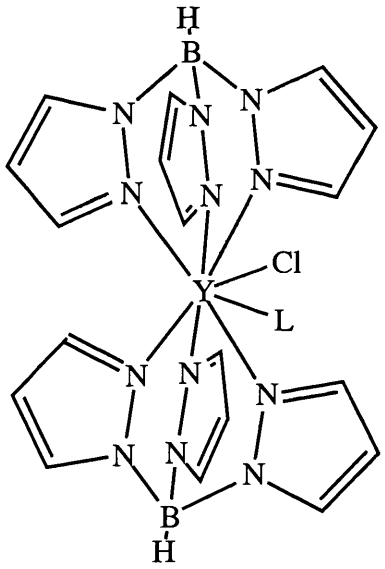

Figure 1.6. Structure of $[Y(Tp)_2Cl(L)]$

In solution the molecular weight of the corresponding complex without coordinated pyrazole, $[Y(Tp)_2Cl]_x$, was found to be concentration dependent and showed that the complex was in a monomer-dimer equilibrium.[122] The unsolvated complex $[Sm(Tp)_2Cl]$ has been shown to be monomeric by mass spectrometry and solution molecular weight studies.[124] The complexes $LnTp_2Cl$

(Ln = Sm, Tb, Er) are reported to be moderately air stable in the solid state, but decompose rapidly in solution to afford $LnTp_2Cl(Hpz)$ as the major decomposition product.[124]

Attempts to replace the chloride ligands in these complexes with other monodentate anions (especially alkyls) have invariably resulted in ligand redistribution reactions and the formation of $[Tp_3Ln]$.[117,125] Only the use of bidentate anions such as β-diketonates, oxalates and carboxylates has enabled a number of well characterised complexes of the type Tp_2LnX to be synthesised and complexes analogous to those obtained for the bis(cyclopentadienyl)lanthanide systems have been reported. The structures of these complexes were found to vary depending both on the size of the metal and the nature of the X ligand.

The first mixed pyrazolylborate β-diketonate Ln(III) complexes were prepared by Takats and coworkers by metathesis between $Ln(Tp)_2Cl.THF$ and the potassium salts of the β-diketones 2,2,6,6-tetramethyl-3,5-heptanedione (dpmH) or 3-trifluoroacetyl-D-camphor (tfacH) (Ln = Yb, Lu).[126]

$$Ln(Tp)_2Cl.THF + K(\beta\text{-diketonate}) \rightarrow Ln(Tp)_2(\beta\text{-diketonate}) + KCl$$

$Yb(Tp)_2(dpm)$ was crystallographically characterised and the β-diketonate ligand shown to bind in bidentate fashion to afford a monomeric structure. Both the dmp and the tfac complexes $Ln(Tp)_2(dmp)$ and $Ln(Tp)_2(tfac)$ are fluxional in solution on the NMR timescale down to -110°C.

The tropolonate ligand is similarly bound in $[Yb(Tp)_2(O_2C_7H_8)]$.[127]

Bis(pyrazolylborate)lanthanide carboxylates are reported to be less tractable than their β-diketonate analogues and although several have been synthesised and characterised by spectroscopic and molecular weight measurements few have been crystallographically characterised, among them $[Sm(Tp)_2(\mu\text{-}O_2CPh)]_2$,[124] $[Y(Tp)_2(O_2CMe)]$,[127] and $[Y(Tp)(\mu\text{-}O_2CMe)_2]_2$.[122]

$$2\ SmCl_3 + 4\ KTp + 2\ NaO_2CPh \rightarrow [Sm(Tp)_2(\mu\text{-}O_2CPh)]_2 + 4\ KCl + 2\ NaCl$$

$[Sm(Tp)_2(\mu\text{-}O_2CPh)]_2$ is dimeric and possesses two unsymmetrical bridging benzoate ligands. The acetate complexes $[Ln(Tp)_2(O_2CMe)]_2$ (Ln = Sm, Tb) were also prepared and $[Sm(Tp)_2(O_2CMe)]_2$ shown to be dimeric by freezing-point-depression measurements in benzene.

The ytterbium analogue was prepared in similar fashion from a 1:1:2 mixture of $YbCl_3.6H_2O$, KTp and sodium benzoate in water and recrystallised from CH_2Cl_2/hexane. In this case the complex was found to adopt a monomeric structure possessing a bidentate benzoate ligand.[127]

$$[YbCl_3.6H_2O] + 2\ KTp + NaO_2CPh \xrightarrow[-\ 2\ KCl]{-\ NaCl} Tp_2Yb(O_2CPh)$$

This discrepancy between the structures of the Sm and Yb compounds is presumably due to the smaller ionic radius of Yb compared to Sm (Sm^{3+} 1.00 Å, Yb^{3+} 0.86 Å) although the different reaction and crystallisation solvents employed may also affect the outcome.

The mono(pyrazolylborate)yttrium bis(acetate) complex $[Y(Tp)(\mu\text{-}O_2CMe)_2]_2$ was also prepared by reaction of YCl_3 with stoichiometric quantities of KTp and NaO_2CMe in THF. This complex was found by X-ray crystallography to possess a dimeric structure with four bridging acetate groups.

$$2\ [YCl_3] + 2\ KTp + 4\ NaO_2CMe \xrightarrow[-\ 4\ NaCl\ -\ 2\ KCl]{THF} [Y(Tp)(\mu\text{-}O_2CMe)_2]_2$$

In addition, mixed cyclooctatetraenyl/*tris*-(pyrazolyl)borate complexes have been synthesised by reaction of $TpLnCl_2(THF)_{1.5}$ with $K_2(COT)$ at low temperature to give [TpLn(COT)] (Ln = Er, Lu and Y),[125] and more recently by metathesis of $[Y(COT)(\mu\text{-}O_3SCF_3)(THF)]_2$ or $[(COT)LnCl(THF)_n]_2$ with a pyrazolylborate anion to give TpLn(COT) and $Tp^{Me2}Ln(COT)$ (Ln = Y, Ce, Pr, Nd and Sm).[128,129] Crystallographic characterisation showed the complexes to have parallel sandwich structures, similar to those observed for the pentamethylcyclopentadienyl analogues.[130,131]

All the structural characterisation obtained for unsubstituted *tris*-(pyrazolyl)borate complexes of the lanthanides indicates fairly normal metal coordination numbers of seven or eight. Most of the compounds were found to be highly fluxional in solution, indicating rapid reorientation of the ligands

on the metal. In addition, Jones and coworkers have shown that intermolecular ligand exchange occurs between complexes such as [Tp_3Yb] and [$Tp_2Lu(acac)$] (acac = acetylacetonate), the mixture coming to equilibrium after a couple of minutes.[132] Such a mechanism accounts for the problems experienced in synthesising derivatives of the $TpLn^{2+}$ and Tp_2Ln^+ fragments.

The reaction of $SmCl_3$ with one equivalent of $KTp^{Me,Me}$ at room temperature affords [$SmTp^{Me,Me}Cl_2$.THF].[133] Attempts to replace the chloride ligands by other groups, such as $C_5H_5^-$, RO^-, Et_2N^- or R^- give only the product of the disproportionation reaction, [$Sm(Tp^{Me,Me})_2Cl$.(THF)]. Oxidation of $Sm(Tp^{Me,Me})_2$ with I_2, or metathesis reaction of SmI_3 with $KTp^{Me,Me}$, afford the analogous complex with iodide as counterion, [$Sm(Tp^{Me,Me})_2$]I [134] (see Chapter 4). Similar compounds of Sm and Yb have been prepared using the large tetraphenylborate and triflate anions as counterions.[135]

Lanthanide(II) compounds of Sm, Eu and Yb with ($Tp^{Me,Me}$) and Tp have been prepared by metathesis reactions of the lanthanide dihalides with potassium or sodium salts of the ligands in 1:2 stoicheiometric ratio.[135-137] Structural characterisation of $Ln(Tp^{Me,Me})_2$ (Ln = Sm,[136] Yb)[137] reveals a linear metallocene-type structure.

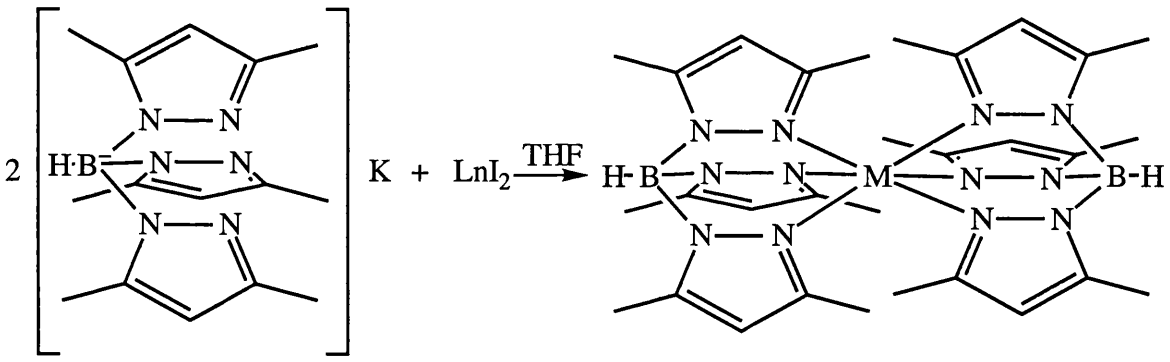

The bis-ligand complexes $Ln(Tp^{R,Me})_2$ (Ln = Sm, Yb; R = Ph, 2'-thienyl)[135] and the "half-sandwich" complexes [$Ln(Tp^{tBu,Me})I(THF)_x$] (Ln = Sm, x = 2; Ln = Yb, x = 1)[136,137] have been reported. The derivatives [$Yb(Tp^{tBu,Me})ER$] (ER = $HBEt_3$, $N(SiMe_3)_2$, C≡CPh, CH_2SiMe_3, $CH(SiMe_3)_2$) have also been obtained by reaction of the half-sandwich complex [$Yb(Tp^{tBu,Me})I(THF)$] with appropriate alkali metal reagents. The acetylide complex has been obtained from $Yb(Tp^{tBu,Me})\{N(SiMe_3)_2\}$ by reaction

with HC≡CPh in hexane. Alkylation of this half-sandwich amide provided a convenient route for the synthesis of the first well-characterised Ln (II) hydrocarbyl complexes. Pure products were obtained in all these reactions at low temperatures with precipitation of NaI or KI, or protonolysis of an acidic hydrogen, providing the main driving force.[135,138]

$$Yb(Tp^{t\text{-}Bu,Me})I(THF) + KR \rightarrow Yb(Tp^{t\text{-}Bu,Me})R + KI$$

R = CH_2SiMe_3, $CH(SiMe_3)_2$).

The amide complex $Yb(Tp^{t\text{-}Bu,Me})\{N(SiMe_3)_2\}$ was prepared by reaction of $Yb(Tp^{t\text{-}Bu,Me})I(THF)$ with $NaN(SiMe_3)_2$ in toluene at -50°C.

$$Yb(Tp^{t\text{-}Bu,Me})I(THF) + NaN(SiMe_3)_2 \rightarrow Yb(Tp^{t\text{-}Bu,Me})\{N(SiMe_3)_2\} + NaI$$

$$Yb(Tp^{tBu,Me})\{N(SiMe_3)_2\} + HR \rightarrow Yb(Tp^{t\text{-}Bu,Me})R + H\{N(SiMe_3)_2\}$$

$Yb(Tp^{t\text{-}Bu,Me})(\mu\text{-}HBEt_3)(THF)$ was prepared by reaction of $Yb(Tp^{t\text{-}Bu,Me})I(THF)$ with $KHBEt_3$ in toluene at low temperature.

$$Yb(Tp^{t\text{-}Bu,Me})I(THF) + KHBEt_3 \rightarrow Yb(Tp^{t\text{-}Bu,Me})(\mu\text{-}HBEt_3)(THF) + KI$$

Attempts to prepare BH_4 compounds have been hampered by the difficulty of replacing the iodide using Li or Na reagents and the extreme insolubility of KBH_4.

The reaction of $[Sm(Tp^{Me,Me})_2]$ with azobenzene gave the mononuclear product $[Sm(Tp^{Me,Me})_2(\eta^2\text{-}PhN{=}NPh)]$. The solid state structure showed that the tridentate coordination mode of the two Tp ligands was retained and that the azobenzene was η^2-bonded to the Sm centre through both N atoms.[136] The same mononuclear product was obtained when a 1:1 or a 2:1 ratio of $Sm(Tp^{Me,Me})_2$ to azobenzene was used, in contrast to the reaction of $[Sm(C_5Me_5)_2]$ with azobenzene, where a 1:1 ratio gave mononuclear $[Sm(C_5Me_5)_2(\eta^2\text{-}N_2Ph_2)(THF)]$ and a 2:1 ratio afforded $[Sm(C_5Me_5)_2(\mu\text{-}\eta^2\text{-}PhN{=}NPh)Sm(C_5Me_5)_2]$.[89] This result presumably arises because the increased bulk of the $Tp^{Me,Me}$ ligand compared with C_5Me_5 prevents formation of the bridged dimer complex. Consistent with this assumption is the recent report of the first lanthanide superoxo complex from reaction of

[$Sm(Tp^{Me,Me})_2$] with O_2 at low temperature.[139] Single crystal X-ray analysis confirms the structure as well-separated monomeric [$Sm(Tp^{Me,Me})_2(\eta^2\text{-}O_2)$] units with the O_2 ligand bound in a symmetrical side-on fashion to Sm. Both ($Tp^{Me,Me}$) ligands remain η^3-coordinated to Sm, providing a protective "cradle" which shields the O_2^- ligand. It has been postulated that this coordination environment may allow the stabilisation of other unusual diatomic moieties.

The mono(pyrazolylborate)yttrium hydrocarbyls and hydrides [$Y(Tp^{Me,Me})R_2(THF)$] have been synthesised recently, although no X-ray crystallographic data have been reported, and they are claimed to be active catalysts for ethylene polymerisation.[140]

New Lanthanide *Tris*-(pyrazolyl)borate Chemistry

Compounds of the lanthanides have displayed some unique reactivities which have been controlled to a large extent by the choice of ancillary ligands.[18,19] Early studies indicated the suitability of the unsubstituted tris-(pyrazolyl)borates as ancillary ligands for these elements; however, the ready formation of [Tp_3Ln] as a result of ligand redistribution presented a serious obstacle to further work.[106,117] By increasing the steric bulk of the pyrazolylborate ligand through the introduction of substituents at the 3-position of the pyrazolyl ring, trivalent complexes have been synthesised in which ligand redistribution reactions are suppressed to some extent and this is underlined by the isolation of complexes with small molecules such as dinitrogen. The pyrazolylborate chemistry of the lanthanides has quite recently been extended to the divalent state, with the preparation of mono- and bis(trispyrazolylborate)lanthanide (II) complexes, and some similar chemistry observed to that of the cyclopentadienyl analogues, although with slightly lower reactivity.

The work presented in this thesis is divided into four chapters. The first of these (Chapter 2) covers the synthesis of bis(pyrazolylborate)samarium chalcogenolate complexes, together with some structural studies. Chapter 3 describes the reactivity of divalent and trivalent complexes of samarium and ytterbium with transition metal carbonyl compounds, including the results of reactions believed to depend upon the presence of adventitious water. Chapter 4 reports the results of attempts to prepare

mono- and bis(pyrazolylborate)lanthanide complexes and reproduce some of the work reported by Bianconi. The experimental details of the work are covered in Chapter 5. This study has resulted in a number of X-ray crystal structure determinations. General comments on the procedures used together with tables of collection data, fractional coordinates and selected bond lengths and bond angles can be found in Appendix 1. Appendices 2 and 3 contain spectroscopic data for Chapters 2 and 4 respectively.

Chapter 1 - References

1) Moeller, T. *Advances in lanthanide chemistry - Comp. Inorg. Chem.*; Moeller, T., Ed.; Pergamon Press: Oxford, 1973; Vol. 4, Chap. 44, pp 1-101.

2) Tompkins, E. R.; Khym, J. X.; Cohn, W. E. *J. Am. Chem. Soc.* **1947**, *69*, 2769.

3) Spedding, F. H.; Voigt, A. F.; Gladrow, E. M.; Sleight, N. R. *J. Am. Chem. Soc.* **1947**, *69*, 2777.

4) Peppard, D. F.; Faris, J. P.; Gray, P. R.; Mason, G. W. *J. Phys. Chem.* **1953**, *57*, 294.

5) Marinsky, J. A.; Glendenin, L. E.; Coryell, C. D. *J. Am. Chem. Soc.* **1947**, *69*, 2781.

6) Freeman, J.; Watson, R. *Phys. Rev.* **1973**, *9*, 217.

7) Connick, R. *J. Chem. Soc. Suppl.* **1949**, 235.

8) Cloke, F. *Chem. Soc. Revs.* **1993**, *22*, 17.

9) Greco, A.; Cesca, S.; Bertolini, G. *J. Organomet. Chem.* **1976**, *113*, 321.

10) McClure, D. S.; Kliss, Z. *J. Chem. Phys.* **1963**, *39*, 3251.

11) Edelmann, F. T. *New. J. Chem.* **1995**, *19*, 535.

12) Wedler, M.; Recknagel, A.; Edelmann, F. T. *J. Organomet. Chem.* **1990**, *395*, C26.

13) Bochkarev, M. N.; Fedushkin, I. L.; Fagin, A. A.; Petrovskaya, T. V.; Ziller, J. W.; Broomhall Dillard, R. N. R.; Evans, W. J. *Angew. Chem., Intl. Ed. Engl.* **1997**, *36*, 133.

14) Cassani, M. C.; Lappert, M. F.; Laschi, F. *J. Chem. Soc., Chem. Commun.* **1997**, 1563.

15) Mikeev, N. B. *Naturwissenschaften* **1989**, *76*, 107.

16) Mikeev, N. B.; Kamenskaya, A. N. *Coord. Chem. Rev.* **1991**, *109*, 1.

17) Johnson, D. A. *Some Thermodynamic Aspects of Inorganic Chemistry*; second ed.; Cambridge University Press: Cambridge, 1982.

18) Evans, W. J. *Polyhedron* **1987**, *6*, 803.

19) Schaverien, C. *Adv. Organomet. Chem.* **1994**, *36*, 283.

20) Birmingham, J. M.; Wilkinson, G. *J. Am. Chem. Soc.* **1956**, *78*, 42.

21) Wilkinson, G.; Birmingham, J. M. *J. Am. Chem. Soc.* **1954**, *76*, 6210.

22) Evans, W. J.; Bloom, I.; Hunter, W. E.; Atwood, J. L. *J. Am. Chem. Soc.* **1981**, *103*, 6507.

23) Evans, W. J.; Bloom, I.; Hunter, W. E.; Atwood, J. L. *Organometallics* **1985**, *4*, 112.

24) Maginn, R. E.; Manastyrskyj, S.; Dubeck, M. *J. Am. Chem. Soc.* **1963**, *85*, 672.

25) Schumann, H.; Meese-Marktscheffel, J. A.; Esser, L. *Chem. Rev.* **1995**, *95*, 865.

26) Evans, W. J.; Keyer, R. A.; Ziller, J. W. *Organometallics* **1993**, *12*, 2618.

27) Coutts, R. S. P.; Wailes, P. C. *J. Organomet. Chem.* **1970**, *25*, 117.

28) Ye, Z.; Ma, H.; Yu, Y. *J. Less Common Met.* **1986**, *126*, 405.

29) Heeres, H. J.; Meetsma, A.; Teuben, J. H.; Rogers, R. D. *Organometallics* **1989**, *8*, 2637.

30) Heeres, H. J.; Meetsma, A.; Teuben, J. H. *J. Chem. Soc.,Chem. Commun.* **1988**, 962.

31) Schavarien, C. J.; Frijns, J. H. G.; Heeres, H. J.; van der Hende, J. R.; Teuben, J. H.; Spek, A. L. *Chem. Commun.* **1991**, 642.

32) Heeres, H. J.; Teuben, J. H. *Recl. Trav. Chim.* **1990**, *109*, 226.

33) Booij, M.; Kiers, B. H.; Heeres, H., J. ; Teuben, J. H. *J. Organomet. Chem.* **1989**, *364*, 79.

34) Heeres, H. J.; Meetsma, A.; Teuben, J. H., 962 *J. Chem. Soc.,Chem. Commun.* **1988**, 962.

35) Tilley, T. D.; Andersen, R. A. *Inorg. Chem.* **1981**, *20*, 3267.

36) Quian, C.; et al *J. Organomet. Chem.* **1983**, *247*, 161.

37) Schumann, H.; Meese-Marktscheffel, J. A.; Dietrich, A. *J. Organomet. Chem.* **1989**, *377*, C5.

38) den Haan, K. H.; Wielstra, Y.; Teuben, J. H. *Organometallics* **1987**, *6*, 2053.

39) Shi, L.; Ma, H.; Yu, Y.; Ye, Z. *J. Organomet. Chem* **1988**, *339*, 277.

40) Deacon, G. B.; Nickel, S.; Tiekink, E. R. T. *J. Organomet. Chem.* **1991**, *409*, C1.

41) Sella, A.; Brennan, J. G. *Specialist Periodical Reports* **1996**, *26*, 28.

42) Wu, Z.-Z. *Polyhedron* **1996**, *15*, 3427.

43) Bielang, G.; Fischer, D. R. *Inorg. Chem. A* **1979**, *36*, L389.

44) Bercaw, J. E.; Davies, D. L.; Wolczanski, P. T. *Organometallics* **1986**, *5*, 443.

45) Heeres, H. J.; Renkema, J.; Booij, M.; Meetsma, A.; Teuben, J. H. *Organometallics* **1988**, *7*, 2495.

46) Nolan, S. P.; Stern, D.; Marks, T., J. *J. Am. Chem. Soc.* **1989**, *111*, 7845.

47) Radu, N. S.; Tilley, T. D.; Rheingold, A. L. *J. Organomet. Chem.* **1996**, *516*, 41.

48) Blackwell, J. A.; Lehr, C.; Sun, Y.; Piers, W. E.; Pearce-Batchilder, S. D.; Zaworotko, M. J.; Young, V. G. J. *Can. J. Chem.* **1997**, *75*, 702.

49) Edelmann, F. T. *Scandium, Yttrium, and the Lanthanide and Actinide elements*; in *Comp. Organomet. Chem.* Pergamon: Oxford, 1995; Vol. 4, p. 11.

50) Deacon, G. B.; Harris, S. C.; Meyer, G.; Stellfeldt, D.; Wilkinson, D. L.; Zelesny, G. *J. Organomet. Chem.* **1996**, *525*, 247.

51) Deacon, G. B.; Wilkinson, D. L. *Aust. J. Chem* **1989**, *42*, 845.

52) Deacon, G. B.; Fallon, G. D.; MacKinnon, P. I.; Newnham, R. H.; Pain, G. N.; Tuong, T. D.; Wilkinson, D. L. *J. Organomet. Chem.* **1984**, *277*, C21.

53) Schumann, H.; Reier, F. W.; Palamidis, E. *J. Organomet. Chem.* **1985**, *297*, C30.

54) Schumann, H.; Jeske, G. *Z. Naturforsch Teil B* **1985**, *40*, 1490.

55) Schumann, H.; Jeske, G. *Angew. Chem. Int. Ed. Engl.* **1985**, *24*, 255.

56) St. Clair, M. A.; Santarsiero, B. D. *Acta. Crystallogr.* **1989**, *C45*, 850.

57) den Haan, K. H.; Luistra, G. A.; Meetsma, A.; Teuben, J. H. *Organometallics* **1987**, *6*, 1509.

58) Holton, J.; Lappert, M. F.; Ballard, D. G. H.; Pearce, R.; Atwood, J. L.; Hunter, W. E. *J. Chem. Soc. Dalton. Trans.* **1979**, *45*, 54.

59) Hammel, A.; Weidlein, J. *J. Organomet. Chem.* **1990**, *388*, 75.

60) den Haan, K. H.; de Boer, J. L.; Teuben, J. H.; Spek, A. L.; Kojic-Prodic, B.; Hays, G. R.; Huis, R. *Organometallics* **1989**, *5*, 1726.

61) Hitchcock, P. B.; Lappert, M. F.; Smith, R. G.; Bartlett, R. A.; Power, P. P. *J. Chem. Soc.,Chem. Commun.* **1988**, 1007.

62) Schumann, H.; Genthe, W.; Bruncks, N.; Pickardt, J. *Organometallics* **1982**, *1*, 1194.

63) Schumann, H.; Genthe, W.; Bruncks, N. *Angew. Chem. Int. Ed. Engl.* **1981**, *20*, 121.

64) Avent, A. G.; Edelman, M. A.; Lappert, M. F.; Lawless, G. A. *J. Am. Chem. Soc.* **1989**, *111*, 3423.

65) Hayes, R. G.; Thomas, J. L. *Inorg. Chem.* **1969**, *8*, 2521.

66) Namy, J. L.; Girard, P.; Kagan, H. B. *Nouv. J. Chim.* **1981**, *5*, 479.

67) Williams, R. A.; Hanusa, T. P.; Huffman, J. C. *Chem. Commun.* **1988**, 1045; Williams, R. A.; Hanusa, T. P.; Huffman, J. C.*Organometallics* **1990**, *9*, 1128.

68) Tilley, T. D.; Andersen, R. A.; Spencer, B.; Ruben, H.; Zalkin, A.; Templeton, D. *Inorg. Chem.* **1980**, *19*, 2999.

69) Evans, W. J.; Drummond, D. P.; Zhang, H.; Atwood, J. L. *Inorg. Chem.* **1988**, *27*, 575.

70) Evans, W. J.; Hughes, L. A.; Hanusa, T. P. *Organometallics* **1986**, *5*, 1285; Evans, W. J.; Hughes, L. A.; Hanusa, T. P. *J. Am. Chem. Soc.* **1984**, *106*, 4270.

71) Kaupp, M.; vonSchleyer, P. R.; Dolg, M.; Stoll, H. *J. Am. Chem. Soc.* **1992**, *114*, 8202.

72) Deacon, G. B.; Koplick, A. J.; Tuong, T. D. *Aust. J. Chem.* **1982**, *35*, 941.

73) Deacon, G. B.; Koplick, A. J. *J. Organomet. chem.* **1976**, *146*, C3.

74) Evans, W. J.; Engerer, S. C.; Coleson, K. M. *J. Am. Chem. Soc.* **1981**, *103*, 6672.

75) Boncella, J. M.; Tilley, T. D.; Andersen, R. A. *J. Chem. Soc.,Chem. Commun.* **1984**, 710.

76) Evans, W. J.; Fazakerly, G. V.; Phillips, R. F. *J. Chem. Soc. A* **1971**, 1931.

77) Evans, W. J.; Grate, J. W.; Levan, K. R.; Bloom, I.; Peterson, T. T.; Doedens, R. J.; Atwood, J. L. *Inorg. Chem.* **1986**, *25*, 3614.

78) Evans, W. B.; Bloom, I.; Grate, J. W.; Hunter, W. E.; Atwood, J. L. *J. Am. Chem. Soc.* **1985**, *107*, 405.

79) Maunder, G. H. *PhDthesis*; University of London, 1995.

80) Berg, D. J.; Burns, C. J.; Andersen, R. A.; Zalkin, A. *Organometallics* **1989**, *8*, 1865.

81) Zalkin, A.; J, B. D. *Acta Crystallogr.* **1988**, *C44*, 1488.

82) Schumann, H.; Albrecht, I.; Gallagher, M.; Hahn, E.; Janiak, C.; Kolax, C.; Loebel, J.; Nickel, S.; Palamidis, E. *Polyhedron* **1988**, *7*, 2307.

83) Schumann, H.; Frisch, G. M. *Z. Naturforsch* **1982**, *37b*, 168.

84) Schumann, H.; Frisch, G. M. *Z. Naturforsch* **1981**, *36b*, 1244.

85) Evans, W. J.; Ulibarri, T.; Ziller, J. W. *J. Amer. Chem. Soc.* **1988**, *110*, 6877.

86) Evans, W. J.; Gonzales, S. L.; Ziller, J. W. *J. Am. Chem. Soc.* **1991**, *113*, 9880.

87) Evans, W. J.; Gonzales, S. L.; Ziller, J. W. *J. Chem. Soc.,Chem. Commun.* **1992**, 1138.

88) Evans, W. J.; Drummond, D. K.; Bott, S. G.; Atwood, J. L. *Organometallics* **1986**, *5*, 2389.

89) Evans, W. J.; Drummond, D. K.; Chamberlain, L. R.; Doedens, R. J.; Bott, S. G.; Zhang, H.; Atwood, J. L. *J. Am. Chem. Soc.* **1988**, *110*, 4983.

90) Evans, W. J.; Drummond, D. K. *J. Am. Chem. Soc.* **1986**, *108*, 7440.

91) Evans, W. J.; Bloom, I.; Hunter, W. E.; Atwood, J. L. *J. Am. Chem. Soc.* **1981**, *103*, 1401.

92) Evans, W. J.; Hughes, L. A.; Drummond, D. K.; Zhang, H.; Atwood, J. L. *J. Am. Chem. Soc.* **1986**, *108*, 1722.

93) Evans, W. J.; Kociok-Kohn, G.; Ziller, J. W. *Angew. Chem. Int. Ed. Engl* **1992**, *31*, 3592.

94) Evans, W. J.; Kociok-Kohn, G.; Ziller, J. W. *Angew. Chem. Int. Ed. Engl* **1992**, *31*, 1081.

95) Evans, W. J.; Drummond, D. K. *J. Am. Chem. Soc.* **1989**, *111*, 3329.

96) Boncella, J. M.; Andersen, R. A. *Inorg. Chem.* **1984**, *23*, 432.

97) Cloke, F. G. N.; de Lemos, H. C.; Sameh, A. A. *J. Chem. Soc.,Chem. Commun.* **1986**, 1344.

98) Cloke, F. G. N. *Abs. Am. Chem. Soc.* **1995**, *207 Part 1*, INOR 403.

99) Bochkarev, M. N.; Trifonov, A. A.; Cloke, F. G. N.; Dalby, C. I.; Matsunaga, P. T.; Andersen, R. A.; Schumann, H.; Loebel, J.; Hemling, H. *J. Organomet. Chem.* **1995**, *486*, 177.

100) Anderson, D.; Cloke, F.; Cox, P.; Edelstein, N.; Green, J.; Pang, T.; Sameh, A.; Shalimoff, G. *J. Chem. Soc., Chem. Commun.* **1989**, 53.

101) Brennan, J.; Cloke, F.; Sameh, A.; Zalkin, A. *J. Chem. Soc., Chem. Commun.* **1987**, 1668.

102) Arnold, P. L.; Cloke, F. G. N.; Hitchcock, P. B. *Chem. Commun.* **1997**, 481.

103) King, W. A.; Marks, T. J.; Anderson, D. M.; Duncalf, D. J.; Cloke, F. G. N. *J. Am. Chem. Soc.* **1992**, *114*, 9221.

104) King, W. A.; Di Bella, S.; Lanza, G.; Khan, K.; Duncalf, D. J.; Cloke, F. G. N.; Fragala, I. L.; Marks, T. J. *J. Am. Chem. Soc.* **1996**, *118*, 627.

105) Trofimenko, S. *J. Am. Chem. Soc.* **1966**, *88*, 1842.

106) Trofimenko, S. *Chem. Rev.* **1993**, *93*, 943.

107) Calabrese, J. S.; Trofimenko, S.; Thompson, J. S. *J. Chem. Soc.,Chem. Commun.* **1986**, 1122.

108) Tolman, C. A. *J. Am. Chem. Soc.* **1970**, *92*, 2956.

109) Shannon, R. D. *Acta Cryst.* **1976**, *A32*, 751.

110) Tolman, C. A. *Chem. Rev.* **1977**, *77*, 313.

111) Maitlis, P. M. *Chem. Soc. Rev.* **1981**, *10*, 1.

112) Rheingold, A. L.; Ostrander, R. L.; Haggerty, B. S.; Trofimenko, S. *Inorg. Chem.* **1994**, *33*, 3666.

113) Calabrese, J. C.; Domaille, P. J.; Trofimenko, S.; Long, G. J. *Inorg. Chem.* **1991**, *30*, 2795.

114) Trofimenko, S. *Pyrazolylborates*; ; Wiley-Interscience, 1986; Vol. 34, pp 115-210.

115) Niedenzu, K.; Trofimenko, S. *Top. Curr. Chem.* **1986**, *131*, 1.

116) Bagnall, K. W.; du Preez, J. G. H.; Warren, R. F. *J. Chem. Soc. Dalton. Trans.* **1975**, 140.

117) Santos, I.; Marques, N. *New J. Chem.* **1995**, *19*, 551.

118) Stainer, M. V. R.; Takats, J. *Inorg. Chem.* **1982**, *21*, 4050.

119) Bagnall, K. W.; Tempest, A. C.; Takats, J.; Masino, A. P. *Inorg. Nucl. Chem. Lett.* **1976**, *12*, 555.

120) Domingos, A.; Marcalo, J.; Marques, N.; Dematos, A. P.; Galvao, A.; Isolani, P. C.; Vicentini, G.; Zinner, K. *Polyhedron* **1995**, *14*, 3067.

121) Stainer, M. V. R.; Takats, J. *J. Am. Chem. Soc.* **1983**, *105*, 410.

122) Reger, D. L.; Lindeman, J. A.; Lebioda, L. *Inorg. Chem.* **1988**, *27*, 3923.

123) Reger, D. L.; Lindeman, J. A.; Lebioda, L. *Inorg. Chim. Acta* **1987**, *139*, 71.

124) Reger, D. L.; Knox, S. J.; Lindemann, J. A.; Lebioda, L. *Inorg. Chem.* **1990**, *29*, 416.

125) Masino, A. P. *PhD thesis*; University of Alberta, 1978.

126) Moffat, W. D.; Stainer, M. V. R.; Takats, J. *Inorg. Chem. Acta* **1987**, *139*, 75.

127) Moss, M. A. J.; Jones, C. J. *J. Chem. Soc., Dalton Trans.* **1990**, 581.

128) Kilimann, U.; Edelmann, F. T. *J. Organomet. Chem.* **1993**, *444*, C15.

129) Kilimann, U.; Edelmann, F. T. *J. Organomet. Chem.* **1994**, *469*, C5.

130) Schumann, H.; Kohn, R. D.; Reier, F.-W.; Dietrich, A.; Pickardt, J. *Organometallics* **1989**, *8*, 1388.

131) Bruin, P.; Booij, M.; Teuben, J. H.; Oskam, A. *J. Organomet. Chem.* **1988**, *350*, 17.

132) Moss, M. A. J.; Jones, C. J. *Polyhedron* **1990**, *9*, 697.

133) Carretas, J.; Marques, N. f-Element conference: Leuven, 1990.

134) Domingos, A.; Marques, N. f-Element conference: Monterey, 1993.

135) McDonald, R.; Zhang, X.; Takats, J. f-Element conference: Monterey, 1993.

136) Takats, J.; Zhang, X. W.; Day, V. W.; Eberspacher, T. A. *Organometallics* **1993**, *12*, 4286.

137) Maunder, G. H.; Sella, A.; Tocher, D. A. *J. Chem. Soc.,Chem. Commun.* **1994**, 885.

138) Takats, J.; Zhang, X.; Bond, A. H.; D, R. R. *J. Am. Chem. Soc.* **1994**, *116*, 8833.

139) Zhang, X. W.; Loppnow, G. R.; McDonald, R.; Takats, J. *J. Amer. Chem. Soc.* **1995**, *117*, 7828.

140) Long, D. P.; Bianconi, P. A. *J. Amer. Chem. Soc.* **1996**, *118*, 12453.

Chapter 2 - Synthesis of bis(pyrazolylborate)samarium complexes with chalcogenolate ligands

Molecular precursors to materials

There is currently considerable interest in the preparation of molecular lanthanide complexes with chalcogenolate ligands. Homoleptic lanthanide chalcogenolates of the type $Ln(ER)_3$ or $Ln(ER)_2$ (E = S, Se, Te; R = bulky organic group) are attractive synthetic targets owing to their potential as molecular precursors to II - VI semi-conducting materials.[1-3] There is also interest in using the lanthanides as dopants in sulfur- and selenium-based fibre optic and laser materials. These applications arise from the unusual magnetic and luminescent properties of the lanthanide ions, such as their sharp optical f-f emission.[4] A low-temperature route to these technologically important binary lanthanide chalcogenide materials is very desirable to avoid problems associated with conventional preparative methods. These routes, utilising metal oxide or halide as starting material, require high temperatures and often suffer from contamination caused by the high oxophilicity of the lanthanide ions. Advantages of the molecular precursor approach include the ability to process materials at lower temperature and the greater ease of purification of soluble lanthanide complexes prior to pyrolysis.

Hard–Soft bonding interactions in lanthanide chalcogenolates

There are more fundamental motivations for studying the coordination chemistry of lanthanides bound to anionic chalcogenolate ligands. The trivalent lanthanide ions, despite their large ionic radii, are considered to be "hard" metal ions, owing to their preference for binding to saturated ligands such as NH_3, H_2O or F^-. These "hard" ligands, so called in allusion to their low polarisability, contain a strong donor atom and are, therefore, particularly suited to stabilising high oxidation state metals which are short of electron density. Low oxidation state metals, on the other hand, (which have

excess electron density) tend to bind unsaturated or polarisable ligands such as I^-, PPh_3 or C_2H_4. These "soft" ligands either contain weaker donor atoms from the second or subsequent rows or are unsaturated by virtue of double or triple bonds. They are capable of stabiling metals in low oxidation states by forming covalent interactions and accepting metal π-electron density through back-bonding into empty ligand orbitals. The group 16 elements, with the exception of oxygen and, to a lesser extent, sulfur, are considered "soft". Marks and co-workers have investigated the thermochemistry of samarium–oxygen and samarium–sulfur bonds and conclude that lanthanide to group 16 element bonds are quite thermodynamically stable.[5] The nature of the bond formed between "hard", Lewis acidic metal ions and the heavier, less electronegative chalcogens is, however, still quite poorly understood. While the bonding in solid state lanthanide chalcogenides has long been discussed in terms of considerable covalent character,[2] molecular lanthanide species are generally considered to possess predominantly ionic bonding interactions, forming stable complexes only with hard, non-polarisable donor anions. The relatively soft selenolate and tellurolate anions were, until recently, considered to be unable to form stable complexes with the lanthanides. A number of thermally stable lanthanide and early transition metal complexes with selenolate and tellurolate anions has, however, recently been prepared.

Formation of polyatomic species

Another area of interest lies in the apparent ability of divalent samarium to assemble atoms and form polynuclear species. Evans has reported the formation of the Zintl ions $(Bi_2)^{2-}$, $(Sb_3)^{3-}$, $(Se_3)^{2-}$ and $(Te_3)^{2-}$ from reaction of $Sm(Cp^*)_2$ or $Sm(Cp^*)_2(THF)_2$ with Ph_3Bi, n-Bu_3Sb and excess elemental Se and Te respectively.[6-8] The chemistry of the group 16 elements is reported as being complicated and highly dependent on reaction conditions and the stoichiometry of the reagents. The cluster $(Cp^*Sm)_6Se_{11}$ has also been reported to crystallise from an NMR sample of $[\{Sm(Cp^*)_2\}_2(\mu\text{-}\eta^1\text{:}\eta^3\text{-}Se_3)(THF)]$ in toluene-d_8.[9]

Homoleptic lanthanide chalcogenolates

A number of divalent and trivalent complexes of the lanthanides with chalcogenolate ligands as the only anion have been reported. Many of these compounds are oligomeric or polymeric and possess bridging chalcogenolate units, such as the THF solvated complexes $[(THF)Sm(SPh)_3]_{4n}$ and $[(THF)_4Ln_3(SePh)_9]_n$ (Ln = Pr, Nd, Sm) reported by Brennan.[4] Low-nuclearity compounds such as $[(py)_3Sm(SePh)_3]_2$,[2] or $Ln(SPh)_3(HMPA)_3$[10] can be obtained utilising a strong base such as pyridine or HMPA to displace the bridging chalcogenolate. Although this could introduce a potential contaminant into the immediate metal coordination sphere and present problems in the conversion to materials, in practice the complexes desolvate readily. An alternative is to utilise a very bulky chalcogen substituent to sterically saturate the metal coordination sphere, as in, for example, $Sm(S\text{-}2,4,6\text{-}Bu^t_3C_6H_2)_3$ synthesised by Lappert and coworkers.[11] The intense colours of the redox active lanthanide complexes have been attributed to chalcogen-to-metal(III) or metal(II)-to-pyridine charge transfer excitations in the visible region.[4]

Thermolysis reactions of the type:

$$2\ M(ER)_3 \rightarrow M_2E_3 + ER_2$$

have been reported to occur cleanly at temperatures below 300°C, with crystalline material obtained by annealing at up to 1000°C.

Heteroleptic Lanthanide Chalcogenolates

Early work in this area, for example in the preparation of $[Ln(NR_2)(\mu\text{-}SBu^t)]_2$ (Ln = Eu, Gd; R = $SiMe_3$) and $Sm(S\text{-}2,4,6\text{-}Bu^t_3C_6H_2)_3$ saw the use of bulky groups such as *tert*-butyl, supermesityl or $Si(SiMe_3)_3$ attached to the chalcogen atom in attempts to prepare soluble, low-nuclearity complexes. The use of fairly bulky ancillary ligands, typically the pentamethylcyclopentadienyl anion, C_5Me_5, has allowed more soluble products to be isolated without the need for a very bulky R-group attached to the

chalcogen atom. The C_5Me_5 ligand also tends to suppress the tendency of the group 16 elements to bridge two or more metal centres and facilitates the preparation of some monomeric complexes with terminal chalcogenolate ligands, notably $[Sm(C_5Me_5)_2(SePh)(THF)]$ and $[Sm(C_5Me_5)_2(TePh)(THF)]$, reported by Edelmann *et all* [12] and analogous complexes of the smaller ytterbium ion $[Yb(C_5Me_5)_2(TePh)(NH_3)]$ and $[Yb(C_5Me_5)_2(SPh)(NH_3)]$.[13,14] It has been noted that the size of the chalcogen substituent is actually relatively unimportant in these heteroleptic complexes in determining the stability of the resulting complex and that a bulkier R group simply results in a larger M–E–R angle to reduce repulsive steric interactions in the second coordination sphere (*vide infra*).

In order to investigate the lanthanide–chalcogenolate interaction it is desirable to obtain a series L_2M–ER (E = O, S, Se, Te) possessing a consistent metal inner coordination sphere with one or more terminal chalcogenolate ligands. In this way comparative information on the M–E bond can be obtained. Whilst a series of homoleptic lanthanide chalcogenolates might be expected to be less sterically congested in the second coordination sphere of the metal, thereby affording more accurate M–E–R bond angle and M–E bond length data, the need for steric saturation of the metal centre could result in less stable complexes than those possessing bulky ancillaries. Indeed, there is no homoleptic series possessing a consistent metal coordination sphere and there are very few examples in the literature of lanthanide chalcogenolates possessing terminal chalcogenolate ligands, supported by ancillary ligands or otherwise.

Synthetic strategies towards lanthanide chalcogenolates

A number of synthetic strategies have been used in the preparation of lanthanide chalcogenolate complexes.

1. Salt Metathesis

The reaction of lanthanide halides with alkali metal chalcogenolates may be used to prepare chalcogenolate complexes.[3,15-19]

$$L_xLnCl + NaER \rightarrow L_xLnER + NaCl$$

(L = Ligand, E =O, S, Se, Te)

This method, however, often suffers from problems arising from the incorporation of units of alkali metal or metal halide into the product, (formation of "ate-complexes") particularly when lithium or sodium reagents are used.[3,17,19]

2. Protonolysis

In order to avoid the formation of "ate-complexes", lanthanide complexes containing amines such as the $-N(SiMe_3)_2$ moiety have been used to prepare chalcogenolate complexes.[15,20] This method relies on the greater acidity of the E-H than the N-H bond, and the volatile amine product is easily separated from the metal complex.

$$L_xLn{-}NR_2 + HER' \rightarrow L_xLn{-}ER' + HNR_2$$

(L = ligand, E = O, S, Se, Te)

This route has also proved successful in early transition metal,[21] group 12[22,23] and uranium[24,25] chemistry.

Complexes containing lanthanide–carbon (alkyl) bonds have similarly been used as precursors in a modified version of this method, with concomitant formation of alkane.[11,26]

$$Lu(C_5Me_5)_2(\mu\text{-}CH_3)_2Li(THF)_2 + 2Bu^tEH \rightarrow Lu(C_5Me_5)_2(EBu^t).THF + LiEBu^t + 2CH_4$$

These synthetic routes can, however, lead to some oxidation of the lanthanide metal centre in attempted syntheses of divalent samarium and ytterbium complexes.[3]

3. Electron Transfer Routes

3a. Reduction of E–E bonds by Ln(0)

The strongly reducing lanthanides can be expected to cleave the weak E-E bonds of dichalcogenides. In the case of Eu and Yb such reactions may conveniently be carried out in liquid ammonia, a solvent in which these metals dissolve.[27] [10,28]

$$Yb + PhE–EPh \rightarrow (pyridine)_4Yb(EPh)_2$$

(E = S, Se or Te)

A modified method, in which lanthanide-mercury amalgams are reacted with diphenyl dichalcogenides to yield trivalent lanthanide chalcogenolate complexes, was reported recently.[2,29-31]

$$Ln + {}^3/_2PhE–EPh \rightarrow (pyridine)_3Ln(EPh)_3$$

(Ln = Ho, Tm or Yb; E = S, or Se)

The presence of excess mercury (or other group 12 metal) can lead to the formation of chalcogenolate-bridged clusters of the type isolated by Brennan, for example $MM'(EPh)_x(L)_y$ (M = Zn, Cd, Hg; M' = Ln(II), x = 4; M' = Ln(III), x = 5; E = S, Se, Te; L = THF, py).

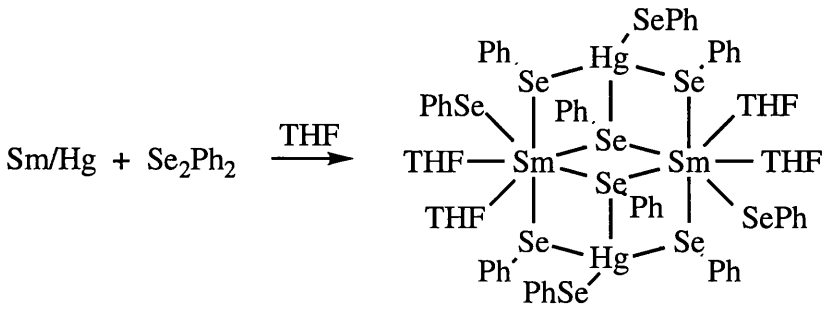

Such reactions have also been carried out in the presence of cyclooctatetraene (COT) to generate organometallic complexes.[32,33]

$$2\ Ln + 2\ COT + RS–SR \rightarrow [Ln(COT)(\mu\text{-}SR)]_2$$

3b. Transmetallation

The reducing ability of the elemental lanthanides has also been utilised in the transmetallation reaction between elemental europium and mercury chalcogenolates to synthesise thiopyridyl complexes.[29]

$$Eu + Hg(SPy)_2 \rightarrow (py)_4Eu(SPy)_2 + Hg$$

3c. Reduction of E–E bonds by Ln(II)

The reducing Sm(II) and Yb(II) ions can be expected to react in a similar fashion to the zerovalent metals. This synthetic method has been used successfully by several groups.[12-14,34 35,36]

$$2\ L_2Ln(II) + REER \rightarrow 2\ L_2Ln(III)–ER \quad (E = S, Se \text{ or } Te)$$

The net reaction is formation of a Ln(III) fragment which is bonded to the reduced ER.

3d. Reduction of C=E bonds

Metallic lanthanides and divalent lanthanide aryloxides[37] have been utilised in the synthesis of lanthanide (II)– and lanthanide (III)–ketone dianion complexes *via* electron transfer reactions with ketones. The reaction greatly depends on the ratio of lanthanide to ketone, with reversible C–O cleavage observed in the reaction of diaryl ketones with excess lanthanide.[38]

Analogous reactions with quinones afford metal alkoxides.[39]

e.g. $2\ [Sm(Tp^{Me,Me})_2] + [O_2\text{-}3,4\text{-}Bu^t{}_2C_6H_2] \rightarrow [Sm(Tp^{Me,Me})_2]_2[O_2\text{-}3,4\text{-}Bu^t{}_2C_6H_2]$

4. Insertion of chalcogen into a metal–carbon bond

By analogy with the behaviour of Grignard and organolithium reagents,[40] the reaction of Ln-R with elemental chalcogens results in the formation of the corresponding

chalcogenolate. Beletskaya's group has thus reported the insertion of tellurium(0) into yttrium carbon bonds.[41]

$$[(Bu^tC_5H_4)_2Y(\mu\text{-}Me)]_2 + 2\ Te \rightarrow [(Bu^tC_5H_4)_2Y(\mu\text{-}TeMe)]_2$$

The complexes $\{Cp'_2Lu(\mu\text{-}TeMe)\}_2$ (Cp' = C_5H_5, $Bu^tC_5H_4$, or $Me_3SiC_5H_4$) were also prepared in an analogous manner.

Piers has reported that insertion of tellurium into a scandium–carbon bond affords a thermally unstable tellurolate which decomposes to form a telluride-bridged dimer in a photochemically reversible reaction.[42,43]

$$Sc(Cp^*)_2\text{–}R + Te \longrightarrow Sc(Cp^*)_2\text{–}TeR \underset{h\nu}{\overset{\Delta}{\rightleftharpoons}} \{Sc(Cp^*)_2\}(\mu\text{-}Te) + TeR_2$$

Results

We have now successfully synthesised and obtained X-ray structural characterisation for a complete series down group 16 of 7-coordinate samarium complexes with terminal arylchalcogenolate ligands, supported by the bulky tris(pyrazolyl)borate ($Tp^{Me,Me}$) ancillaries. We have additionally prepared the dinuclear $[Sm(Tp^{Me,Me})_2]_2(\mu\text{-}O_2C_{14}H_8)$ and the 8-coordinate $[Sm(Tp^{Me,Me})_2S_2CNEt_2]$, identified a rational route to $[Sm(Tp^{Me,Me})_2][Te_3Ph_3]$ and the analogous $[Sm(Tp^{Me,Me})_2][I_3]$ and carried out further spectroscopic characterisation of the complexes $[Sm(Tp^{Me,Me})_2O\text{-}4\text{-}t\text{-}BuC_6H_4]$ and $[Sm(Tp^{Me,Me})_2][Te_3Ph_3]$ synthesised originally by Liu.

Synthesis of $[Sm(Tp^{Me,Me})_2OAr]$ (2.2)

The preparation of $[Sm(Tp^{Me,Me})_2OAr]$ (Ar = 4-Bu^t-C_6H_4, **2.2**) *via* salt metathesis of $[Sm(Tp^{Me,Me})_2Cl]$ with one equivalent of sodium phenoxide in THF has been described previously by Liu.[44]

$$[Sm(Tp^{Me,Me})_2Cl] + NaOPh \rightarrow [Sm(Tp^{Me,Me})_2OPh] + NaCl$$

The structure of **2.2** has been reported previously and is 7-coordinate at Sm, with pentagonal bipyramidal coordination geometry. Bond lengths and angles pertinent to the discussion are listed in table 2.1. This structure will only be discussed further in relation to the prepared chalcogenolate series $[Sm(Tp^{Me,Me})_2(EAr)]$.

Attempted Preparation of $[Sm(Tp^{Me,Me-4-Et})_2]_2[O_2C_6H_4]$

Working in parallel with Takats and Marques we attempted to prepare a wider range of samarium alkoxides *via* reduction of the C=O double bond in a number of quinones utilising the electron transfer route (3d) outlined above. Takats has synthesised $[Sm(Tp^{Me,Me})_2]_2[O_2\text{-}3,4\text{-}Bu^t{}_2C_6H_2]$ by this method [39] and $[Sm(Tp^{Me,Me})_2]_2[O_2C_6H_4]$ has recently been recrystallised and fully characterised by Marques and co-workers.[45] The attempted preparation of analogous complexes utilising the more soluble $[Sm(Tp^{Me,Me-4-Et})_2]$ as reducing agent did not yield tractable products. Thus, in an effort to synthesise $[Sm(Tp^{Me,Me-4-Et})_2][O_2C_6H_4]$ and $[Sm(Tp^{Me,Me-4-Et})_2]_2[O_2C_6H_4]$ by reaction of *p*–benzoquinone with one or two equivalents of $Sm(Tp^{Me,Me-4-Et})_2$ respectively green and yellow solutions in THF were obtained. ^1H NMR spectroscopy of the crude materials indicated that mixtures of products were present and no resonance was observed for the pyrazolyl ring protons. The green 1:1 compound decomposed during several attempts at recrystallisation from different solvent systems, giving some yellow material, presumably through decomposition to the $[O_2C_6H_4]^{2-}$ dianion and a pure sample could not be isolated. A yellow microcrystalline material was obtained on cooling a toluene solution of the crude product of the reaction using two equivalents of $Sm(Tp^{Me,Me-4-Et})_2$ but elemental microanalysis indicated that the C:H:N ratio was close to that expected for $[Sm(Tp^{Me,Me-4-Et})_2][O_2C_6H_4]$. The difference in stability between $[Sm(Tp^{Me,Me-4-Et})_2][O_2C_6H_4]$ and $[Sm(Tp^{Me,Me})_2][O_2C_6H_4]$ could arise from the more soluble nature of the $[Sm(Tp^{Me,Me-4-Et})_2]$ system, which reacts more rapidly than the insoluble system. It is possible that a secondary reaction such as C–O bond cleavage

occurs, as has been observed by Hou in the reaction of diaryl ketones with excess lanthanide metal.[38]

Synthesis of $[Sm(Tp^{Me,Me})_2]_2[O_2C_{14}H_8]$ (2.1)

Because of the difficulties encountered in reproducing these experiments and our failure to grow crystals, we attempted the synthesis of analogous complexes utilising 9,10-anthraquinone, The reaction of $[Sm(Tp^{Me,Me-4-Et})_2]$ with anthraquinone[$O_2C_{14}H_8$] gave a deep red product which could not be isolated with sufficient purity to obtain elemental microanalysis, although NMR and IR spectroscopy indicated the presence of the desired product. $[Sm(Tp^{Me,Me})_2]_2[O_2C_{14}H_8]$ (**2.1**) has, on the other hand, been successfully synthesised using this method. Thus on stirring anthraquinone with two equivalents of $[Sm(Tp^{Me,Me})_2]$ in THF the purple solid disappeared and a deep red solution was formed. Filtration, followed by cooling a concentrated solution in CH_2Cl_2/toluene to –30°C afforded a red crystalline product in good yield. This product was soluble in THF and CH_2Cl_2 but only sparingly soluble in the less polar solvents toluene, diethyl ether, DME and petrol. Elemental analysis was consistent with a 2:1 ratio of $Sm(Tp^{Me,Me})_2$ to anthraquinone, suggesting that reduction to the dianion had occurred. The IR spectrum exhibited two B–H stretches in the normal 2550cm^{-1} region, consistent with there being two pyrazolylborate environments in the solid state and the bands associated with the free anthraquinone C=O stretches were no longer present. These stretches presumably shift to around 1200 cm^{-1} and were not located owing to overlap with C–C bands in the fingerprint region. The ^1H NMR spectrum of **2.1** at room temperature was quite complex and indicated that one major product had been formed. The presence of six resonances attributed to the pyrazolylborate methyl protons and three for the pyrazolyl ring protons suggested that the molecule possesses a C_2 axis in solution. The resonances associated with the anthraquinone moiety were shifted upfield to around 3 ppm, presumably because the aromatic ring current of the outer rings is disrupted in the dianion, together with the close proximity to the paramagnetic

samarium centre. The ^{1}H NMR spectrum in toluene-d_8 remained temperature invariant between +90° and -80°C.

X-ray structure of 2.1

X-ray quality crystals were grown from dichloromethane/THF solution as red plates in space group $P\bar{1}$. The molecular structure is shown in Fig. 2.1 and the final atomic coordinates and lists of selected bond lengths and angles are given in Appendix 1. No significant intermolecular contacts were noted. The molecule lies on an inversion centre hence only half of the molecule is unique. The molecule consists of two 7-coordinate samarium atoms linked by a planar (μ-$C_{14}H_8O_2$) unit which is coordinated through each oxygen to one $Sm(Tp^{Me,Me})_2$ in a molecular structure. Thus each samarium atom is directly coordinated to two tridentate ($Tp^{Me,Me}$) ligands and an anthraquinone oxygen atom. The coordination geometry at samarium is pentagonal bipyramidal with N(3) and N(7) occupying axial sites. The Sm–N(axial) distances are slightly shorter than those in the equatorial girdle, as expected for these less crowded sites.[46] The axial sites are bent with a N(3)-Sm(1)-N(7) angle of 157.3°, slightly larger than the equivalent angle in $[Sm(Tp^{Me,Me})_2(OC_6H_4\text{-}4\text{-}Bu^t)]$ (153.32°), **2.2**, a distortion that arises from the geometrical requirements of the $Tp^{Me,Me}$ ligands. The two $Tp^{Me,Me}$ ligands are mutually staggered and bent back from each other at an angle of 143°, as measured by the B-Sm-B angle, a bend angle quite typical of lanthanide bis-$Tp^{Me,Me}$ systems.

The boron atoms are tetrahedral and the $Tp^{Me,Me}$ ligands show the typical twisting of the pyrazolyl rings about the B-N bond, whereby the pyrazolyl rings rotate in such a way that the ring planes are no longer parallel to the B–Sm vectors with B–N–N–Sm torsion angles for pyrazolyl rings 3 (N5-N6) and 6 (N11-N12) are 22.0° and 23.7° respectively. We presume that this deviation from the ideal C_3 symmetry of the pyrazolylborates is necessary to accommodate the anthraquinone group. The coordination site so created for the anthraquinone is such that the plane of the anthraquinone lies at an angle of *ca* 24.5° relative to the plane defined by Sm(1), B(1) and B(2). In this position it fits snugly between the "front" pyrazolyl rings 3 and 6.

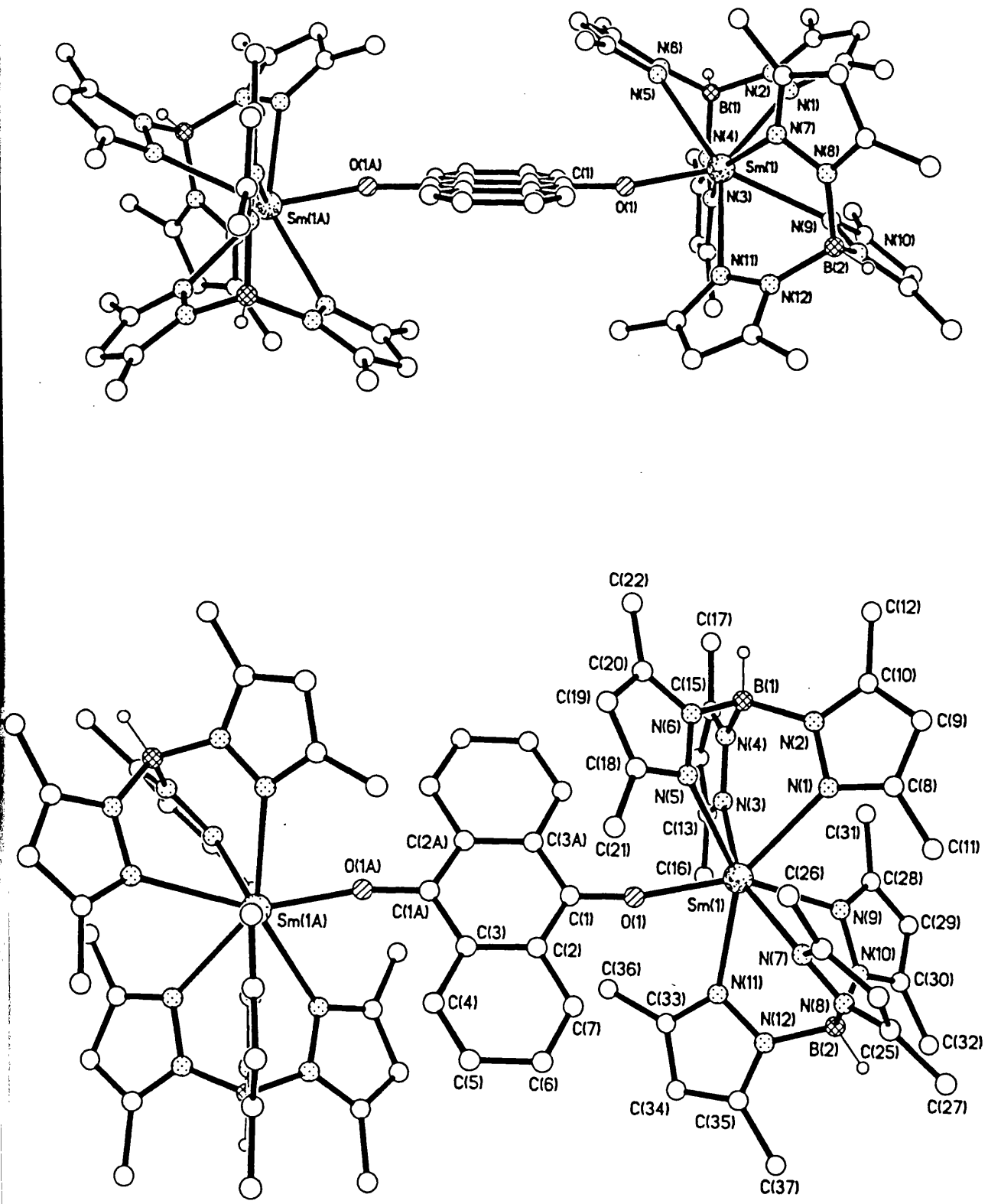

Figure 2.1 X-ray structure of 2.1

The average M-N(pyrazolyl) distance 2.572(4) Å (range 2.482(10) – 2.624(10) Å) is equivalent to that observed in **2.2** (2.572(5) Å) and similar to the corresponding seven-coordinate chloride complex (2.565(3) Å).[47]

The Sm–O bond in **2.1**, 2.138(8)Å, is marginally shorter than those in **2.2** (2.159(2) Å) and in $[Sm(Tp^{Me,Me})_2(O\text{-}3,4\text{-}Bu^tC_6H_2O)]$ (2.213 Å), suggesting either a stronger ionic interaction between the anthraquinone dianion and the $Sm(Tp^{Me,Me})_2$ units or a more effective π-interaction (*vide infra*). This Sm–O bond is slightly longer than the M–O bonds observed in the related metallocene systems $Cp^*_2Sm(O\text{-}2,3,5,6\text{-}Me_4C_6H)$ 2.13(1) Å,[48] $[Cp^*_2Sm]_2(O_2C_{16}H_{10})$ 2.08(2) Å and $[Cp^*_2Sm]_2(O_2C_{16}H_{10})$ 2.099(9) Å.[49] and the average terminal aryloxide distance in $\{Sm(\mu\text{-}O\text{-}\eta^6\text{-}Ar)(OAr)_2\}$ (Ar = 2,6-$Pr^i_2C_6H_3$) 2.101(6) Å.[50] This may reflect the greater crowding around the third ligand in the tris(pyrazolyl)borate system than in the relatively open wedge of the metallocene. The Sm–O–C angle of 167.6(8)° is approaching linearity, which may be ascribed to a need to relieve steric crowding with the pyrazolylborate methyl groups together with possible π-donation by oxygen to the samarium (*vide infra*). Although this bond angle is less acute than those noted for **2.2** (153.7(2)°) and $[Sm(Tp^{Me,Me})_2(O\text{-}3,4\text{-}Bu^tC_6H_2O)]$ (154.5°), comparable M-O-C bond angles are observed for the terminal alkoxide groups in $Cp^*_2Sm(O\text{-}2,3,5,6\text{-}Me_4C_6H)$ (172.3(13)°),[48] $[Cp^*_2Sm]_2(O_2C_{16}H_{10})$ 173(2)°, $[Cp^*_2Sm]_2(O_2C_{16}H_{10})(THF)$ 166.3(7)°,[49] and the group 4 complexes $[TiCl_2(OPh)_2]_2$ (165.9(6)° [51] and $[Ti(OPh)_4]_2.2PhOH$ (175 and 169°).[52]

The sum of the angles around the bridgehead carbon C(1) indicate that it is planar, suggesting that it is still sp^2-hybridised and that compound **2.1** is a quinone dianion metal complex, consistent with the fact that it is formed via an electron transfer route. The C(1)–O(1) bond length of 1.326(14) Å is similar to C–O distances in other reported metal alkoxide systems (e.g. 1.340(3) Å in **2.2**, 1.301 Å in $[Sm(Tp^{Me,Me})_2(O\text{-}3,4\text{-}Bu^tC_6H_2O)]$, 1.29(2) Å in $Cp^*_2Sm(O\text{-}2,3,5,6\text{-}Me_4C_6H)$[48], 1.39(6) Å in $[\{Yb(OCPh)_2(HMPA)_2\}_2]$.[53]

While it is plausible that the more stable anthraquinone dianion facilitates the isolation of complex **2.1**, in contrast to the intractability of the benzoquinone complexes, it is likely that a major contribution to the stability of the system is provided by the $[Sm(Tp^{Me,Me})_2]$ unit which crystallises more readily with these systems than does the soluble $[Sm(Tp^{Me,Me\text{-}4\text{-}Et})_2]$, as evidenced by the isolation of $[\{Sm(Tp^{Me,Me})_2\}_2(\mu\text{-}O_2C_6H_4)]$ by Marques and coworkers.

Preparation of $[Sm(Tp^{Me,Me})_2]$ thiolates

Attempts by Liu to use the salt metathesis strategy for the preparation of thiolates were not successful as mixtures of products were obtained, presumably as a result of salt incorporation. This parallels the experience of Bianconi who reported extensive chloride incorporation when preparing divalent ytterbium and samarium tellurolates.[3] For these complexes an oxidative strategy was therefore utilised, starting from the samarium (II) complex $[Sm(Tp^{Me,Me})_2]$, in a manner analogous to that used by Schumann and coworkers for the preparation of metallocene complexes.[54] Liu found that the reaction conditions were of crucial importance, with the use of THF as solvent resulting in no pure products being isolated. In the reaction with diphenyldisulfide the use of toluene as a solvent and milder conditions, namely starting the reaction at –78°C and warming slowly to room temperature, yielded a clear, pale yellow solution from which $[Sm(Tp^{Me,Me})_2SPh]$ could be recovered at low temperature as a pale yellow solid in acceptable yields.

$$2[Sm(Tp^{Me,Me})_2] + PhSSPh \rightarrow 2\ Sm(Tp^{Me,Me})_2SPh$$

Preparation of samarium chalcogenolates $[Sm(Tp^{Me,Me})_2(EAr)]$ (E = S, 2.3; E = Se, 2.4; E = Te, 2.5)

The reductive cleavage of E-E bonds can be extended to the other members of group 16. Thus $[Sm(Tp^{Me,Me})_2SPh^{Me}]$, **2.3**, $[Sm(Tp^{Me,Me})_2SePh^{4\text{-}t\text{-}Bu}]$, **2.4**, and $[Sm(Tp^{Me,Me})_2TePh]$, **2.5** could be obtained in high yields and are thermally robust

although rather air sensitive. Consistent with an electron transfer mechanism the reactions were complete within an hour for the ditellurides, were somewhat slower for the diselenides and required overnight stirring at room temperature in the case of the disulfides. We have now been able to obtain crystals suitable for X-ray diffraction studies for all of these complexes. Analogous compounds were obtained in NMR reactions starting from the toluene-soluble $[Sm(Tp^{Me,Me,4\text{-}Et})_2]$. These reactions proceeded more rapidly than with $[Sm(Tp^{Me,Me})_2]$ and the products were only analysed by ^1H NMR spectroscopy.

The analogous ytterbium complexes, $[Yb(Tp^{Me,Me})_2EPh]$, could not be synthesised in this way and only starting material was recovered from the reaction mixture. Although there are several examples of $Yb(Cp^*)_2$ reducing the E–E bond in diaryldichalcogenides and other reducible systems, this apparent inconsistency is ascribed to the generally lower reactivity conferred on the divalent lanthanides by the $Tp^{Me,Me}$ ligand system (compared to C_5Me_5) and has been observed in a number of reaction systems.

The nature of the structures of these complexes is intriguing as, including the phenoxide synthesised by Liu, compounds **2.2** to **2.5** represent a complete series down the chalcogenolate group and provide a unique set of compounds for which structural comparisons can be made, permitting us to explore directly changes in bonding as a function of hardness and softness. It has recently been shown that in the corresponding series for the halogens, $[Sm(Tp^{Me,Me})_2X]$, the steric demand of the halide ions leads to expulsion of iodide from the coordination sphere, while the smaller chloride and fluoride anions yield seven-coordinate molecular structures.[47] The structure of the bromide remains a matter of conjecture and our attempts to prepare this complex are described in Chapter 4. The solvent system utilised for reaction and recrystallisation together with the length of time for which the lanthanide and alkali metal reagents are stirred appears to be of crucial importance to the outcome (see Chapter 4).

^{1}H NMR spectroscopic studies on [Sm(Tp^{Me,Me})$_2$(EAr)]

The room temperature ^{1}H NMR spectra of complexes **2.2**, **2.3**, **2.4**, and **2.5** are broadly similar, with three peaks in the ratio of 3:3:1 assigned to the tris-pyrazolylborate ligands, somewhat shifted by the presence of the paramagnetic samarium(III) centre, and corresponding peaks for the phenyl groups. Figure 2.2 shows the room temperature ^{1}H NMR spectrum of **2.4**. The doublet assigned to the *ortho* protons of the phenyl groups showed quite marked shifts downfield, particularly for the phenoxides. The chemical shifts of the Tp^{Me,Me} groups are very similar to those of the pyrazolyl groups of [Sm(Tp^{Me,Me})$_2$X] (X = F, Cl, OTf) which are known to be seven-coordinate both in the solid state and in solution.[55] Thus the room temperature NMR spectra of these compounds are rather structurally uninformative but possibly suggestive of molecular complexes with a fluxional coordination sphere.

Cooling **2.2** to –80°C in toluene-d$_8$ resulted in some broadening of the ^{1}H NMR signals associated with the pyrazolylborate ligands but no limiting spectrum was observed. The changes were considerably more marked for **2.3**, **2.4** and **2.5**. In particular, cooling **2.4** in toluene led to progressive broadening of the resonances in the ^{1}H NMR spectrum associated with the pyrazolylborates, together with small shifts in the peaks associated with the selenolate group which arise as a result of the Curie dependence of chemical shift of a paramagnetic molecule. By –95°C the spectrum had become sharp once more and six resonances assigned to the methyl groups and three owing to the methine protons of the Tp^{Me,Me} ligand had been resolved, consistent with a structure of C_2 symmetry, implying a molecular nature for the complex. **2.3** and **2.5** exhibited similar, but less well resolved, low temperature spectra. The variable temperature spectra are shown in Appendix 2.

X-ray crystallographic data for the series [Sm(Tp^{Me,Me})$_2$(EAr)]

In view of the small number of complexes possessing terminal chalcogenolate ligands and the relative scarcity of structural data, it was of interest to collect X-ray crystallographic data on complexes **2.2** to **2.5**.

X-ray structure of $[Sm(Tp^{Me,Me})_2(SPh^{Me})]$, 2.3

The thiolate **2.3** crystallized from toluene in the space group $P2_1/n$. The molecular structure is shown in Fig. 2.2 and the final atomic coordinates and lists of selected bond lengths and angles are given in Appendix 1. No significant intermolecular contacts were noted. The structure is broadly similar to that reported for **2.2**, with a seven-coordinate pentagonal bipyramidal metal centre coordinated to two pyrazolylborates in η^3 fashion with a terminal thiolate ligand. Nitrogen atoms N(11) and N(1) adopt axial positions with N(11)-Sm(1)-N(1) slightly bent (150.1°). The equatorial plane has mean deviation from planarity of 0.2502 Å. The pyrazolylborate ligands are bent back by 152.8°, as measured by the B(1)-Sm(1)-B(2) angle. The average Sm-N distance is 2.531(6) Å (range 2.456(3) to 2.634(3) Å), slightly shorter than in **2.2**, presumably owing to the less effective donation to the Lewis acidic metal centre by the softer thiolate ligand, which results in the ancillary ligands being drawn in to compensate. The Sm–S distance, 2.8260(9) Å is *ca.* 0.6 Å longer than the Sm–O distance in **2.2**, far greater than can be accounted for in terms of the change in ionic radius from alkoxide to thiolate. While the Sm–S distance can be predicted quite accurately by summation of ionic radii, which gives a theoretical bond length of 2.84 Å,[56] the Sm–O bond falls short of the expected distance by 0.16 Å. This suggests that the alkoxide-samarium interaction may have considerable multiple bond character (*vide infra*). The Sm–S bond length in **2.3** is similar to those observed in other complexes possessing terminal thiolate ligands, for example $[Sm(SPh)_3(HMPA)_3]$ (2.821(1)Å), $[(py)_2(THF)Sm(SC_6H_2Pr^i_3)_3]$ (2.740(2) Å) and $[(THF)_3Sm(\mu\text{-}(SC_6H_2Pr^i_3)(SC_6H_2Pr^i_3)_3]$ (2.908(6) Å) and slightly longer than that observed in $Sm(SC_6H_2\text{-}2,4,6\text{-}Bu^t_3)$ (av.Sm–S 2.644(5) Å)[11] which relies on Sm–CH_3 interactions to saturate the metal coordination sphere. The only system comparable to that of **2.3**, possessing bulky ancillaries together with a single terminal thiolate ligand, is provided by the metallocene $[YbCp^*_2(SPh)(NH_3)]$[13] which has two independent molecules in the asymmetric unit, with Yb–S distances of 2.670(3) and 2.679(3) respectively. On changing the metal(III) ion from Sm to Yb ionic radius decreases by 0.14 Å[56] or

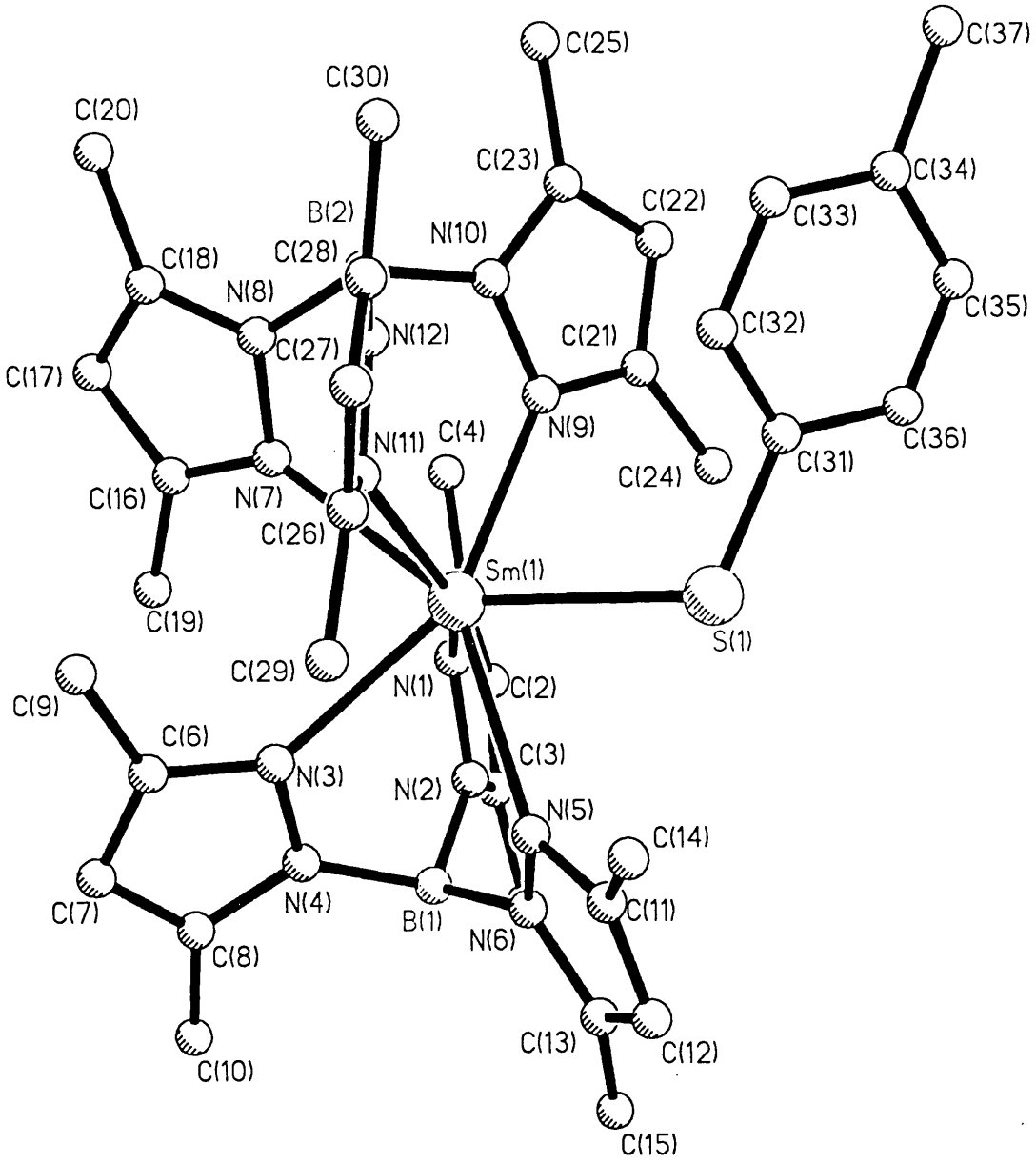

Figure 2.2 X-ray structure of 2.3

0.09Å.[57] The average difference in M–S bond length between [Sm($Tp^{Me,Me}$)$_2$SPh-4-Bu^t] and [YbCp*$_2$(SPh)(NH_3)] is 0.153 Å, suggesting that summation of ionic radii allows us to make reasonably accurate predictions for Sm from Yb bond distances using the ionic radii quoted by Emsley. The difference between average M–S distance in the homoleptic complexes [(py)$_2$(THF)Ln($SC_6H_2Pr^i_3$)$_3$] and [Ln(SPh)$_3$(HMPA)$_3$] (Ln = Sm, Yb), with Δ(Sm–S/Yb–S) of 0.092 and 0.093 Å respectively (and equivalent, therefore, to the value calculated applying Shannon's data) suggests, however, that "consistent" data concerning metal ionic radii are only reliable for complexes possessing directly comparable metal coordination sphere.

The thiolate ligand is significantly bent with a Sm-S-C angle of 114.6(1)°, consistent with there being comparatively little overlap between the lone pairs on the sulfur and the vacant samarium 5 d orbitals, and also with the longer M–S separation conferring greater freedom of movement on the phenyl group. The C–S bond length, 1.772(3) Å, is consistent with that expected for a single covalent bond.

Pyrazolyl rings 1 (N1N2), 3 (N5N6) and 6 (N11N12) are twisted about their B–N bonds such that the ring planes are at angles of 28.9, 31.3 and 34.4° respectively to the Sm–B vectors. This type of distortion of the pyrazolylborate groups away from their ideal C_3 symmetry is commonly observed in 7- and 8-coordinate lanthanide systems and is presumed to arise from the need to minimise steric congestion in the second coordination sphere arising from the accommodation of the third ligand.

X-ray structure of [Sm($Tp^{Me,Me}$)$_2$($SePh^{t\text{-}Bu}$)], 2.4

The selenolate **2.4** crystallized from toluene as large, air sensitive orange blocks in the space group P $\bar{1}$. The molecular structure is shown in Fig. 2.3 and the final atomic coordinates and lists of selected bond lengths and angles are given in Appendix 1. No significant intermolecular contacts were noted. The complex consists of two $Tp^{Me,Me}$ ligands and a phenyl selenolate in the metal coordination sphere. However, in contrast to **2.1**, **2.2**, **2.3** and **2.5** (*vide infra*) which are rigorously seven coordinate at samarium, one of the Tp ligands in **2.4** binds through three nitrogens (N7, N9, N11)

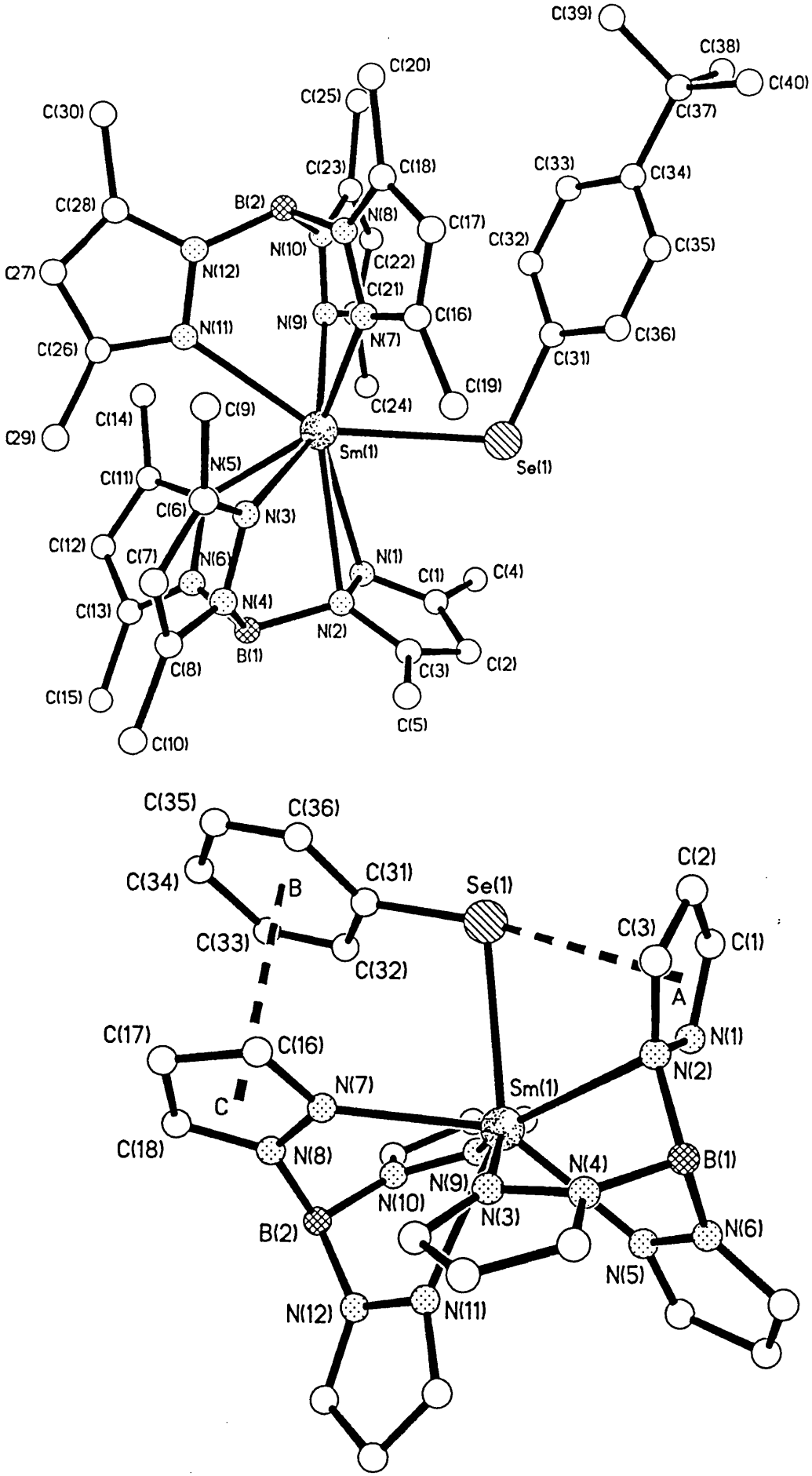

Igure 2.3 X-ray structure of 2.4

while the other is severely distorted away from the normal C_3 symmetry. Thus two of the pyrazolyl groups are aligned approximately parallel to the B–Sm vector while the third is twisted sideways such that both nitrogens interact with the metal. Such a distortion has been observed only once before in the structurally related $[Tp^{Me,Me}{}_2UI]$.[58] The distortion in the case of **2.4** is more pronounced, with N(2) closer to the samarium than N(1) (2.736(2) *vs.* 2.858(2) Å) and the sum of the angles around N(1) (348°) suggesting the atom to be slightly pyramidal.

The two pyrazolylborate groups are mutually staggered and the phenyl group of the selenolate ligand lies in the wedge between two pyrazolyl groups of the undistorted Tp ligand. The phenyl group lies parallel to one of the pyrazolyl rings with a centroid to centroid distance of 3.607 Å suggesting a possible graphitic interaction. This is shown in figure 2.3b.

The Sm-Se distance in **2.4** is 2.9457(3) Å, which is slightly longer than those observed by Edelmann and coworkers in the metallocene analogue $[Cp^*{}_2Sm(SeC_6H_2(CF_3)_3\text{-}2,4,6)]$ 2.919(2) Å[12] and by Brennan in the seven-coordinate terminal selenolates $[(py)_2Sm(SePh)(\mu\text{-}SePh)_3Na(py)_2]_2$, (2.908(1) Å)[30] and $[(py)_3Sm(\mu\text{-}SePh)(SePh)_2]_2$ (2.9129(14) and 2.8968(11) Å).[4] The Sm-Se-C angle, 108.29(9)°, is even more acute than in **2.3**. This is less open than the angle at selenium in $[Cp^*{}_2Sm(SeC_6H_2(CF_3)_3\text{-}2,4,6)]$ (126.4(1)°)[12] but compares with the corresponding angles in $[(py)_3Sm(\mu\text{-}SePh)(SePh)_2]_2$ of 109.2(2) and 114.2(2)° and in $Yb(SePh)_2(Py)_4$ of 103.7(2)°.[27] Presumably the bulky CF_3 *ortho*-substituents are responsible for the straightening of the M–Se–C bond in the metallocene complex.

A further possible secondary interaction occurs between the selenium atom and pyrazolyl ring 1 (N1N2), which lies below the selenium with Se–pyrazolyl ring centroid distance of 3.232 Å.

Assuming the distorted Tp ligand to occupy a coordination site midway between N(1) and N(2), the coordination geometry at the metal may again be described as distorted pentagonal bipyramidal, with N(3) and N(9) in axial positions, bent away from linearity with N(3)-Sm-(N9) of 150.9°. The equatorial plane is defined by N(5), N(11), N(7),

Se(1) and the mid-point between N(1) and N(2) and is more distorted than the other members of the series with mean deviation from the equatorial plane of 0.3502 Å (see Fig. 2.9 and table 2.3). The average metal-nitrogen distance, excluding N(1) and N(2), is 2.5072(4) Å, shorter than in **2.3**, consistent with the decreasing ability of the chalcogen to satisfy the Lewis acidity of the metal on descending group 16 resulting in a closer approach of the ancillary pyrazolylborate ligands.

X-ray structure of [Sm(Tp^{Me,Me})$_2$(TePh)], 2.5

The tellurolate **2.5** crystallized as small orange blocks in the space group $P2_1/c$ as a toluene solvate and the structure is shown in figure 2.4. The molecular structure of the complex is quite similar to that of **2.3**, consisting of discrete [Sm(Tp^{Me,Me})$_2$(TePh)] units. No significant intermolecular contacts were noted. The metal centre is seven-coordinate with a distorted pentagonal bipyramidal geometry. The samarium-tellurium distance of 3.1874(4) Å is slightly longer than that observed by Edelmann in [Cp*$_2$Sm(TeC$_6$H$_2$(CH$_3$)$_3$-2,4,6)], 3.088(2) Å[12]. The acute Sm–Te–C angle in **2.5** of 104.83° does not correlate with the considerably wider angle of 123.5(3)° observed for Edelmann's metallocene, consistent with the observation for the corresponding selenolates that the bend at the chalcogen atom is relatively "soft" and highly dependent upon steric congestion in the second coordination sphere of the metal centre. There are, to our knowledge, no other examples of samarium complexes possessing terminal tellurolate ligands, although a number of ytterbium tellurolates have been reported. Although no major distortion of the pyrazolylborate ligands occurs as in **2.4**, one ring on each ligand twists significantly (19.3° and 47.7°) around the B-N bond, presumably to accommodate the tellurium atom in the metal coordination sphere. A graphitic-type interaction similar to that believed to partially stabilise the distortion in the selenolate is noted between the phenyl ring and pyrazolyl ring 6 (N11N12), with centroid-to-centroid distance of 3.537 Å. The average Sm-N distance is 2.538 Å (range 2.455(4) to 2.633(3) Å), slightly longer than in the thiolate, again presumably due to the

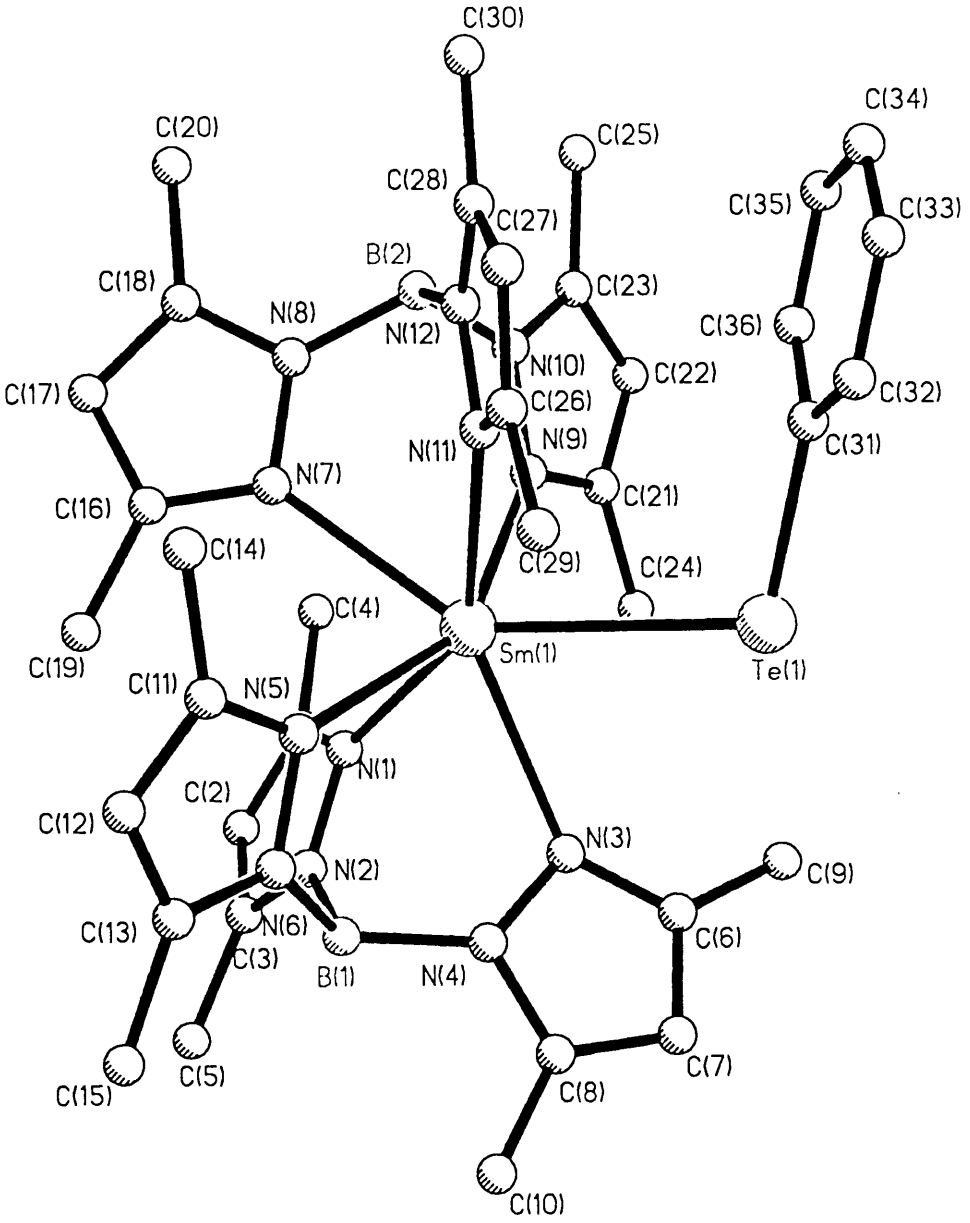

Figure 2.4 X-ray structure of 2.5

larger size of the tellurium atom. The axial nitrogens N(5) and N(9) of the pentagonal bipyramid are bent with a N(5)–Sm(1)–N(9) angle of 151.5°. The equatorial plane has mean deviation from planarity of 0.2847Å, larger than that observed for **2.2** (0.2239Å) and comparable to the thiolate. The pyrazolylborate ligands are bent back from each other, with B(1)–Sm–B(2) angle of 148.4°.

Preparation of $[Sm(Tp^{Me,Me})_2(SBz)]$ and $[Sm(Tp^{Me,Me})_2(SeBz)]$

All of the complexes described so far are aryl substituted. In order to explore the electronic effect of having a better donor alkyl substituent, complexes with benzyl substituents were prepared. Reaction of $[Sm(Tp^{Me,Me})_2]$ with dibenzyl disulphide in toluene resulted in a similar colour change to the diaryldisulfides. The petrol soluble product gave elemental analyses consistent with the stoicheiometry $[Sm(Tp^{Me,Me})_2(SBz)]$ and the ^1H NMR spectrum contained the three peaks expected for a fluxional molecule with equivalent $Tp^{Me,Me}$ ligands. The benzyl group, however, gave multiplets in the aryl region together with two broad singlets integrating for approximately one proton each, and consistent with a methylene group with inequivalent hydrogen environments. The observation that one of these peaks was significantly shifted upfield may suggest an agostic interaction of one of the methylene protons with the metal centre. This interaction may be sufficiently strong to give rise to differentiate between the two protons but apparently not enough to constrain rotation of the $Tp^{Me,Me}$ ligands. Attempts to prepare the corresponding benzyl selenolate were not successful as the reaction was not fully reproducible and consistent elemental analyses on the yellow product isolated were not obtained.

Synthesis of $[Sm(Tp^{Me,Me})_2S_2CNEt_2]$, 2.6

The oxidative synthetic strategy was extended to the reaction with thiuram disulfides. No tractable product was obtained with tetramethylthiuram disulfide,[59] but the analagous reaction utilising tetraethylthiuram disulfide afforded $[Sm(Tp^{Me,Me})_2(S_2CNEt_2)]$, **2.6**. Addition of $\{Et_2NC(S)S\}_2$ to $[Sm(Tp^{Me,Me})_2]$ in toluene resulted in the gradual disappearance of the purple colour on stirring overnight.

Filtration and recrystallisation from Et_2O afforded pale yellow crystalline material in reasonable yield.

^{1}H NMR Spectroscopy of 2.6

The room temperature ^{1}H NMR spectrum of **2.6** (shown in Appendix 2) exhibited six resonances attributed to the $Tp^{Me,Me}$ methyl protons and three for the pyrazolyl ring protons, consistent with a C_2-symmetric structure. Resonances associated with the dithiocarbamate protons were also observed. It appears that while the 7-coordinate bis(pyrazolylborate)samarium chalcogenolate complexes (with the exception of the dimeric anthraquinone complex) exhibit fluxionality at room temperature on the NMR time scale, the increase in coordination number to eight freezes out the fluxional processes. Although not observed for $[Sm(Tp^{Me,Me})_2(L_2)]$ systems (L = unidentate ligand), which are fluxional at all accessible temperatures,[60] this seems to be quite a common feature of the 8-coordinate $[Sm(Tp^{Me,Me})_2]$ systems with a bidentate third ligand. $[Sm(Tp^{Me,Me})_2(PhNNPh)$ is reported to possess C_2 symmetry in solution as high as 90°C[61] and Marques has recently synthesised $[Sm(Tp^{Me,Me})_2(EPy)]$ (E = S, Se) and found them to possess rigid C_1-symmetric structures in solution at elevated temperature, exhibiting 12 pyrazolyl-methyl resonances and 6 pyrazolyl-methine resonances in their ^{1}H NMR spectra.[45] The analogous 2-hydroxypyridine complex, on the other hand, exhibits only a single set of pyrazolyl resonances in the typical 3:3:1 ratio in the room temperature ^{1}H NMR spectrum,[45] as does the dioxygen complex $[Sm(Tp^{Me,Me})_2](O_2)$, remaining temperature invariant at accessible temperatures.[62] On warming a sample of complex **2.6** in toluene-d_8 the peaks associated with the pyrazolylborate ligands started to broaden but a limiting spectrum was not reached at 100°C.

X-ray structure of 2.6

X-ray quality crystals of **2.6** were grown from a concentrated diethyl ether solution as pale yellow plates in space group $P\bar{1}$. The molecular structure is shown in Fig. 2.5 and the final atomic coordinates and lists of selected bond lengths and angles are given in

Appendix 1. The metal centre is eight-coordinate, with the samarium atom bound in tridentate fashion to two pyrazolylborate ligands and in bidentate fashion to the dithiocarbamate ligand through both sulfur atoms. The metal coordination geometry is dodecahedral, the trapezia being defined by the atoms N21, S2, S1, N61 and N11, N31, N41, N51 respectively which intersect with a dihedral angle of 102° rather than the ideal 90°. While the trapezoid containing the sulfur atoms is almost planar, the second is somewhat distorted, as defined by the normalised ϕ angles of 0.3 and 10.9° respectively. There is very little distortion of the trapezia of the type observed by Maunder and coworkers in the eight-coordinate lanthanum complex $[La(Tp^{Me,Me})_2(MeCN)_2][O_3SCF_3]$ where significant distortion towards trigonal bicapped prismatic geometry was noted.[60]

The two pyrazolylborate groups are mutually staggered and bent back with a B–Sm–B angle of 137.2°. The resulting open metal coordination site is considerably larger than in the comparable 8-coordinate complexes $Sm(Tp^{Me,Me})_2(O_2)$, $Sm(Tp^{Me,Me})_2(PhNNPh)$ and $Sm(Tp^{Me,Me})_2(NO_2)$ with B–Sm–B angles of 144.1, 152.6 and 159.0° respectively but close to the 142.7° observed for the larger metal lanthanum in $La(Tp^{Me,Me})_2(MeCN)(O_3SCF_3)$. The arrangement of the pyrazolyl groups around the dithiocarbamate ligand gives an effective C_2 symmetry to the binding site. Similar pseudo-C_2 symmetry has been noted in the above 8-coordinate $[Sm(Tp^{Me,Me})_2]^+$ complexes.

The average Sm–N bond length in **2.6** of 2.626(2) Å (range 2.503(5) to 2.728(5) Å) is close to those reported for $Sm(Tp^{Me,Me})_2(O_2)$ (2.58 Å), $Sm(Tp^{Me,Me})_2(PhNNPh)$ (2.59 Å) and $Sm(Tp^{Me,Me})_2(NO_2)$ (2.559(4) Å) and longer than the corresponding distance in the thiolate **2.3**, as expected on increasing coordination number from seven

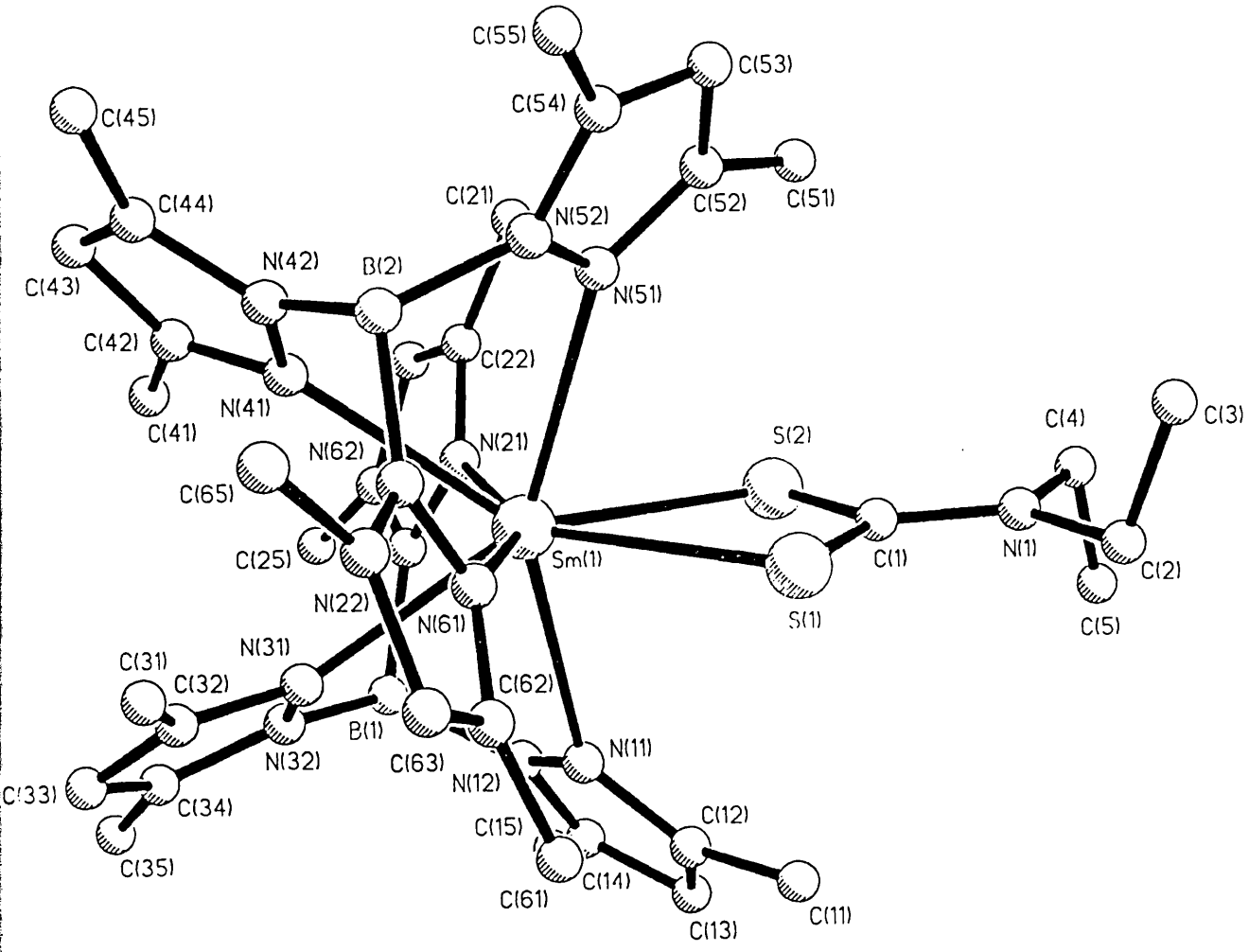

Figure 2.5 X-ray structure of 2.6

to eight. Pyrazolyl rings 1 (N11N12) and 5 (N51N52) are considerably twisted about their B–N bond, with B-N-N-Sm torsion angles of 32.1 and 23.9° respectively.

The greater steric demand of $Tp^{Me,Me}$ relative to other ancillary ligands is evidenced in the smaller dithiocarbamate bite angle (S–Sm–S = 61.31(6)°) and longer Sm–S bond lengths (2.891(2) and 2.873(2) Å) observed for **2.6**, against corresponding angles of 64.1° in $[Sm(Cp^*)_2(S_2CNEt_2)]$, 65.6(1)° in $[\{PhC(NTMS)_2\}_2Yb(S_2CNMe_2)]$ and 59.6(10)° in $[Yb(Cp^*)_2(S_2CNEt_2)]$, and Sm–S distance for $[Sm(Cp^*)_2(S_2CNEt_2)]$ of 2.808(2) Å.

Discussion

The differences between the structures of **2.2**, **2.3**, **2.4** and **2.5** are intriguing. It has previously been shown that the structures of the bis-$Tp^{Me,Me}$ complexes depend quite critically upon the ionic radius of the metal ion, and on the bonding properties and the steric demand of the potential third ligand. Where the third ligand is a particularly poor donor such as the triflate anion, changing the ionic radius of the metal results in expulsion of the ligand from the coordination sphere.[55] On the other hand, the halide complexes of $Sm(Tp^{Me,Me})_2$ are seven coordinate when the halide is small and hard, fluoride and chloride, while the iodide adopts a six-coordinate ion-separated structure.[63]

In the present case the structural differences between the phenoxide and the heavier congeners can be interpreted in two ways, differing in the extent to which the mismatch between hard and soft donors and acceptors contributes to bonding. In the first scenario, it is assumed that the mismatch between hard and soft donors and acceptors plays a significant role in determining structure in these complexes. On the one hand the σ-donor lone pair on the chalcogenolate ligand leads to coordination to the metal. On the other hand, only the harder π-donor oxygen overlaps effectively with the empty samarium 5d orbitals and presumably reduces the Lewis acidity of the metal. Such a π-interaction, with consequent M–O multiple bond character, results in a substantially

shorter and more linear M–O–C bond angle than that expected from a simply σ-bound ligand. In the case of sulfur such π-overlap is much less favourable and this leads to a marked increase in metal-ligand bond length, reflecting not simply the larger size of sulfur but also the reduced bond order in the absence of π bonding, and a much more acute Sm-S-C angle. This trend continues for **2.4** and **2.5**. In comparison with these heavier chalcogenolates, which exhibit significant bending at the chalcogen atom, the aryloxide ligands in **2.1** and **2.2** are considerably more open. (Relevant bond angles and lengths are given in table 2-1). Taken with the shorter than expected Sm–O distance, it is feasible that π-interactions are responsible for this large angle. This interpretation is consistent with the structures of **2.1** and **2.2**, with the steric influence of the methyl substitutent on one of the pyrazolyl groups presumed responsible for the deviation from linearity of the alkoxide. In the case of $[(Sm(Tp^{Me,Me})_2)_2(\mu\text{-}C_{10}H_8O_2)]$ (**2.1**) the angle at oxygen is significantly greater (167.6(8)°) suggesting that bending this angle is quite a soft deformation.

Table 2-1. Selected bond lengths and angles for $[Sm(Tp^{Me2})_2(EPh^{4\text{-}R})$.

E	d(Sm–E)Å	d(E–C)Å	d(Sm–N_{av})Å	Sm-E-C(°)	B-Sm-B(°)
O (**2.1**)	2.138(8)	1.326(14)	2.572(4)	167.6(8)	143
O (**2.2**)	2.159(2)	1.340(3)	2.572(5)	153.7(2)	143
S (**2.3**)	2.827(1)	1.772(3)	2.531(6)	114.6(1)	152.8
Se (**2.4**)	2.9457(3)	1.918(3)	2.5072(4)	108.29(9)	150.1
Te (**2.5**)	3.1874(4)	2.119(5)	2.538(4)	104.83(13)	148.4

It is nevertheless possible that the significantly more open Sm–O–C angle is simply a result of the greater steric congestion in the secondary coordination sphere of the alkoxide compared with the larger thiolate and that any Sm–O π-interaction is insignificant. In this second interpretation it is argued that the bond angle pattern in the chalcogenolates merely mirrors that observed for the chalcogen hydrides H_2E, [H_2O

(104.5°), H_2S (92.2°), H_2Se (91.0°), H_2Te (89.5°)] where no π-bonding is possible. Parkin has argued this to be the case for the series $Zr(Cp^*)_2(EPh)_2$ (E = O, S, Se, Te) where an anomalously short Zr–O bond (*ca.* 0.17 Å shorter than the sum of the covalent bond radii for zirconium and oxygen) was noted, together with a Zr–O–C angle of 172.7(2)°, compared to 119.0(1)° for the corresponding thiolate.[64] The magnitude of the difference in angle on exchanging O for S, however, suggests that other factors are strongly influential. The most plausible explananation is that suggested by Parkin, namely that repulsive steric interactions in the second coordination sphere of the metal between the chalcogenolate phenyl substituent and the ancillary ligands are much greater where the chalcogen is oxygen (and, therefore, the phenyl ring held much closer to the ancillaries) than with the larger group 16 elements. The short Zr–O distance in $Zr(Cp^*)_2(OPh)_2$ is attributed to a stronger ionic interaction between the metal and oxygen than the other chalcogens, *i.e.* to a greater degree of polarisation of the metal–oxygen bond, $Zr^{\delta+}$–$O^{\delta-}$.

By comparison with other samarium alkoxides the observed metal–oxygen distances and Sm–O–C angles observed in **2.1** and **2.2** are quite typical. In addition, they conform to the pattern noted for transition metal alkoxides and aryloxides; namely that short M–O and, to a lesser extent, short O–C distances are often coupled with large M–O–C angles.[48] (Some relevant M–O bond lengths and M-C-O angles for lanthanide and early transition metal complexes are given in table 2.2 for comparison). Without preparing a series of directly comparable alkoxide complexes, however, differing only in the steric bulk of either the ancillaries or the oxygen substituent, it is not possible to state definitively which of the above conjectures paints the more accurate picture. It is, however, probable that steric effects play the more influential rôle in determining structure.

It appears that the less efficient satisfying of the metal centre's Lewis acidity by the softer atoms is compensated by a reduction in the metal-nitrogen distances in the ancillary $Tp^{Me,Me}$ ligands. We presume that in the selenolate **2.4** a closer approach of the pyrazolylborate is not possible, in part due to the larger size of the chalcogen itself.

The result is that the pyrazolylborate ligand collapses inwards towards the metal and assumes the distorted arrangement seen here. The fact that the distortion is far smaller for **2.5** would, however, suggest that crystal packing forces and in particular the apparent π-stacking interactions noted above between two of the pyrazolyl rings and the selenium atom and the phenyl ring respectively may play a significant role in stabilizing the unusual structure in **2.4**. Furthermore, a C_1 symmetric structure is not observed in solution, suggesting that crystal packing forces are responsible for the magnitude of the distortion in the solid state. The fact that the shortest metal-nitrogen distances are observed in the selenolate is consistent with the better resolved low temperature ^1H NMR spectrum observed for **2.4**. This is indicative of the greater steric constraints in the more crowded second coordination sphere of the selenolate which more effectively "locks" the fluxionality of the pyrazolylborate ligands in **2.4** than in **2.2**, **2.3** and **2.5**. The longer metal-nitrogen distances in **2.5**, approaching those observed in **2.2**, presumably occur because the large size of the tellurium atom prevents a closer approach of the ancillary pyrazolylborate ligands.

The distortion of the pyrazolylborate in **2.4** is intriguing in view of the many examples of pyrazolylborate fragmentation that have been reported anecdotally. The present distortion may represent a step along the trajectory towards B–N cleavage.[65] Several examples of minor twisting of the pyrazolyl groups have been noted previously.[60] In addition the selenolate appears to be significantly more air sensitive than either the phenoxides or the thiolate and indeed fragmented products have been isolated during attempts to crystallize the complex.[59]

A further point of interest in the solid state structures of these terminal chalcogenolates is that the deviation from planarity of the equatorial plane of the pentagonal bipyramid is almost entirely due to the accommodation of the chalcogen atom. In the case of the tellurolate, in particular, the mean deviation of the N1N3N7N11 plane is neglible (0.0023 Å), increasing to 0.2847 Å upon inclusion of the tellurium atom. This effect is most pronounced in the selenolate and is considerably less important in the

anthraquinone complex. Table 2-3 describes the environment at samarium with regard to the pyrazolylborate ligands in more detail.

Table 2-2. Sm–O bond lengths and Sm-O-C bond angles in samarium alkoxides.

^{a}Ar = 2,6-$Pr^{i}_{2}C_{6}H_{3}$); ^{b}r(Ti^{4+}) = 0.69 Å ; ^{c}r(Zr^{4+}) = 0.87 Å.

Complex	d(M–O) Å	M-Ô-C (°)
2.1	2.138(8)	167.6(8)
2.2[44]	2.159(2)	153.7(2)
$Sm(Tp^{Me,Me})_2(OC_6H_2(^tBu)_2\text{-}O)$[39]	2.213	154.5
$[Sm(Tp^{Me,Me})_2]_2(\mu\text{-}O_2C_6H_4)$[45]		
$Cp^*_2Sm(O\text{-}2,3,5,6\text{-}Me_4C_6H)$[48]	2.13(1)	172.3(13)
$[Cp^*_2Sm]_2(O_2C_{16}H_{10})$[48]	2.08(2)	
$[Cp^*_2Sm]_2(O_2C_{16}H_{10})(THF)$[49]	2.099(9)	
$\{Sm(\mu\text{-}O\text{-}\eta^6\text{-}Ar)(OAr)_2\}$[a] 50	2.101(6)	
$[TiCl_2(OPh)_2]_2$[b] 51	1.74(1)	165.9(6)
$[Ti(OPh)_4]_2.2PhOH$[52]	1.789, 1.842, 2.200	175, 169, 132
$Cp^*_2Zr(OPh)_2$[c] 64	1.989(3)	172.7(2)
$Cp_2Zr(OPh)_2$ 64	2.01(1)	147(1)

Table 2-3a Metrical data concerning the pentagonal bipyramidal structure at samarium.

$^{d}N_{ax}$ = axial nitrogen of pentagonal bipyramid; $^{e}N_{front}$ = nitrogen atom adjacent to chalcogen in equatorial plane.

	N_{ax}-Sm-N_{ax}(°)[d]	N_{front}-Sm-N_{front}(°)	d(N_{front}–N_{front})Å[e]
2.1	157.3	147.1	5.030
2.2	153.3	144.3	4.985
2.3	150.1	140.9	4.765
2.4	150.9	142.5	4.918
2.5	151.5	142.8	4.861

Table 2-3b Metrical data concerning the equatorial plane of the pentagonal bipyramidal structure at samarium in complexes 2.1 - 2.5.

Complex	Mean deviation from N_4 plane (Å)	Mean deviation from N_4E plane (Å)	Angle of NNE plane to N_4 plane (°)
2.1	0.1328	0.1343	12.3
2.2	0.1031	0.2239	31.1
2.3	0.085	0.2502	22.8
2.4	0.0919	0.3502	35.6
2.5	0.0023	0.2847	27.8

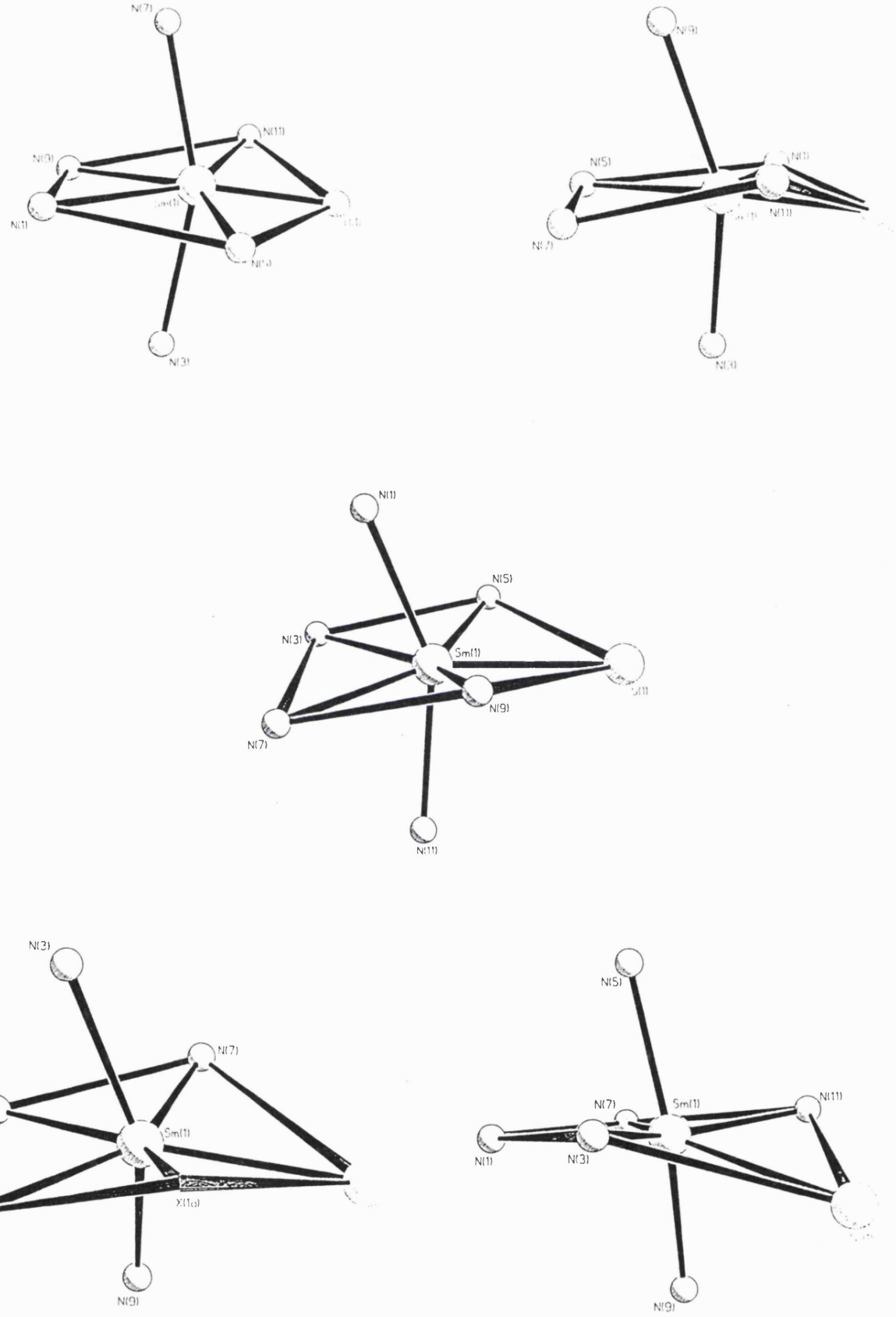

Figure 2.6 Pentagonal bipyramidal coordination geometry in 2.1 - 2.5

The NMR spectra of the seven-coordinate $[Sm(Tp^{Me,Me})_2]^+$ system have hitherto been consistently uninformative with regards to the coordination sphere and have failed to give any hint of the kinds of structural equilibria taking place.[55] In the case of the selenolate the distortion is such that such fluxionality can be frozen out, although only a C_2 symmetric species has been observed, in contrast to the crystallographic evidence. In contrast the presence of bidentate ligands in the eight-coordinate complexes of samarium with the $(Tp^{Me,Me})$ ligand appears to lock the coordination sphere and frozen out spectra of C_2 or C_1 symmetry are observed at room temperature. This is in contrast to complexes of the type $(Tp^{Me,Me})_2LnL_2$ (L = unidentate) which are fluxional at all accessible temperatures.[60] The 7-coordinate complex **2.1** is unusual in that C_2-symmetry is observed at room temperature. This is credited to the bulky anthraquinone unit and the dimeric structure of the complex. Detailed simulation of the spectra for these fluxional processes is not possible owing to the paramagnetism of the samarium (III) centre.

Preparation of $[Sm(Tp^{Me,Me})_2](TePh)_3$ 2.7

During several attempts to crystallise **2.5** dark red crystals of $[Sm(Tp^{Me,Me})_2](TePh)_3$, **2.7**, were obtained.[44] The formation of the $(TePh)_3^-$ anion was unexpected and is likely to have resulted from a small amount of oxygen leaking into the schlenk flask as the compound was being crystallized. This would result in oxidation of a small amount of $PhTe^-$ to diphenylditelluride which then coordinates a further $PhTe^-$ unit. In fact, complex **2.7** has now been prepared directly by reaction of $Sm(Tp^{Me,Me})_2$ with 1.5 equivalents of diphenylditelluride in toluene and isolated as dark red microcrystals in good yield.

$$[Sm(Tp^{Me,Me})_2] + {}^3/_2\,PhTeTePh \rightarrow [Sm(Tp^{Me,Me})_2](TePh)_3$$

The chemistry of tellurium is an intriguing area for solid state chemists because of the wealth of structural types arising from subtle changes in bonding and connectivity. Numerous and unexpected examples of structures not easily rationalized by simple

models of bonding have come to light in recent years.[66,67] Considerable effort has been devoted to developing rational syntheses of such polytellurides starting from smaller building blocks. Tritelluride units are a recurring motif in this chemistry, among them the classic Zintl ion Te_3^{2-} first isolated by Corbett.[68] Numerous attempts have been made to relate such hypervalent structures to those of the polyhalides, in particular to I_3^-, although the direct analogue, the Te_3^{4-} ion has remained elusive.[69,70] A cluster containing the linear selenium analogue Se_3^{4-} has recently been reported.[6] The synthesis of a formal, but cationic, triiodide analogue, pentamesityl tritellurium, was reported recently by addition of a Te_1 cation to a Te_2 unit.[71] Complex **2.7** may be regarded as the corresponding direct *anionic* analogue of triiodide.

X-ray strucure of 2.7[44]

The $[Te_3Ph_3]^-$ anion is virtually linear (∠Te-Te-Te = 174.57(8)°). This is in contrast to the diorganyltritellurides which show significant bending at the central tellurium (100-103°)[72,73] and the recently reported $[Mes_2TeTe(Mes)Te(Mes)_2]^+$ cation which, with a bend angle of 159.51(3)°, is reported as being "almost linear".[71] The anion of **2.7** is unsymmetrical with Te-Te distances of 2.929(3) and 3.101(3) Å respectively. Both distances are significantly longer than in singly bonded materials such as organoditellurides (typically of the order of 2.69-2.75 Å),[74-78], in the Te_2^{2-} bridging group in $[(SmCp^*_2)_2(\mu\text{-}Te_2)]$ 2.773(1) Å[6] or in the tritellurides $((Me_3Si)_3Si)_2Te_3$ 2.710(1) Å[72] and $(2\text{-}pyrPh)_2Te_3$ (2.776(1) Å)[73], the crown-shaped Te_8 rings of Cs_3Te_{22} (2.80(2) Å),[79] and in elemental tellurium itself (2.8345(8) Å).[80][Adenis, 1989 #25] Rather, the distances are comparable to those observed in the pentamesitylditellurium cation 3.0491(10) and 2.9791(10) Å[71], and to the linear polyiodide analogue Te_5^{4-} ion found in NaTe (2.82-3.08 Å).[81] They fall between the two sets of distances observed in the tridentate, chelating Te_7^{4-} anion which is reported to possess a linear (*ca.*174°) Te_3 unit. This unit is asymmetrical in $AgTe_7^{3-}$ (Te–Te 2.866(2) and 3.230(2) Å) and almost symmetrical in $HgTe_7^{2-}$ (Te–Te 2.997(2) and

3.050(2)Å).[82] A similarly long Te-Te distance is also found in the bridging intact ditelluride complex $[Ru_2(\eta\text{-}C_5Me_5)_2(\mu\text{-}TePh)_2(\mu\text{-}PhTeTePh)]$ (2.901(3) pm).[83]

The phenyl groups lie in the typical cisoid conformation across the short Te-Te bond and in a transoid conformation across the longer Te-Te bond. The C31-Te1-Te2-C37 torsion angle of 63.6° is smaller than those commonly found in organic tellurides for which the typical range is 72.4 - 92.2°.

Preparation of $[Sm(Tp^{Me,Me})_2]I_3$, 2.8

The asymmetry of the ion $(TePh)_3^-$, suggesting a neutral diphenyl ditelluride unit bound to a phenyltellurolate anion, is reminiscent of the triiodide ion which has been isolated in both symmetrical[84] and unsymmetrical structures.[85] depending upon the counter-cation. The analogy is further supported by the fact that we have been able to prepare the corresponding triiodide by reaction of $[Tp^{Me,Me}{}_2Sm]$ with excess iodine in toluene. Thus, a red-brown complex of stoichiometry $[Sm(Tp^{Me,Me})_2][I_3]$ (**2.8**) has been prepared by stirring 1.5 equivalents of iodine with $[Sm(Tp^{Me,Me})_2]$.

$$[Sm(Tp^{Me,Me})_2] + {}^3/_2\, I_2 \rightarrow [Sm(Tp^{Me,Me})_2]I_3$$

This product has been characterised by IR, ^1H and ^{13}C NMR spectroscopy and by elemental microanalysis and is further discussed in Chapter 4. No crystallographic data have yet been collected so it is not known whether the I_3 anion is symmetrical or unsymmetrical. By analogy with the tritelluride anion, given that the nature of the counterion bears a strong influence on the mode of crystallisation the asymmetrical triiodide is expected.

Low temperature NMR spectroscopy

The ^1H NMR spectrum of **2.7** consisted of three singlets in the ratio of 3:3:1 plus three peaks assigned to the phenyl groups of the tritelluride unit. The chemical shifts of the latter peaks were normal, apparently unaffected by the paramagnetic samarium centre. In addition the ^1H and ^{13}C NMR spectra were found to be temperature invariant, consistent with a symmetrical and non-fluxional samarium coordination sphere. These

consistent with a symmetrical and non-fluxional samarium coordination sphere. These observations are consistent with the salt-like structure containing a six-coordinate metal coordination sphere and correlate with the spectra observed for **2.8**. The absence of significant shifting of the peaks due to the phenyl groups in the ^{1}H NMR spectrum of **2.7** at low temperature suggests that complexes **2.5** and **2.7** are not in equlibrium *via* dissociation of diphenylditelluride in toluene solution.

The ^{125}Te NMR spectrum of **2.7** at room temperature (figure 2.7) consists of a single peak at 415 ppm, very similar to the chemical shift of diphenylditelluride (422 ppm), presumably indicating rapid exchange between the central and terminal environments. Although a considerable temperature dependence of the chemical shift was observed no broadening of the signal was observed down to -80 °C in toluene suggesting that the chemical shift difference between the central and terminal environments is quite small. The poor solubility in toluene-d_8 and freon solvents at temperature below -80°C has precluded further low temperature NMR experiments.

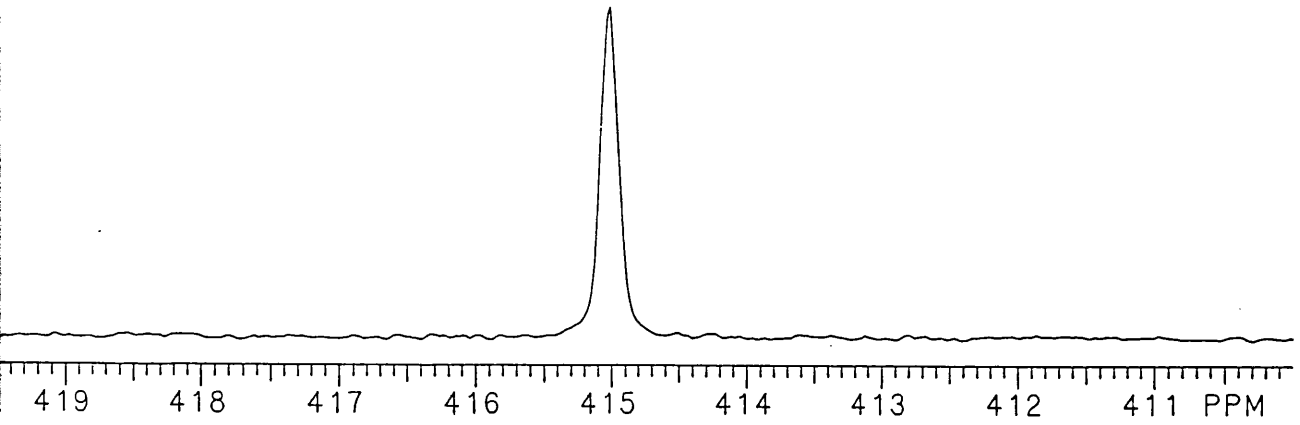

Figure 2.7. ^{125}Te NMR spectrum of 2.7 (298K)

Given the amount of effort concentrated in this field it is quite suprising that the $(TePh)_3^-$ anion should not have been reported previously since it appears so simple to prepare in high yield. It is noteworthy that many of the tritelluride ions reported are supported either within a polymeric or Zintl ion framework or as bridging (μ-Te_3) ligands. Presumably in this case it is stabilized in the solid state by the presence of the large $[(Tp^{Me,Me})_2Sm]^+$ cation.

Conclusions

In this chapter the syntheses of the sandwich complexes $[Sm(Tp^{Me,Me})_2]_2O_2C_{14}H_8$ (**2.1**), $[Sm(Tp^{Me,Me})_2EAr]$ (EAr = SPh^{Me} (**2.3**), $SePh^{t\text{-}Bu}$ (**2.4**), TePh (**2.5**)) and $[Sm(Tp^{Me,Me})_2S_2CNEt_2]$ (**2.6**) have been described and their X-ray structures presented. Complexes **2.1** to **2.5** represent a series of bis(pyrazolylborate)samarium complexes with terminal chalcogenolate ligands possessing consistent coordination sphere, permitting comparison of the effects on the metal coordination environment of varying the size and donating ability of the chalcogen. The influence of the chalcogenolate aryl substituent on the structure, in the form of secondary interactions with the pyrazolylborate ancillary ligands, has also been noted. In the case of **2.4**, these two factors contribute to the severe distortion of one of the pyrazolylborate groups in the solid state, which may represent a step along the pathway to B–N bond cleavage as observed in the hydrolysis product **4.5**. Variable temperature ^{1}H NMR spectroscopy on **2.3** - **2.5** showed that these complexes were fluxional in solution at room temperature and exhibited spectra consistent with C_2 symmetric structures at low temperature. In contrast the 8-coordinate complexes **2.1** and **2.6** displayed ^{1}H NMR spectra consistent with C_2 symmetry at room temperature and were fluxional on warming, although no high temperature limiting spectra were reached.

Further characterisation data have also been obtained on $[Sm(Tp^{Me,Me})_2](TePh)_3$ (**2.7**). Variable temperature ^{13}C and ^{125}Te NMR spectroscopy was carried out, but the insolubility of the compound at low temperature prevented observation below –80°C.

Chapter 2 - References

1) Berardini, M.; Lee, J.; Freedman, D.; Lee, J.; Emge, T. J.; Brennan, J. G. *Inorg. Chem.* **1997**, *36*, 5772.

2) Lee, J.; Brewer, M.; Berardini, M.; Brennan, J. G. *Inorg. Chem.* **1995**, *34*, 3215.

3) Strzelecki, A.; Liker, C.; Helsel, B.; Utz, T.; Lin, M.; Bianconi, P. *Inorg. Chem.* **1994**, *33*, 5188.

4) Lee, J.; Freedman, D.; J. H, M.; Brewer, M.; Sun, L.; Emge, T. J.; Long, F. H.; Brennan, J. G. *Inorg. Chem.* **1998**, *37*, 2512.

5) Nolan, S. P.; Stern, D.; Marks, T., J. *J. Am. Chem. Soc.* **1989**, *111*, 7845.

6) Evans, W. J.; Rabe, G. W.; Ziller, J. W.; Doedens, R. J. *Inorg. Chem.* **1994**, *33*, 2719.

7) Evans, W. J.; Gonzales, S. L.; Ziller, J. W. *J. Am. Chem. Soc.* **1991**, *113*, 9880.

8) Evans, W. J.; Gonzales, S. L.; Ziller, J. W. *J. Chem. Soc., Chem. Commun.* **1992**, 1138.

9) Evans, W. J.; Rabe, G. W.; Ansari, M. A.; Ziller, J. W. *Angew. Chem. Int. Ed. Engl.* **1994**, *33*, 2110.

10) Mashima, K.; Nakayama, Y.; Shibahara, T.; Fukumoto, H.; Nakamura, A. *Inorg. Chem.* **1996**, *35*, 93.

11) Cetinkaya, B.; Hitchcock, P. B.; Lappert, M. F.; Smith, R. G. *J. Chem. Soc., Chem. Commun.* **1992**, 932.

12) Recknagel, A.; Noltemeyer, M.; Stalke, D.; Pieper, U.; Schmidt, H.-G.; Edelmann, F. T. *J. Organomet. Chem.* **1991**, *411*, 347.

13) Zalkin, A.; Henly, T. J.; Andersen, R. A. *Acta Crystallogr.* **1987**, *C43*, 233.

14) Berg, D. J.; Andersen, R. A.; Zalkin, A. *Organometallics* **1988**, *7*, 1858.

15) Aspinall, H. C.; Bradley, D. C.; Hursthouse, M. B.; Sales, K. D.; Walker, N. P. C. *J. Chem. Soc., Chem. Commun.*, **1985**, 1585.

16) Tatsumi, K.; Amemiya, T.; Kawaguchi, H.; Tani, K. *J. Chem. Soc., Chem. Commun.* **1993**, 773.

17) Berardini, M.; Emge, T. J.; Brennan, J. G. *J. Chem. Soc., Chem. Commun.* **1993**, 1537.

18) Strzelecki, A.; Timinski, P. A.; Helsel, B.; Bianconi, P. *J. Am. Chem. Soc.* **1992**, *114*, 3159.

19) Khasnis, D. V.; Brewer, M.; Lee, J.; Emge, T. J.; Brennan, J. G. *J. Am. Chem. Soc.* **1994**, *116*, 7129.

20) Cary, D. R.; Arnold, J. *Inorg. Chem.* **1994**, *33*, 1791.

21) Christou, V.; Arnold, J. *J. Am. Chem. Soc.* **1992**, *114*, 6240.

22) Bochmann, M.; Webb, K. J. *J. Chem. Soc. Dalton Trans.* **1991**, 2325.

23) Bochmann, M.; Webb, K. J.; Hursthouse, M. B.; Mazid, M. *J. Chem. Soc., Dalton Trans.* **1991**, 2317.

24) Leverd, P. C.; Lance, M.; Vigner, J.; Nierlich, M.; Ephritikhine, M. *J. Chem. Soc., Dalton Trans.* **1995**, 237.

25) Leverd, P. C.; Arliguie, T.; Ephritikhine, M.; Nierlich, M.; Lance, M.; Vigner, J. *New J. Chem.* **1993**, *17*, 769.

26) Schumann, H.; Albrecht, I.; Hahn, E. *Angew. Chem. Int. Edn. Engl.* **1985**, *24*, 985.

27) Brewer, M.; Khasnis, D.; Buretea, M.; Berardini, M.; Emge, T. J.; Brennan, J. G. *Inorg. Chem.* **1994**, *33*, 2743.

28) Mashima, K.; Nakayama, Y.; Fukumoto, H.; Kanehisa, N.; Kai, Y.; Nakamura, A. *J. Chem. Soc., Chem. Commun.* **1994**, 2523.

29) Berardini, M.; Brennan, J. G. *Inorg. Chem.* **1995**, *34*, 6179.

30) Berardini, M.; Emge, T. J.; Brennan, J. G. *Inorg. Chem.* **1995**, *34*, 5327.

31) Brewer, M.; Lee, J.; Brennan, J. G. *Inorg. Chem.* **1995**, *34*, 5919.

32) Mashima, K.; Nakayama, Y.; Nakamura, A.; Kanehisa, N.; Kai, Y.; Takaya, H. *J. Organomet. Chem.* **1994**, *473*, 85.

33) Mashima, K.; Nakayama, Y.; Kanehisa, N.; Kai, Y.; Nakamura, A. *J. Chem. Soc., Chem. Commun.* **1993**, 1847.

34) Wedler, M.; Noltemeyer, N.; Pieper, U.; Schmidt, H.-G.; Stalke, D.; Edelmann, F. T. *Ang. Chem. Int. Ed. Engl.* **1990**, *29*, 894.

35) Edelmann, F. T.; Rieckhoff, M.; Haiduc, I.; Silaghi-Dumitrescu, I. *J. Organomet. Chem.* **1993**, *447*, 203.

36) Wedler, M.; Recknagel, A.; Gilje, J. W.; Noltemeyer, N.; Edelmann, F. T. *J. Organomet. Chem.* **1992**, *426*, 295.

37) Hou, Z. M.; Fujita, A.; Zhang, Y.; Miyano, T.; Yamazaki, H.; Wakatsuki, Y. *J. Am. Chem. Soc.* **1998**, *120*, 754.

38) Hou, Z.; Yamazaki, H.; Fujiwara, Y.; Taniguchi, H. *Organometallics* **1992**, *11*, 2711.

39) Takats, J., *personal communication.*

40) Greenwood, N. N.; Earnshaw, A. *Chemistry of the Elements*; Pergamon: Oxford, 1986, p.1497.

41) Beletskaya, I. P.; Voskoboynikov, A. Z.; Shestakova, A. K.; Schumann, H. *J. Organomet. Chem.* **1993**, *463*, C1.

42) Piers, W. E.; MacGillivray, L. R.; Zaworotko, M. *Organometallics* **1993**, *12*, 4723.

43) Piers, W. E. *J. Chem. Soc., Chem. Commun.* **1994**, 304.

44) Liu, S.-Y. *PhD thesis*; University of London, 1996.

45) Marques, N., *Personal Communication.*

46) Drew, M. G. B. *Prog. Inorg. Chem.* **1977**, *23*, 67.

47) Liu, S. Y.; Maunder, G. H.; Day, V. W.; Sella, A.; Takats, J.; Marques, N.; Santos, I. *manuscript in preparation.*

48) Evans, W. J.; Hanusa, T. P.; Levan, K. R. *Inorg. Chim. Acta* **1985**, *110*, 191.

49) Evans, W. J.; Drummond, D. K.; Hughes, L. A.; Zhang, H.; Atwood, J. L. *Polyhedron* **1988**, *7*, 1693.

50) Barnhart, D. M.; Clark, D. L.; Gordon, J. C.; Huffman, J. C.; Vincent, R. L.; Watkin, J. G.; Zwick, B. D. *Inorg. Chem.* **1994**, *33*, 3487.

51) Watenpaugh, K.; Caughlan, C. N. *Inorg. Chem.* **1966**, *5*, 1782.

52) Sretich, G. W.; Voge, A. A. *J. Chem. Soc., Chem. Commun.* **1971**, 676.

53) Hou, Z.; Yamazaki, H.; Kobayashi, K.; Fukiwara, Y.; Taniguchi, H. *J. Chem. Soc., Chem. Commun.* **1992**, 722.

54) Beletskaya, I. P.; Voskoboynikov, A. Z.; Shestakova, A. K.; Yanovsky, A. I.; Fukin, G. K.; Zacharov, L. N.; Struchkov, Y. T.; Schumann, H. *J. Organomet. Chem.* **1994**, *468*, 121.

55) Liu, S.-Y.; Maunder, G. H.; Sella, A.; Stephenson, M.; Tocher, D. A. *Inorg. Chem.* **1996**, *35*, 76.

56) Emsley, J. *The Elements*; Oxford University Press: Oxford, 1989.

57) Shannon, R. D. *Acta Cryst.* **1976**, *A32*, 751.

58) Sun, Y. M.; McDonald, R.; Takats, J.; Day, V. W.; Eberspacher, T. A. *Inorg. Chem.* **1994**, *33*, 4433.

59) Liu, S. Y.; Sella, A.; Elsegood, M. R. J., *unpublished results* .

60) Clark, R. J. H.; Liu, S. Y.; Maunder, G. H.; Sella, A.; Elsegood, M. R. J. *J. Chem. Soc., Dalton Trans.* **1997**, 2241.

61) Takats, J.; Zhang, X. W.; Day, V. W.; Eberspacher, T. A. *Organometallics* **1993**, *12*, 4286.

62) Zhang, X. W.; Loppnow, G. R.; McDonald, R.; Takats, J. *J. Amer. Chem. Soc.* **1995**, *117*, 7828.

63) Maunder, G.; Sella, A.; Takats, J.; Zhang, X. *unpublished results.*

64) Howard, W. A.; Trnka, T. M.; Parkin, G. *Inorg. Chem.* **1995**, *34*, 5900.

65) Day, V.; Liu, S.; Sella, A. , *unpublished results.*

66) Bottcher, P. *Angew. Chem., Intl. Ed. Engl.* **1988**, *27*, 759.

67) Ansari, M. A.; Ibers, J. A. *Coord. Chem. Rev.* **1990**, *100*, 223.

68) Cisar, A.; Corbett, J. D. *Inorg. Chem.* **1977**, *16*, 623.

69) Kanatzidis, M. G. *Angew. Chem., Intl. Ed. Engl.* **1995**, *34*, 2109.

70) Liu, Q.; Goldberg, N.; Hoffmann, R. *Chem. Eur. J.* **1996**, *2*, 390.

71) Jeske, J.; du Mont, W.-W.; Jones, P. G. *Angew. Chem. Int. Ed. Engl.* **1997**, *36*, 2219.

72) Sladky, F.; Bildstein, B.; Rieke, C.; Gieren, A.; Betz, H.; Hübner, T. *J. Chem. Soc., Chem. Commun.* **1985**, 1800.

73) Hamor, T. A.; AlSalim, N.; West, A. A.; McWhinnie, W. R. *J. Organomet. Chem.* **1986**, *310*, C5.

74) Llabres, G.; Dideberg, O.; Dupont, L. *Acta Cryst., B* **1972**, *28*, 2438.

75) Spirlet, M. R.; Van de Bossche, G.; Dideberg, O.; Dupont, L. *Acta Cryst., B* **1979**, *35*, 1727.

76) Becker, J.; Bernstein, J.; Dayan, M.; Shahal, L. *J. Chem. Soc., Chem. Commun.* **1992**, 1048.

77) Sandman, D. J.; Li, L.; Tripathy, S.; Starck, J. C.; Acampora, L. A.; Foxman, B. M. *Organometallics* **1994**, *13*, 348.

78) Edelmann, A.; Brooker, S.; Bertel, N.; Noltemeyer, M.; Roesky, H. W.; Sheldrick, G. M.; Edelmann, F. T. *Z. Naturf. B* **1992**, *47*, 305.

79) Sheldrick, W. S.; Wachhold, M. *Angew. Chem., Intl. Ed. Engl.* **1995**, *34*, 450.

80) Cherin, P.; Unger, P. *Acta. Cryst.* **1967**, *23*, 670.

81) Böttcher, P.; Keller, R. *J. Less Common Met.* **1985**, *109*, 311.

82) McConnachie, J. M.; Anari, M. A.; Bollinger, J. C.; Salm, R. J.; Ibers, J. A. *Inorg. Chem.* **1993**, *32*, 3201.

83) Matsuzaka, H.; Ogino, T.; Nishio, M.; Noshibashi, Y. A.; Uemura, S.; Hidai, M. *J. Chem. Soc.,Chem. Commun.* **1994**, 223.

84) Mooney-Slater, R. C. *Acta Cryst. B* **1959**, *12*, 187.

85) Tasmin, H. A.; Bozwijk, K. H. *Acta. Cryst.* **1955**, *8*, 59.

Chapter 3 - The reactivity of (pyrazolylborate)lanthanide complexes with transition metal carbonyls

Introduction

Transition metal carbonyl complexes and related clusters are ubiquitous in organometallic chemistry, many containing metal-metal bonds, both direct and carbonyl-bridged. Over recent years there has been much interest in the study of metal carbonyl complexes, with particular emphasis on activation of the C–O bond.[1-3] One reason for this interest arises from the potential of transition metal carbonyl complexes and their derivatives as homogeneous catalysts for industrially important processes. Of particular interest are heterometallic complexes which exhibit catalytic activity in the Fischer-Tropsch and related syn-gas processes.

Fischer-Tropsch Chemistry

Heterogeneous Catalysis

The Fischer-Tropsch (FT) reaction converts synthesis gas ($CO + H_2$) to a mixture of long chain hydrocarbons and alcohols. It allows for the use of coal as a source of liquid or gaseous fuel or chemical feedstock.

$$H_2 + CO \rightarrow CH_3(CH_2)_nCH_3 + CH_3(CH_2)_nOH + CH_3(CH_2)_nCH{=}CH_2 + H_2O$$

This process is catalysed heterogeneously on an industrial scale. The alkali-iron catalysed reaction was discovered in 1923 - 1925 by Fischer and Tropsch and the first commercial plant opened in Germany in 1936. The cobalt-catalysed process utilised in this plant satisfied to a substantial extent Germany's wartime liquid hydrocarbon fuel requirements. From 1957 South Africa operated a large iron catalysed coal-based FT plant (SASOL). The economics of producing liquid hydrocarbon fuels or chemical feedstock from synthesis gas are unfavourable (with the exception of ethylene glycol)

except when petroleum prices are prohibitively high or out of political necessity. The petroleum embargo in the early 1970s resulted in sufficiently high prices for the FT process to become commercially viable and extensive research effort was expended on this and related processes.

The most likely mechanism of the heterogeneously catalysed process is believed to involve dissociative chemisorption of CO onto the solid surface of the catalyst to give surface carbides which are hydrogenated by H_2 to afford carbene fragments. A surface hydride then inserts CH_2 to form a methyl group, which then inserts CH_2 again in the chain-propagation step. A lack of product selectivity and an inability to control the propagation step are drawbacks of the FT reaction. In addition a substantial quantity of the carbon content of coal is lost as CO_2 in forming H_2 *via* the water-gas shift reaction (*vide infra*), with approximately 4 tonnes of coal required to produce 1 tonne of liquid fuel.

Homogeneous Catalysis

The scope for homogeneous analogues to effect such conversions with higher selectivity has focused much effort into identifying effective homogeneous Fischer-Tropsch type catalysts. The major requirements for a potential such catalytic system are that it possess a reducible carbonyl ligand and that it be able to effect carbon-carbon coupling.

The direct formation of alkanes from reaction of metal carbonyls with reducing agents generally affords only low yields of hydrocarbons. The use of $Os_3(CO)_{12}$ or $Ir_4(CO)_{12}$ as homogeneous catalyst, for example, results in only 10 - 15% conversion to methane after 5 days at 180°C. $Rh_{12}(CO)_{34}$ gives similarly poor yields.

$$Os_3(CO)_{12} \text{ or } Ir_4(CO)_{12} + CO/H_2 \rightarrow CH_4$$

On addition of a Lewis acid such as $AlCl_3$ to the system, however, the yield and rate of alkane formation are greatly increased.

$$Ir_4(CO)_{12} \xrightarrow[\substack{NaCl/AlCl_3 \text{ melt} \\ 170\text{-}180^\circ C}]{CO/H_2,\ 1\ atm} \text{C1 to C8 saturated hydrocarbons}$$

The coordination of the strongly Lewis acidic aluminium to the oxygen of a carbonyl group reduces the bond order of the CO ligand and activates it towards reduction. The promotion by Lewis acids of carbon-carbon bond formation, for example in the preparation of acyl complexes *via* migratory insertion into a M–C bond and reduction of CO is well known.[4-6]

It is thought that in the course of catalytic hydrogenation of CO, very small, undetectable quantities of formyl complexes form and are transformed into formaldehyde by subsequent reduction.[3] While there are numerous examples of metal formyls in the literature, the majority are prepared by reaction of metal carbonyl with a hydride source.[7] Although migratory insertion of CO into the M–C bond of a coordinated alkyl group is well known as a synthetic route, the equivalent reaction involving a M–H bond has only been observed in a very limited number of cases. This can be explained by reference to the M–H bond dissociation energy which is sufficiently high to suggest that insertion to form a formyl complex should be thermodynamically uphill.[3,8] This is borne out experimentally, with only one example of a transition metal formyl complex having been prepared by carbonylation of metal hydride, in a binuclear tantalum hydride complex.[9] Many transition metal formyls are thermodynamically unstable with respect to transition metal hydride and CO.[7]

On the other hand some special cases are known. The rhodium porphyrin hydride Rh(OEP)(H) inserts carbon monoxide in the presence of $[Rh(OEP)]_2$ in a free radical chain process to afford Rh(OEP)(CHO) (figure 3.1).[3]

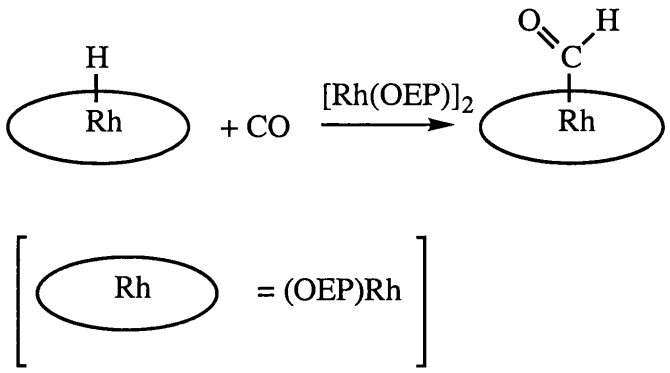

Figure 3.1. Insertion of CO into Rh–H bond.

Organoactinide hydrides can give formyls via CO insertion (figure 3.2).[3,10]

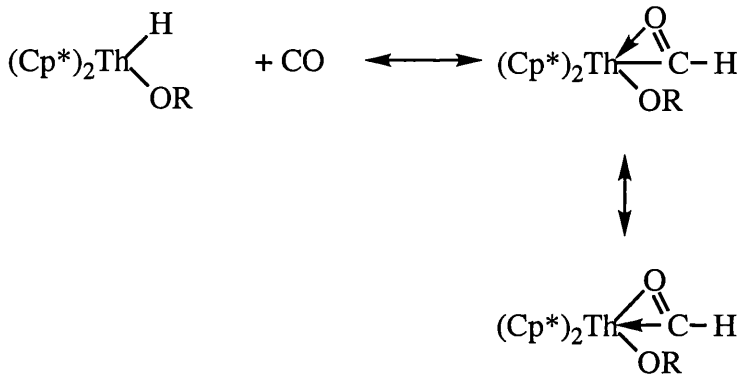

Figure 3.2. Intramolecular CO to formyl conversion.

To date, although there is still no commercially effective homogeneous catalyst for the FT process, work on such systems has afforded many insights into the Fischer-Tropsch reaction mechanism, through the isolation of potential intermediates.

Water-Gas Shift Chemistry

The water-gas shift (WGS) reaction alters the ratio of CO to H_2 in synthesis gas:

$$H_2O + CO \leftrightarrow H_2 + CO_2 \qquad \Delta H = -42 kJmol^{-1}$$

The reaction is industrially important, providing a means by which the H_2 content of synthesis gas can be enhanced, exploiting the reducing power of carbon monoxide to

produce H_2 from H_2O under mild conditions. It also allows for the removal of CO from "mixed gas" (50% N_2, 30% CO, 15% H_2, 5% CO_2) for the Haber-Bosch process.

The reaction is catalysed heterogeneously by Cr_2O_3, Fe_3O_4 or Cu/ZnO at temperatures greater than 200°C. The relatively high temperature required by these catalysts is, however, unfavourable for the position of the equilibrium. The development of homogeneous catalysts which might more effectively affect the equilibrium is of great interest. Among the homogeneous catalysts that have been studied are $Fe(CO)_5$[11], $Ru_3(CO)_{12}$, $[Rh(CO)_2I]^-$ and $Pt(PPr^i_3)_3$.[12]

The proposed mechanism for the homogeneous metal carbonyl WGS catalytic system involving known reaction types is shown in figure 3.3. A metal-bound CO ligand is activated towards nucleophilic attack by an OH^- ion at the carbon atom to form an unstable carbohydroxy complex which decarboxylates to give a metal hydride. The mechanism of decarboxylation is complicated, involving either one of two paths. A coordinatively unsaturated metallacarboxylic acid, MCO_2H, can lose CO_2 in a process analogous to β-hydride elimination. Alternatively, the anionic form, MCO_2^-, loses CO_2 to give a metal anion which then combines with a proton.

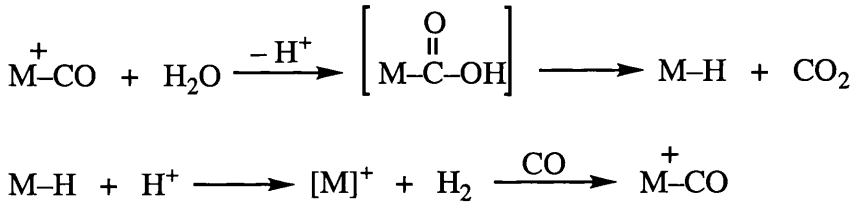

Figure 3.3 Mechanism of homogeneously catalysed WGS reaction.

The platinum alkyl catalyst is sufficiently basic to deprotonate water, thereby generating an OH^- anion, so no added base is required.

There is some evidence that other intermediates, such as the formate anion, could play a role in the homogeneous and heterogeneous catalysis of the water gas shift reaction.[13,14]

The formate anion is known to be formed readily by uncatalysed reaction of CO with hydroxide in solution and to decompose in the absence of CO to H_2 and CO_2.[13]

Evidence for the formation of metalloformates from CO and metal hydride has, on the other hand, been largely circumstantial. $M(CO)_6$ (M = Cr, W) in the presence of crypt-222-solubilised HCO_2K in acetonitrile is reported to exhibit infrared bands assignable to the corresponding $[M(CO)_5(O_2CH)]$ species (approximately 5% conversion) after 24 hours.[15] A surface formate has been formed by treatment at 110°C of $Ir_4(CO)_{12}$ adsorbed onto a dehydroxylated alumina support, with mechanism suggested to involve nucleophilic attack of surface OH^- groups at the coordinated CO followed by β-H elimination and concerted coordination of the resulting carboxylic group to the Lewis acidic aluminium site.

Darensbourg, on the other hand, believes that while formate species are likely to be present during catalysis of the WGS reaction, the metallacarboxylic acid structural isomer MCOOH is actually involved as intermediate.[15]

In order to understand how the reactivity and activation of CO operate it is necessary to examine the bonding in the MCO fragment.

Metal Carbonyls

The carbonyl group is an unsaturated ligand, by reason of the C–O multiple bond. It is generally considered to be a soft ligand since although it is a σ-donor through the carbon atom, it is also a strong π-acceptor and can accept metal dπ electron density *via* backbonding interactions. In this way CO is able to stabilise metals in low oxidation state and polyanionic species, providing a means of relieving a central metal atom of excess π-electron density and delocalising negative charge over the carbonyl oxygens.

Bonding in free CO

In figure 3.4a both C and O are sp hybridised. The singly occupied sp and p_z orbitals on C and O overlap to form a σ and a π bond respectively. The $\pi(p_y)$ orbital is orthogonal to the $\pi(p_z)$ bond and is not shown in figure 3.4b. In order to make this π molecular orbital, it is necessary to donate one electron from $p_y(O)$ to $p_y(C)$. This

transfer results in polarisation of the $\pi(p_y)$ molecular orbital and hence of the C–O bond, C^-–O^+. On the other hand, this polarisation is largely canceled by a partial C^+–O^- polarisation of all three bonding orbitals because the higher electronegativity of oxygen results in the bonding orbitals having more O than C character (see Fig. 3.5). The overall result is that free CO has net dipole moment close to zero.

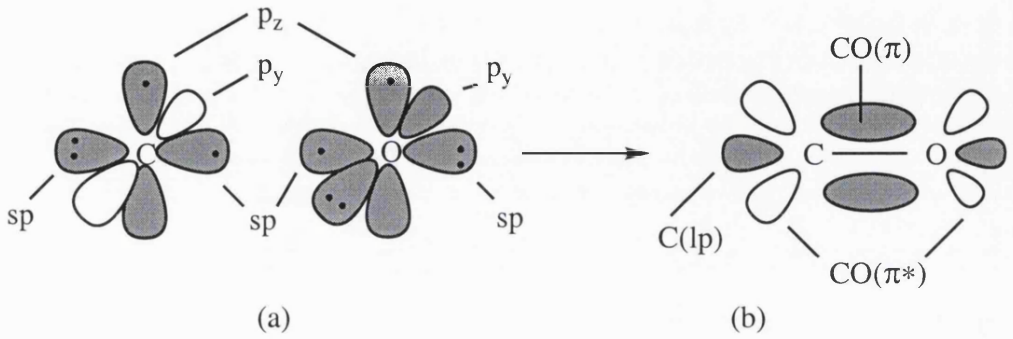

Fig. 3.4 **Hybridisation model for the electronic structure of (b) CO, building up from (a) C and O, each atom having two p orbitals and two sp hybrids. Shading represents occupied orbitals. In (b) only one of the two mutually perpendicular sets of p orbitals is shown.[2]**

The negative end of the dipole is at carbon, even though oxygen is more electronegative. This can be explained by reference to the MO diagram of CO shown in figure 3.5. The HOMO of the system is the anti-bonding σ^* (5σ) orbital, which lies predominantly on carbon, since the major contribution to an anti-bonding orbital is made by the atomic orbitals of the less electronegative atom. It follows, therefore, that if that orbital is occupied there may be sufficient electron density on the carbon atom for it to possess a partial negative charge. In the case of CO the overall result is the very small non-zero dipole moment of 0.12D.

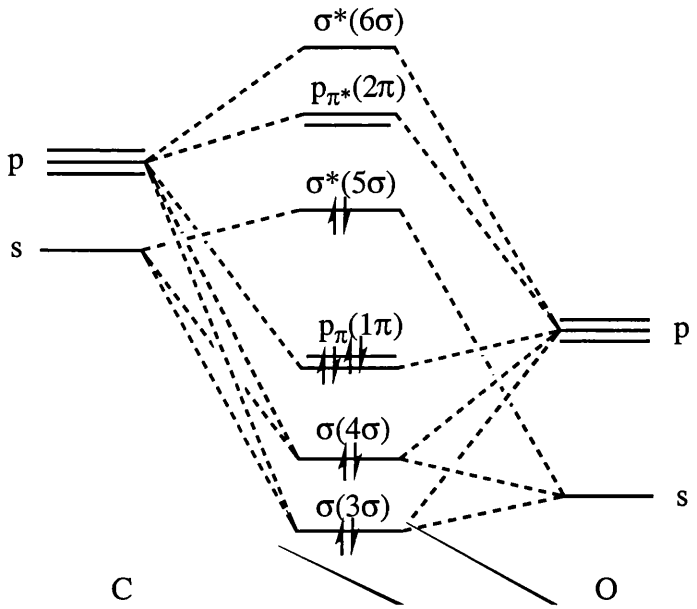

Fig.3.5 **Simplified energy-level diagram for CO. The symbols in brackets refer to the energetic sequence of the molecular orbitals that results if all atomic orbitals, including C(1s) and O(1s) are considered.** [1]

Metal-bound CO

The transition metal binds to the carbon atom, not to the oxygen, because the ligand HOMO is the lone pair on carbon rather than on oxygen. The description of the metal–CO bond as a resonance hybrid involving the two structures shown in figure 3.6 leads to a bond order of between 1 and 2 for the M–C bond and between 2 and 3 for the C–O bond.

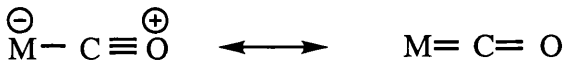

Fig. 3.6 **Resonance hybrids for the M–CO bond.**

The M–C–O bond may, therefore, be considered to contain a degree of M=C doubly bonded carbenoid character. This is most effectively identified by X-ray crystallography, where the short M–C distances are evident.

There are three types of interaction, one σ- and two π-interactions, between the metal and a carbonyl ligand in a single M–C–O moiety. These are depicted in figure 3.7.

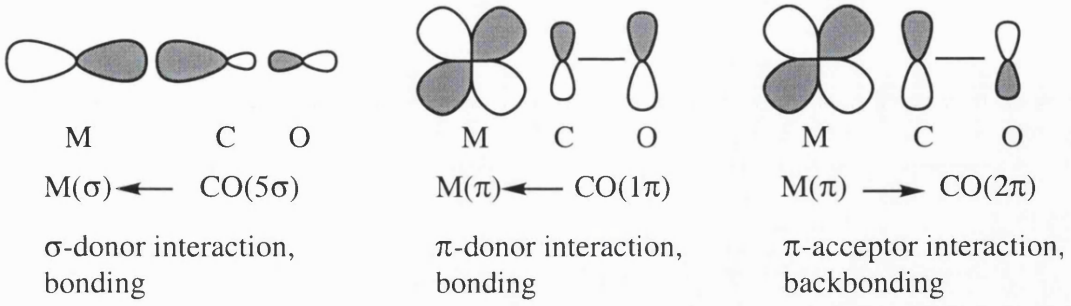

Fig. 3.7. Bonding interactions in M–C–O fragment.

A σ bond is formed by donation of the carbon lone pair (5σ) into the metal dσ orbitals. A weaker π-donation from the CO (1π) bonding orbital also occurs. These bonding interactions are reinforced by a backbonding π-interaction between the metal dπ orbitals and the CO 2π(π*) antibonding orbital. The extent of backbonding is influenced to varying degree by the other ligands attached to the metal and by the net charge on the complex. If the metal is coordinated to other π-acceptors or if the metal is cationic, *e.g.* $Mo(CO)_6$ or $[Mn(CO)_6]^+$, the resultant competition for the metal's π electron density reduces M→CO backdonation and the C→M σ donation is the dominant interaction. The dative σ bond builds up electron density on the metal and is favoured in complexes where the metal bears a formal positive charge. This results in the CO carbon having pronounced δ^+ character and consequently being particularly susceptible to nucleophilic attack. Where the metal carbonyl complex is anionic, or if the other ligands are good π donors, for example in $W(Cp)_2(CO)$ or $[W(CO)_5]^{2-}$, M→CO backdonation is enhanced and the carbonyl carbon loses its pronounced δ^+ charge. In this case the CO oxygen bears a significantly greater δ^- charge. Since such backbonding populates the CO $p_{\pi^*}(2\pi)$ antibonding orbital the M–C π bond is strengthened at the expense of the C–O π bond. These effects may also be expressed in terms of orbital overlap, *i.e.* a negative charge on the metal leads to expansion and a positive charge to contraction of the metal d orbitals, with attendant increase or decrease in the overlap M(d,π)–CO(π*) respectively.

Infrared Spectroscopy

The net result of coordination of CO to a metal is polarisation of the C–O bond, $C^{\delta+}$–$O^{\delta-}$, accompanied by a reduction in bond order, the degree of which may conveniently be investigated by infrared spectroscopy. A significant amount of backbonding results in a longer, weaker C–O bond, which is observed at lower wavenumber compared to a CO ligand in a complex where little back-donation occurs. Whereas, for example, the C–O stretch in free CO is at 2143 cm^{-1}, ν_{CO} in $[Mn(CO)_6]^+$ is observed at 2090, in $[Cr(CO)_6]$at 2000 and in $[V(CO)_6]^-$ at 1860 cm^{-1}.[1]

Another factor affecting the C–O polarisation is whether the carbonyl ligand is in a terminal or a bridging environment. The consequent change in bond order results in characteristic shifts of the vibrational stretching frequencies, shown in figure 3.8.

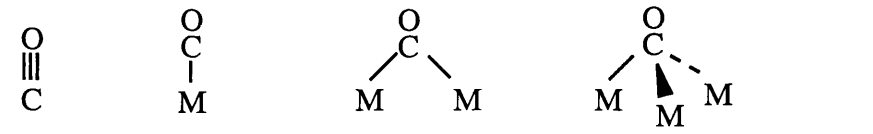

Free	Terminal	μ_2-CO	μ_3-CO	
2143	1850-2120	1750-1850	1620-1730	cm^{-1}

Fig. 3.8. Change in vibrational stretching frequency with different bonding modes of CO

Thus it is apparent that the more metal centres a given carbonyl group bridges, the weaker and more polarised the C–O bond becomes.

It is also possible for a metal-bound carbonyl group to function as a Lewis base and coordinate to a strong Lewis acid through the oxygen lone pair to afford an interaction of the type M–CO–M' (*vide infra*). The isocarbonyl interaction is particularly favoured for anionic transition metal carbonyls or where the other ligands are good π-donors, owing to the associated concentration of negative charge onto the carbonyl oxygen that occurs in many cases.[16]

This type of interaction weakens the C–O bond to the same extent that is observed for triply bridging carbonyl groups, as measured by the change in vibrational stretching frequency in the infrared. For a bridging isocarbonyl group ν_{CO} typically falls in the range 1600 - 1750 cm^{-1}. This interaction is believed to involve the C–O $p\pi$ (1π) bonding orbitals rather than the $p\sigma$ (4σ) orbital that formally contains the oxygen lone pair. Since such M–O–C interactions are not observed in reactions of L_xM with carbon monoxide, it is reasonable to assume that initial polarisation of the C–O bond, by prior coordination to a metal through carbon, is necessary for the formation of an isocarbonyl linkage. Indeed, in many cases, it is a prerequisite that the carbonyl ligand should be a bridging one in order for the oxygen to exhibit sufficient Lewis basicity to coordinate to a Lewis acid. Such a high degree of polarisation of the C–O $p\pi(1\pi)$ bonding orbitals results in the π electron density being localised on the oxygen atom and effectively functioning as a lone pair. The fact that almost all of the crystallographically characterised complexes possessing bridging isocarbonyl interactions are linear at carbon and bent at oxygen (*e.g.* in $Mg(py)_4[(\mu\text{-}OC)MoCp(CO)_2]_2$, the Mo-C-O angle is 177.2(1)°, *vs.* 155.0(2)° for C-O-Mg) further supports this view, since the 4σ lone pair on oxygen is axial to the C–O bond and should give rise to a linear C-O-M' interaction.

Transition Metal Carbonyl Basicity

The concept of transition metal carbonyl basicity, whereby the lone pair of electrons on the CO oxygen functions as a Lewis base, is well known.[17] Much of the early work in this area was centred around the formation of Lewis acid-Lewis base adducts between trialkyl aluminium and transition metal carbonyl complexes. It was noted that the increased polarisation of CO and hence basicity of oxygen exhibited by bridging carbonyl groups compared to their terminal counterparts permitted the coordination of the μ-CO oxygen to aluminium and other Lewis acidic metal complexes. Transition metal carbonyl compounds possessing only terminal carbonyl ligands were observed not to interact in this way. Whilst, for example, the reaction of $[Fe(Cp)(CO)_2]_2$ with

triethylaluminium yielded the isocarbonyl-bridged complex $[Fe(Cp)CO(\mu\text{-}CO)AlEt_3]_2$, the analogous reaction utilising $Fe(Cp)(CO)_2CH_3$ was found not to give the characteristic shift of the CO stretch to lower frequency in the infrared spectrum.[18,19] This tendency of carbonyl-bridged transition metal compounds to coordinate to Lewis acids was utilised in the preparation of a number of complexes possessing μ_3-CO groups. Many of these complexes were characterised primarily by IR spectroscopy, since the characteristic shift of ν_{CO} to low frequency is very easily observed, confirming the bridging isocarbonyl nature of the ligand. Crystallographic data, where available, provided further evidence for the carbenoid nature of the M–C interaction, in the short M–C and long C–O distances observed for such Lewis acid - Lewis base adducts.

The first crystallographically characterised example of such a complex, containing M–C–O–M' linkages, was $[Fe(Cp)(CO)(\mu\text{-}CO)AlEt_3]_2$ reported by Shriver in 1969.[19]

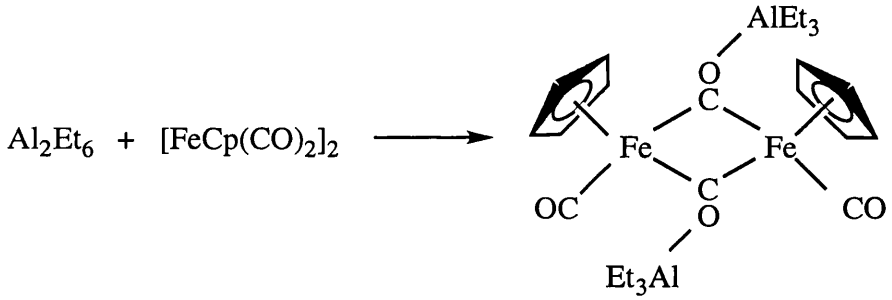

The infrared spectrum of this complex exhibited the expected increase in CO stretching frequency for the terminal carbonyl ligands and a marked decrease of *ca.* 110 cm^{-1} in ν_{CO} for the bridging carbonyls, to 1682 cm^{-1} in heptane solution, attributed to the weakening of the CO bond on coordination of the oxygen to aluminium.

Similar adducts were prepared utilising a variety of transition metal carbonyl complexes, all possessing bridging carbonyl ligands, with aluminium or other main group metal, early transition metal or lanthanide complexes acting as the Lewis acid. Examples of crystallographically characterised compounds with main group Lewis acidic metal complexes include $Al(THF)_3\{(\mu\text{-}OC)W(CO)_2Cp\}_3$,[20] isolated from the reaction of aluminium metal or amalgam with the mercury reagent $Hg\{W(CO)_3Cp\}_2$ and $Mg(py)_4\{(\mu\text{-}OC)MoCp(CO)_2\}_2$, prepared in similar fashion,which was the first

definitive example of oxygen coordination of a carbonyl ligand to a main group metal other than aluminium.[21]

Reactions involving early transition metals gave less predictable outcomes. Whilst the titanium complex $Ti(C_5Me_5)_2Me(\mu\text{-}OC)MoCp(CO)_2$ has been prepared, the reaction of $ZrCp_2Me_2$ with $HMoCp(CO)_3$ results in migratory insertion to afford the acyl-bridged complex $Zr(Cp)_2(\eta^2\text{-}COMe)MoCp(CO)_2$.[5] The similarly unexpected reductive coupling of two carbonyl ligands occurs in the reaction of $[(C_5Me_5)_2ZrN_2]_2N_2$ with the iron carbonyl derivative $[FeCp(CO)_2]_2$. [22]

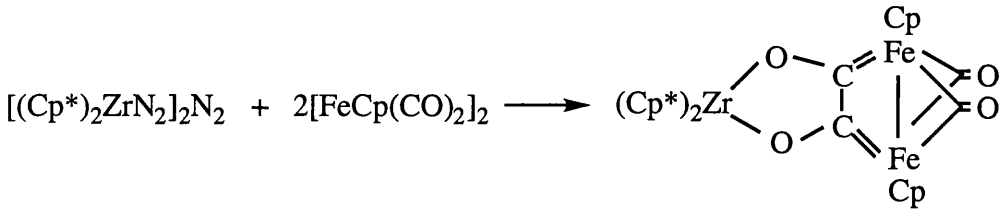

This carbon-carbon coupling reaction is unusual because the reductant is divalent decamethylzirconocene, which reacts with free carbon monoxide to afford the stable $[(C_5Me_5)_2Zr(CO)_2]$ and with $[CoCp(CO)_2]$ to give the mixed metal species $[Zr(C_5Me_5)_2(\mu_2\text{-}CO)(\mu_3\text{-}\eta^1,\eta^2\text{-}CO)CoCp]$.[23] The different reactivity in this case is attributed to the disposition of the carbonyl groups of $[FeCp(CO)_2]_2$, which has a rigid $Fe(\mu\text{-}CO)_2Fe$ unit.

Lanthanide - Transition Metal Carbonylates

Reactivity towards adduct formation with main group and early transition metal complexes has generally been observed only with transition metal complexes possessing bridging carbonyl groups (*vide supra*). There is, for example, no reaction between trialkylaluminium and $Mn_2(CO)_{10}$, in which all the carbonyl ligands are in terminal positions in solution and in the solid state. Complexes of the lanthanides are weaker Lewis acids than the corresponding aluminium compounds and are not, therefore, expected to form adducts with metal carbonyls that do not coordinate to aluminium complexes. The use of different synthetic routes, however, such as the

electron transfer processes that are possible for the di- or zero-valent lanthanides, has allowed the preparation of compounds containing a lanthanide cation linked *via* an isocarbonyl bridge to a transition metal carbonylate anion. In such complexes the lanthanide acts as an electron-transfer reagent, reducing the transition metal fragment to form an anionic species, with concomitant oxidation of Ln(II) to Ln(III), and as a Lewis acid. A greater degree of backdonation occurs from the anionic transition metal centre to the carbonyl ligands, with consequent increase of negative charge on oxygen. Reactivity has thus been observed with transition metal carbonyls such as $Mn_2(CO)_{10}$ and $Re_2(CO)_{10}$ in which the terminal CO groups were previously considered not basic enough to coordinate to a Lewis acidic metal centre. Andersen, for example, has reacted $Yb(C_5Me_5)_2(OEt)_2$ with $Mn_2(CO)_{10}$ to afford the polymeric chain $[Yb(C_5Me_5)_2(\mu\text{-}OC)_3Mn(CO)_2]_\infty$ and the dimeric complex $[Yb(C_5Me_5)_2(\mu\text{-}OC)_2Mn(CO)_3]_2$. Rhenium carbonyl was reported to give analogous products which were not, however, characterised by X-ray crystallography.[24]

Synthetic Routes to Lanthanide-Transition Metal Carbonyl Complexes

1. Adduct Formation

Tris(cyclopentadienyl) lanthanides have been utilised as Lewis Acids towards potential electron donors possessing bridging carbonyl ligands such as $[FeCp(CO)_2]_2$ and $[MnCp(Me)(CO)_3]$[25,26] in reactions analogous to those carried out with main group Lewis acids. The products have been characterised by infrared spectroscopy from the characteristic shift on coordination of terminal and bridging ν_{CO} to high and low frequency respectively. The reaction of $[FeCp(CO)_2]_2$ with $Sm(Cp)_3$, for example, with product assumed to be $[Sm(Cp)_3(\mu\text{-}OC)FeCp(CO)]_2$, increases the CO stretching frequencies for the terminal carbonyl groups by up to 65 cm^{-1} from 1955 and 1938 cm^{-1} in the uncoordinated iron complex to 2020 and 1985 cm^{-1} in the product. The band for the bridging carbonyl is likewise shifted to lower frequency, from 1752 to 1700 cm^{-1}.

2. Salt Metathesis

The reaction of lanthanide halides with alkali metal salts of transition metal carbonylates is expected to afford the corresponding lanthanide complex. Bruno *et al* have prepared the tetrametallic Ce - W compound $[Ce(Cp')_2(\mu\text{-}OC)W(CO)Cp(\mu\text{-}CO)]_2$ in this way ($Cp' = C_5H_3\{NSiMe_3\}_2$).[27]

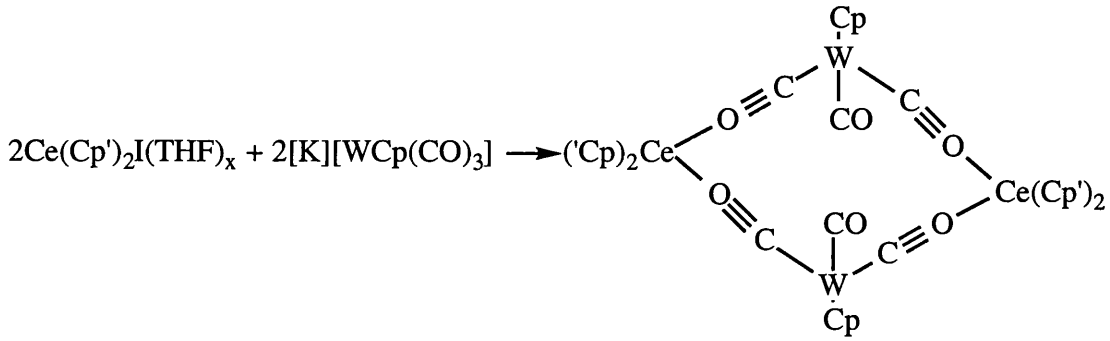

This method does not appear to be widely used in the preparation of such complexes, presumably owing to problems with incorporation of halide salts and to the ready availability of dimeric or polynuclear carbonyl complexes which exhibit reactivity with low-valent lanthanides.

3. Protonolysis

Reaction of a lanthanide alkyl or amide with a transition metal complex possessing an acidic proton is not a much used synthetic route. A divalent and a trivalent ytterbium complex have, however, been prepared from the ytterbium-benzophenone dianion complex $[Yb(\mu\text{-}OCPh_2)(HMPA)_2]_2$.[28]

$$[Yb(\mu\text{-}OCPh_2)(HMPA)_2]_2 + 2\ MoCp(CO)_3H \rightarrow Yb(HMPA)_4[(\mu\text{-}OC)MoCp(CO)_2]_2$$

$$[Yb(\mu\text{-}OCPh_2)(HMPA)_2]_2 + 4\ MoCp(CO)_3H \rightarrow$$

$$Yb(HMPA)_5[(\mu\text{-}OC)MoCp(CO)_2][MoCp(CO)_3].THF$$

4. Electron Transfer Routes

4a. Reduction of M–M bonds by Ln(0)

The zerovalent lanthanides are sufficiently reducing to cleave metal-metal bonds in similar fashion to the cleavage of chalcogen-chalcogen bonds (see Chapter two). Ytterbium metal has been reacted with $Fe_3(CO)_{12}$ in liquid ammonia to afford two structurally related polymers containing direct Yb–Fe links.[29,30]

$$Yb + Fe_3(CO)_{12} \rightarrow (NH_3)_2YbFe(CO)_4 \rightarrow [\{(MeCN)_3YbFe(CO)_4\}_2.MeCN]_\infty + [(NH_3)YbFe(CO)_4]_\infty$$

4b. Reduction of M–M bonds by Ln(II)

The use of divalent lanthanides to reductively cleave element-element bonds is also well-precedented and this is the most widely used synthetic method for the preparation of lanthanide-transition metal heterometallic complexes. A recent example is the synthesis of $[Sm(C_5Me_5)_2(\mu\text{-}OC)_2FeC_5Me_5]_2$ by Recknagel *et al.*[31] This heterometallic complex has a similar structure to that established for $[Ce(Cp')_2(\mu\text{-}OC)W(CO)Cp(\mu\text{-}CO)]_2$.

$$2\ Sm(C_5Me_5)_2(THF)_2 + [FeC_5Me_5(CO)_2]_2 \rightarrow [Sm(C_5Me_5)_2(\mu\text{-}OC)_2FeC_5Me_5]_2$$

This route can also result in the formation of polynuclear carbonyl complexes such as $[Yb(C_5Me_5)_2\{Co_3(Cp^R)_2(\mu_3\text{-}CO)_2\}]$ (R = H, Me, $SiMe_3$).[32]

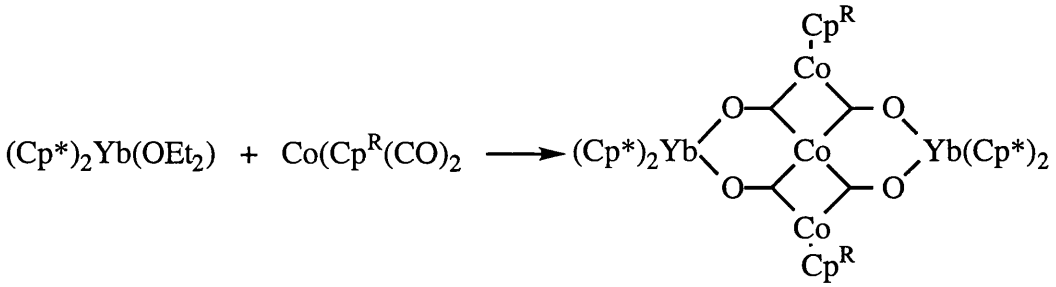

4c. Transmetallation

This route has been utilised by Wong and Lin in the preparation of $[(THF)_4I_2Sm(\mu\text{-}OC)Mo(CO)_2Cp]$ from divalent samarium with mercury reagent.[33]

$$SmI_2(THF)_x + Hg[Mo(CO)_2Cp]_2 \rightarrow [(THF)_4I_2Sm(\mu\text{-}OC)Mo(CO)_2Cp] + Hg$$

Product types

Three major structural types have been observed for lanthanide - transition metal heterometallic complexes.

1. Separated ion pair

Where the negative charge of the transition metal carbonylate anion is delocalised over a highly symmetrical structure, or if a more effective nucleophile such as a donor solvent is present, a salt-like complex possessing a well-separated ion pair with no direct interionic contacts between cation and anion is often formed. An example of such a complex is $[SmI_2(THF)_5][Co(CO)_4]$, containing the tetrahedral tetracarbonylcobaltate anion, which was isolated from the reaction of $SmI_2(THF)_2$ with $Co_2(CO)_8$.[34]

$$SmI_2(THF)_x + Co_2(CO)_8 \rightarrow [SmI_2(THF)_5][Co(CO)_4]$$

2. Bridging isocarbonyl

In cases where the anionic negative charge is localised onto the carbonyl oxygens a bridging isocarbonyl interaction (*vide supra*) is favoured. This type of interaction is most commonly observed in these systems. Recent crystallographically characterised examples include $[(THF)_4I_2Sm(\mu\text{-}OC)Mo(CO)_2Cp]$,[33] $[(Tp^{Me,Me})_2Sm(\mu\text{-}OC)Mo(CO)_2Cp]$,[35] and $[Ce(Cp')_2(\mu\text{-}OC)W(CO)Cp(\mu\text{-}CO)]_2$.[27]

$$[(Tp^{Me,Me})_2Sm] + {}^1/_2\,[Mo(CO)_3Cp]_2 \rightarrow [(Tp^{Me,Me})_2Sm(\mu\text{-}OC)Mo(CO)_2Cp]$$

The isocarbonyl interaction also supports cluster and polymeric structures such as those observed by Andersen in $[Yb(C_5Me_5)_2(Fe_3(CO)_{11})]$[36] and $[Yb(C_5Me_5)_2(\mu\text{-}OC)_3Mn(CO)_2]_\infty$.[24]

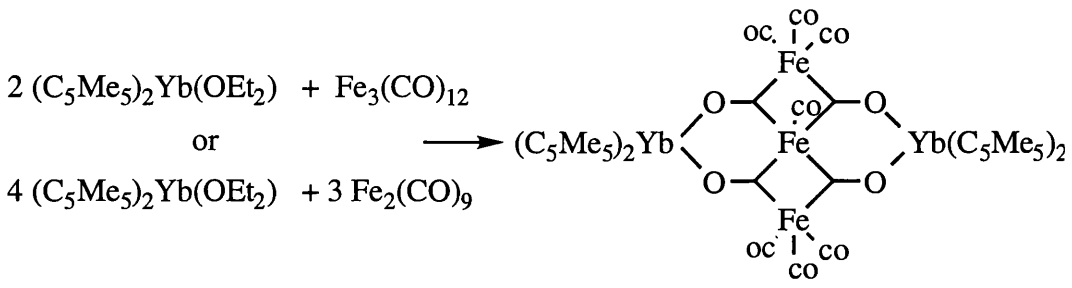

3. Metal-metal bond

Localisation of anionic charge onto the metal, as has been predicted by Bursten and Gatter[16] for iron and ruthenium cyclopentadienyl carbonyl complexes, results in the metal carbonyl moiety acting as a Lewis base at the metal centre, allowing the possibility of metal-metal bond formation. This type of interaction is quite rare and only two examples have been reported. Beletskaya *et al* have prepared $(THF)(Cp)_2Lu–RuCp(CO)_2$ by reaction of $Lu(Cp)_2Cl(THF)$ with the salt $Na[RuCp(CO)_2]$[37] and two polymeric compounds containing direct Yb–Fe interactions have been reported by Shore and co-workers from the reaction of ytterbium metal with the cluster $Fe_3(CO)_{12}$.[29,30]

$$Lu(Cp)_2Cl(THF) + Na[RuCp(CO)_2] \rightarrow (THF)(Cp)_2Lu–RuCp(CO)_2$$

Results

Reactivity of half sandwich complexes $[LnTp^{t\text{-}Bu,Me}I(Et_2O)_m(THF)_n]$ (Ln = Sm, m = 0.5, n = 2; Ln = Yb, m = 0 n = 1)

Synthesis of $[LnTp^{t\text{-}Bu,Me}(THF)(\mu\text{-}OC)_2Mo(\eta\text{-}C_5H_4CH_3)(CO)]_2$, Ln = Sm, 3.1; Ln = Yb, 3.2

Following the preparation of $[LnTp^{Me,Me}(\mu\text{-}OC)Mo(\eta\text{-}C_5H_4CH_3)(CO)_2]$ by Liu,[35] it was of interest to synthesise analogous divalent lanthanide complexes, in order to ascertain whether the pyrazolyborate - Ln(II) system exhibited sufficient Lewis acidity to coordinate to a carbonyl oxygen. An electron transfer route was not possible, so a salt metathesis reaction was carried out, utilising $[LnTp^{t\text{-}Bu,Me}I(THF)_n]$ and the salt $[Na][Mo(\eta\text{-}C_5H_4CH_3)(CO)_3]$.

$$[Ln(Tp^{tBu,Me})I(THF)] + Na[Mo(\eta\text{-}C_5H_4CH_3)(CO)_3] \rightarrow$$

$$[Ln(Tp^{tBu,Me})(THF)Mo(\eta\text{-}C_5H_4CH_3)(CO)_3]_2 + NaI\downarrow$$

A solution of $Na[Mo(\eta\text{-}C_5H_4CH_3)(CO)_3]$ was freshly prepared by stirring $[Mo(\eta\text{-}C_5H_4CH_3)(CO)_3]_2$ with sodium amalgam in THF, then filtered onto a solution of $[LnTp^{t\text{-}Bu,Me}I(THF)_n]$ in THF at –78°C. No colour change was observed in the blue/black (Sm) or canary yellow (Yb) THF solutions on warming to room temperature, but the solution IR spectra of both exhibited a band at low frequency in the carbonyl region, consistent with the presence of a bridging isocarbonyl group. Recrystallisation from a concentrated diethyl ether solution yielded dark blue/black and canary yellow crystals respectively, which desolvated fairly quickly on removal from the mother liquor. Both compounds are quite air sensitive, the solids decomposing within seconds on exposure to air. They dissolve easily in hydrocarbon and ether solvents but decompose quickly in wet or halogenated solvents. The solid state infrared spectra show the expected B-H stretching absorption around 2555 cm^{-1}, compared with

2463 cm^{-1} in $KTp^{Me,Me}$, consistent with a tridentate Tp ligand bound to a lanthanide.[38] A number of intense bands appear in the carbonyl region of the ytterbium complex corresponding to the stretches of the terminal CO groups at approximately 1920 and 1834 cm^{-1} and low energy bands at 1745 and 1687 cm^{-1}, diagnostic of bridging isocarbonyl groups. The corresponding peaks in the infrared spectrum of the samarium complex are at closely similar frequencies, with the small differences attributed to the slightly different Lewis acidities of samarium and ytterbium.

The spectrum of **3.1** is also slightly more complicated, presumably owing to the greater sensitivity to air of this complex, with some decomposition occurring during the time taken to obtain the spectrum. The frequency of the bands attributed to bridging isocarbonyl groups compares with the band at 1654 cm^{-1} observed in the related trivalent complex $[Sm(Tp^{Me,Me})_2(\mu\text{-}OC)Mo(\eta\text{-}C_5H_4CH_3)(CO)_2]$[35] which is in a range similar to those observed by others previously. The IR spectrum of $[Sm(C_5Me_5)_2(\mu\text{-}OC)_2FeC_5Me_5]_2$, for example, exhibits low energy bands at similar frequencies, 1760 and 1691 cm^{-1}.[31] The higher frequency of the bands in the divalent Ln - Mo complexes is consistent with the lower Lewis acidity of Ln(II) compared to Ln(III). That the complexes retain their integrity in toluene solution is suggested by the presence of three IR bands at closely similar wavenumbers to those recorded in the solid state. The peaks in the ^1H NMR spectrum of **3.2** are sharp, consistent with the diamagnetic f^{14} metal centre. No changes in the spectrum were observed on cooling a sample in toluene-d_8 to -90°C.

X-Ray structures of $[LnTp^{t\text{-}Bu,Me}(THF)(\mu\text{-}OC)_2MoCpMe(CO)]_2$, 3.1, 3.2

Compounds **3.1** and **3.2** crystallized from diethyl ether as isomorphous triclinic blue-green or yellow blocks respectively (which tended to lose solvent) in the space group $P\bar{1}$, incorporating two molecules of diethyl ether in the lattice for each Mo_2Sm_2 unit. A view of the molecule of **3.1** is shown in Figure 3.9 and of **3.2** in Figure 3.10. The molecules consist of "molecular squares" lying on an inversion centre, making half of each molecule unique. The two lanthanide centres are linked to the molybdenum atoms

via isocarbonyl bridges. The overall structure therefore resembles those observed before with trivalent lanthanides such as $[(\eta\text{-}C_5H_3\{N(SiMe_3)_2\}_2)_2Ce(\mu\text{-}OC)W(Cp)(CO)]_2$[27] and $[(C_5Me_5)_2Sm(\mu\text{-}CO)_2Fe(C_5Me_5)]_2$.[31] The core of the molecule is puckered, the central 12-membered ring adopting a chair-like conformation, with two coplanar $Mo(CO)_2$ units facing each other and the two lanthanide atoms closing the ring at either end, one above and one below the $Mo_2(CO)_4$ plane. The cyclopentadienyl ring centroids lie in equatorial positions and the terminal carbonyls axial to the ring.

Each lanthanide atom is six coordinate with a geometry best described as bicapped trigonal pyramidal (figure 3.11). The tridentate tris(pyrazolyl)borate ligand defines the base of the pyramid with the oxygen atoms of the bridging carbonyls defining the apex and capping a face. The THF caps a second face, binding in the cleft between two pyrazolyl rings of the $Tp^{t\text{-}Bu,Me}$ ligand. The geometry is, therefore, very similar to that seen in the divalent starting material with the two capping ligands effectively perpendicular to the apical carbonyl {OC at 87.46(6)° **3.1**, 83.91(9)°, **3.2** and the THF at 74.66(6)°, **3.1**, 75.38(9)°, **3.2**}.

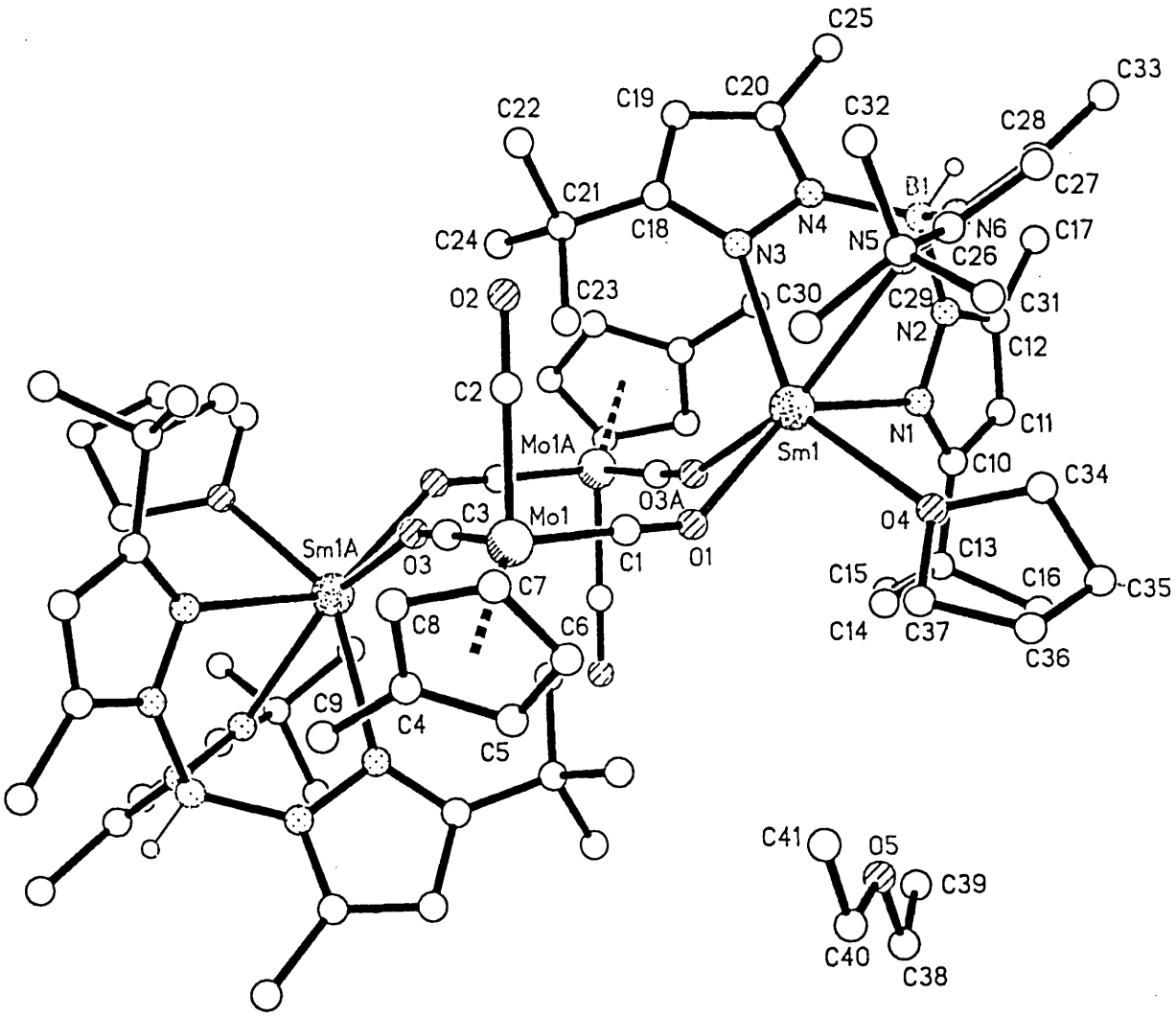

Figure 3.9. X-ray Structure of 3.1.

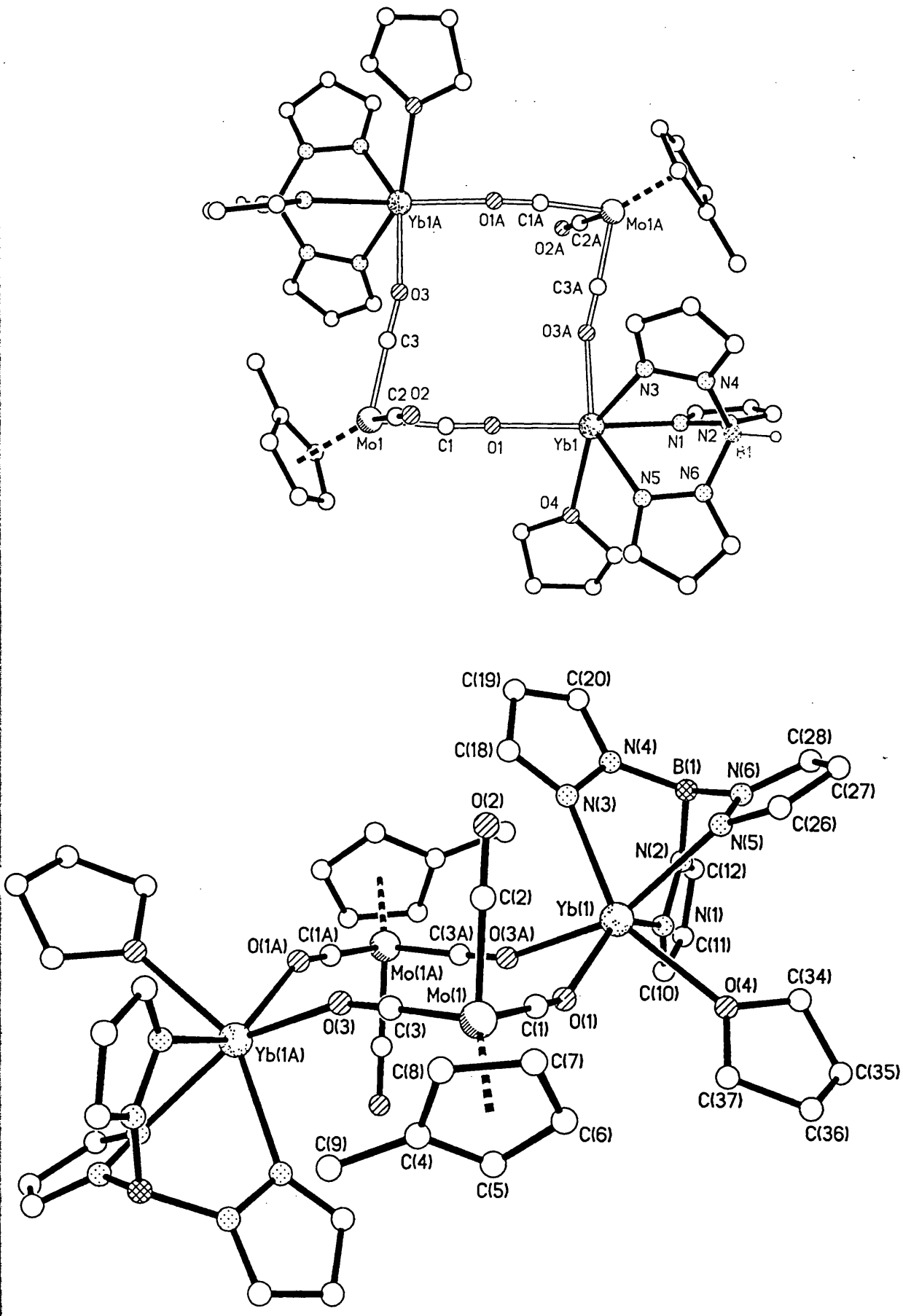

Figure 3.10. X-ray Structure of 3.2.

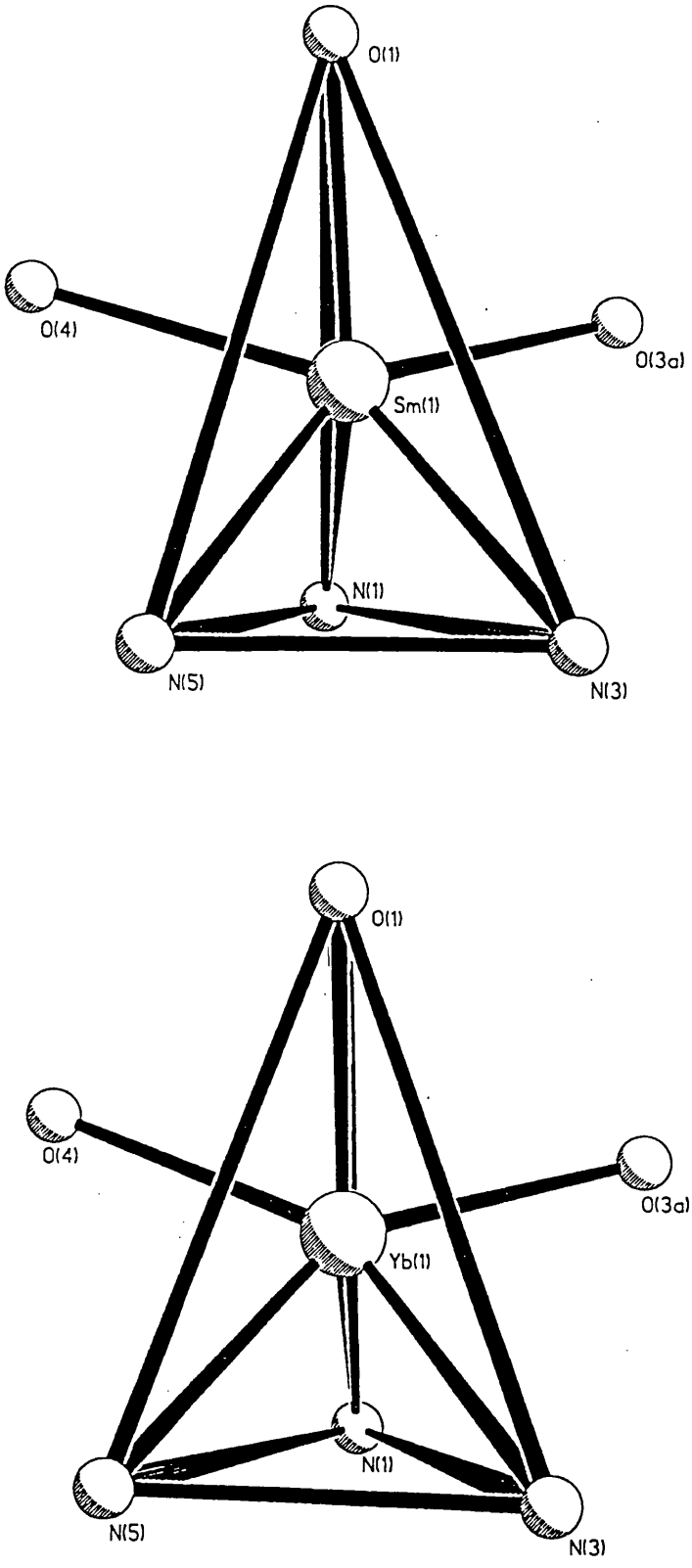

Figure 3.11. Bicapped trigonal pyramidal coordination geometry of 3.1 and 3.2.

As expected the average samarium-nitrogen distance in **3.1**, 2.603(3)Å, is similar to that in the starting material, 2.637(9)Å. On the other hand the samarium-oxygen distances to the isocarbonyls are significantly different. The apical oxygen lies 2.524(2) Å from the metal atom while the face-cap is longer at 2.577(2) Å. These are markedly longer than the Sm–OC distances observed both in trivalent samarium isocarbonyls, such as $[(Tp^{Me,Me})_2Sm(\mu\text{-}OC)Mo(\eta\text{-}Cp)(CO)_2]$, 2.335(4) Å,[35] and $[SmI_2(THF)_4(\mu\text{-}OC)Mo(\eta\text{-}Cp)(CO)_2]$ 2.41(2) Å,[33] and in the tetrametallic $[(C_5Me_5)_2Sm(\mu\text{-}OC)_2Fe(C_5Me_5)]_2$, 2.348(4) and 2.339(4),[31] as well as in four-coordinate samarium (II) alkoxides 2.339(9) Å.[39] There are no divalent samarium isocarbonyls reported in the literature with which to draw further comparison. The corresponding distances in the ytterbium complex **3.2**, Yb–O 2.390(3) (apical) and 2.449(3) Å (face-cap) are comparable to those observed in the Yb (II) compounds $Yb(HMPA)_4[(\mu\text{-}OC)MoCp(CO)_2]_2$, 2.47(2)Å,[28] $[\{(MeCN)_3YbFe(CO)_4\}_2.MeCN]_\infty$, 2.389(5) and 2.374(5) Å and $[(MeCN)_3YbFe(CO)_4]_\infty$, 2.444(8), 2.541(6) and 2.459(6) Å.[29,30] These distances are somewhat longer than the Yb–O (isocarbonyl) bond lengths in trivalent ytterbium complexes, for example 2.268(4) Å in the structurally similar $[Yb(C_5Me_5)_2(\mu\text{-}OC)_2Mn(CO)_3]_2$ [24] and 2.258(2) Å in $[Yb(C_5Me_5)_2(THF)(\mu\text{-}OC)Co(CO)_3]$.[40]

The isocarbonyl C–O distances in **3.1** and **3.2** {1.194(3) and 1.195(4) Å (apical); 1.181(3) and 1.184(5) Å (face-cap)}, are significantly longer than those in the terminal carbonyls, 1.160(3) and 1.155(5) Å respectively. In trivalent samarium isocarbonyls the analogous C–O (isocarbonyl) distances are generally at least 1.20 Å, for example 1.22(2) Å in $[SmI_2(THF)_4(\mu\text{-}OC)Mo(\eta\text{-}Cp)(CO)_2]$ and 1.206(7) Å in $[(Tp^{Me,Me})_2Sm(\mu\text{-}OC)Mo(\eta\text{-}Cp)(CO)_2]$ suggesting that the divalent lanthanide centre may be considered a somewhat weaker Lewis acid. The bridging C–O separations in $Yb(HMPA)_4[(\mu\text{-}OC)MoCp(CO)_2]_2$ (1.14(4) and 1.20(3) Å),[28] $[\{(MeCN)_3YbFe(CO)_4\}_2.MeCN]_\infty$ (1.198(8) Å) and $[(MeCN)_3YbFe(CO)_4]_\infty$ (1.17(1), 1.20(1) and 1.19(1) Å) are, on the whole, comparable. The shorter μ-C–O bonds observed in $Yb(HMPA)_4[(\mu\text{-}OC)MoCp(CO)_2]_2$ and $[(MeCN)_3YbFe(CO)_4]_\infty$ are

almost equivalent to the terminal C–O bonds, probably arising in the one case from the strong donating ability of the HMPA ligands and in the other due to structural constraints within the polymeric framework. Shorter C–O distances have also been observed for trivalent ytterbium with other transition metal systems, such as the average C–O separations of 1.186 Å in $[Yb(C_5Me_5)_2(\mu\text{-}OC)_2Mn(CO)_3]_2$ and 1.188(3) Å in $[Yb(C_5Me_5)_2(THF)(\mu\text{-}OC)Co(CO)_3]$. A short C–O bond of 1.182 Å has also been noted in $[(\eta\text{-}C_5H_3R_2)_2Ce(\mu\text{-}OC)_2W(\eta\text{-}C_5H_5)(CO)]_2$. The attendant shortening of the Mo–C (isocarbonyl) distances (1.897(3) (apical) and 1.899(3) Å (face-cap), **3.1**; 1.900(4) and 1.905(4) Å, **3.2**) compared to the terminal Mo–C bonds (1.955(3) Å, **3.1**; 1.960(5) Å, **3.2**) is as expected for the more "carbene-like" nature of the isocarbonyls.[41]

The angles in the isocarbonyl unit are consistent with those observed in other isocarbonyl bridged systems, which are somewhat bent at oxygen and essentially linear at carbon. The Ln-O-C angles of 144.27(17) and 149.1(3)° (apical) and 158.71(19) and 159.4(3)° (face-cap) for **3.1** and **3.2** respectively correspond reasonably well to the 151.0(4)° observed for $[(Tp^{Me,Me})_2Sm(\mu\text{-}OC)Mo(Cp)(CO)_2]$ and 149(1)° for $[SmI_2(THF)_4(\mu\text{-}OC)Mo(Cp)(CO)_2]$ and to the Ce-O-C angle of 154.4° in $[(\eta\text{-}C_5H_3\{N(SiMe_3)_2\}_2)_2Ce(\mu\text{-}OC)_2W(Cp)(CO)]_2$. The Sm-O-C angles of 164.5(5) and 168.8(5)° in $[(C_5Me_5)_2Sm(\mu\text{-}OC)_2Fe(C_5Me_5)]_2$, are somewhat more open, as are the Yb-O-C angles of 163.0(2) and 170.6(4)° in $[Yb(C_5Me_5)_2(THF)(\mu\text{-}OC)Co(CO)_3]$ and $[Yb(C_5Me_5)_2(\mu\text{-}OC)_2Mn(CO)_3]_2$ respectively. The divalent ytterbium complex $Yb(HMPA)_4[(\mu\text{-}OC)MoCp(CO)_2]_2$ displays similarly large angles (166(2) and 172(2)°) while the corresponding angles in $[(MeCN)_3YbFe(CO)_4]_\infty$ (167.3(7), 146.9(7) and 161.1(8)°) and $[\{(MeCN)_3YbFe(CO)_4\}_2.MeCN]_\infty$ (168.4(5), 134.8(6)°) appear to depend on ligand environment and are presumably dictated by the polymeric structures of these complexes. The Mo-C-O angles are almost linear and therefore comparable to the 175 to 178° generally observed for such systems, at 175.3(2) (apical), 176.2(2)° (face-cap) for **3.1** and 175.2(3) (apical), 176.4(3)° (face-cap) in **3.2**. The more acute angle at oxygen observed for the apical isocarbonyl group compared to the face-capping

isocarbonyl is consistent with the shorter Ln–OC (apical) distance and the longer C–O separation, indicating a higher degree of polarisation of the axial C–O bond.

The lanthanide–O (THF) distances of 2.6173(17) (**3.1**) and 2.510(3) Å (**3.2**) are longer than the average Sm–O (THF) bond of 2.453 Å in $[SmI_2(THF)_4(\mu\text{-}OC)Mo(\eta\text{-}Cp)(CO)_2]$ and Yb–O (THF) of 2.335(2) Å in $[Yb(C_5Me_5)_2(THF)(\mu\text{-}OC)Co(CO)_3]$, consistent with the increase in ionic radius on exchanging Ln (III) with Ln (II).

Fluxionality in 3.1 and 3.2

The X-ray structure implies that we might expect to observe three different ^{t}Bu and Me environments in the solution NMR spectra. In fact the complexes are fluxional on the NMR timescale at room temperature and only one ^{t}Bu and one Me environment are observed even at low temperature. The fact that the ^{1}H NMR spectra of **3.1** and **3.2** are temperature invariant suggests that there is very rapid interconversion of the pyrazolyl environments in solution, as has been observed for $[Ln(Tp^{tBu,Me})I(py)_n]$ (Ln = Sm, Yb).[42] Since the IR spectra in solution and in the solid state are closely similar this is unlikely to occur by breakage of the isocarbonyl links. It is more probable that dissociation of one arm of the Tp ligand occurs allowing the resulting 5-coordinate intermediate to rearrange. Such dissociations are presumed to be facile in view of the known fluxionality of $[Sm(Tp^{tBu,Me})_2]$ in which the two Tp ligands are tridentate and bidentate respectively.[43]

Reactivity of 3.1 and 3.2

The lanthanide to isocarbonyl interaction is presumed to be fairly weak. Addition of pyridine to solutions of **3.1** and **3.2** results in deep blue-green and red solutions repectively. The infrared spectra of these solutions are essentially identical to each other, with three bands in the carbonyl region at 1910, 1820 and 1670 cm^{-1} consistent with a break up of the tetramer, displacement of THF, and the coordination of one or more pyridine ligands in the lanthanide coordination sphere as was seen for $[Ln(Tp^{t\text{-}Bu,Me})I(py)_n]$ (Ln = Sm, Yb).[42,44] The CO region of the IR spectra is essentially superimposable with that of $[Sm(Tp^{Me,Me})_2(\mu\text{-}OC)Mo(Cp^{Me})(CO)_2]$.

Reactions with group 8 metal carbonyl complexes

In view of the success of Beletskaya and coworkers in isolating the Lu–Ru metal-metal bonded complex $[(THF)(Cp)_2Lu–RuCp(CO)_2]$[37] and the formation of polymers containing Yb–Fe interactions by Shore and coworkers,[29,30] the possibility of observing similar structural features with group 8 metal carbonyl derivatives prompted us to attempt reactions of "half-sandwich" and "sandwich" samarium and ytterbium pyrazolylborates. The synthetic routes employed were either salt metathesis, utilising $[Ln(Tp^{tBu,Me})I(THF)]$ or $[Sm(Tp^{Me,Me})_2Cl]$ as starting materials, or electron transfer routes from $[Sm(Tp^{Me,Me})_2]$ (*vide infra*).

Attempted preparation of $[LnTp^{t\text{-}Bu,Me}]_2[Fe(CO)_4]$

Stirring a solution of two equivalents of $[SmTp^{t\text{-}Bu,Me}I(THF)_n]$ with $Na_2Fe(CO)_4$ in THF followed by extraction into diethyl ether and cooling afforded a brown powder which displayed a broad band at 2000 cm^{-1} in the infrared spectrum, but no BH stretch. The corresponding reaction utilising $[YbTp^{t\text{-}Bu,Me}I(THF)_n]$ gave a yellow solid after workup. which exhibited three poorly resolved bands in the carbonyl region at 1996, 1922 and 1907 cm^{-1} and three bands associated with the pyrazolylborate BH stretch, at 2551, 2521 and 2499 cm^{-1}, indicative of a possible polynuclear structure in the solid state or of a mixture of products. The number of bands expected for the $[Fe(CO)_4]^{2-}$ unit in the carbonyl region depends on the symmetry and hence the coordination mode of this anion. A tetrahedral $[Fe(CO)_4]^{2-}$ anion would display a single CO stretch, at the lower frequency end of the terminal carbonyl region (*ca.* 1790 cm^{-1}) owing to the negative charge on the unit. A metal-coordinated $[Fe(CO)_4]^{2-}$ anion, on the other hand, possessing reduced symmetry, should display infrared bands in both the terminal and the bridging CO regions No crystals were obtained from diethyl ether or toluene solutions and no NMR spectroscopic data obtained.

Attempted preparation of $[YbTp^{t\text{-}Bu,Me}][FeCp(CO)_2]$

The reaction of $[YbTp^{t\text{-}Bu,Me}I(THF)_n]$ with $KFeCp(CO)_2$ in THF afforded a brown solution, from which the only isolable product was a red/brown crystalline solid which

exhibited bands at 1995, 1953, 1783 and 1778 cm^{-1} in the infrared spectrum, consistent with the presence of a $[FeCp(CO)_2]$-containing species. No peaks were observed, however, in the BH stretching region. The analogous reaction utilising $[SmTp^{t\text{-}Bu,Me}I(THF)_n]$ was not attempted.

Discussion

The preparation of complexes **3.1** and **3.2** provides further examples of how polynuclear conjugated systems can be built up using carbonyls to bridge between both lanthanides and transition metals. The presence of the ancillary ligands serves to constrain the oligomerization. This is the first example of an isocarbonyl linkage to samarium(II) and only the third to divalent ytterbium. The carbonyl groups appear resistant to electron transfer- this is to be expected in view of the back-bonding from the transition metal centre. In the present case calculations suggest that a partial negative charge is localized on the oxygens of the $MeCpMo(CO)_3$ unit.[16]

Our inability to isolate clean products from the reactions with iron carbonyl derivatives could be attributed to the possible formation of complexes containing $Ln^{(II)}$-Fe interactions, which would be extremely sensitive to oxidation by trace amounts of oxygen or moisture. The likelihood that polymeric species are formed might also explain the relative intractability of the products. It is, however, possible that some incorporation of alkali metal halide salt occurs, given the relatively open lanthanide metal coordination sphere in these "half-sandwich" complexes. In the reaction of $[YbTp^{t\text{-}Bu,Me}I(THF)_n]$ with $KFeCp(CO)_2$, we believe that some oxidation of $KFeCp(CO)_2$ to $[FeCp(CO)_2]_2$ occurred, presumably due to leakage of oxygen into the flask.

Salt Metathesis Reactions of $[Sm(Tp^{Me,Me})_2Cl]$

Attempted preparation of $[Sm(Tp^{Me,Me})_2][FeCp(CO)_2]$

The reaction of $[Sm(Tp^{Me,Me})_2Cl]$ with $KFeCp(CO)_2$ in THF, followed by extraction into diethyl ether solution, afforded red/brown crystals which exhibited three bands in

the carbonyl region of the solid state infrared spectrum at 1987, 1933 and 1776 cm^{-1}. Only a weak B–H stretch was observed at 2525 cm^{-1}. The major product was, therefore, formulated to be $[FeCp(CO)_2]_2$, which has ν_{CO} of 1975, 1934 and 1767 cm^{-1} in the solid state. This apparent oxidation of iron is supported by the fact that if the reaction mixture is left stirring for several hours at room temperature some reduction of $[Sm^{(III)}(Tp^{Me,Me})_2Cl]$ to $[Sm^{(II)}(Tp^{Me,Me})_2]$ occurs, as evidenced by the formation of a purple insoluble material, presumably with concomitant formation of potassium chloride.

$$2\,[Sm(Tp^{Me,Me})_2Cl] + 2\,K[FeCp(CO)_2] \rightarrow 2\,[Sm(Tp^{Me,Me})_2] + [FeCp(CO)_2]_2 + 2\,KCl$$

This hypothesis also correlates with our inability to isolate $[Sm(Tp^{Me,Me})_2][FeCp(CO)_2]$ from the electron transfer reaction of $[Sm(Tp^{Me,Me})_2]$ with $[FeCp(CO)_2]_2$ (*vide infra*).

Attempted preparation of $[Sm(Tp^{Me,Me})_2]_2[Fe(CO)_4]$

The reaction of two equivalents of $[Sm(Tp^{Me,Me})_2Cl]$ with $Na_2Fe(CO)_4$ in toluene afforded very low yields of an off-white powder which displayed one fairly intense band at 1874 cm^{-1} and three weak bands at 2000, 1906 and 1747 cm^{-1} in the infrared spectrum, as well as two B–H stretches at 2572 and 2523 cm^{-1}. The same reaction carried out in THF/Et_2O gave a product of similar appearance, but the infrared spectrum exhibited a number of B–H stretching bands in the region 2562 - 2524 cm^{-1} and the low frequency ν_{CO} was no longer present. The low yields prevented satisfactiory characterisation by elemental microanalysis or NMR spectroscopy. Attempts to crystallise the product from toluene and diethyl ether solutions were not successful, precluding crystallographic studies.

Electron Transfer reactions of $[Sm(Tp^{Me,Me})_2]$

The use of cyclopentadienyl and halide complexes of divalent lanthanides in electron transfer routes, with concomitant oxidation of Ln(II) to Ln(III), has proved successful in the preparation of a number of transition metal carbonylate species. It was of interest to see whether this type of reactivity was also accessible with the bulky

tris(pyrazolyl)borate ligand system. While $[Sm(Tp^{Me,Me})_2]$ has proved reactive with transition metal carbonyl systems, no reaction has been observed for the analagous $[Yb(Tp^{Me,Me})_2]$ system with $[MoCp(CO)_3]_2$, $Mn_2(CO)_{10}$ or $[FeCp(CO)_2]_2$, indicating that the reduction potential of $[Yb(Tp^{Me,Me})_2]$ is not sufficiently negative to reduce the metal centre and cleave metal-metal bonds in these transition metal carbonyls.

The reaction of $[Sm(Tp^{Me,Me})_2]$ with $[MoCp(CO)_3]_2$ afforded the heterobimetallic complex $[Sm(Tp^{Me,Me})_2(\mu\text{-OC})MoCp(CO)_2]$ in which the two metal atoms are linked *via* an isocarbonyl bridge.[35] The tungsten analogue has also been prepared and is presumed to be isostructural on the basis of infrared and NMR. The reaction of $[Sm(Tp^{Me,Me})_2]$ with $Co_2(CO)_8$, on the other hand, produced $Co_4(CO)_{12}$ and an off white solid formulated to be $[Sm(Tp^{Me,Me})_2][Co(CO)_4]$, owing to the presence of a single sharp ν_{CO} at 1839 cm^{-1} in the infrared spectrum together with appropriate ν_{BH} and ^1H NMR signals. Evidently, while $[MCp(CO)_3]^-$ coordinates to the lanthanide via an isocarbonyl bridge, the $[Co(CO)_4]^-$ anion remains isolated. Evans *et al* made a similar observation in the reaction of $[SmI_2]$ with $Co_2(CO)_8$ which also gave a salt-like product.[34] $[Yb(C_5Me_5)_2]$, on the other hand, yields an isocarbonyl-linked complex, $[Yb(C_5Me_5)_2(\mu\text{-CO})Co(CO)_3]$.[40] It is likely that the Sm–OC link is relatively weak and that the structure of the complex depends on a number of factors, including the charge-to-radius ratio of the metal and the lattice energy of the crystal. In the case of $[Sm(Tp^{Me,Me})_2][Co(CO)_4]$ lattice energy may be maximised with a salt-like structure. Indeed, $[Sm(Tp^{Me,Me})_2]$ seems to favour the formation of salts where the anion is large and reasonably symmetrical, and the separated ion structure has been observed for several complexes, among them $[Sm(Tp^{Me,Me})_2][I]$,[45] $[Sm(Tp^{Me,Me})_2][Te_3Ph_3]$[46] and $[Sm(Tp^{Me,Me})_2][TCNE]$.[47]

Reactions of $[Sm(Tp^{Me,Me})_2]$ with iron carbonyl derivatives

Given our failure to isolate complexes of samarium and ytterbium in salt metathesis reactions with iron carbonyl anions (*vide supra*), the syntheses of a number of iron

carbonylates of $[Sm(Tp^{Me,Me})_2]$ and $[Sm(Tp^{Me,Me,4\text{-}Et})_2]$ *via* the electron transfer route were attempted.

Attempted preparation of $[Sm(Tp^{Me,Me})_2][FeCp(CO)_2]$

The reaction of a slight excess of $[Sm(Tp^{Me,Me})_2]$ with $[FeCp(CO)_2]_2$ afforded a deep red solution. Recrystallisation from petroleum ether afforded a red/brown crystalline solid which exhibited some weak bands in the infrared spectrum consistent with the presence of the $[FeCp(CO)_2]^-$ anion, at 1993, 1952(sh), 1936 and 1757 cm^{-1} although the most intense bands indicated that $[FeCp(CO)_2]_2$ was the major product isolated.

Attempted preparation of $[Sm(Tp^{Me,Me\text{-}4\text{-}Et})_2][FeCp(CO)_2]$

The analogous reaction utilising the soluble samarium pyrazolylborate complex as starting material afforded a deep red product. Weak bands at 1987, 1953 and 1941 cm^{-1} in the carbonyl region of the infrared spectrum of this material were consistent with the presence of the$[FeCp(CO)_2]^-$ anion but the overall appearance of the spectrum was such that it was almost superimposable with that for $[FeCp(CO)_2]_2$. The three intense bands displayed were in the form of doublets, presumably due to solid state effects.

Reaction of $[Sm(Tp^{Me,Me})_2]$ and $[Sm(Tp^{Me,Me,4\text{-}Et})_2]$ with $[Fe(CO)_5]$

On stirring $[Sm(Tp^{Me,Me})_2]$ and $Fe(CO)_5$ in toluene the purple colour disappeared and a yellow/orange solution was formed. Filtration, followed by cooling a toluene solution to -30°C, afforded a pink microcrystalline product which lost solvent, becoming opaque on drying under vacuum. Since the resulting solid was insoluble in hydrocarbon solvents, the analogous reaction utilising the more soluble $[Sm(Tp^{Me,Me,4\text{-}Et})_2]$ starting material was carried out, reacting in the same way. The reaction product was, however, also quite insoluble. The toluene reaction solution and solid state infrared spectra of both compounds were quite complex, exhibiting a large number of stretches in the carbonyl region. Both complexes displayed infrared bands at similar frequencies, *ca.* 2000 and 1880 cm^{-1} but were not otherwise superimposable. The insolubility of the complexes precluded NMR spectroscopic studies beyond identification of the

resonances associated with the pyrazolyborate ligands in the ^1H NMR spectrum. The insolubility of the products in hydrocarbon solvent suggests they might be salt-like; if this is the case the large number of infrared bands observed (including bands at the lower wavenumbers associated with bridging carbonyls) indicates that the carbonyl-containing species is not uncoordinated $Fe(CO)_4^{2-}$ or $Fe(CO)_5^-$, which should display only 1 or 2 bands respectively. Although elemental microanalysis was consistent with the compositions $\{[Sm(Tp^{Me,Me})_2][Fe(CO)_5]\}_3.(C_7H_8)_2$ and $[Sm(Tp^{Me,Me,4\text{-}Et})_2][Fe(CO)_5]$, the formulation of the complexes as $[Sm(Tp^{Me,Me,R})_2]_2[Fe_3(CO)_{11}](C_7H_8)_2$ (R = H, Et) also correlated well with the elemental analysis data and avoids invoking the 19 electron species $[Fe(CO)_5]^-$. The trinuclear iron carbonyl anion $[Fe_3(CO)_{11}]^{2-}$ has previously been isolated by Andersen *et al* from $Yb(C_5Me_5)_2.OEt_2$ reduction of $Fe(CO)_5$ and $Fe_2(CO)_9$ and exhibits three infrared bands at high frequency (2048, 1998 and 1973 cm^{-1}) and two at low frequency (1667 and 1604 cm^{-1}). Whilst the samarium complexes display several CO stretches at high wavenumber, the bands at low wavenumber are quite weak and broad. The composition of these products therefore remains to be confirmed.

Attempted reaction with $Fe_2(CO)_9$

Only starting materials were recovered from the reaction of $[Sm(Tp^{Me,Me})_2]$ with $Fe_2(CO)_9$, even on heating or irradiating the reaction mixture.

Reactivity with group 7 metal carbonyls

Synthesis of $[Sm(Tp^{Me,Me})_2][Mn(CO)_5]$, 3.3

Stirring purple $Sm(Tp^{Me,Me})_2$ with freshly recystallized $[Mn_2(CO)_{10}]$ in toluene at -80°C and allowing the reaction mixture to warm to room temperature overnight yielded a yellow/orange solution from which yellow crystals were isolated by cooling to low temperature. Elemental analysis of this product showed that it could be formulated as $[Sm(Tp^{Me,Me})_2][Mn(CO)_5]$. The solid state infrared spectrum displayed ν_{BH} at 2564 cm^{-1} and ν_{CO} at 1911, 1887 and 1852 cm^{-1}, consistent with terminal carbonyl groups on

an anionic metal rather than with isocarbonyls as seen previously for $(C_5Me_5)_2YbMn(CO)_5$.[24] The presence of bands at 1980 - 1950 and 1738 cm^{-1} in both solid state and solution infrared spectra suggests that small amounts of a secondary product containing a bridging carbonyl group are also formed. Reaction of the yellow material with sodium tetraphenylborate afforded a colourless product which exhibited an infrared spectrum with loss of all the bands in the carbonyl region and a fingerprint region superimposable with the $[Sm(Tp^{Me,Me})_2][Mn(CO)_5]$ starting material; this indicates that **3.3** is a salt-like product containing a manganese carbonyl anion, presumably $[Mn(CO)_5]^-$ on the basis of stoicheiometry. This counterion can be exchanged for the tetraphenylborate anion in a straightforward metathesis reaction with sodium tetraphenylborate. $[Sm(Tp^{Me,Me})_2][BPh_4]$ has been previously prepared from $[Sm(Tp^{Me,Me})_2]$ by reaction with $AgBPh_4$.[48]

X-ray structure of 3.3

The crystals diffracted weakly but the resulting structure clearly showed the connectivity of the compound and confirmed it to be salt-like, $[Sm(Tp^{Me,Me})_2][Mn(CO)_5]$. The molecular structure is shown in Fig. 3.12. The cation is essentially identical to those observed by us and by others in $[Tp^{Me,Me}{}_2Sm]I$, $[Tp^{Me,Me}{}_2Sm]BPh_4$, $[Tp^{Me,Me}{}_2Sm](TePh)_3$, with average Sm–N distance of 2.421 Å (range 2.406(9) to 2.430(9) Å). The counterion is trigonal bipyramidal as expected. No significant interionic interactions were observed. In this respect therefore the reaction proceeds analogously to the reaction with $Co_2(CO)_8$ which yields the salt-like $[Sm(Tp^{Me,Me})_2][Co(CO)_4]$.

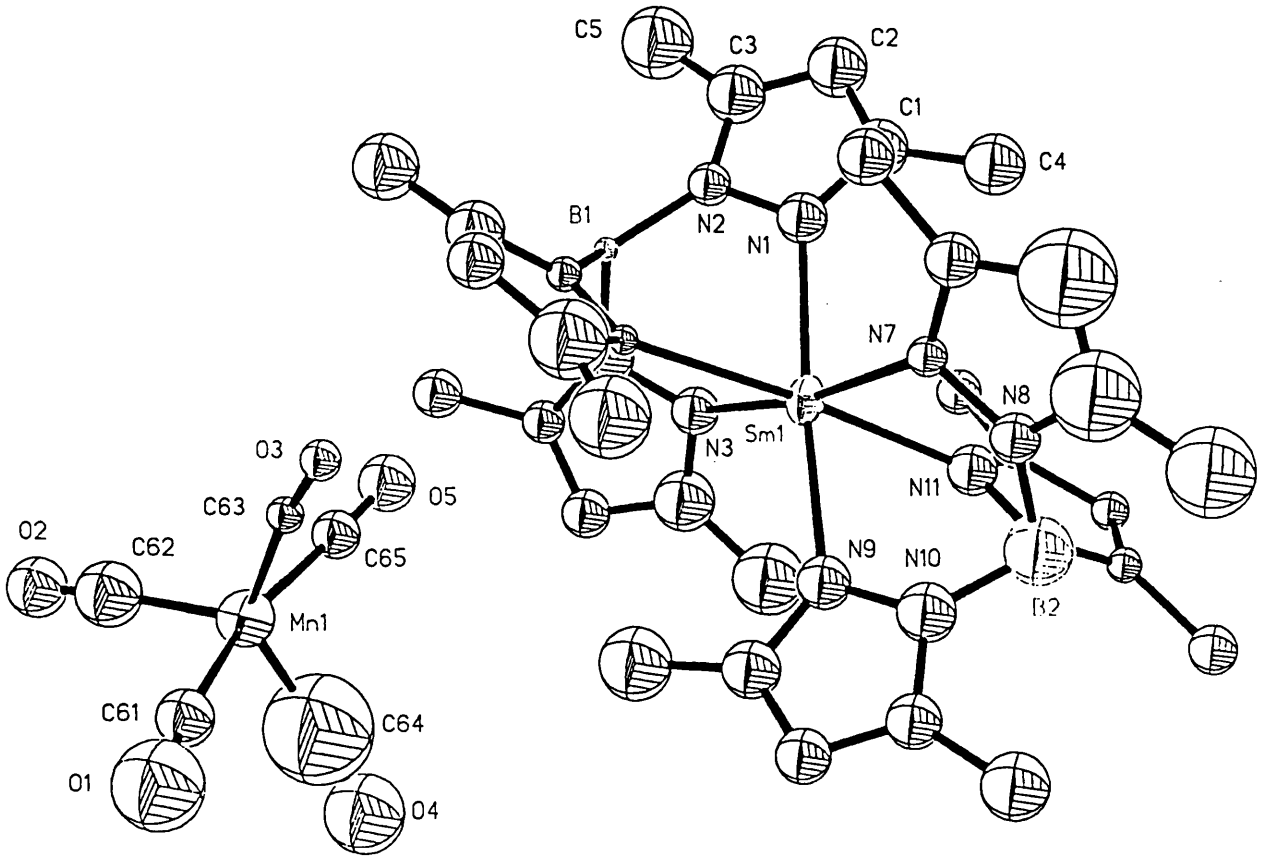

Figure 3.12. X-ray Structure of 3.3.

Synthesis of $[Sm(Tp^{Me,Me})_2]_2(\mu\text{-}O_2CH)][Mn(CO)_5]$, 3.4

During one synthesis of **3.3** yellow crystals were obtained which exhibited both BH and CO peaks in the infrared spectrum but which differed significantly from those of **3.3**.

X-ray structure of 3.4

A single crystal X-ray diffraction study revealed a salt-like structure in which a bimetallic cation, $[(Tp^{Me,Me})_2Sm(\mu\text{-}O_2CH)Sm(Tp^{Me,Me})_2]^+$, crystallizes with $[Mn(CO)_5]^-$ as counterion (figure 3.13). The cation consists of two essentially normal $(Tp^{Me,Me})_2Sm$ units linked by a formate group. The Sm-N distances are in the range 2.435(3) to 2.601(3)Å {Sm(1), average 2.516 Å} and 2.441(3) to 2.591(3) Å {Sm(2), average 2.522 Å), slightly shorter than those observed for **2.1** and $[Sm(Tp^{Me,Me})_2(O\text{-}4\text{-}Bu^t\text{-}C_6H_4)]$[48] (average Sm–N 2.572 Å) but comparable to those observed for the dimeric benzoate bridged complex $[Sm(Tp)_2(\mu\text{-}O_2CPh)]_2$ (2.527 and 2.523 Å).[49] The pyrazolylborate groups on each samarium atom are bent away from the bridging formate group, as measured by the B-Sm-B angles of 147.4 and 149.3° for Sm(1) and Sm(2) respectively. The plane of the formate moiety is almost coplanar with the B-Sm-B planes, at 3.7° to the B-Sm(1)-B plane and at 6.3° to the B-Sm(2)-B plane, nestling between pyrazolyl groups 5 (N9N10) and 6 (N11N12) on Sm(1) and 7 (N13N14) and 9 (N17N18) on Sm(2). Four of the pyrazolyl rings, rings 1, 6, 9 and 10 are somewhat twisted about the B–Sm vector, with torsion angles of 22.4, 20.4, 18.3 and 18.2° respectively, presumably to accommodate the formate anion and to minimise interactions between the two halves of the dimer. The larger torsion angles for the pyrazolylborates attached to Sm(1) correlate with the shorter C(61)–O(1) and Sm(1)–N distances. In this respect the molecule is dissimilar to the pyrazolylborate samarium benzoate complex $[Sm(Tp)_2(\mu\text{-}O_2CPh)]_2$ which exhibits no significant twisting of the pyrazolyl rings.

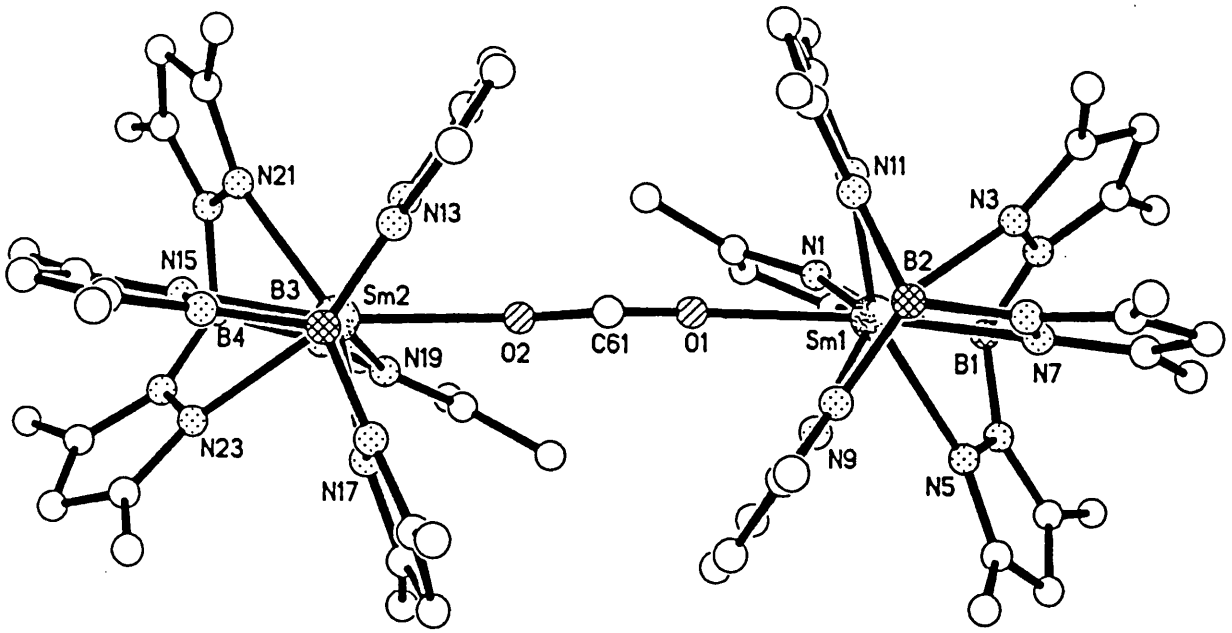

Figure 3.13. X-ray Structure of 3.4.

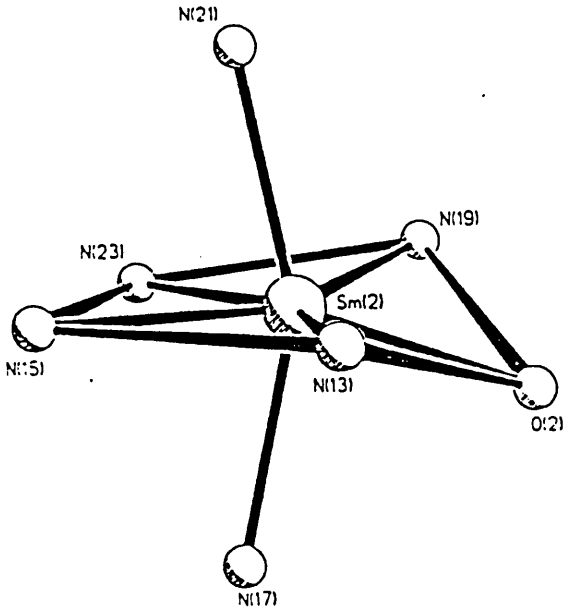

Figure 3.14. Pentagonal bipyramidal geometry in 3.4.

The coordination geometry at each samarium atom is best described as distorted pentagonal bipyramidal (figure 3.14). N(5) and N(11) on Sm(1) and N(21) and N(17) on Sm(2) adopt axial positions, with the equatorial planes defined by O(1), N(1), N(3), N(7) and N(9), or O(2), N(13), N(15), N(23) and N(19) respectively. The arrangement of the ligands around Sm(1) is such that the axial nitrogens are bent away from linearity, with N(5)-Sm(1)-N(11) angle of 155.8° and the mean deviation from the equatorial plane is 0.3009 Å. The equivalent data at Sm(2) are closely similar, N(21)-Sm(2)-N(17) (155.3°) and mean deviation from equatorial plane (0.2701 Å).

The Sm–O distances of 2.344(3) and 2.345(2) Å are comparable to the 2.32(1), 2.30(2), 2.34(2) and 2.38(2) Å observed in the dimeric samarium benzoate complex $[Sm(Tp)_2(\mu\text{-}O_2CPh)]_2$,[49] but shorter than those in other trivalent samarium carboxylates, for example $[Sm(O_2CMe)_4]_2$,[50] (Sm–μ-O 2.402 and 3.074 Å) and $[Sm(O_2CPh)_2(\mu\text{-}O_2CPh)_2]_2$,[51] (average Sm–μ-O 2.38 Å). The samarium atoms are separated by 6.888 Å, a much greater distance than that of 5.42 Å for the doubly bridged dimer $[Sm(Tp)_2(\mu\text{-}O_2CPh)]_2$. The tris(pyrazolyl)borate groups at each samarium are staggered (taking the boron atom as the centre of the ligand), similar to those in $[Sm(Tp)_2(\mu\text{-}O_2CPh)]_2$.

The formate group is unsymmetrical, with C–O distances of 1.230(5) and 1.250(5) Å, slightly longer than those in $[Sm(Tp)_2(\mu\text{-}O_2CPh)]_2$, 1.208 and 1.227 Å in one benzoate moiety and 1.218 and 1.261 Å in the second. The O-C-O angle of 126.3(4)° is comparable to those observed in $[Sm(Tp)_2(\mu\text{-}O_2CPh)]_2$, 124(2) and 121(2)° and to the angles of 124 and 127° in $[Sm(O_2CPh)_2(\mu\text{-}O_2CPh)_2]_2$.

Mechanism of formation of $[Sm(Tp^{Me,Me})_2]_2(\mu\text{-}O_2CH)][Mn(CO)_5]$

The formation of a formate group in this reaction is surprising. We believe that the overall reaction is most likely to be the conversion of carbonyl to formate *via* addition of water. Activation of CO_2, is excluded on the basis of several observations. First, $Sm(C_5Me_5)_2(THF)_2$ reductively couples CO_2 at room temperature to form the oxalate complex $[Sm(C_5Me_5)_2](\mu\text{-}\eta^2\text{:}\eta^2\text{-}O_2CCO_2)$.[52]

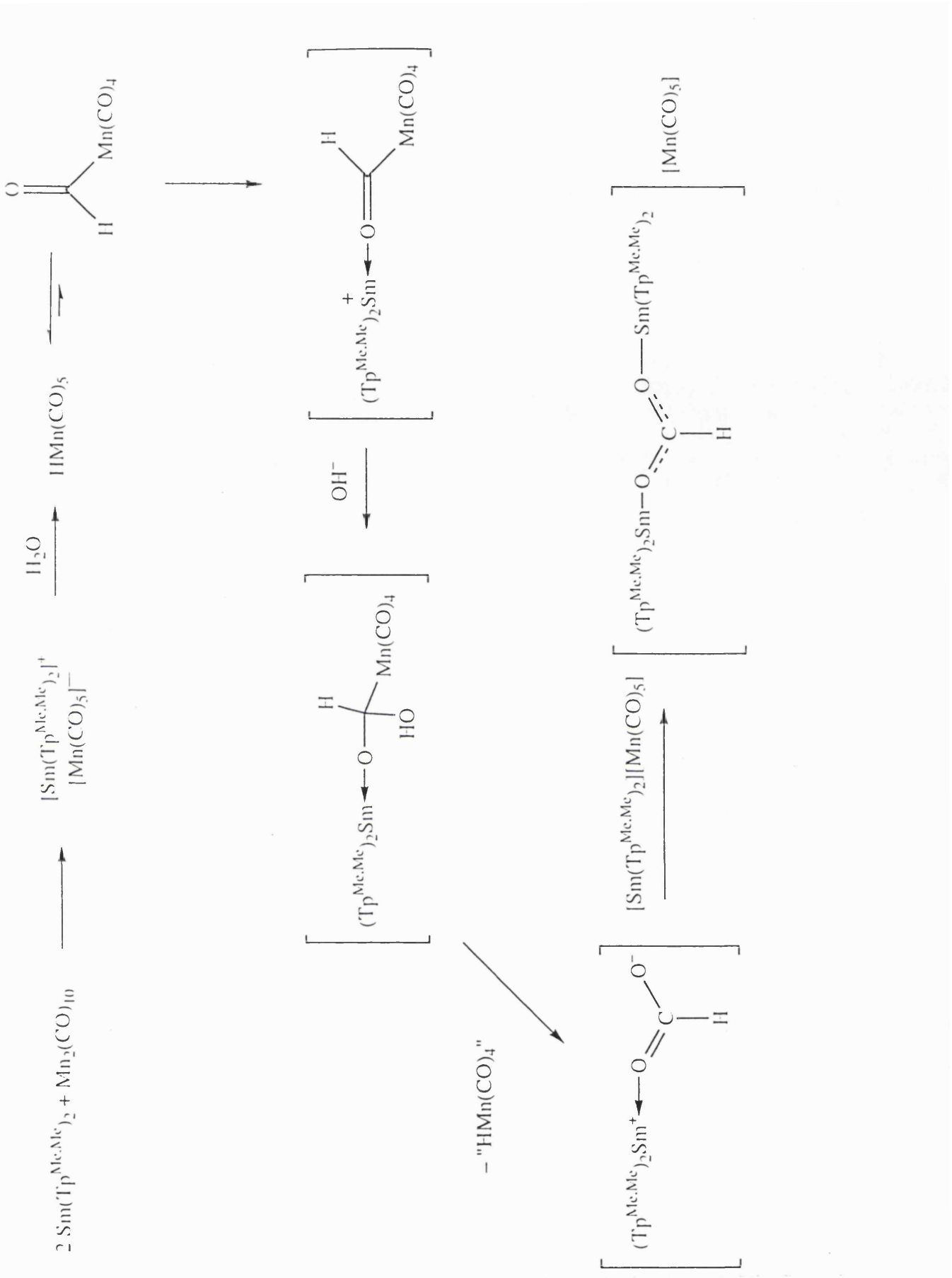

Figure 3.15. Proposed mechanism for CO to formate conversion.

Second, our attempts to activate CO_2 using $Sm(Tp^{Me,Me})_2$ gave very slow reactions and intractable products. Third, atmospheric carbon dioxide, (which should not in any case be present in any quantity), can be excluded since O_2 would react more rapidly to give in the first instance a side-bound O_2, then oxidation products. We therefore suppose the mechanism to involve adventitious water; in this case, several mechanisms can be envisaged. The addition of one oxygen and one hydrogen atom to a carbonyl group is reminiscent of water gas shift chemistry. It is known that neither $Mn_2(CO)_{10}$ nor $Mn(CO)_5^-$ reacts with water to give a formate group. Indeed, this is the first report of the generation of formate with manganese, which suggests that samarium plays a key role in driving the reaction. We are, therefore, suggesting a mechanism which we believe to be the most plausible given the constraints of the system. This is shown in Figure 3.15.

Initial reduction of $Mn_2(CO)_{10}$ by Sm^{2+} cleaves the Mn–Mn bond and affords the anionic $Mn(CO)_5^-$. In rigorously anhydrous conditions the salt **3.3** is obtained. If, however, traces of moisture are present in the solution, the $Mn(CO)_5^-$ anion could be protonated to give $HMn(CO)_5$; this could then insert CO into the Mn–H bond, generating a manganese-bound formyl group. While insertion of CO into metal-alkyl bonds is well precedented,[53,54] formation of formyl by this "direct" method is rarely observed; although many examples of reduction of metal-bound CO to formyl are known, such reactions tend to be intermolecular reductions of coordinated CO effected by the strongly reducing hydrides of, for example, Zr, Ti, B and Al.[3] The Mn–H bond dissociation energy for $HMn(CO)_5$ is 59 kcal/mol - sufficiently high to suggest that insertion of free carbon monoxide to form a formyl derivative should be thermodynamically uphill, even considering the extra energy gained on adding an external ligand.[2,3] This is borne out experimentally; whilst only one example is known involving formation of transition metal formyl complexes by carbonylation of the corresponding hydride,[9] the reverse decarbonylation reaction occurs quite readily.[55]

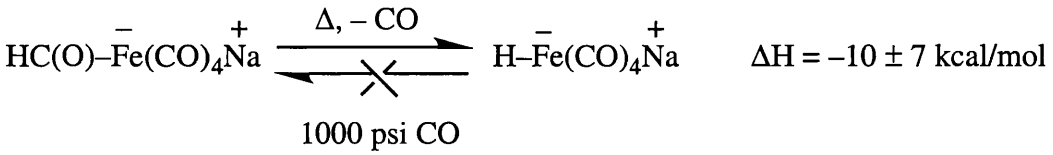

If, on the other hand, the metal involved is sufficiently oxophilic to bind the formyl in the η^2 form, additional driving force for the reaction is provided. This has been found to be the case for the early d-[56,57]and the f-block[4] metals. The mechanism of the reaction of decamethyl zirconocene dihydride with CO, which gives a coordinated enediolate complex (by coupling of the carbene form of the η^2-formyl), is believed to involve insertion of CO into a Zr–H bond to afford an η^2 formyl as shown.[56,57]

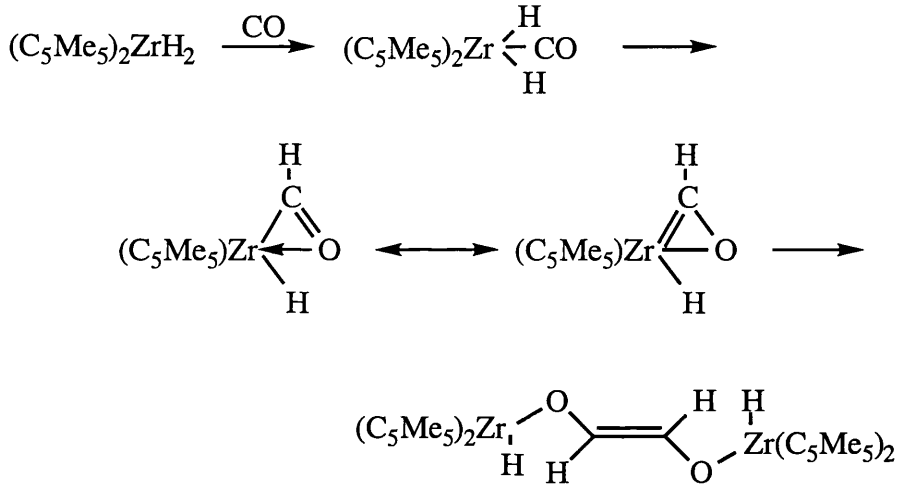

A related, intermolecular, conversion of a coordinated CO to formyl has been observed.[58]

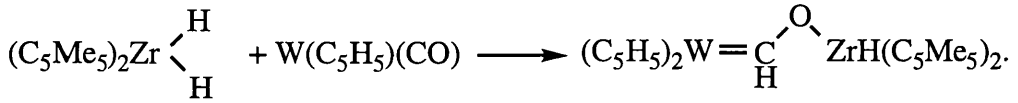

The presence of a Lewis acid is also known to facilitate CO insertion into metal alkyl bonds, presumably *via* a similar mechanism.[6] It is conceivable, therefore, that $HMn(CO)_5$ is in equilibrium with the corresponding formyl (with the equilibrium to the left hand side under normal conditions) and that a strong Lewis acid such as samarium drives the equilibrium to the right hand side.

$$H\text{–}Mn(CO)_5 \leftrightarrow HOC\text{–}Mn(CO)_4$$

A number of steps in the homogeneously catalysed hydrogenation of CO to formaldehyde are believed to be facilitated by coordination of a metal carbonyl with Lewis acids, which are known to promote both migratory insertion and reduction of CO through coordination to oxygen.[3,6]

The bridging Mn-Sm formyl would then be susceptible to attack by a hydroxyl group to give the sp^3 hybridised intermediate shown in figure 3.15. Nucleophilic attack at a formyl carbon by water or hydroxide is in accord with the expected polarisation of the C–O bond. In this case the resulting bridging formate can undergo β-elimination to give the coordinatively unsaturated $[HMn(CO)_4]^-$ fragment, which would be expected to oligomerise and form hydrido- and/or carbonyl-bridged clusters such as $[H_3Mn_3(CO)_{12}]$. This might explain the fact that a small amount of an unidentified red material was always obtained (alongside the yellow product) in the reaction of $[Sm(Tp^{Me,Me})_2]$ with $[Mn_2(CO)_{10}]$. Mass spectrometry of a mixture of the yellow and the red materials shows only the parent ion, $[Sm(Tp^{Me,Me})_2]^+$, and the red product could not be isolated cleanly in sufficient quantity to obtain unambiguous infrared data.

At the same time the samarium formate complex reacts with a further equivalent of $[Sm(Tp^{Me,Me})_2][Mn(CO)_5]$ to give the less soluble $[Sm(Tp^{Me,Me})_2](\mu\text{-}O_2CH)][Mn(CO)_5]$.

A number of reactions was attempted with a view to clarifying the mechanism of the reaction. Addition of water to the reaction solution was not successful, owing to the difficulty in adding sufficiently small quantities to prevent problems with pyrazolylborate hydrolysis. Rinsing the reaction vessel with D_2O, then drying it *in vacuo* before introducing the reagents, afforded red and yellow crystals optically similar to those previously obtained. It was hoped that formation of a deutero-formate (DCO_2) would permit the identification of the infrared band associated with the formate C–H stretch by observing the change in frequency arising from the isotope shift. The infrared spectra of these materials, however, did not differ significantly from those observed in

other reactions and it was not possible to identify a band that had shifted to lower frequency. This is not altogether surprising since the formate C–H stretch is not expected to give rise to an intense band and the C–D stretch should fall at the higher frequency end of the carbonyl range, possibly obscured, therefore, by a carbonyl peak. Alternative methods included the use of unrecrystallised $Mn_2(CO)_{10}$ in a well flamed schlenk and recrystallised $Mn_2(CO)_{10}$ in a less well dried reaction flask, again giving material that exhibited essentially identical infrared spectra to those observed previously.

Whereas most of the known dimeric carboxylate or oxalate bridged samarium pyrazolylborate complexes possess two bridging groups, in this case only a single formate group links the two metal centres, with a separate counterion to balance the resulting cationic charge. This difference is attributed to the different mode of formation of complex **3.4** since on steric grounds the 8-coordination at samarium in either the monomeric complex $[Sm(Tp^{Me,Me})_2(O_2CH)]$ or the doubly bridged dimer $[\{Sm(Tp^{Me,Me})_2\}_2(\mu\text{-}O_2CH)_2]$ would more effectively saturate the samarium centres. The reaction is not very reproducible as it is difficult to introduce sufficiently small amounts of water to avoid problems with pyrazolylborate hydrolysis.

There is, to our knowledge, only one example of CO to formate conversion by a coordination complex in the literature. This occurs during reduction of $Ir_4(CO)_{12}$ by sodium in THF, with the authors believing trace amounts of water in the solvent to be responsible. No mechanism or further details were reported.[59] A number of metal formate complexes has been reported from reactions with formic acid. The reaction between a cobalt hydride complex and carbon dioxide or formic acid affords the corresponding cobalt complex.[60]

$$H(N_2)Co(PPh_3)_3 + CO_2 \text{ or } HCOOH \rightarrow (HCO_2)Co(PPh_3)_3$$

The rhodium (I) complex $Rh(C_6H_4PPh_2)(PPh_3)_2$ is also known to catalyse the decomposition of formic acid to CO_2 and hydrogen. The initial step in the reaction is presumed to be cleavage of the rhodium–σ-carbon bond by formic acid to give the

intermediate $[Rh(HCO_2)(PPh_3)_3]$. This step is followed by β-hydrogen elimination to afford the metal hydride, which reacts with a further molecule of formic acid to regenerate $[Rh(HCO_2)(PPh_3)_3]$ and release H_2.[61]

$$Rh(HCO_2)L_3 \rightarrow RhHL_3 + CO_2$$

L = PPh_3

Metal formate complexes have, in addition, been isolated from reactions between formic acid and ruthenium or osmium carbonyls. These have all been reported to possess a monodentate "terminal" formate on the basis of the infrared stretching frequency of the HCO_2 group, typically around 1615 to 1630 cm^{-1}.[61] The possible presence of intermediate complexes containing a formate ligand has been postulated by a number of authors, for example by Darensbourg in phase-transfer-catalysed reactions of hydroxide with metal-bound carbon monoxide, which afford metal hydride as final organometallic product, [62] and by Laine *et al* in the homogeneously catalysed water gas shift reaction utilising $Ru_3(CO)_{12}$/KOH as catalyst.[63]

Our attempts to reproduce the CO to formate conversion have yielded products that exhibit no bands consistent with the presence of formate in the infrared spectra.

Synthesis of $[Sm(Tp^{Me,Me})_2][Re_4H(CO)_{17}]$, 3.5

Given the unusual reactivity observed in reactions of $[Sm(Tp^{Me,Me})_2]$ with $Mn_2(CO)_{10}$, it was of interest to ascertain whether Re exhibited similar chemistry. Stirring purple $[Sm(Tp^{Me,Me})_2]$ with $Re_2(CO)_{10}$ in toluene at 80°C for several hours yielded an orange solution from which orange crystals of $[Sm(Tp^{Me,Me})_2][Re_4H(CO)_{17}]$, **3.5**, could be isolated on cooling to low temperature. Elemental analysis figures were consistent with the composition $[Sm(Tp^{Me,Me})_2]_2[Re_4(CO)_{17}]$. The infrared spectrum shows peaks at 1881, 1919, 1967, 2009, 2031 and 2028 cm^{-1} consistent with terminal carbonyl groups on an anionic multimetallic rather than with the presence of isocarbonyl groups between the d- and f-block elements as seen previously for the products of the electron transfer reactions of divalent ytterbium with $Re_2(CO)_{10}$.[24] The ^1H NMR spectrum showed the

three peaks expected for the $[Sm(Tp^{Me,Me})_2]^+$ unit and a sharp signal at –17 ppm, consistent with a metal hydride.

A red product crystallised alongside the orange crystals, with bands in the carbonyl region at 1892, 1908, 1947, 1972, 1992, 2034 and 2089 cm^{-1} as well as bands associated with the pyrazolylborates. This product is presumably a rhenium cluster of different order, however no further characterisation of this material has been attempted.

X-ray structure of 3.5

Orange crystals of **3.5** grew from toluene in the space group $P\bar{1}$. The structure consists of discrete $[Re_4H(CO)_{17}]^{2-}$ anions with $[Sm(Tp^{Me,Me})_2]^+$ cations and a toluene of solvation with no short interionic contacts. The cations lie on crystallographic inversion centres and are essentially identical to those observed previously in the structures of $[Sm(Tp^{Me,Me})_2]I$,[64] $[Sm(Tp^{Me,Me})_2]BPh_4$,[45] and $[Sm(Tp^{Me,Me})_2](Te_3Ph_3)$.[65] The average metal-nitrogen distance is 2.447 Å, consistent with the trivalent oxidation state of the samarium.

The structure of the anion is shown in figure 3.16 and consists of a spiked triangular array of rhenium atoms, consistent with a 64 electron count, but unusual in rhenium chemistry. The rhenium atom of the spike is equatorial and almost coplanar with the Re_3 triangle (0.086 Å above the plane) in a manner reminiscent of tetraosmium and other clusters.[66] The carbonyl groups on the spike are staggered with respect to those on the adjacent rhenium atom. Thus the 18 electron $Re(CO)_5^-$ unit of the spike may be viewed as acting as a two electron donor at the unsaturated triangular $Re_3H(CO)_{12}$ species with an unsupported dative bond to the triangle, as shown in figure 3.17. The structure is, therefore, in contrast to the only other spiked triangular tetrarhenium clusters, $[Re_4H_4(CO)_{15}]^{2-}$ and $[Re_4H_4(CO)_{15}I]^-$ in which the spiked ruthenium atom is bridged by a hydride to the metal triangle and is in an axial rather than equatorial position.[67] In $[Re_4H_4(CO)_{15}I]^-$,[68] prepared from $[Re_4H_4(CO)_{15}]^{2-}$, the iodide occupies a formerly CO site on the apical rhenium atom and the terminal hydride migrates to bridge the previously unbridged (in $[Re_4H_4(CO)_{15}]^{2-}$) Re–Re bond.

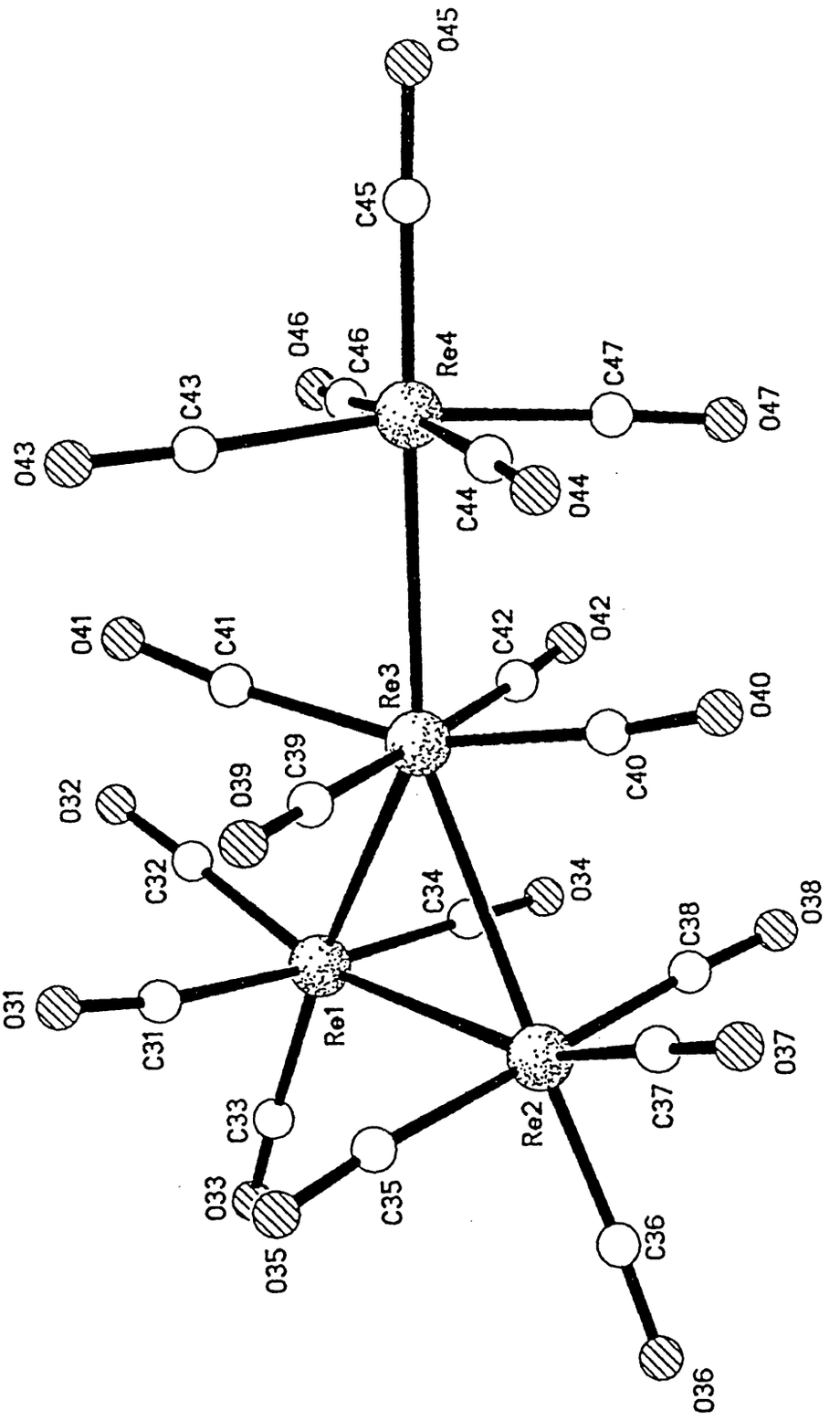

Figure 3.16 X-ray structure of 3.5

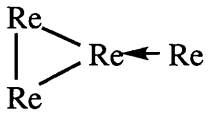

Figure 3.17. Donation from spike to triangle

In the case of **3.5**, evidence for the presence of a hydride was found in the ^{1}H NMR spectrum in acetone-d_6 solution, with a signal at –17 ppm. Although the hydride has not been located in the X-ray structure and the Re–Re bonds are all much the same length, the disposition of the carbonyl groups within the cluster indicates that the most probable location is bridging between the two rhenium atoms opposing the spike, Re(1) and Re(2). The symmetrical nature of the Re(4)$(CO)_5$ unit with respect to the Re(1)Re(2)Re(3) triangle suggests that there is no μ–H along Re(3)–Re(4), Re(1)–Re(3) or Re(2)–Re(3). The "top" and the "bottom" of the triangle Re(1)Re(2)Re(3) appear much the same, which tends to rule out a triply-bridging μ_3-H since this would open up the face on which it was bridged. The Re-Re-CO angles for the equatorial carbonyls are larger for Re(1)–Re(2) than for Re(1)–Re(3) and Re(2)–Re(3) (110.3 and 110.6 compared with 97.7 and 100.8). This extra 10° indicates the Re(1)–Re(2) edge is bridged. The Re(1)–Re(2) bond, at 3.0659(6) Å, is not significantly longer than the other, non-hydride bridged, Re–Re distances in the triangle as might be expected on the evidence of the previously X-ray characterised ReH(CO) spiked triangular clusters. Although it is slightly longer than the Re(1)–Re(3) distance of 3.0610(6) Å, it is, in fact, comparable to the Re(2)–Re(3) bond (3.0776(6) Å). It is also considerably shorter than the hydride-bridged Re–Re bonds on the triangle in $[Re_4H_4(CO)_{15}]^{2-}$, (3.192(8) and 3.211(8) Å). In **3.5** the average rhenium-rhenium bond distance in the triangle is 3.068 Å, somewhat longer than in $Re_2(CO)_{10}$ (3.02 Å)[69] and $[Re_4(CO)_{16}]^{2-}$ (2.98-3.02 Å) [70] and for the non-hydride-bridged Re–Re bond in $[Re_4H_4(CO)_{15}]^{2-}$ (3.032(8) Å).

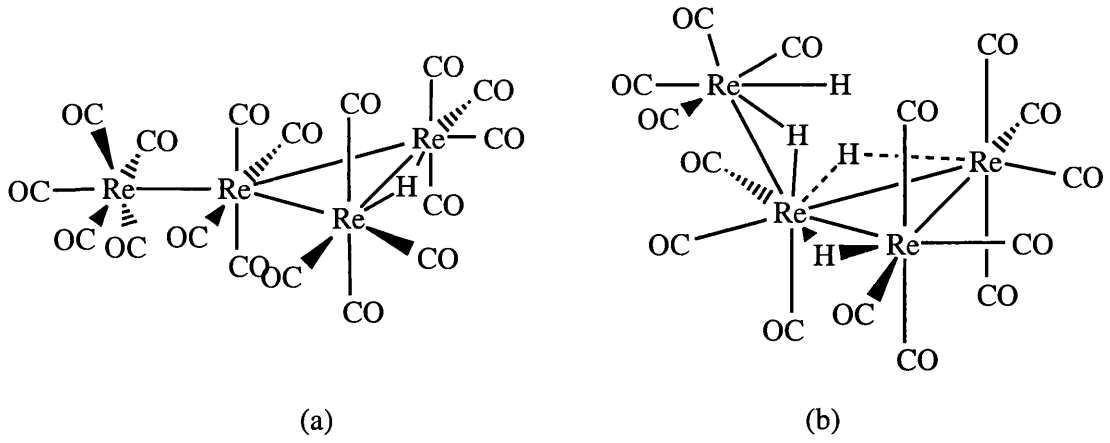

Figure 3.18 (a) $[Re_4H(CO)_{17}]^-$ (b) $[Re_4H_4(CO)_{15}]^{2-}$

The fact that all the Re–Re bonds are particularly long could explain why there is little lengthening of the Re(1)–Re(2) bond on introducing a hydride bridge. The distance from the spike to the triangle is significantly shorter than the bonds in the triangle, 3.0392(6) Å, in contrast to the equivalent, but hydride-bridged, Re–Re separation in $[Re_4H_4(CO)_{15}]^{2-}$ (3.288(9) Å) which is longer than the hydride-bridged metal-metal distances on the triangle. This is suggestive of strong donation from the 18 electron $[Re(CO)_5]^-$ unit to the $[Re_3H(CO)_{12}]^-$ triangle (Figure 3.17). In contrast to the osmium triangles described by Pomeroy, for example $[Os_4(CO)_{15}(PMe_3)]$, which exhibits a longer Os–Os bond *cis* to the (spike) phosphine substituent and a shorter *trans* Os–Os distance (2.923(1) and 2.849(1) Å respectively) no particular shortening of any Re-Re bond is observed. It should, however, be noted that the spike in the osmium clusters is significantly bent towards the *cis*-$Os(CO)_4$ unit, with Os-Os-Os angles of 60.17(3) (*cis*) and 165.32(3)° (*trans*) respectively. No significant leaning of the $Re(4)(CO)_5$ moiety is observed for **3.5** {Re(4)-Re(3)-Re(2) 148.098(19)°, Re(4)-Re(3)-Re(1) 151.897(19)°}, presumably because the spike substituents are all equivalent.

The chemistry of 64-electron M_4 clusters has attracted considerable interest because of the different topologies possible when linking four metal centres through four bonds.[71] For a tetrahedral cluster the EAN rule requires a total of 60 electrons. If the cluster is

electron deficient, containing fewer then 60 electrons, formation of metal-metal multiple bonds can occur. Electron rich tetrametallic clusters with electron count greater than 60, on the other hand, need to break metal-metal bonds. In a 64 electron complex, therefore, two of the tetrahedral edges are cleaved. Most tetranuclear metal carbonyl clusters with 64 valence electrons adopt either the puckered square or spiked-triangular geometry, structures which may indeed be derived from a tetrahedron via cleavage of two metal-metal bonds and these have been identified for a range of transition metals.[72] Each structure contains four metal-metal bonds. In the case of rhenium only a relatively small number of tetranuclear clusters has been identified,[72,73] only two of which adopt the spiked triangle structure. Pomeroy has argued convincingly that in tetra-osmium clusters, $Os_4(CO)_{15}(L)$, the spike acts as a two electron donor to the remaining triangular framework *via* an unbridged, dative metal-metal bond.[74] He concludes that the electron-richness of the cluster, which differs only with the electronic properties of L, is of greater importance in determining the structure adopted than are steric considerations arising from the ligand L. Thus in osmium chemistry the structure can be tuned simply by altering the equatorial (L) substituents on the spike. [66,74] With good σ donors, such as trialkylphosphines and isonitriles, a spiked triangle is isolated, while with better π-acceptors such as CO and PF_3 a closed square structure results. In the present case, presumably the anionic nature of the cluster is sufficient to tip the balance in favour of the spiked structure.

Compound **3.5** appears to be quite thermally stable, since it is prepared in toluene at 80°C. There are several theoretical studies that suggest that in trinuclear clusters an important component of the metal-metal bonding is provided by a central molecular orbital, together with edge-bridging molecular orbitals (figure 3.18).

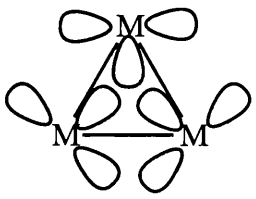

Figure 3.18. Metal-metal bonding in triangular clusters.

The occupancy of this orbital contributes significantly to the stability of the cluster, hence a spike moiety which is a good donor could be expected to stabilise a spiked triangle in preference to a puckered square geometry.

The mechanism of formation of the cluster is unclear since the stoicheiometry of the reaction itself leads to the expectation of $Re(CO)_5^-$ as the principal product while the formation of $[Re_4H(CO)_{17}]^-$ requires the addition of one electron and a hydride, together with the loss of three carbonyl units. This suggests that the formation of this M_4 cluster may be related to the rate at which the samarium(II) reagent is able to transfer electrons to the rhenium starting material. Owing to the extreme insolubility of the $[Sm(Tp^{Me,Me})_2]$ starting material in common solvents, the rate of electron transfer may be assumed to be quite slow, allowing time for carbonyl elimination to occur. It is believed that originally $[Sm(Tp^{Me,Me})_2]_2[Re_4(CO)_{17}]$ is formed and the hydride is thought to derive from attack by adventitious water present during recrystallisation, since the original elemental analysis figures for rwo batches are consistent with the composition $[Sm(Tp^{Me,Me})_2]_2[Re_4(CO)_{17}]$.

The synthesis of transition metal cluster compounds is an area of wide interest to inorganic and materials chemists. A number of methods have been developed for the synthesis of large clusters. These include ligand dissociation via photolysis, thermolysis, or chemically-induced ligand elimination using reagents such as trimethylamine-N-oxide, or by displacement of anionic and weakly coordinated ligands. Oligomerization of unsaturated or multiply-bonded systems provides another approach to the creation of larger clusters. In some case the use of potentially bridging ligands encourages the formation of M-M bonds.[71] Redox condensation reactions initiated by electron transfer have been used to synthesize clusters either by conproportionation or through carbonyl labilization. Sodium benzophenone ketyl has been widely used for such reactions. The reaction of sodium with $M_3(CO)_{12}$ (M = Ru, Os) at reflux in THF gives good yields of $[M_6(CO)_{18}]^{2-}$.[75] The reduction of $Re_2(CO)_{10}$ with sodium in glyme-like solvents results in the efficient formation of $[Re_4(CO)_{16}]^{2-}$ [76] and, at higher temperatures, of the carbido clusters $[HRe_6C(CO)_{18}]^{3-}$ and $[HRe_5C(CO)_{16}]^{2-}$.[77]

The use of samarium(II) as a mild one-electron reducing agent in organic chemistry suggests that it might have a useful role as an alternative reductant in cluster synthesis. The formation of the $[Re_4H(CO)_{17}]^-$ cluster, of a structure only rarely observed in rhenium chemistry and without a supporting hydride bridge to the spike, suggests that samarium(II) reagents may provide a possible alternative to other more powerful reducing agents such as sodium or sodium benzophenone ketyl for the preparation of higher clusters.

Conclusions

In this chapter the syntheses and X-ray characterisation of the half-sandwich complexes $[LnTp^{t\text{-}Bu,Me}(THF)(\mu\text{-}OC)_2Mo(\eta\text{-}C_5H_4CH_3)(CO)]_2$, Ln = Sm, **3.1**; Ln = Yb, **3.2**, have been described, as has their reactivity with pyridine. The results of attempts to prepare half-sandwich and sandwich complexes of Sm with iron carbonyls has been described. $Yb(Tp^{Me,Me})$ has been found to be insufficiently reactive to prepare transition metal carbonylate complexes via reductive routes. The preparation of the sandwich complex $[Sm(Tp^{Me,Me})_2][Mn(CO)_5]$, (**3.3**) by reduction of $Mn_2(CO)_{10}$, has been described, as well as the isolation and X-ray characterisation of the dimeric formate-bridged compound **3.4**. A mechanism for the formation of **3.4** has been proposed, based on the intervention of adventitious water. This unusual transformation of CO to formate is believed to be dependent on the presence of the Lewis acidic Sm with the manganese carbonyl species and illustrates the potential of such heterobimetallic systems in the activation of small molecules. The formation of a new rhenium cluster $[Re_4H(CO)_{17}]^-$ with spiked triangle structure has also been achieved, (**3.5**) presumably owing to the mildly reducing conditions provided by Sm(II) and to the preference of the large $[Sm(Tp^{Me,Me})_2]$ cation for a large anion.

Chapter 3 - References

1) Elschenbroich, C.; Salzer, A. *Organometallics. A Concise Introduction*; VCH Publishers (UK) Ltd.: Cambridge, 1989.

2) Crabtree, R. H. *The Organometallic Chemistry of the Transition Metals 2nd Edition*; Wiley Interscience:, 1994.

3) Collman, J. P.; Hegedus, L. S.; Norton, J. R.; Finke, R. G. *Principles and Applications of organotransition metal chemistry*; University Science books: Mill Valley, California.

4) Manriquez, J. M.; Fagan, P. J.; Marks, T. J.; Day, C. S.; Day, V. W. *J. Am. Chem. Soc.* **1978**, *100*, 7112.

5) Longato, B.; Norton, J. R.; Huffman, J. C.; Marsella, J. A.; Caulton, K. G. *J. Am. Chem. Soc.* **1981**, *103*, 209.

6) Butts, S. B.; Holt, E. M.; Strauss, S. H.; Alcock, N. W.; Stimson, R. E.; Shriver, D. F. *J. Am. Chem. Soc.* **1979**, *101*, 5864.

7) Gladysz, J. A. *Adv. Organomet. Chem.* **1982**, *20*, 1.

8) Berke, H.; Hoffmann, R. *J. Am. Chem. Soc.* **1978**, *100*, 7224.

9) Belmonte, P. A.; Cloke, F. G. N.; Schrock, R. R. *J. Am. Chem. Soc.* **1983**, *105*, 2643

10) Fagan, P. J.; Moloy, K. G.; Marks, T. J. *J. Am. Chem. Soc.* **1981**, *103*, 6959.

11) Reppe, J. W. *Annalen* **1953**, *582*, 121.

12) Yoshida, T.; Ueda, Y.; Otsuka, S. *J. Am. Chem. Soc.* **1978**, *100*, 3941.

13) Slegeir, W. A. R.; Sapienza, R. S.; Rayford, R.; Lam, L. *Organometallics* **1982**, *1*, 1728.

14) King, J., A. D. ; King, R. B.; Yang, D. B. *J. Am. Chem. Soc.* **1981**, *103*, 2699.

15) Darensbourg, D. J.; Rokicki, A. *Organometallics* **1982**, *1*, 1685.

16) Bursten, B. E.; Gatter, M. G. *J. Amer. Chem. Soc.* **1984**, *106*, 2554.

17) Shriver, D. F. *J. Organomet. Chem.* **1975**, *94*, 259.

18) Marks, T. J.; Kristoff, J. S.; Alich, A.; Shriver, D. F. *J. Organomet. Chem.* **1971**, *33*, C35.

19) Nelson, N. J.; Kime, N. E.; Shriver, D. F. *J. Am. Chem. Soc.* **1969**, *91*, 5173.

20) Peterson, R. B.; Stezowski, J. J.; Wan, C.; Burlitch, J. M.; Hughes, R. E. *J. Am. Chem. Soc.* **1971**, *93*, 3532.

21) Ulmer, S. W.; Skarstad, P. M.; Burlitch, J. M.; Hughes, R. E. *J. Am. Chem. Soc.* **1973**, *95*, 4469.

22) Berry, D. H.; Bercaw, J. E.; Jircitano, A. J.; Mertes, K. B. *J. Am. Chem. Soc.* **1982**, *104*, 4712.

23) Barger, P. T.; Bercaw, J. E. *J. Organomet. Chem.* **1980**, *201*, C39.

24) Boncella, J. M.; Andersen, R. A. *Inorg. Chem.* **1984**, *23*, 432.

25) Crease, A. E.; Legzdins, P. *J. Chem. Soc.,Chem. Commun.* **1972**, 268.

26) Crease, A. E.; Legzdins, P. *J. Chem. Soc., Dalton Trans.* **1973**, 1501.

27) Hazin, P. N.; Huffman, J. C.; Bruno, J. W. *J. Chem. Soc.,Chem. Commun.* **1988**, 1473.

28) Hou, Z. M.; Aida, K.; Takagi, Y.; Wakatsuki, Y. *J. Organomet. Chem.* **1994**, *473*, 101.

29) Deng, H.; Shore, S. G. *Inorg. Chem.* **1996**, *35*, 3891.

30) Deng, H.; Shore, S. G. *J. Amer. Chem. Soc.* **1991**, *113*, 8538.

31) Recknagel, A.; Steiner, A.; Brooker, S.; Stalke, D.; Edelmann, F. T. *Chem. Ber.* **1991**, 1373.

32) Boncella, J. M.; Andersen, R. A. *J. Chem. Soc.,Chem. Commun.* **1984**, 809.

33) Lin, G.; Wong, W. T. *J. Organomet. Chem.* **1996**, *522*, 271.

34) Evans, W. J.; Bloom, I.; Grate, J. W.; Hughes, L. A.; Hunter, W. E.; Atwood, J. L. *Inorg. Chem.* **1985**, *24*, 4620.

35) Hillier, A. C.; Liu, S.-Y.; Sella, A.; Zekria, O.; Elsegood, M. R. J. *J. Organomet. Chem.* **1997**, *528*, 209.

36) Tilley, T. D.; Andersen, R. A. *J. Amer. Chem. Soc.* **1982**, *104*, 1772.

37) Beletskaya, I. P.; Voskoboynikov, A. Z.; Chuklanova, E. B.; Kirillova, N. I.; Shestakova, A. K.; Parshina, I. N.; Gusev, A. I.; Magomedov, G. K.-I. *J. Amer. Chem. Soc.* **1993**, *115*, 3156-3166.

38) Apostolidis, C.; Rebizant, J.; Kanellakopoulos, B.; Ammon, R. V.; Dornberger, E.; Müller, J.; Powietzka, B.; Nuber, B. *Polyhedron* **1997**, *16*, 1057.

39) Evans, W. J.; Anwander, R.; Ansari, M. A.; Ziller, J. W. *Inorg. Chem.* **1995**, *34*, 5-6.

40) Tilley, T. D.; Andersen, R. A. *J. Chem. Soc.,Chem. Commun.* **1981**, 985.

41) Lukehart, C. M. *Fundamental Transition Metal Organometallic Chemistry*; Brooks Cole: Belmont, CA, 1985.

42) Maunder, G. H.; Sella, A.; Tocher, D. A. *J. Chem. Soc.,Chem. Commun.* **1994**, 2689-2690.

43) Zhang, X. W.; McDonald, R.; Takats, J. *New J. Chem.* **1995**, *19*, 573-585.

44) Maunder, G.; Sella, A.; Takats, J.; Zhang, X. *unpublished results.*

45) Marques, N. *personal communication.*

46) Liu, S.-Y. *PhD thesis*; University of London, 1996.

47) Maunder, G. H. *PhD thesis*; University of London, 1995.

48) Takats, J., *personal communication.*

49) Reger, D. L.; Knox, S. J.; Lindemann, J. A.; Lebioda, L. *Inorg. Chem.* **1990**, *29*, 416.

50) Lossin, A.; Meyer, G.; Fuchs, R.; Strahle, J. *Z. Naturforsch, Teil. B* **1992**, *47*, 179.

51) Moore, J. W.; Glick, M. D.; Baker Jr, W. A. *J. Am. Chem. Soc.* **1972**, *94*, 1858.

52) Evans, W. J.; Seibel, C. A.; Ziller, J. W. *Inorg. Chem.* **1998**, *37*, 770.

53) Calderazzo *Angew. Chem. Int. Ed. Engl.* **1977**, *16*, 299.

54) Wojcicki, A. *Adv. Organomet. Chem.* **1973**, *11*, 87.

55) Lane, K. R.; Sallans, L.; Squirer, R. R. *Organometallics* **1985**, *4*, 408.

56) Bercaw, J.; *et al. J. Am. Chem. Soc.* **1976**, *98*, 6733.

57) Bercaw, J.; *et al. J. Am. Chem. Soc.* **1974**, *96*, 5087.

58) Wolczanski, P. T.; Threlkel, R. S.; Bercaw, J. E. *J. Am. Chem. Soc.* **1979**, *101*, 218.

59) Angoletta, M.; Malatesta, L.; Caglio, G. *J. Organomet. Chem.* **1975**, *94*, 99.

60) Pu, L. S.; Yamamoto, A.; Ikeda, S. *J. Am. Chem. Soc.* **1968**, *90*, 3896.

61) Strauss, S. H.; Whitmire, K. H.; F., S. D. *J. Organomet. Chem.* **1979**, *174*, C59.

62) Darensbourg, D. J.; Baldwin, B. J.; Froelich, J. A. *J. Am. Chem. Soc.* **1980**, *102*, 4688.

63) Laine, R. M.; Pinker, R. G.; Ford, P. C. *J. Am. Chem. Soc.* **1977**, *99*, 252.

64) Liu, S. Y.; Maunder, G. H.; Day, V. W.; Sella, A.; Takats, J.; Marques, N.; Santos, I. *manuscript in preparation.*

65) Hillier, A. C.; Liu, S. Y.; Marques, N.; Sella, A.; Elsegood, M. R. J. *manuscript in preparation* .

66) Einstein, F. W. B.; Johnston, V. J.; Pomeroy, R. K. *Organometallics* **1990**, *9*, 2762.

67) Albano, V. G.; Ciani, G.; Freni, M.; Romiti, P. *J. Organomet. Chem.* **1975**, *96*, 259.

68) Ciani, G.; D'Alfonso, G.; Freni, M.; Romiti, P.; Sironi, A. *J. Organomet. Chem.* **1979**, *170*, C15.

69) Dahl, L. F.; Ishishi, E.; Rundle, R. E. *J. Chem. Phys.* **1957**, *26*, 1750.

70) Churchill, M. R.; Bau, R. *Inorg. Chem.* **1968**, *7*, 2606.

71) Shriver, D. F.; Kaesz, H. D.; Adams, R. D. *The Chemistry of Metal Cluster Complexes*, VCH, New York, 1990.

72) Henly, T. J. *Coord. Chem. Rev.* **1989**, *93*, 269.

73) O'Connor, J. M. *Comp. Organomet. Chem. II* , Pergamon, **1995**, Vol. 6, Chapter 9.

74) Einstein, F. W. B.; Johnston, V. J.; Ma, A. K.; Pomeroy, R. K. *Organometallics* **1990**, *9*, 52.

75) Hayward, C.-M. T.; Shapley, J. R. *Inorg. Chem.* **1982**, *21*, 3816.

76) Hayward, C.-M. T.; Shapley, J. R. *Organometallics* **1988**, *7*, 448.

77) Healy, T. J.; Wilson, S. R.; Shapley, J. R. *Inorg. Chem.* **1987**, *6*, 2618.

Chapter 4 - New sandwich and half-sandwich complexes of lanthanides with pyrazolylborates as ancillary ligands.

Introduction

In this chapter we present the results of attempts to prepare mono- and bis(pyrazolylborate)lanthanide complexes with uninegative "X" ligands. The chapter is divided into three sections. The first deals with the preparation of bis(pyrazolylborate)lanthanide complexes [Ln($Tp^{Me,Me}$)$_2$X] (Ln = Sm, X = F, Cl, Br, I, Ph, C≡CPh, O_2CH, O_2CMe, O_2CPh; Ln = Y, X = Cl, I; Ln = Yb, X = Cl). The structural changes that occur in the samarium complexes as a result of increasing ionic radius of the halide ion are noted. The preparation of [Sm($Tp^{Me,Me}$)$_2$]I_3, analogous to the tritelluride complex described by Liu and in Chapter 2, is reported. Attempts to isolate Sm($Tp^{Me,Me}$)$_2$Br are also discussed.

The second section outlines our efforts to produce tractable mono(pyrazolylborate) complexes of Y and Yb (III). The primary motivation for this work was the preparation of a (pyrazolylborate)lanthanide imido complex. Whilst 5f element imido compounds are known, 4f element imidos have yet to be reported. Since there seem no obvious electronic or thermodynamic reasons for the Ln–N imido bond to be intrinsically unstable, it was hoped that by using the bulky substituted $Tp^{Me,Me}$ ligand such an interaction might be stabilised kinetically. This part of the chapter describes the synthetic routes employed, including the attempted preparation of a number of mono(pyrazolylborate) alkyls and amides, and the problems encountered in this work.

In the third section of the chapter, the synthesis and attempted synthesis of a number of mono- and bis(pyrazolylborate)lanthanide borohydrides and aluminohydrides is described. A brief literature survey of organolanthanide borohydride and aluminohydride compounds is included.

A number of the reactions in the latter two sections involved the use of lithium reagents and a particular problem was noted in these routes, namely that the major product in many cases was the ligand redistribution product $LiTp^{Me,Me}$. This has also been observed by Piers *et al.* in mono(pyrazolylborate)scandium chemistry.[1]

Results

Section 1 - Preparation of bis(pyrazolylborate)lanthanide complexes

Bis(pyrazolylborate)samarium halides: halide = F, Cl, I

The preparation of a series of bis(pyrazolylborate)lanthanide halides is of interest, in order to probe the steric demands of the bulky bis($Tp^{Me,Me}$) ligand environment at a single metal centre, changing only the size of the halide, and to make comparisons with analogous bis(cyclopentadienyl)lanthanide complexes. While salt incorporation (formation of "ate" complexes) is quite common for the cyclopentadienyl complexes, it might be expected that the greater steric demand of the bis(pyrazolylborate) ligand system would not permit the inclusion of salt molecules. Similarly, the pyrazolylborate groups are likely to prevent formation of halide bridged dimeric or oligomeric species, owing to repulsive steric interaction between two $[Sm(Tp^{Me,Me})_2]$ groups.

The $[Sm(Tp^{Me,Me})_2]$ halide complexes (X = F, Cl, I) can be prepared from $[Sm(Tp^{Me,Me})_2]$, either by reaction with halocarbon in the case of the fluoro and the chloro complex, or by oxidation with iodine. In the attempted preparation of $[Sm(Tp^{Me,Me})_2(\eta^2\text{-}F_3CC{\equiv}CCF_3)$ by Takats, the Sm (II) abstracted a fluoride ion from $F_3CC{\equiv}CCF_3$. The organic byproduct was not characterised.[2]

$$[Sm(Tp^{Me,Me})_2] + F_3CC{\equiv}CCF_3 \rightarrow [Sm(Tp^{Me,Me})_2F]$$

The complex has since been prepared by reaction of $[Sm(Tp^{Me,Me})_2]$ with PbF_2.[2] Other attempted preparations have been less successful; the extreme insolubility of the

lanthanide trifluorides precluded a metathetical route and an attempted preparation with $NaBF_4$ afforded a white powder which exhibited three bands in the B–H stretching region, suggesting that more than one species is present or possibly that the pyrazolylborate groups in one product are inequivalent in the solid state. The elemental microanalysis figures were not consistent with the product having composition $[Sm(Tp^{Me,Me})_2]F$ or $[Sm(Tp^{Me,Me})_2]BF_4$, although salt incorporation could be responsible for lowering the found values.

Although the chloro compound could be prepared analogously to the fluoride, by removal of a chloride ion from chloroform or other chlorinated hydrocarbons;[2]

$$[Sm(Tp^{Me,Me})_2] + CHCl_3 \rightarrow [Sm(Tp^{Me,Me})_2Cl]$$

a more convenient preparative route is the salt metathesis reaction between $SmCl_3$ and $KTp^{Me,Me}$ in THF, precipitating KCl.

$$SmCl_3 + 2\ KTp^{Me,Me} \rightarrow [Sm(Tp^{Me,Me})_2Cl] + KCl$$

Oxidation of $[Sm(Tp^{Me,Me})_2]$ with elemental iodine in 1:1 Sm:I ratio affords pale yellow $[Sm(Tp^{Me,Me})_2]I$.[3]

$$2\ [Sm(Tp^{Me,Me})_2] + I_2 \rightarrow 2\ [Sm(Tp^{Me,Me})_2]I$$

Increasing the ratio of iodine to samarium to 3:1 resulted in formation of a brown solid which has been formulated as $[Sm(Tp^{Me,Me})_2]I_3$ (**2.8**) on the basis of elemental analysis, infrared and NMR spectroscopy and by comparison with the analogous preparation of $[Sm(Tp^{Me,Me})_2][Te_3Ph_3]$ (see Chapter 2). A single sharp band at 2554 cm^{-1} was displayed in the solid state infrared spectrum, consistent with pyrazolylborate coordinated to samarium. The ^1H and ^{13}C NMR spectra exhibited signals for the pyrazolylborate ligands and no coordinated solvent or other impurities were observed.

$$2\ [Sm(Tp^{Me,Me})_2] + 3\ I_2 \rightarrow 2\ [Sm(Tp^{Me,Me})_2]I_3$$

Structure of Bis(pyrazolylborate)samarium halides: halide = F, Cl, I

X-ray crystallographic studies show that whilst the smaller, harder halides fluoride and chloride form molecular complexes [Sm($Tp^{Me,Me}$)$_2$X], with the halide lying in the inner coordination sphere of the metal (figure 4.1a.), the larger, more polarisable iodide ion remains in the outer coordination sphere, giving a salt-like structure (figure 4.1b).

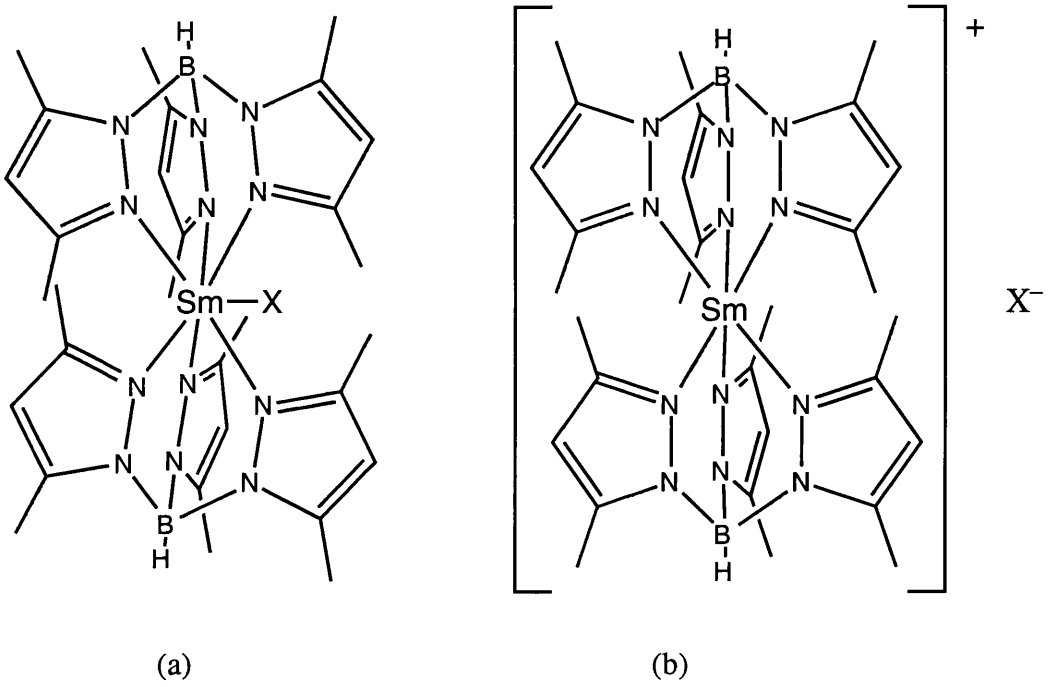

(a) (b)

Figure 4.1. Structure of halide complexes of [Sm($Tp^{Me,Me}$)$_2$] a) X = F, Cl; b) X = I, I_3.

The reason for this disparity is likely to be that the iodide ion is simply too large to be accommodated in the pocket defined at the samarium atom by the methyl groups on the ancillary ligands. In addition, the iodide is not a "hard" enough ligand for trivalent samarium; this is, however, likely to be a secondary factor since lanthanide–iodide bonds are known, for example in [Yb(C_5Me_5)$_2$(μ-I)$_2$Li(OEt_2)$_2$][4] and also by analogy with the formation of the Sm–Te bond in [Sm($Tp^{Me,Me}$)$_2$TePh] (see Chapter 2). The hard-soft mismatch probably contributes to the structure, however, in that it makes for a weaker Sm–X interaction. In this case the steric congestion causes the structure to be salt-like, presumably increasing the electrostatic lattice energy gained by the system.

Bis(pyrazolylborate)samarium halides: halide = Br

The structure of the corresponding bromide has not yet been fully elucidated despite many attempts at preparation and crystallisation. It is noteworthy that the ionic radius of the bromide ion (Br^-, 1.96 Å) is very close to that of Se^{2-} (1.91 Å),[5] so there might be some distortion of the pyrazolylborate groups in $[Sm(Tp^{Me,Me})_2Br]$ of the type observed for $[Sm(Tp^{Me,Me})_2SePh\text{-}4\text{-}Bu^t]$ (**2.4**, see Chapter 2) and $[U(Tp^{Me,Me})_2I]$,[6] rendering the molecule more prone to secondary reactions such as hydrolysis.

A number of routes has been explored for the preparation of $[Sm(Tp^{Me,Me})_2Br]$. Reaction of $[Sm(Tp^{Me,Me})_2]$ with bromocarbons afforded intractable products,[7] as did preparations involving reduction of elemental bromine.

$$[Sm(Tp^{Me,Me})_2] + CHBr_3 \rightarrow ??$$

$$[Sm(Tp^{Me,Me})_2] + Br_2 \rightarrow ??$$

Metathetical reaction of $SmBr_3$ with $KTp^{Me,Me}$ seemed a promising route, although preparation of $SmBr_3$ from Sm metal and bromine in petrol afforded only very low yields.

Quite recently, however, $SmBr_3$ became commercially available. Stirring $SmBr_3$ with two equivalents of $KTp^{Me,Me}$ in THF for 2 days resulted in formation of a white precipitate. Filtration and recrystallisation from THF afforded a white microcrystalline material for which elemental analysis was consistent with the formulation $[Sm(Tp^{Me,Me})_2Br.THF]$.

$$SmBr_3 + 2\ KTp^{Me,Me} \xrightarrow[2\ days]{THF} Sm(Tp^{Me,Me})_2Br.THF$$

The compound appears to decompose progressively in solvent. The ^1H NMR spectrum of a sample in $CDCl_3$ was rather complicated, exhibiting a greater number of resonances than expected. On leaving the chloroform-d solution for 3 days the spectrum was found to be different, with a number of new peaks. The ^1H NMR spectrum of the same compound in benzene-d_6 similarly displayed more signals than expected. The infrared

spectrum was also somewhat complicated, exhibiting, as well as the expected ν_{BH} for pyrazolylborate attached to samarium, a sharp peak at slightly lower frequency and a number of broader bands in the range 2250 - 2550 cm^{-1} which could be due to pyrazole. The presence of a very broad band centred around 1855 cm^{-1} could not be explained, although it is possible that the recrystallised product is in fact the dimeric complex $[(Tp^{Me,Me})\{(pz^{Me,Me})_2B(H)O\}Sm]_2$ (**4.5**) which results from hydrolysis of one pyrazolylborate ligand; this compound has been isolated by us and by other groups on a number of occasions during crystallisation attempts (*vide infra*).[2,3,7-9] Whilst no spectroscopic data has ever been obtained for this complex, it would be expected to exhibit a fairly complex ^1H NMR spectrum; the formation of this compound would also be consistent with the presence of pyrazole (as observed in the infrared spectrum).

Carrying out the same preparation with a shorter reaction time afforded a white microcrystalline product which gives elemental analysis consistent with a half-sandwich "ate" complex formulation $[Sm(Tp^{Me,Me})Br_3][K(THF)_2]$, **4.1**.

$$SmBr_3 + 2\ KTp^{Me,Me} \xrightarrow[\text{overnight}]{THF} [Sm(Tp^{Me,Me})Br_3][K(THF)_4]$$

The ^1H NMR and infrared spectra show that one major species is present and are consistent with pyrazolylborate bound to samarium. Crystals of the complex were grown from THF. An X-ray data set was collected by Professor V. W. Day at the University of Nebraska and the crystals found to be hexagonal; however, severe disorder was encountered and a full solution is as yet unavailable. Preliminary results suggest that the molecule lies on a threefold axis, possessing a salt-like structure, with an octahedral "3-legged piano stool" $[Sm(Tp^{Me,Me})Br_3]^+$ cation and a tetrahedral $[K(THF)_4]^-$ counterion in the lattice. Both species sit on the C_3 axis.[10]

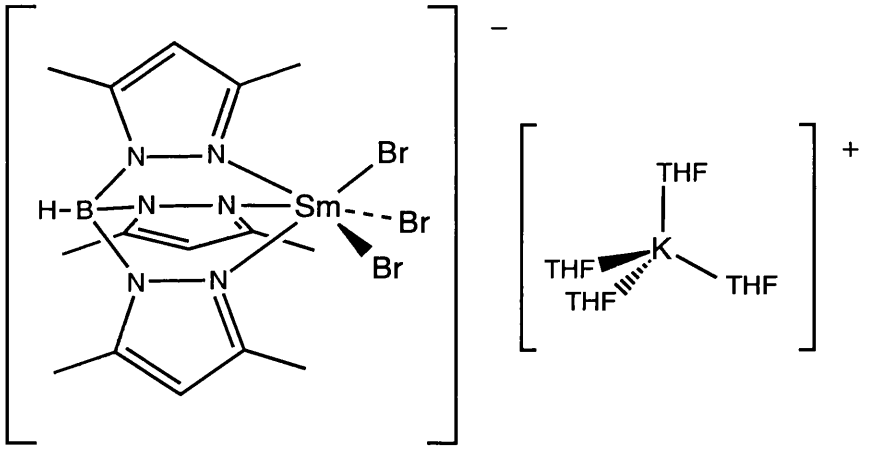

Figure 4.2. Structure of 4.1.

It appears that the product obtained depends upon the length of time for which the reagents are stirred. The fact that different products were isolated from preparations with different reaction times suggests that formation of $[Sm(Tp^{Me,Me})_2Br]$ occurs in a stepwise manner, with initial coordination of one pyrazolylborate group to form the half-sandwich complex **4.1**, followed by coordination of the second pyrazolylborate and loss of associated KBr. This is consistent with the preparation of $[Sm(Tp^{Me,Me})_2]$ by reaction of SmI_2 with $KTp^{Me,Me}$, which is believed to be formed *via* $[Sm(Tp^{Me,Me})I]$ (which has been isolated and crystallographically characterised by Takats[2]) and similar to the formation of $[Yb(C_5Me_5))_2I_2Li(OEt_2)_2]$ *via* $[Yb(C_5Me_5)(I)_3Li(OEt_2)_2]$ reported by Watson.[4,11]

Preparation of bis(pyrazolylborate)samarium carboxylates

The isolation of the dimeric formate-bridged complex $[Sm(Tp^{Me,Me})_2]_2(\mu\text{-}O_2CH)$ (**3.4**) raises questions about its mechanism of formation and about the fact that a singly bridged structure was obtained, when previous syntheses of unsubstituted (pyrazolylborate)lanthanide carboxylates *via* metathesis routes have given doubly carboxylate-bridged dimers (see chapter 1).

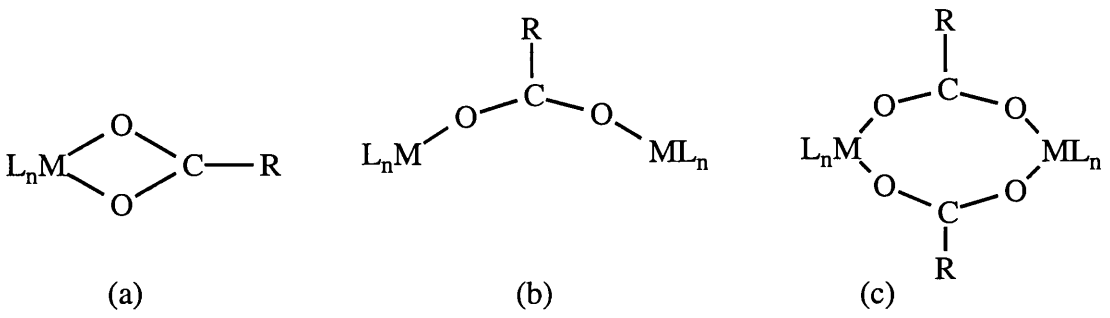

Figure 4.3. Carboxylate binding modes (a) bidentate, (b) singly bridging, (c) doubly bridging.

We were, therefore, interested to know whether the mode of formation or the steric demands of the $Tp^{Me,Me}$ ligand were responsible for the unusual structure. In order to probe the constraints placed upon these systems by the bis($Tp^{Me,Me}$) environment we prepared [$Sm(Tp^{Me,Me})_2$] complexes with formate, acetate and benzoate ligands. These complexes were prepared *via* the salt metathesis reaction of [$Sm(Tp^{Me,Me})_2Cl$] with the appropriate sodium carboxylate.

$$[Sm(Tp^{Me,Me})_2Cl] + NaO_2CR \rightarrow Sm(Tp^{Me,Me})_2O_2CR + NaCl$$

$Sm(Tp^{Me,Me})_2O_2CH$, 4.2

[$Sm(Tp^{Me,Me})_2Cl$] and NaO_2CH were mixed in a schlenk and THF added at room temperature. Following overnight stirring at ambient temperature the solvent was removed and the white residue extracted into toluene. After reducing the volume of solvent, cooling to -30°C afforded a colourless microcrystalline solid.

The ^1H NMR spectrum in $CDCl_3$ was quite complicated, exhibiting a large number of signals in the range 13.2 to -8.0 ppm, possibly owing to some decomposition in the halogenated solvent. The insolubility of the complex in benzene precluded further NMR studies. Four bands were displayed in the B–H stretching region of the infrared spectrum, two consistent with pyrazolylborate coordinated to a lanthanide and two at the slightly lower frequency more commonly associated with alkali metal pyrazolylborate. The separation of *ca.* 50 cm^{-1} between the two carboxylate CO_2 bands (at 1644 and 1593 cm^{-1}) suggests that the formate bridges the metal centres (*vide infra*).

Although the elemental analysis figures obtained for C and H were in good agreement with the calculated values, the value found for N was rather low.

$Sm(Tp^{Me,Me})_2O_2CMe$, 4.3

The reaction of $Sm(Tp^{Me,Me})_2Cl$ with NaO_2CMe in THF at toom temperature followed by recrystallisation from toluene afforded a mixture of white powder and four crystals which appeared fractured. The ^1H NMR spectrum in benzene-d_6 and elemental analysis of the powder were consistent with the formulation $Sm(Tp^{Me,Me})_2O_2CMe$. Infrared bands consistent with the lanthanide pyrazolylborate B–H stretch were displayed, as were very weak bands at 1627 - 1609 cm^{-1} in the CO_2 region. The FAB mass spectrum exhibited the parent ion $[Sm(Tp^{Me,Me})_2]^+$ at 749.

$Sm(Tp^{Me,Me})_2O_2CPh$, 4.4

The reaction of $[Sm(Tp^{Me,Me})_2Cl]$ with NaO_2CPh in THF at toom temperature, followed by recrystallisation from toluene afforded a colourless crystalline solid. The infrared spectrum displayed 2 bands in the B–H stretching region and ν_{CO2} at 1596 cm^{-1}. ^1H NMR spectroscopy indicated the presence of the phenyl ring and the pyrazolyl ring proton, as well as two signals in the pyrazolylborate methyl region, one sharp and one very broad. Elemental microanalysis was consistent with the composition $Sm(Tp^{Me,Me})_2O_2CPh$. It is possible that this complex is dimeric, by analogy with $[Sm(Tp)_2O_2CPh]_2$ prepared by Reger *et al*[12], althought the presence of the methyl groups in the 3-position on the pyrazolyl rings might be expected to prevent dimerisation, particularly with the benzoate ligand; the two sides of the dimer are held in much closer proximity in $[Sm(Tp)_2O_2CPh]_2$ than in $[Sm(Tp^{Me,Me})_2]_2(\mu\text{-}O_2CH)$.

A data set was collected on a sample of crystals that had been stored in solution for a period of several months. This sample was found to consist of the dimeric complex $[Sm(Tp^{Me,Me})(HB(pz^{Me,Me})_2O)]$ (**4.5**) which results from hydrolysis of a B–N bond in one of the pyrazolylborate ligands. Several examples of this dimer have been seen before, invariably obtained during recrystallisation of products.

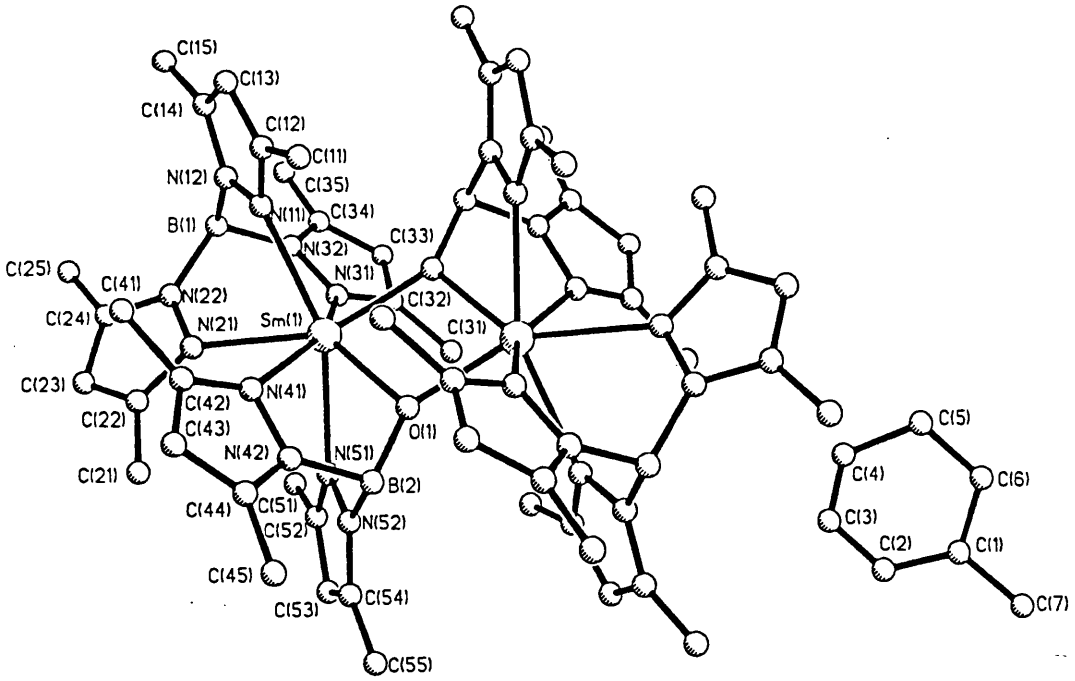

Figure 4.4. Structure of 4.5.

Infrared spectroscopy of (pyrazolylborate)lanthanide carboxylates

Whilst infrared spectroscopy is potentially a powerful tool for carboxylate complexes, allowing assignment of infrared vibrational frequencies to particular binding modes, in this case few infrared data have been obtained in conjunction with crystallographic characterisation. It is, therefore, difficult to make detailed assignments relating the carboxylate vibrational frequencies to specific carboxylate binding modes. Jones has assigned bands at 1535 - 1525 (antisymmetric stretch) and 1635 - 1625 cm^{-1} to bidentate coordination of the acetate group in $[Ln(Tp)_2(O_2CMe)]$ (Ln = Yb, Lu, Y), while the bands at 1600 and 1555 cm^{-1} in the spectra of acetate and benzoate complexes of the larger lanthanides have been tentatively attributed to a bridging bonding mode.[13] Since the $Tp^{Me,Me}$ ligand displays infrared bands in the fingerprint region up to 1540 cm^{-1} it is probable that in our complexes the relatively weak CO_2 antisymmetric stretch at lower frequency lies beneath one of the pyrazolylborate bands. On the basis of Jones' assignments, the separation of *ca.* 50 cm^{-1} between the two bands observed in the spectrum of the formate complex (rather than *ca.* 100 cm^{-1} expected for a bidentate bonding mode) suggests that the formate is bridging. The infrared data for the acetate and the benzoate are insufficient to deduce structural information.

Preparation of bis(pyrazolylborate)samarium hydrocarbyls

Salt metathesis and, to a much lesser extent, protonolysis reactions have been utilised to good effect in the preparation of lanthanide hydrocarbyl complexes. Previous attempts by Maunder using Grignard and organolithium reagents caused either reduction of the metal or ligand redistribution of the pyrazolylborate to magnesium.[14] Reductive transmetallation starting from divalent lanthanides, employing "soft" metal reagents, has been successfully employed to synthesise halide, carboxylate and hydrocarbyl species (see Chapter 1). It was, therefore, of interest to determine whether this might be an effective route for the synthesis of bis(pyrazolylborate)samarium hydrocarbyl complexes.

$$2\ [Sm(Tp^{Me,Me})_2] + HgR_2 \rightarrow 2\ Sm(Tp^{Me,Me})_2R + Hg$$

Since planar or rod-like ligands such as NO_2 or acetonitrile were known to give tractable products with the $[Sm(Tp^{Me,Me})_2]$ moiety, it was decided to attempt the reaction with similarly "flat" hydrocarbyl groups, which should be easily accommodated by the bulky 3,5-disubstituted pyrazolylborates.

Attempted preparation of $Sm(Tp^{Me,Me})_2Ph$

Stirring $[Sm(Tp^{Me,Me})_2]$ with $HgPh_2$ in toluene for several days at room temperature and then at elevated temperature did not result in any decolourisation or formation of mercury. Changing the solvent system to THF, DME or combinations of the three had no effect on the reactivity. This is in contrast to samarocene which reacts with $HgPh_2$, illustrating the extent to which the steric bulk of $Tp^{Me,Me}$ reduces the reactivity of the divalent lanthanides.

Preparation of $Sm(Tp^{Me,Me})_2C{\equiv}CPh$, 4.6

On stirring a slurry of purple $[Sm(Tp^{Me,Me})_2]$ with $Hg(C{\equiv}CPh)_2$ in toluene at –78°C, then warming to room temperature, the mixture decolourised over several hours and small grey droplets of mercury were formed. Filtration and removal of solvent afforded a cream/white solid. The ^1H NMR spectrum of this material was consistent with the

presence of pyrazolylborate and phenyl groups and the infrared spectrum displayed a band for the pyrazolylborate B–H stretch; a band at 2146 cm^{-1} was assigned to the C≡C stretch. Recrystallisation of the crude product from 30/40 petrol afforded a colourless microcrystalline product which displayed the same resonances in the ^1H and infrared spectra. The crystals were not, unfortunately, suitable for X-ray crystallography.

The analogous reaction utilising the soluble precursor $[Sm(Tp^{Me,Me,4\text{-}Et})_2]$ decolourised more rapidly; recrystallisation from 30/40 petrol afforded a similarly colourless crystalline product which appeared to lose solvent rapidly and became oily on removal from the mother liquor. Again, signals in the ^1H NMR and infrared spectra were consistent with the presence of both pyrazolylborate and phenylalkynyl groups.

While this work was in progress the Takats group, working in parallel, succeeded in growing crystals of the $Sm(Tp^{Me,Me})_2C{\equiv}CPh$ product and obtained X-ray characterisation data which showed that the alkynyl ligand was bound in terminal fashion to samarium (figure 4.5),[2] rather than bridging between two metal centres as is often observed in analogous cyclopentadienyl complexes (see introduction).

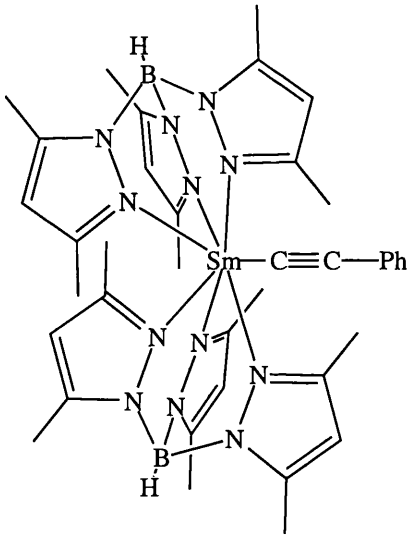

Figure 4.5. Structure of 4.6.

Bis(pyrazolylborate)yttrium and ytterbium halides: halide = Cl, I

Whilst the X-ray structures of the yttrium complexes $[Y(Tp)_2Cl(L)]$ (L = H_2O, Hpz) have been reported[15,16] to our knowledge no analogous $Tp^{Me,Me}$ compounds have been structurally characterised. We were, therefore, interested to ascertain whether the additional steric bulk afforded by the 3-methyl ring substituent would alter the structure significantly. By analogy with the different structures of the bis($Tp^{Me,Me}$)Sm halides, which depend on the halide size, a further point of interest was to compare the effect of changing the lanthanide metal, in particular to ascertain the crossover point between molecular and separated ion pair structures for the smaller metal ions.

Another significant factor is the way in which the size of the metal centre affects the coordination of the ancillary pyrazolylborate ligands. These ligands possess very flexible "jaws" and have been shown to accommodate a large range of metal centres of different ionic radius by altering the ligand bite angle. In the case of the 3- or the 3,5-substituted pyrazolyborate groups, however, on increasing or decreasing the bite angle the inter- and intraligand steric interactions between the pyrazolyl ring substituents can force the rings to twist about their B–N bond. Such twisting has been observed in the (3,5-disubstituted pyrazolylborate)indium complex $[In(Tp^{tBu,tBu})]$, in which all three pyrazolyl rings are highly twisted, adopting a propeller-like motif in which the local symmetry of ($Tp^{tBu,tBu}$) is reduced from the normal C_{3v} to C_3.[17] This twisting has been attributed to intraligand steric repulsions between the substituents in the 5-position and has also been observed for other $[M(Tp^{tBu,tBu})]$ and $[M(Tp^{tBu,tBu})X]$ derivatives.[18] The way in which interligand repulsions can affect structure is illustrated by the studies of tris(trispyrazolylborate)lanthanide complexes for which both 8- and 9-coordinate metal centres have been observed, depending on the size of the central metal ion. Whilst, for example, the complexes $[M(Tp)_3]$ of the larger metal (III) ions (M = Sc, Y, La, Ce - Gd) possess three tridentate pyrazolylborate ligands, the central metal ion in the analogous complexes of the heavier lanthanides (M = Tb - Lu) is 8-coordinate see Chapter 1). For the smaller lanthanides the metal coordination sphere in the solid state is defined by two pyrazolylborate ligands bound in tridentate fashion and one bidentate

ligand with a pendant pyrazolyl ring. NMR spectroscopic studies showed that all the pyrazolyl rings were inequivalent in solution, presumably through retention of the solid state structure.[19,20]

Similar problems to those noted in the preparation of $[Sm(Tp^{Me,Me})_2Br]$ were encountered in the syntheses of the bis($Tp^{Me,Me}$) halide complexes of yttrium and ytterbium. Again, the cleanness of the reaction appears to depend on the length of time for which the reagents are stirred. Thus, stirring two equivalents of $KTp^{Me,Me}$ with one of YCl_3 in THF for 1 hour, followed by filtration and recrystallisation from THF afforded a product formulated to be $[Y(Tp^{Me,Me})_2Cl.^1/_2(THF)]$ (**4.7**) on the basis of ^1H NMR and elemental analysis. The ^1H NMR in $CDCl_3$ indicated that small quantities of minor products were also present; these are, however, believed to arise through some decomposition in the halogenated solvent, since the intensity of these signals increases on allowing the chloroform solution to stand for several days. Analogous results were obtained in the reaction to prepare the complex of the smaller metal ytterbium, starting from ytterbium chloride. The formation of a single major product was observed, presumed to be $[Yb(Tp^{Me,Me})_2Cl.^1/_2(THF)]$ (**4.8**) on the basis of ^1H NMR spectroscopy and elemental analysis.

Longer reaction times resulted in a mixture of products, with different combinations obtained on stirring for one night to those obtained over 48 hours. These mixtures gave elemental analysis figures consistent with the formulation $[Ln(Tp^{Me,Me})_2Cl.^1/_2(THF)]$ (Ln = Y, Yb) but the ^1H NMR spectra indicated the presence of more than one product. Whilst the spectrum of the Yb compound was rather broad owing to the f^{13} electronic configuration, preventing reliable integration values, the ^1H NMR spectrum of the Y product clearly indicated that two major products had been obtained, in 2:3 ratio. It was initially believed that a complex containing one tridentate and one bidentate pyrazolylborate ligand, with a pendant pyrazolyl group, had been formed. This would be in contrast to the structure observed by X-ray crystallography for the analogous unsubstituted bis(pyrazolylborate)yttrium complexes $[Y(Tp)_2Cl.L]$ (L = H_2O, Hpz) but

could be feasible given the greater steric constraints associated with the 3,5-dimethyl substituted pyrazolylborate ligand. Variable temperature ^{1}H NMR studies, however, showed that whilst one component of the system was fluxional, broadening into the baseline as the sample was cooled, the other resonances merely shifted relative to the toluene reference peak. The fluxionality observed for one component could be due to processes such as those observed in the chalcogenolates. Alternatively it could be attributed to ligand redistribution reactions. No interpretable limiting spectra were observed.

In the hope of obtaining cleaner reactions and suppressing the chances of formation of "ate" complexes we attempted to prepare the corresponding iodide. On adding THF to a mixture of YI_3 and $KTp^{Me,Me}$ in 1:2 ratio a dense white precipitate formed almost immediately. This attempted preparation of $[Y(Tp^{Me,Me})_2I]$ afforded, after filtration and removal of solvent, mixtures of products. The composition of these mixtures differed depending on the reaction time, which was varied from 1 hour to 3 days. No attempts were made to separate the components, although variable temperature ^{1}H NMR indicated that again one of them exhibited fluxional behaviour, with some signals broadening into the baseline as the temperature was increased and new resonances appearing at high temperature. However, again no interpretable limiting spectra were observed. Elemental analysis was consistent with the composition $[Y(Tp^{Me,Me})_2I.^1/_2(THF)]$. The infrared spectrum exhibited several bands in the B-H stretching region.

The fact that the elemental analyses of these mixtures correspond to the expected formulation $[Ln(Tp^{Me,Me})_2X]$ (Ln = Y, X = Cl, I; Ln = Yb, X = Cl) may indicate that significant ligand redistribution occurs in these systems in solution, giving a mixture of compounds whose overall stoicheiometry is in the correct ratio of metal to $Tp^{Me,Me}$ to halide. This ligand redistribution also hinders attempts to grow crystals for X-ray diffraction studies. Our inability to obtain a single product in the attempts to prepare $Y(Tp^{Me,Me})_2I$, even employing a fairly short reaction time, might be explained by reference to the problems encountered in the preparation of $[Sm(Tp^{Me,Me})_2Br]$.

Section 2 - Preparation of mono(pyrazolylborate)lanthanide complexes

Metal imido complexes, $L_nM{\equiv}NR$, are attractive synthetic targets, permitting access to a wide range of reactivity, both catalytic and stoicheiometric. Given the different reactivity observed for organolanthanide complexes to that displayed by similar transition metal systems, the preparation of lanthanide imido complexes is of interest and one of the objectives of this project was to synthesise a (pyrazolylborate)lanthanide imido complex. Whilst Teuben and coworkers have synthesised compounds in which the combination of an anchored nitrogen donor group with a mobile hydrogen could give rise to degree of Y=N double bonding,[21] no lanthanide complexes containing "free" Ln–N multiple bond character have, to our knowledge, been reported. Attempts to prepare lanthanide imido complexes with the very electron withdrawing di(pentafluorophenyl)amide group, *via* initial formation of the lanthanide amide then protonolysis of one phenyl substituent, resulted in the formation of homoleptic tris(amido)lanthanide compounds with M–F interactions.[22]

The bonding in metal imido systems is best described in terms of both σ- and π-donation from the nitrogen to the metal d orbitals, forming one σ and two π bonds. The metal-nitrogen bond order is considered to be 3 and imido groups usually adopt linear geometry at N. Although bent imido complexes are also known, formally containing a M=N double bond, this structural type is quite rare.

(a) (b)

Figure 4.6. a) Linear imido; b) bent imido.

The relative energies of the metal (d_π) and the nitrogen (p_π) orbitals control the electrophilic or nucleophilic character (*i.e.* the basicity) of the imido ligand. The high electronegativity of N gives the imido ligand "Schrock" character (by analogy with carbenes), that is, it can be regarded as NR^{2-}, in the same way that oxo and nitrido

ligands are considered as O^{2-} and N^{3-} respectively (figure 4.7a). As the electronegativity of the metal centre increases on moving to the right in the Periodic Table the orbital energies move to a situation where the M(d_π) and the N(p_π) orbitals have comparable energy (figure 4.7b), with the result that the basic character of the N decreases and the metal d_π contribution to the metal-nitrogen π bonding MOs increases.

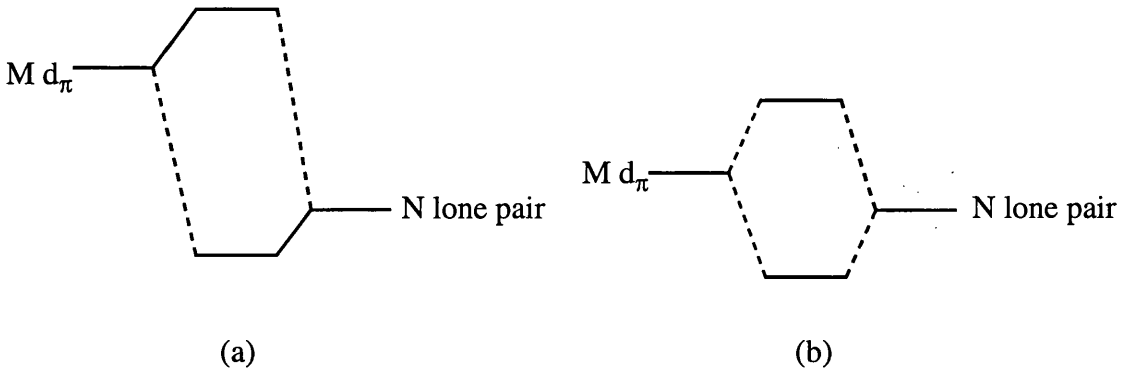

Figure 4.7. Relative energies of M (d_π) and N (p) orbitals: a) early d-block metal; b) late d-block metal.

Figure 4.7 may also be used to represent the relative energies of the metal d_π and nitrogen p_π orbitals for metals in (a) low and (b) high oxidation states. The better d_π/p_π energy match in high valent transition metal imido complexes (such as those of group 4, 5 and 6 d^0 metals) results in these systems being stable and quite straightforward to prepare, by contrast to low valent metal complexes which tend to be much more reactive. Given this ability of the imido ligand to stabilise high oxidation states, it seems strange that no analogous group 3 or lanthanide M^{3+} complexes have been reported. Although this could be owing to orbital energy mismatch, it could simply be that the narrow, rod-like imido group requires a very bulky ancillary ligand system capable of kinetically stabilising such large metal centres (for example, with respect to ligand redistribution). In this context, it is noteworthy that no nitrido or terminal oxo lanthanide complexes are known. The cup-shaped 3-substituted pyrazolylborate ancillary ligand seems well-suited to stabilising such ligand systems. We anticipated

that the substitution in the 3-position of the Tp ligand would also provide sufficient steric protection for the imido group to prevent dimerisation.

Traditional routes to imido complexes, involving reaction of a metal oxo compound with an isocyanate, are not possible for the lanthanides; the terminal oxo ligand is unknown on a lanthanide centre and bridging oxo complexes are uncommon.

$$L_nM{=}O + RNCO \rightarrow L_nM{\equiv}NR + CO_2$$

On the other hand imido complexes have been prepared in the past by deprotonation of primary amides. We therefore attempted to prepare a half-sandwich bis(primary amide). It was believed that the use of a very bulky primary amide ligand possessing an acidic hydrogen might force the elimination of amine with concomitant formation of a formal metal-nitrogen multiple bond (figure 4.8).

Two preparative routes were employed initially in the attempted preparation of the diamide complexes, salt metathesis starting from the mono(pyrazolylborate)lanthanide dihalide and protonolysis of a hydrocarbyl with an amine. These routes are shown in the scheme in figure 4.8. The alternative protonolysis reaction between $Ln(NHR)_3$ and TpH was precluded by the lack of suitable primary amido starting materials.

With the imido as a target, therefore, we decided initially to develop the chemistry of the halide and the hydrocarbyl precursors.

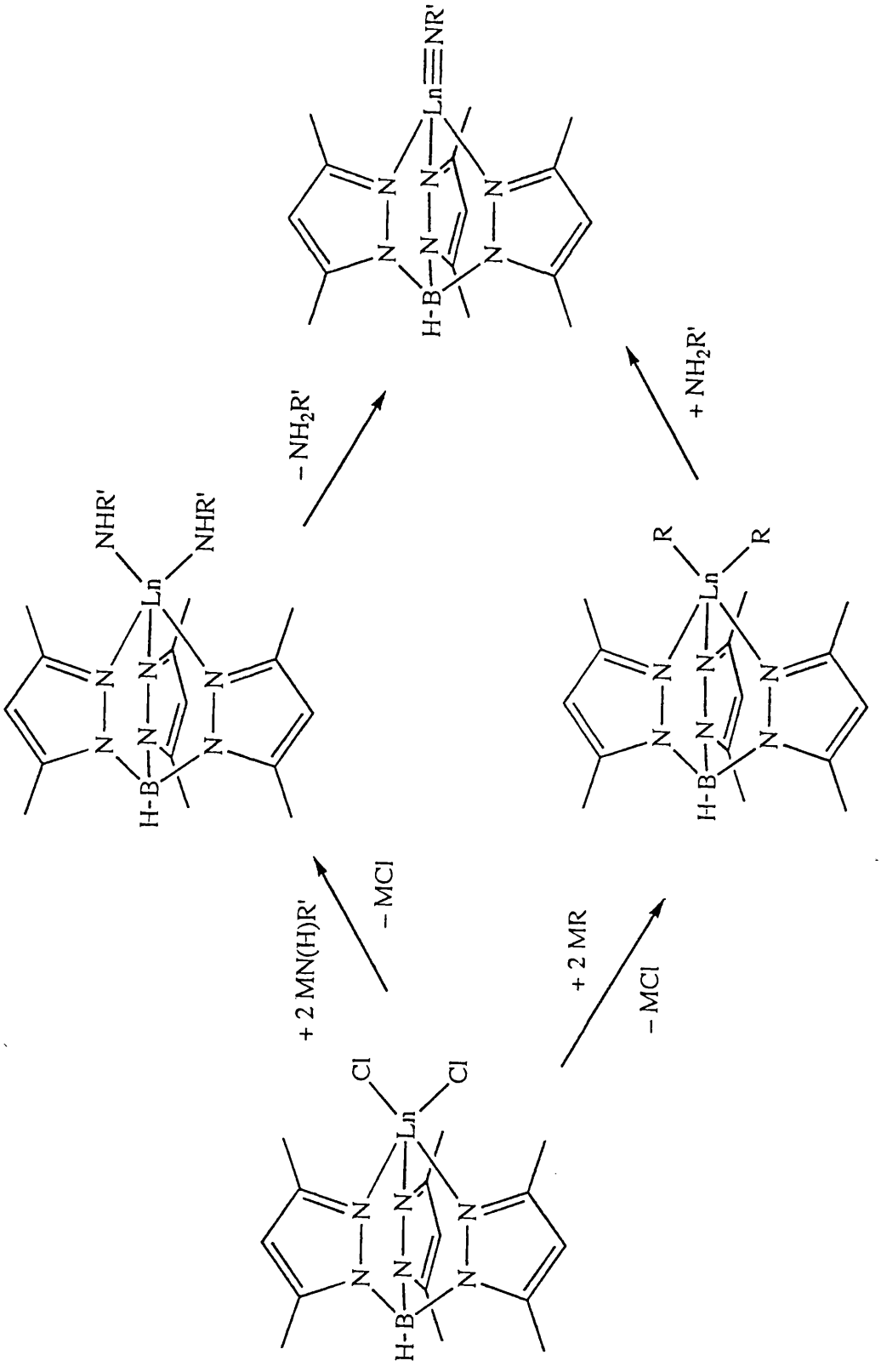

Figure 4.8. **Possible route to a lanthanide imido complex. R' = bulky organic group, e.g. Bu^t, 2,6-Pr^i_2.C_6H_3. (Ln = Y, X = Cl, I; Ln = Yb, X = Cl; R = Ph, CH_2SiMe_3, $CH\{SiMe_3\}_2$; M = Li, R' = Bu^t, 2,4,6-$Me_3C_6H_2$, 2,6-$Pr^i_2C_6H_3$; M = K, R' = Bu^t; M = Na, R' = $N\{SiMe_3\}_2$).**

Preparation of Mono(pyrazolylborate)lanthanide halides [Ln($Tp^{Me,Me}$)X_2] (Ln = Y, X = Cl (4.9), I (4.10); Ln = Yb, X = Cl (4.11))

The preparation of half-sandwich pyrazolylborate lanthanide halide complexes was carried out in analogous fashion to the sandwich compounds, *via* metathesis of lanthanide trihalide with potassium pyrazolylborate in THF.

$$LnX_3 + KTp^{Me,Me} \rightarrow Ln(Tp^{Me,Me})X_2 + KCl$$

On stirring YCl_3 with $KTp^{Me,Me}$ in THF, followed by filtration and recrystallisation from THF a white crystalline material was obtained. The ^1H NMR and infrared spectra indicated that no impurities were present. Elemental analyses on different reaction batches were, however, inconsistent. In one case the analysis figures were consistent with the stoicheiometry of the desired product. In other cases, however, instead of the expected composition elemental analysis was more consistent with the formation of the salt-incorporated product $YTp^{Me,Me}Cl_3K(THF)$ (**4.9**). The retention of alkali metal salt is common in the preparation of mono(pentamethylcyclopentadienyl) lanthanide complexes but has not been observed in half-sandwich pyrazolyborate lanthanide compounds containing the more bulky $Tp^{t\text{-}Bu,Me}$ ligand. This could be linked to the reaction time, by analogy with the preparation of **4.1**, although in general the reaction mixtures were stirred for similar periods. Presumably the steric requirements of the metal centre are only poorly satisfied by the $Tp^{Me,Me}$ ancillary ligand. Indeed, most attempts to prepare divalent lanthanide complexes of the type $LnTp^{Me,Me}X$ have been unsuccessful, with the exception of [$SmTp^{Me,Me}I$],[2] and only the products of ligand rearrangement were recovered. On the other hand, attempted preparations of $YTp^{t\text{-}Bu,Me}Cl_2$ have failed and starting materials were recovered even after extended reaction times.

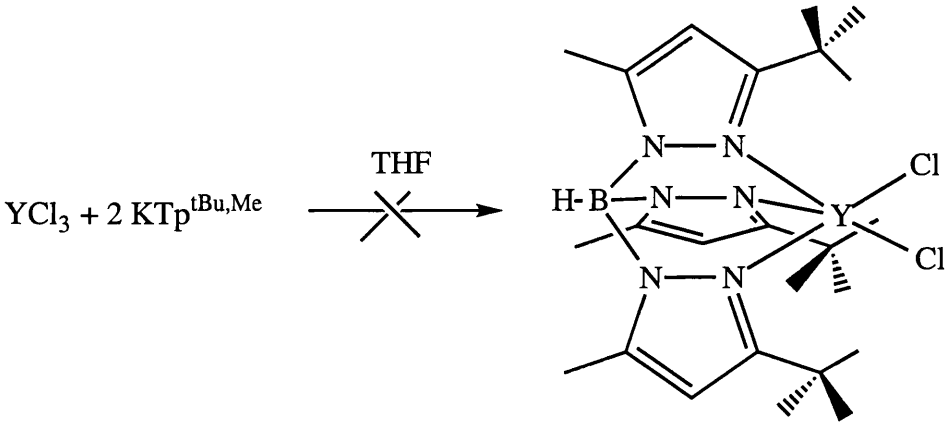

Since the chloride product suffered from problems with salt incorporation the iodide complex was also prepared, which should be less prone to such effects. Thus reaction of YI_3 with $KTp^{Me,Me}$ afforded $YTp^{Me,Me}I_2$.THF (**4.10**), characterised by ^1H NMR and infrared spectroscopy and by elemental analysis; only quite low yield was obtained. The reaction of the smaller metal $YbCl_3$ with one equivalent of $KTp^{Me,Me}$ similarly afforded fairly low yields of $YbTp^{Me,Me}Cl_2.{}^1/_2THF$ (**4.11**). Infrared spectroscopy and elemental analysis were consistent with this formulation, but the ^1H NMR resonances were too broad to assign reliably. This complex has previously been isolated and crystographically characterised by Marques.[3]

Preparation and attempted preparation of half sandwich complexes $[Ln(Tp^{Me,Me})R_2]$ (R = alkyl)

Since problems with incorporation of alkali metal salt are common for the sterically unsaturated half-sandwich lanthanide complexes it was decided in the first instance to attempt the protonolysis route in the preparation of imido complexes. It was, therefore, necessary to prepare (pyrazolylborate)lanthanide hydrocarbyls. A recent communication by Bianconi has outlined the preparation of $[Y(Tp^{Me,Me})R_2(THF)]$ (Ln = Y; R = Ph, CH_2SiMe_3) by reaction of organolithium reagents with the halide precursor complex $[Y(Tp^{Me,Me})Cl_2(THF)]$.[23]

Following what we believed to be the method of Bianconi (which was not reported in detail) a hexane/Et_2O solution of LiPh was added to **4.9** in toluene at -78°C, then the

reaction mixture was allowed to warm to ambient temperature and stirred overnight. Removal of solvent and extraction into pentane followed by cooling to -30°C afforded a pale brown powdery product which displayed only three resonances in the ^{1}H NMR spectrum, at 5.744, 2.315 and 1.728 ppm, in 1:3:3 ratio and an intense infrared band at 2515 cm^{-1}. On this basis it was identified as $LiTp^{Me,Me}$, which has also been isolated from reactions of $[Sc(Tp^{Me,Me})Cl_2(THF)]$ and $[Sc(Tp^{t\text{-}Bu,Me})Cl_2]$ with organolithium reagents.[1] Shorter reaction times and filtration of the reaction mixture at –78°C, followed by a second filtration at room temperature, resulted in the isolation of a product of similar optical appearance, which exhibited signals in the ^{1}H NMR spectrum attributed to $[Y(Tp^{Me,Me})Ph_2(Et_2O)]$ as well as the peaks associated with $LiTp^{Me,Me}$. Attempts to separate the components by fractional recrystallisation were unsuccessful and further efforts to isolate $[Y(Tp^{Me,Me})Ph_2(Et_2O)]$ were abandoned.

$LiTp^{Me,Me}$ was also isolated from the reactions of **4.9** with $Li(CH_2SiMe_3)$ and $Li(CH\{SiMe_3\}_2)$, depending on the reaction conditions. The attempted preparation of $[Y(Tp^{Me,Me})(CH_2SiMe_3)_2]$ in toluene solution, after filtration and removal of solvent, afforded an off-white product which did not contain $LiTp^{Me,Me}$, and gave elemental analysis figures consistent with the formulation $Y(Tp^{Me,Me})Cl(CH_2SiMe_3)$. Signals associated with the pyrazolylborate and trimethylsilyl groups were identified in the ^{1}H NMR spectrum, although integration suggested that both the 3- and the 5-methyl pyrazolyl substituents appeared at the same chemical shift. On the other hand, the same reaction carried out in diethyl ether solution followed by extraction into 30/40 petrol, afforded only $LiTp^{Me,Me}$.

The reaction of **4.9** with $Li(CH\{SiMe_3\}_2)$ in toluene gave, in one instance, a crude product believed to be a mixture of $LiTp^{Me,Me}$ and $[Y(Tp^{Me,Me})(CH\{SiMe_3\}_2)_2(THF)_n]$ on the basis of the ^{1}H NMR spectrum. No attempt at recrystallisation was made and no elemental analysis data obtained.

The use of $K(CH_2SiMe_3)$, prepared from the lithium reagent by stirring with $KOBu^t$, afforded a marginally higher degree of success – the reaction with **4.10** afforded a product which exhibited pyrazolylborate and trimethylsilyl resonances in the ^{1}H NMR

spectrum, albeit at different chemical shifts to those reported by Bianconi. The methylene protons, however, were not observed, although Bianconi reported them to be located at –0.637 ppm.

The attempted preparation of $[Yb(Tp^{Me,Me})(CH\{SiMe_3\}_2)_2]$ by reaction of **4.11** with $Li(CH\{SiMe_3\}_2)_2$ resulted in reduction of ytterbium, as evidenced by the formation of an insoluble purple material, presumed to be $[Yb(Tp^{Me,Me})_2]$.

Our attempts to reproduce the work of Bianconi were largely unsuccessful and we were unable to isolate clean products. One reason for the apparent intractability of these compounds in our hands appears to be owing to ligand redistribution reactions which are quite common for the large labile lanthanides. The use of organolithium and Grignard reagents in attempted preparations of bis(pyrazolylborate)lanthanide hydrocarbyl complexes has previously been observed to lead to problems associated with ligand redistribution and salt incorporation, resulting in largely intractable products.[8] It is therefore surprising to us that the compounds $[Y(Tp^{Me,Me})R_2(THF)]$ (R = Ph, CH_2SiMe_3) were reported to be isolated cleanly in yields as high as 70%. It appears from our work that the reaction conditions are essential; filtration at low temperature and the choice of solvent system seem to be key factors in obtaining even a small quantity of product. Even with careful attention to reaction conditions, mixtures and products giving ambiguous spectroscopic data were obtained.

A more effective synthetic route that avoids such problems has been reported recently by Piers. Whilst attempted preparations of the analogous scandium complexes from $[Sc(Tp^{Me,Me})Cl_2(THF)]$ and $LiCH_2SiMe_3$ resulted in formation of $LiTp^{Me,Me}$, the alternative route, starting from the tris(hydrocarbyl)scandium complexes and reacting with $KTp^{Me,Me}$, permitted access to the desired product with no side reactions.[1]

Preparation and attempted preparation of half sandwich complexes $[Ln(Tp^{Me,Me})X_2]$ (X = amide)

Given our inability to isolate well-defined hydrocarbyl complexes from the reactions described above, it was decided to prepare the amido complexes by metathesis methods utilising the halide complexes $[Ln(Tp^{Me,Me})X_2]$ as precursors in reactions with alkali metal amides.

The salt metathesis route was, therefore, attempted employing **4.9** or **4.10** with alkali metal salts of bulky primary amides MNHR'. The reactions were carried out in THF at low temperature and the products extracted into toluene.

The reaction of **4.9** with $LiNHBu^t$ afforded an off-white product which displayed three resonances in a 1:3:3 ratio in the ^1H NMR spectrum, but no signals for the amide *tert*-butyl group. The preparation of $[Y(Tp^{Me,Me})(NHBu^t)_2]$ was then attempted starting from **4.10**, employing a potassium reagent, in the hope that the insolubility of the KI byproduct would drive the reaction. The ^1H NMR spectrum of the product was rather broad, surprisingly since yttrium(III) is diamagnetic. Signals consistent with the coordination of THF to the metal and resonances presumed to be due to the pyrazolyl rings were displayed but the poor resolution of the spectrum precluded reliable assignment of the resonances associated with the amide group.

The analogous reactions of **4.9** with $LiNH(2,4,6\text{-}Me_3C_6H_2)$ and $LiNH(2,6\text{-}Pr^i_2C_6H_3)$ afforded white powders that gave superimposable infrared spectra. The products were not very soluble in benzene and the signals in the ^1H NMR spectrum of the product of the $LiNH(2,4,6\text{-}Me_3C_6H_2)$ reaction could not be assigned reliably beyond the lack of evidence for either the pyrazolylborate or the amide ligands, in particular the fact that no signals were displayed in the phenyl region. Insufficient quantities of the diisopropylphenylamide reaction product were isolated to obtain NMR data.

The elemental analysis figures obtained for all of these products were similarly inconsistent with any reasonable formulation given the starting materials and reaction conditions. Our failure to isolate either the desired imido or diamide products was

attributed to ligand redistribution reactions, particularly in the reactions involving lithium reagents, and possibly to the fragmentation of the complex in the presence of the reactive potassium reagent. The product isolated in the reaction between **4.9** and $LiNHBu^t$ was later assigned as $LiTp^{Me,Me}$ (*vide supra*).

The preparation of $Y(Tp^{Me,Me})(N\{SiMe_3\}_2)_2$ was also attempted, by reaction of **4.10** with $NaN\{SiMe_3\}_2$ in a mixture of THF and diethyl ether. The ^1H NMR spectrum was consistent with $Y(Tp^{Me,Me})(N\{SiMe_3\}_2)_2$ as the major product, exhibiting resonances for the pyrazolylborate and the trimethylsilyl groups, although there also appeared to be a second pyrazolylborate-containing complex present.

Section 3: Preparation and attempted preparation of mono- and bis(pyrazolylborate)lanthanide borohydride and aluminohydride complexes.

Given the apparent intractability of the half-sandwich yttrium and ytterbium amide and alkyl complexes and the problems encountered in the preparation of the bis(pyrazolylborate)lanthanide halides, it was decided to prepare complexes with potentially multidentate borohydride and aluminohydride ligands. We believed this might allow the isolation of more tractable products and prevent ligand redistribution reactions, as well as giving access to potentially reactive M–H bonds.

Borohydrides

There are many reported lanthanide borohydrides, with a large contribution to the field from the groups of Bulychev, Mirsaidov and Semenenko; a review of f-element borohydride and aluminohydride chemistry has been published recently.[24] The class of organolanthanide borohydrides largely consists of bis(cyclopentadienyl) compounds. One reason for the interest in lanthanide borohydride complexes is owing to their potential as hydroboration catalysts and as precursors to metal hydrides. Different binding modes are observed for the borohydride ligand depending on the mode of preparation and the steric considerations at the metal centre (figure 4.9).[24,25]

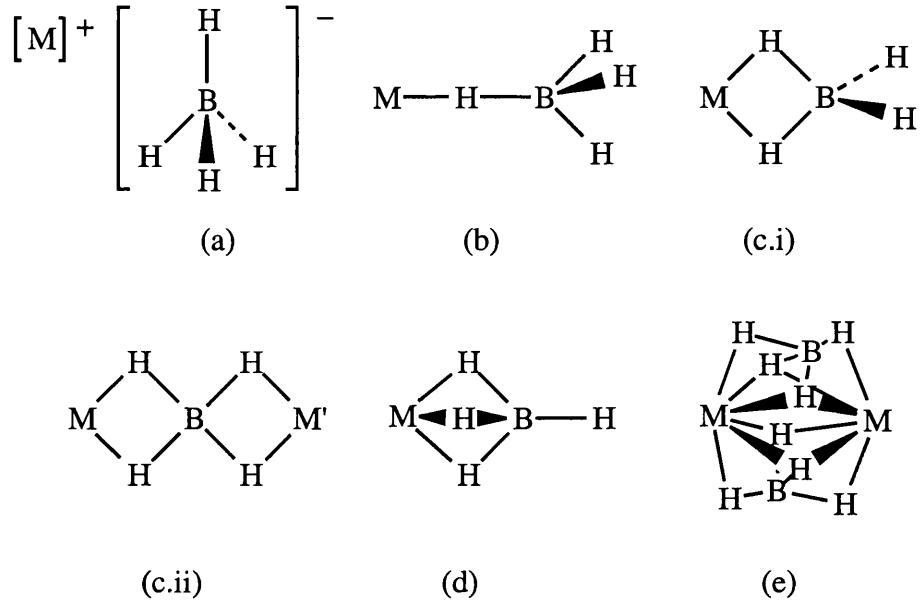

Figure 4.9. Coordination types for tetrahydroborate group with metal atom. (a) Ionic; (b) unidentate; (c) bidentate (i) monomer, (ii) dimer or higher nuclearity; (d) tridentate; (e) tetradentate.

It is fairly straightforward to distinguish between the different coordination modes on the basis of their IR spectra (see table 4.1). In cases where two or more borohydride groups are present and adopt different denticity the spectra can become more complex.

Organolanthanide borohydrides have been synthesised by reaction of a halide precursor with $LiBH_4$ or $NaBH_4$.

$$Ln(Cp)_2Cl.THF + M(BH_4) \rightarrow Ln(Cp)_2(BH_4)(THF)$$

The denticity of the borohydride ligand depends upon a number of factors. The size of the ancillary ligands contributes to the overall steric considerations at the metal centre. For example the BH_4 group in $Sc(Cp)_2(BH_4)$ was found to be tridentate by infrared and multinuclear NMR studies,[26] but a bidentate BH_4 was observed in the ring-substituted analogue $Sc\{C_5H_3(SiMe_3)_2\}_2(BH_4)$, characterised by X-ray crystallography.[27] The ionic radius of the metal centre is the major factor upon which the ligation mode of the borohydride group depends. In the complexes $LnCp_2(BH_4)(THF)$ the borohydride ligands are bidentate for Ln = Lu or Yb and tridentate for Ln = Sm, reflecting the larger

ionic radius of the earlier lanthanide metal samarium. The infrared spectrum of $ErCp_2(BH_4)(THF)$ apparently indicates a structure in which the BH_4 ligand adopts coordination intermediate between bi- and tridentate. The novel tetradentate ligation mode was observed in the complexes of the larger metals Ce[28] and Sm[29] $[(1,3\text{-}Bu^t_2\text{-}C_5H_3)_2Ln(BH_4)]_2$, with the lanthanide metal and boron bonded through triple hydrogen bridges, as shown in Figure 4.9(e) above.

Table 4.1. Infra-red vibrational transitions observed for MBH_4 species [24,25]

Structure	Approx. freq., cm^{-1}	Type of internal coordinate change	Symmetry type
(a) ionic	2200 - 2300	B-H_t stretch	T_2
	1050 - 1150	BH_2 deformation	T_2
(b) monodentate	2300 - 2450	B-H_t stretch	A_1, E
	2000	B-H_b stretch	A_1
	2000 - 1700	M-H_b stretch	A_1
	1000 - 1150	BH_3 deformation	A_1, E
(c.i) bidentate	2400 - 2600	B-H_t stretch	A_1, B_1
(monomer)	1650 - 2150	B-H_b stretch	A_1, B_2
	1300 - 1500	Bridge stretch	A_1
	1100 - 1200	BH_2 deformation	B_2
(c.ii) bidentate	*ca.* 2290	B-H_b stretch	A_1
(dimer, polymer)	*ca.* 1200	BH_2 deformation	B_2
(d) tridentate	2450 - 2600	B-H_t stretch	A_1
	2100 - 2200	B-H_b stretch	A_1
	1150 - 1250	BH_3 deformation	A_1
(e) tetradentate	2400 - 2420	B-H_b stretch (η^3)	
	2250 - 2280	B-H_b stretch (η^2)	

Coordination of solvent also affects the mode of bonding of the borohydride ligand. THF can be removed from the complexes $LnCp_2(BH_4)(THF)$ where Ln = Lu, Yb or Er to afford the unsolvated complexes $LnCp_2(BH_4)$ which were suggested to be polymeric by comparison of their infrared spectra with those of $[Be(BH_4)_2]_n$ and $[ZnMe(BH_4)]_n$, exhibiting $(\mu\text{-}\eta^2\text{-}H_2)_2B$ units bridging between lanthanide centres (Figure 4.10a).[30]

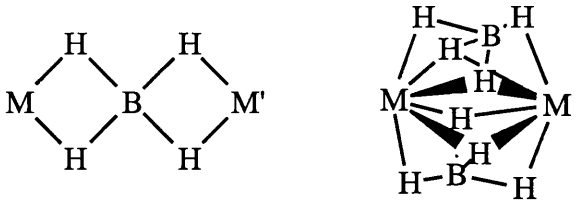

Figure 4.10. BH_4 binding mode in (a) $[Be(BH_4)_2]_n$ and $[ZnMe(BH_4)]_n$; (b) $[(1,3\text{-}Bu^t_2\text{-}C_5H_3)_2Ln(BH_4)]_2$, (Ln = Ce, Sm).

It has also been suggested, by comparison of the broad infrared bands at 2250 - 2280 cm^{-1}, that these complexes exhibit the same tetradentate $(\mu_3\text{-}H)_2B(\mu_2\text{-}H)_2$ BH_4 ligation mode observed in the dimeric Ce and Sm complexes (Figure 4.10b).

Monomeric unsolvated bis(cyclopentadienyl)lanthanide borohydrides have been obtained by employing ancillary ligands that incorporate donor groups. Deng has prepared a series of complexes $[(2\text{-}MeOCH_2CH_2C_5H_4)_2Ln(BH_4)]$ (Ln = La, Pr, Nd, Sm, Gd)[31] and carried out X-ray crystallography on the Pr and Nd compounds. The BH_4 ligand in the complexes of the smaller lanthanides Sm and Gd was reported to bind in bidentate fashion, while the larger lanthanide complexes possessed a tridentate borohydride. The analogous yttrium complex has also been prepared.[32]

Ephritikhine and coworkers have recently developed a new synthetic route to organolanthanide borohydrides starting from the solvated complex $Nd(BH_4)_3(THF)$. The cyclooctatetraenyl neodymium borohydride complex $[(\eta\text{-}C_8H_8)Nd(BH_4)(THF)]_2$[33] and the cycloheptatrienyl complex $(THF)(BH_4)_2[(\mu\text{-}\eta^7\text{:}\eta^7\text{-}C_7H_7)Nd(BH_4)(THF)_2$[34] have been isolated from reactions of $Nd(BH_4)_3(THF)_3$ with the appropriate organopotassium reagent. The COT complex exhibits the $(\mu_3\text{-}H)_2B(\mu_2\text{-}H)_2$ borohydride coordination mode observed in $[(1,3\text{-}Bu^t_2\text{-}C_5H_3)_2Ln(BH_4)]_2$ (Ln = Ce, Sm). The

reactivity of these complexes has also been investigated. The tetraphenylborate complex $[(COT)Nd(THF)_4][BPh_4]$, containing the novel (cyclooctatetraenyl)lanthanide cation, was prepared by treatment of $[(COT)Nd(BH_4)(THF)]_2$ with $NHEt_3BPh_4$. Both of these compounds react with KCp to afford the mixed ligand complex (COT)Nd(Cp)
Quite recently the reaction of $[Sm(Bu^t_2\text{-}C_5H_3)_2Cl]$ with $NaHBEt_3$ was reported to afford either monomeric $[Sm(Bu^t_2\text{-}C_5H_3)_2HBEt_3(THF)]$ or $[Sm(Bu^t_2\text{-}C_5H_3)_2H]_2$.[35]

Aluminohydrides

Lanthanide aluminohydride complexes are of interest both as precursors to hydrides and as potentially reactive heterometallic systems. Organolanthanide aluminohydrides are generally prepared by reaction of a lanthanide chloride with $LiAlH_4$ or AlH_3.

$$[LnCp_2Cl]_2 + LiAlH_4 \rightarrow [LnCp_2(AlH_4)]_2 + 2\ LiCl$$

An alternative route involves oxidation of a divalent lanthanide with solvated alane.

$$Na[Sm(Bu^t_2\text{-}C_5H_3)_3]THF + 2AlH_3.THF \rightarrow$$

$$[\{Sm(Bu^t_2\text{-}C_5H_3)_2.(\mu_3\text{-}H)\}\{(\mu_2\text{-}H)_2AlH.THF\}_2$$

A variety of coordination modes has been observed in mono- and polynuclear compounds. Dimeric complexes are quite commonly obtained in reactions of $[LnCp_2Cl]_2$ with $LiAlH_4$ in the presence of a Lewis base and one of two ligating modes adopted (figure 4.11). Structural type (a) has been reported for $[Ln(C_5H_5)_2(AlH_4).NEt_3]_2$ where Ln = Y,[36] Yb,[37] Lu[38] and for $[Ln(C_5H_5)_2(AlH_4).THF]_2$ where Ln = Y [39] and type (b) where Ln = Sm,[40]Lu.[37]

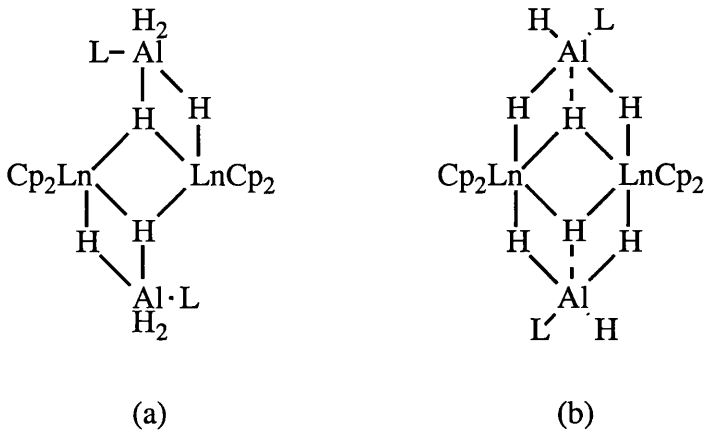

Figure 4.11. AlH_4 ligating modes in dimeric bis(cyclopentadienyl)lanthanide aluminohydrides.

The diethyl ether solvate of the yttrium complex $[Y(C_5H_5)_2(AlH_4)]_2.Et_2O$, on the other hand, adopts a non-centrosymmetric structure with two non-equivalent aluminium atoms, one of which is connected to the ether molecule (Figure 4.12).[39]

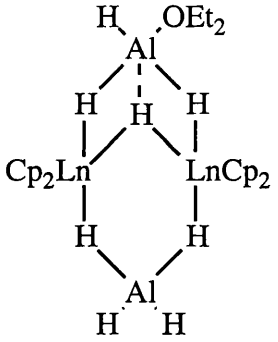

Figure 4.12. Structure of $[YCp_2(AlH_4)]_2.Et_2O$

The lutetium complex $[Ln(Cp_2(AlH_4).NEt_3]_2$ dissociates on exposure to X-ray radiation to afford the monomeric compound $[LuCp_2(\mu_2\text{-}H)AlH_3.NEt_3]$ (Figure 4.13.).[38]

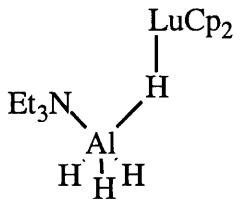

Figure 4.13. Structure of $[LuCp_2(\mu_2\text{-}H)AlH_3.NEt_3]$

Higher nuclearity complexes have been obtained as products in reactions of divalent samarium. An example is provided in the reactions of $Sm(Bu^t_2\text{-}C_5H_3)_2.THF$ with AlH_3 in THF or of $Sm(Bu^t_2\text{-}C_5H_3)_2$ with AlH_3 in Et_2O in the presence of excess TMEDA and pentane which both afford the octanuclear species $[Sm(Bu^t_2\text{-}C_5H_3)\{(\mu_2\text{-}H)_2(\mu_3\text{-}H)_2Al(TMEDA)\}_2\{Sm(Bu^t_2\text{-}C_5H_3)H\}_2\{(\mu_2\text{-}H)_3Al(\mu_2\text{-}H)Al(\mu_2\text{-}H)_3\}\{(\mu_3\text{-}H)_2Sm(Bu^t_2\text{-}C_5H_3)_2\}]$. The metallic framework is shown in figure 4.11. All the metal atoms are bonded by double or triple hydrogen bridges and there is a short non-bonding contact between the two Al atoms adjacent to the $Sm(Bu^t_2\text{-}C_5H_3)_2$ fragment.[41]

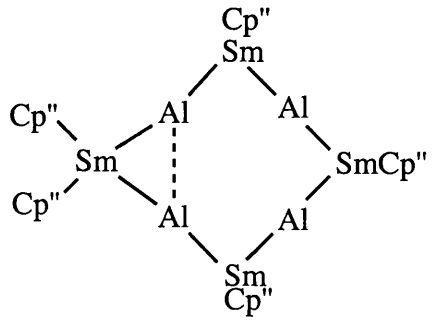

Figure 4.14. Metallic framework of octanuclear $Sm(Bu^t_2\text{-}C_5H_3)$ aluminohydride.

One reason for the interest in organolanthanide aluminohydrides is owing to their potential as alternative precursors to lanthanide hydrides, which are usually synthesised by hydrogenolysis of hydrocarbyl complexes. Teuben has reported the facile synthesis of $[YCp'_2(\mu\text{-}H)]_2$ by treatment of the unsolvated ether-functionalised $[YCp'_2(AlH_4).NEt_3]_2$ with triethylamine($MeOCH_2CH_2C_5H_4$).[32] Similar reactivity has been observed for bis(di-tert-butylcyclopentadienyl) complexes of Ce and Sm.[29] The transition metal aluminohydrides stabilised by cyclopentadienyl ligands are also believed to be convenient models for the study of reactive sites in Ziegler-type systems.[36]

Preparation and attempted preparation of (pyrazolylborate)lanthanide aluminohydrides

The preparation of aluminohydrides of bis- and mono(pyrazolylborate)lanthanides was attempted by reaction of the appropriate precursor chlorides or triflates with lithium aluminium hydride in THF or in diethyl ether.

A pale yellow solid was obtained from the reaction of $[Ce(Tp^{Me,Me})_2OTf]$ with $LiAlH_4$ in THF, followed by extraction into toluene. The chemical shifts and integration of the ^1H NMR spectrum suggested that a mixture of $LiTp^{Me,Me}$ and $[Ce(Tp^{Me,Me})_2AlH_4]$ had been obtained, with the resonance at 3.5 ppm attributed to the AlH_4 protons.

The analogous reaction between $[Sm(Tp^{Me,Me})_2Cl]$ and $LiAlH_4$ in diethyl ether afforded a pale yellow microcrystalline solid in reasonable yield which decomposed under inert (N_2) atmosphere over a period of days, yielding a grey solid, possibly owing to extrusion of aluminium metal. $[Y(Cp)_2(AlH_4)L_n]$ (L = NEt_3, Et_2O, THF) has similarly been reported to decompose on storage.[36] The decomposition product in this case has not been identified. However, the ^1H NMR spectrum of the pale yellow solid was at odds with the presence of an aluminohydride ion and instead was consistent with the formation of $LiTp^{Me,Me}$ as the major product, with the presence of a second product suggested by weak resonances in the baseline. The infrared spectrum displayed a B–H stretch at 2521 cm^{-1}, slightly higher than the 2515 cm^{-1} expected for $LiTp^{Me,Me}$.

The inconsistency between the ^1H NMR and the infrared spectra could be explained by the $[Sm(Tp^{Me,Me})_2AlH_4]$ product undergoing ligand redistribution at room temperature in solution (rather than decomposition as observed in the solid state), with formation of insoluble products such as $[Sm(Tp^{Me,Me})(AlH_4)_2]$ and $[Sm(AlH_4)_2]$ which are not observed in the NMR spectrum.

The reaction of $[Eu(Tp^{Me,Me})_2OTf]$ with $LiAlH_4$ in THF at low temperature resulted in a rapid colour change from pale yellow to deeper yellow/orange and slight effervescence. Reduction of Eu (III) to Eu (II) offers a possible reason for the colour change, although the fluorescent orange colour characteristic of $[Eu(Tp^{Me,Me})_2]$ was not observed. The product was purified by sublimation onto a liquid nitrogen-cooled probe. Elemental

microanalysis gave figures which were very low for C, H and N. The fact that these three elements were found to be present in the correct ratio for $Eu(Tp^{Me,Me})_2AlH_4(THF)$ could indicate that there is some salt coordination, although the characteristic infrared bands for the triflate anion at 1200 and 1272 cm^{-1} were not observed. There was, however, a similar lack of evidence for the presence of Al–H. It was not possible to obtain ^1H or ^{27}Al NMR spectra owing to severe line broadening caused by the paramagnetic Eu centre. The insolubility of the complex in common non-halogenated or "non-reactive" organic solvents hampered attempts at recrystallisation, although it might be possible to recrystallise the compound by slow sublimation. This has not been attempted owing to the small yields of product obtained.

$[Ln(Tp^{Me,Me})(AlH_4)_2]$

Attempts were also made to prepare the corresponding half-sandwich complexes $[Ln(Tp^{Me,Me})(AlH_4)_2]$ (Ln = Y, Yb).

The reaction between **4.9** and $LiAlH_4$ in diethyl ether, followed by recrystallisation from the same solvent, afforded a colourless microcrystalline material. The infrared spectrum of this complex displayed two bands in the B–H stretching region but no peaks that could be construed as Al–H stretches. The ^1H NMR spectrum showed that both THF and Et_2O were present. Resonances attributed to the pyrazolylborate ligand were observed, although one signal, at 2.7 ppm, could be assigned to either a methyl group or to the two aluminohydride groups. No resonances attributed to $LiTp^{Me,Me}$ were observed, in contrast to the problems encountered in the attempted preparation of the bis(pyrazolylborate)lanthanide hydrocarbyl complexes and of the cerium and samarium aluminohydrides.

The elemental analysis values found for C and H correlated well with the calculated values, although the nitrogen content was again very low.

The analogous reaction of **4.11** with $LiAlH_4$ resulted in some reduction to purple $[Yb(Tp^{Me,Me})_2]$, illustrating the reducibility of $[Yb^{III}(Tp^{Me,Me})_2]$ complexes. Following filtration and removal of solvent the infrared spectrum of the crude product (which was

pale pink owing to the presence of a small amount of the divalent [Yb($Tp^{Me,Me}$)$_2$]) displayed two B–H bands consistent with lanthanide-coordinated $Tp^{Me,Me}$ and a broad band around 1900 - 1750 cm^{-1}, which could be attributed to AlH_4. The Al–H stretching region in bis(cyclopentadienyl)lanthanide complexes occurs at lower frequency than the corresponding borohydride B–H stretches, in the range 1580 to 1890 cm^{-1} compared to 2100 - 2530 cm^{-1}.[24] A broad band at similar frequency was observed in the yttrium complex [Y(Cp)$_2$)]$_2$(μ-Cl)(μ-AlH_4.NEt_3).C_6H_6.[42] The ^{1}H NMR spectrum displayed peaks over a chemical shift range of +80 to -15 ppm and the multitude of resonances was unassignable.

Preparation and attempted preparation of (pyrazolylborate)lanthanide borohydrides

The reaction of [Ce($Tp^{Me,Me}$)$_2$OTf] with $NaBH_4$ afforded a pale yellow microcrystalline solid which exhibited infrared bands attributed to the pyrazolylborate group and weak bands in the borohydride B–H (terminal region). Two intense bands at 2391 and 2304 cm^{-1} were also displayed. By analogy with the work of Bulychev *et al* in the preparation of [Ln(C_5H_3-Bu^t_2)$_2$(BH_4)]$_2$ (Ln = Ce,[28] Sm[29]) which display infrared bands in the region of 2400 and 2300 cm^{-1} the structure could be assigned as a dimer possessing two η^4-BH_4 groups as shown in figure 4.9e.

The insolubility of our product in hydrocarbon solvents precluded NMR spectroscopy; the C,H,N ratio determined by elemental microanalysis, however, is consistent with the formulation Ce($Tp^{Me,Me}$)$_2$(BH_4).THF. Whilst the poor solubility could reasonably be assigned to a different, possibly polymeric structure it could, alternatively, be due to the low solubility conferred by the $Tp^{Me,Me}$ ligand in these solvents since it seems unlikely that the bulky $Tp^{Me,Me}$ ligands would accommodate either a dimeric or a polymeric structure containing bridging BH_4 groups.

Mono(pyrazolylborate)lanthanide borohydride complexes.

The half-sandwich mono(pyrazolylborate)lanthanide bis(borohydrides) were also prepared. The yttrium complex was prepared by stirring either **4.9** or **4.10** with 2

equivalents of sodium borohydride in THF. Following addition of solvent at -78°C, then warming to room temperature and filtering, a clear colourless solution was obtained. Concentration of this solution and cooling to -30°C afforded a colourless microcrystalline solid. As well as the pyrazolylborate band in the infrared spectrum, the B–H region also exhibited two intense bands at 2286 (with a shoulder) and 2228 cm^{-1} and some weaker bands in both the terminal and the bridging B–H regions. The splitting of *ca.* 50 cm^{-1} between the ν_{BH} (bridging) bands in the infrared spectrum suggest that the BH_4 groups are bound in tridentate fashion. The presence of the weaker bands, while possibly indicative of a minor species, could indicate that the borohydride groups exhibit different ligation modes, with one bidentate and one tridentate BH_4 (figure 4.15). The infrared spectrum is shown in Appendix 3.

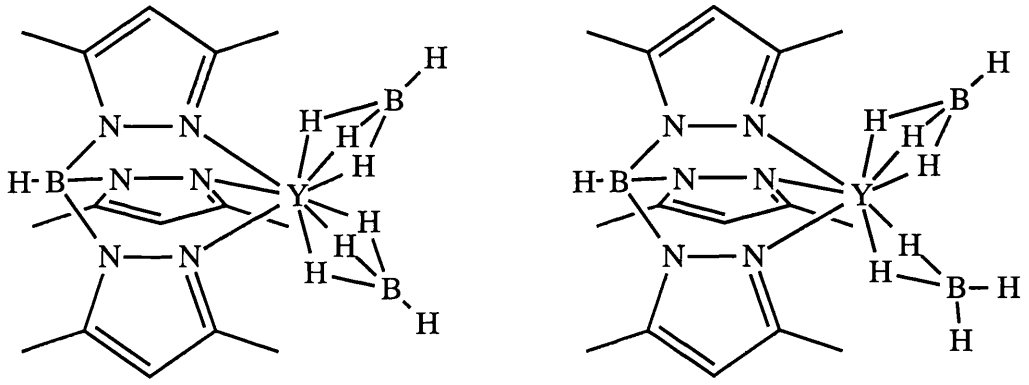

FIgure 4.15. Possible structures of "[Y($Tp^{Me,Me}$)(BH_4)$_2$]"

The ^1H NMR spectrum in benzene-d_6 displayed resonances assigned to the pyrazolylborate protons and to solvent although the integral for one THF peak is larger than that for the other. The expected broad 1:1:1:1 quartet for BH_4 was not observed, although on cooling a sample in toluene-d_8 to -80°C a new peak emerged at 2.9 ppm which could be attributed to the borohydride group. The ^{11}B NMR spectrum is consistent with a single BH_4 environment, displaying, in addition to the pyrazolylborate resonance, a quintet at -24.6 ppm with coupling constant J_{BH} = 83.5 Hz.

The reaction of **4.11** with $NaBH_4$ in THF followed by extraction into toluene and removal of solvent afforded a white powdery solid. The infrared spectrum displayed a

weak band in the terminal, and two intense bands with separation of 20 cm^{-1} in the bridging ν_{BH} region, suggestive of tridentate coordination for both BH_4 groups. The ^1H NMR spectrum exhibits a large number of quite sharp signals in the range +80 to -90 ppm, the assignment of which has not been possible. The spectrum is shown in Appendix 3. The ^{11}B NMR spectrum displayed one broad resonance centred at *ca.* -8.43 ppm, attributed to the pyrazolylborate group. No other signals were observed, presumably due to broadening caused by the paramagnetic f^{13} ytterbium metal centre.

Preparation and attempted preparation of (pyrazolylborate)lanthanide phenylborohydrides

In order to improve the solubility of the reaction products and to have a reliable ^1H NMR handle for the borohydride ligand the NMR and infrared spectra, it was decided to use a substituted borohydride group. The phenyl-substituted borohydride group was chosen because the distinctive ^1H NMR phenyl resonances would not overlap with pyrazolylborate signals and because lithium phenylborohydride is easily prepared from the commercially available phenylboronic acid. The phenyl ring should also improve the solubility of the products in hydrocarbon solvent.

The same reaction procedure was employed in the preparation of all the phenylborohydride complexes, namely, the reagents (the appropriate (pyrazolylborate)lanthanide halide or triflate and one or two equivalents of $Li\{BH_3Ph\}$) were mixed in a schlenk and diethyl ether added at -78°C. The solutions were stirred for several hours while warming to ambient temperature, then filtered. In the case of the bis(pyrazolylborate) samarium and the mono(pyrazolylborate) yttrium and ytterbium complexes, cooling a concentrated ether solution afforded colourless microcrystalline material. The products of the reactions involving complexes of neodymium, europium and gadolinium were isolated by removal of solvent from the diethyl ether filtrate in order to obtain structural information by spectroscopic techniques.

[Nd(Tp^{Me,Me})$_2$(BH$_3$Ph)]

A pale blue/mauve powder was obtained from the reaction between [Nd(Tp^{Me,Me})$_2$OTf] and Li(BH$_3$Ph). The solid state infrared spectrum exhibited a sharp band at 2557 cm^{-1} for the Tp B–H stretch and two bands at lower frequency. These bands, at 2293 and 2224 cm^{-1} (ν_{BHb}), together with the absence of bands in the terminal B–H region, indicate a tridentate coordination mode for the BH$_3$Ph group, similar to that observed by Edelstein *et al* in the Lewis base adducts Ln(BH$_3$Me)$_3$.L (Ln = Lu, Yb, Ho; L = OEt$_2$, THF).[43]

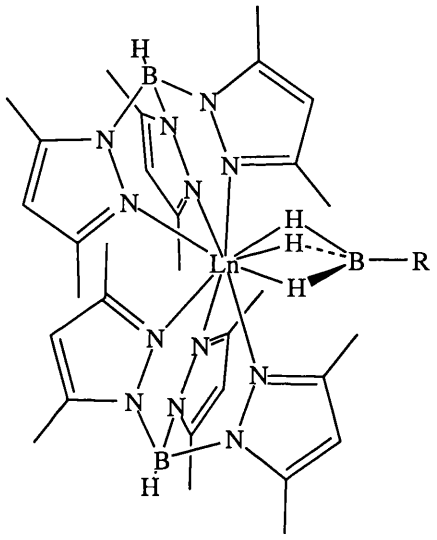

The ^{1}H NMR spectrum in benzene-d$_6$ displayed many resonances in the range +15 to -25 ppm. By analogy with the spectrum of [Nd(Tp^{Me,Me})$_2$OTf] the peaks at -8.87 and 4.45 ppm were assigned to the pyrazolylborate methyl substituents and the signal at 7.85 ppm to the pyrazolyl ring proton. The phenyl signals were located in the normal chemical shift range. Resonances attributed to LiTp^{Me,Me} were also observed. In addition a fairly large number of smaller signals was present which we presume to arise from an as yet unidentified impurity of low symmetry; this prevented assignment of the BH$_3$Ph hydride resonances. ^{11}B NMR spectroscopy was attempted but the paramagnetism of the Nd centre resulted in severe line broadening and no resonances were observed.

[Sm($Tp^{Me,Me}$)$_2$(BH_3Ph)]

The infrared spectrum of the microcrystalline solid obtained in the reaction of [Sm($Tp^{Me,Me}$)$_2$Cl] and Li(BH_3Ph) displayed a broad band centred on 2195 cm^{-1}, of similar appearance to the spectra of other complexes in which the borohydride coordination mode has been assigned as tridentate, for example [Sm(Cp)$_2BH_4$.THF].[30] In addition to the Sm($Tp^{Me,Me}$) B–H stretch at 2553 cm^{-1}, a second pyrazolylborate B–H stretch was present at 2515 cm^{-1}, indicative of formation of $LiTp^{Me,Me}$. The ^1H NMR spectrum revealed that the major product in solution was indeed $LiTp^{Me,Me}$, with at least two other pyrazolylborate- and phenylborohydride- containing species present, identified by the additional four signals attributed to pyrazolylborate methyl substituents and the two 4-CH resonances. Two broad resonances were displayed in the $^{11}B\{^1H\}$ NMR spectrum. The J_{B-H} coupling constants could not, however, be resolved.

The elemental microanalysis figures were somewhat lower than expected, believed to be due to salt coordination and to the presence of $LiTp^{Me,Me}$.

[Eu($Tp^{Me,Me}$)$_2$(BH_3Ph)]

The reaction between [Eu($Tp^{Me,Me}$)$_2$OTf] and Li(BH_3Ph) afforded a pale yellow powder which exhibited infrared stretching frequencies consistent with tridentate coordination of the BH_3Ph group, as well as the pyrazolylborate B–H stretch at 2561 cm^{-1}. No band was observed at 2515 cm^{-1}, indicating that in this case $LiTp^{Me,Me}$ was absent. This observation was confirmed by the ^1H NMR spectrum which displayed no resonances at the chemical shifts characteristic of $LiTp^{Me,Me}$. By analogy with the ^1H NMR spectrum of [Eu($Tp^{Me,Me}$)$_2$(OTf)] the peaks at 2.04 and 9.81 ppm were assigned to the pyrazolylborate methyls and the signal at 5.15 ppm to the 4-CH. Resonances attributed to the phenyl substituent were also located in the aromatic region. Although a number of sharp singlets were displayed at high (27 to 28 ppm) and low (-9 to -0.6 ppm) chemical shift, it is unlikely that they arise from the borohydride protons (given their proximity to the paramagnetic f^7 Eu^{3+} centre). A single, very broad resonance centred around 11 ppm

was observed in the $^{11}B\{^{1}H\}$ NMR spectrum. No signals were observed in the proton-coupled ^{11}B spectrum.

[Gd($Tp^{Me,Me}$)$_2$(BH_3Ph)]

The white powder isolated from the reaction of [Gd($Tp^{Me,Me}$)$_2$OTf] with Li(BH_3Ph) exhibited two bands in the pyrazolylborate B–H stretching region, one consistent with lanthanide pyrazolylborate and the other with the presence of $LiTp^{Me,Me}$. A broad, weak band centred around 2360 cm^{-1} was attributed to a phenylborohydride bound in η^3 mode. The resonances in the ^{1}H NMR spectrum were broad and at the chemical shifts associated with $LiTp^{Me,Me}$. No other signals were observed, presumably owing to the increased broadening of the resonances associated with groups bound directly to the f^7 gadolinium metal centre.

Half-sandwich complexes [Ln($Tp^{Me,Me}$)(BH_3Ph)$_2$]

The mono(pyrazolylborate)lanthanide complexes [Ln($Tp^{Me,Me}$)(BH_3Ph)$_2$] (Ln = Y, Yb) have also been prepared.

The reaction of **4.9** with Li(BH_3Ph) in Et_2O, followed by recrystallisation from the same solvent, afforded colourless crystals. The broad infrared band centred on 2214 cm^{-1} (Appendix 3) suggests that tridentate coordination is adopted for both BH_3Ph groups. The ^{1}H NMR spectrum in benzene-d_6 exhibited resonances attributed to the pyrazolylborate group, to the phenyl rings and to Et_2O. A number of very broad signals were also displayed, possibly indicating the presence of a fluxional species. Three different boron environments were displayed in the ^{11}B NMR spectrum, a broad doublet at -8 ppm attributed to the Tp ligand, a triplet at -12 ppm (*vide infra*) and quartet with coupling constant of 70 Hz assigned to the phenylborohydride moiety, at *ca* -14 ppm relative to $B(OEt_3)$.

The elemental microanalysis figures were very low for C, H and N, suggesting that coordinated LiCl salt was affecting the values. The ratios of C and H to N were slightly high, consistent with coordination of solvent.

[Yb($Tp^{Me,Me}$)($BH_3Ph)_2$]

Stirring **4.10** with Li(BH_3Ph) in Et_2O, then cooling a concentrated ether solution, afforded a colourless microcrystalline solid. The infrared spectrum was almost superimposable with that of the yttrium analogue, with the broad band centred at 2220 cm^{-1} suggesting that the borohydride groups were ligated in tridentate fashion. The $^{11}B\{^1H\}$ NMR spectrum in diethyl ether displayed a sharp singlet at -12.51 ppm which split into a triplet in the coupled spectrum with coupling constant of 70 Hz, as well as three broad resonances at -13, -14 and -22 ppm. The signal at -22 ppm split into a quartet (J_{BH} = 81.7 Hz) on coupling to ^1H while the resonances at -12 and -14 ppm became too broad to assign. We presume that one of these signals arises from the Tp ligand and the other from the second BH_3Ph group. The presence of a sharp triplet is unexpected and is believed to arise from formation of a borane, $BH_2Ph.Et_2O$ in ether solution.

The ^1H NMR spectrum displayed signals in the chemical shift range +30 to -75 ppm, although the majority of peaks were located in the 0 to 20 ppm region. On the basis of their integrals, the resonances at -2.8 and 0.95 ppm were assigned to the pyrazolyl methyl substituents and the peak at 4.1 ppm to the pyrazolyl ring proton. The phenyl ring protons were located at 20.22 (*o*-CH), 13.07 (*m*-CH) and 8.63 (*p*-CH) ppm. It was not possible to assign the borohydride proton resonances, although it is probable that the signals would appear at very high or low frequency, by analogy with the ^1H NMR spectra of $Yb(BH_3Me)_3.nTHF$ (n = 1, 2) which exhibited chemical shift ranges of -160 to +85 and -70 to +27 ppm respectively.[43]

Conclusions

In this chapter the preparation and attempted preparation of a number of sandwich and half-sandwich complexes of trivalent lanthanides has been presented. Considerable problems have been encountered in many of these syntheses. Our attempts to complete the series of bis(pyrazolylborate)samarium halides and prepare the corresponding bromide have resulted in the isolation of the half-sandwich "ate" complex **4.1**, rather

than the sandwich complex $Sm(Tp^{Me,Me})_2Br$. Similarly the syntheses of bis(pyrazolylborate)yttrium and ytterbium chlorides **4.7** and **4.8** and (to an even greater extent) the corresponding yttrium iodide afforded mixtures of products if allowed to remain in solution for extended periods of time, illustrating the proclivity of these systems to undergo ligand redistribution, even with the bulky 3,5-dimethyl trispyrazolylborate ancillary ligands. The bis(pyrazolylborate)samarium carboxylate complexes **4.2** - **4.4** have been prepared and characterised by elemental microanalysis and ^1H NMR and infrared spectroscopy. The structures have not been elucidated; although crystals of the benzoate **4.4** were grown they were in fact found to be the hydrolysed dimer **4.5**.

Attempts to prepare half-sandwich yttrium and ytterbium amide and hydrocarbyl complexes suitable for investigations into the preparation of imido complexes were frustrated by major problems with ligand redistribution; although NMR spectroscopy indicated the presence of the desired product in some cases, essentially no tractable products were obtained.

Reaction of sandwich and half-sandwich complexes with $LiAlH_4$ afforded products which exhibited no identifiable infrared bands in the Al–H region and no signals in the ^{27}Al NMR spectra. In some cases, $LiTp^{Me,Me}$ was identified as a major (or the sole) product. Reactions with sodium borohydride and lithium phenylborohydride gave products whose infrared spectra were consistent with tridentate coordination of the borohydride group to the metal, although $LiTp^{Me,Me}$ was again identified on several occasions from the latter reactions.

The $Tp^{Me,Me}$ ligand is appearing increasingly fragile when coordinated to the lanthanides. The susceptibility of $Tp^{Me,Me}$ to hydrolysis, in particular *via* cleavage of one B–N bond, seems much greater than the unsubstituted Tp ligand; the dimeric hydrolysis product **4.5** has been isolated on many occasions, by a number of workers, with samarium and other lanthanides. Reactivity towards this particular hydrolytic route could be attributed to the increased steric bulk around the boron atom at the "back" of the ligand causing

twisting of the pyrazolyl rings of the type observed in **2.4**, thereby opening the B–N bond to attack by water. Although the use of 3-substituted pyrazolylborates, unsubstituted in the 5-position of the pyrazolyl rings, might reduce the risk of hydrolysis *via* this route, the consequent exposure of the B–H bond could offer an alternative site for hydrolysis. The tendency of the $Tp^{Me,Me}$ ligand to undergo redistribution, in particular with small group 1 and 2 metals has also been amply demonstrated and $LiTp^{Me,Me}$ has been obtained as a major product in a number of reactions involving lithium reagents, including attempts to reproduce literature preparations of half-sandwich yttrium hydrocarbyl complexes. This mirrors the problems encountered by Maunder using Grignard reagents in the preparation of (pyrazolylborate)lanthanide hydrocarbyl complexes and by Piers in analogous scandium chemistry. More effective synthetic routes appear to be transmetallation with soft metal reagents, as in the preparation of **4.6**, (although this method was found to be ineffective for the preparation of $Sm(Tp^{Me,Me})_2Ph$) or protonolysis from tris(hydrocarbyl)lanthanide complexes, as reported by Piers (*vide supra*).

Chapter 4 - References

1) Blackwell, J. A.; Lehr, C.; Sun, Y.; Piers, W. E.; Pearce-Batchilder, S. D.; Zaworotko, M. J.; Young, V. G. J. *Can. J. Chem.* **1997**, *75*, 702.

2) Takats, J., *personal communication.*

3) Marques, N., *personal communication.*

4) Watson, P. L.; Whitney, J. F.; Harlow, R. L. *Inorg. Chem.* **1981**, *20*, 3271.

5) Emsley, J. *The Elements*; Oxford University Press: Oxford, 1989.

6) Sun, Y. M.; McDonald, R.; Takats, J.; Day, V. W.; Eberspacher, T. A. *Inorg. Chem.* **1994**, *33*, 4433.

7) Liu, S.-Y. *PhD thesis*; University of London, 1996.

8) Maunder, G. H. *PhD thesis*; University of London, 1995.

9) Day, V.; Liu, S.; Sella, A., *unpublished results.*

10) Day, V. W., *personal communication.*

11) Watson, P. L. *J. Chem. Soc.,Chem. Commun.* **1980**, 652.

12) Reger, D. L.; Knox, S. J.; Lindemann, J. A.; Lebioda, L. *Inorg. Chem.* **1990**, *29*, 416.

13) Moss, M. A. J.; Jones, C. J. *J. Chem. Soc., Dalton Trans.* **1990**, 581.

14) Maunder, G.; Sella, A.; Takats, J.; Zhang, X. ; Maunder, G.; Sella, A.; Takats, J.; Zhang, X., Ed., *unpublished results.*

15) Reger, D. L.; Lindeman, J. A.; Lebioda, L. *Inorg. Chem.* **1988**, *27*, 3923.

16) Reger, D. L.; Lindeman, J. A.; Lebioda, L. *Inorg. Chem. Acta* **1987**, *139*, 71.

17) Kuchta, M. C.; Dias, H. V. R.; Bott, S. G.; Parkin, G. *Inorg. Chem.* **1996**, *35*, 943.

18) Dowling, C. M.; Leslie, D.; Chisholm, M. H.; Parkin, G. *Main Group Met. Chem.* **1995**, *1*, 29.

19) Apostolidis, C.; Rebizant, J.; Kanellakopoulos, B.; Ammon, R. v.; Dornberger, E.; Müller, J.; Powietzka, B.; Nuber, B. *Polyhedron* **1997**, *16*, 1057.

20) Stainer, M. V. R.; Takats, J. *Inorg. Chem.* **1982**, *21*, 4050-4053.

21) Duchateau, R.; Brussee, E. A. C.; Meetsma, A.; Teuben, J. H. *Organometallics* **1997**, *16*, 5506.

22) Watkin, J. G., *personal communicatio*n.

23) Long, D. P.; Bianconi, P. A. *J. Amer. Chem. Soc.* **1996**, *118*, 12453.

24) Ephritikhine, M. *Chem. Rev.* **1997**, *97*, 2193.

25) Marks, T. J.; Kolb, J. R. *Chem. Rev.* **1977**, *77*, 263.

26) Mancini, M.; Bougeard, P.; Burns, R. C.; Mlekuz, M.; Sayer, B. G.; Thompson, J. I. A.; McGlinchey, J. *Inorg. Chem.* **1984**, *23*.

27) Lappert, M. F.; Singh, A.; Atwood, J. L.; Hunter, W. E. *J. Chem. Soc.,Chem. Commun.* **1983**, 206.

28) Lobkovsky, E. B.; Gun'ko, Y. K.; Bulychev, B. M.; Belsky, V. K.; Soloveichik, G. L.; Antipin, M. Y. *J. Organomet. Chem.* **1991**, *406*, 343.

29) Gun'ko, Y. K.; Bulychev, B. M.; Soloveichik, G. L.; Belsky, V. K. *J. Organomet. Chem.* **1992**, *424*, 289.

30) Marks, T. J.; Grynkewich, G. W. *Inorg. Chem.* **1976**, *15*, 1302.

31) Deng, D.; Zheng, X.; Qian, C.; Sun, J.; Zhang, L. *J. Organomet. Chem.* **1994**, *466*, 95.

32) Laske, D. A.; Duchateau, R.; Teuben, J. H.; Spek, A. L. *J. Organomet. Chem.* **1993**, *462*, 149.

33) Cendrowski-Guillaume, S. M.; Nierlich, M.; Lance, M.; Ephritikhine, M. *Organometallics* **1998**, *17*, 786.

34) Arliguie, T.; Lance, M.; Nierlich, M.; Ephritikhine, M. *J. Chem. Soc. Dalton Trans.* **1997**, 2501.

35) Baudry, D. *J. Organomet. Chem.* **1997**, *547*, 157.

36) Belsky, V. K.; Erofeev, A. B.; Bulychev, B. M.; Soloveichik, G. L. *J. Organomet. Chem.* **1984**, *265*, 123.

37) Knjazhansky, S.; Bulychev, B.; Kireeva, O. K.; Belsky, V.; Soloveichik, G. *J. Organomet. Chem.* **1991**, *414*, 11.

38) Knjazhanski, S. Y.; Bulychev, B. M.; Belsky, V. K.; Soloveichik, G. L. *J. Organomet. Chem.* **1987**, *327*, 173.

39) Bel'skii, V. K.; Bulychev, B. M.; Erofeev, A. B.; Soloveichik, G. L. *J. Organomet. Chem.* **1984**, *268*, 107.

40) Gun'ko, Y. K.; Bulychev, B. M.; Sizov, A. I.; Soloveichik, G. L.; Belsky, V. K. *J. Organomet. Chem.* **1990**, *390*, 153.

41) Belsky, V. K.; Gun'ko, Y. K.; Bulychev, B. M.; Soloveichik, G. L. *J. Organomet. Chem.* **1991**, *420*, 43.

42) Erofeev, A. B.; Bulychev, B. M.; Bel'skii, V. K.; Soloveichik, G. L. *J. Organomet. Chem.* **1987**, 189.

43) Shinomoto, R.; Zalkin, A.; Edelstein, N. M. *Inorg. Chim. Act.* **1987**, *139*, 97.

Chapter 5 - Experimental Details

General Procedures

All manipulations were carried out under an atmosphere of dry nitrogen [1] either using standard Schlenk line techniques or in a Braun Lab Star 50 or a Vacuum Atmospheres HE-493 glove box. All air sensitive compounds and the reagents required for their synthesis were stored in a glove box after preparation. Sublimations were generally carried out in horizontal tubes of diameter *ca.* 8-35 mm, depending on the scale, with a tube furnace as the heat source. On account of their toxicity, all manipulations involving hexamethylphosphoramide (HMPA) and thallium salts were carried out in a fume cupboard. Molecular sieves were predried in an oven at 150°C for several days and activated prior to use by heating to *ca.* 200°C under vacuum.

Purification of Reagents

Oxygen-free nitrogen (% BOC) was further dried and deoxygenated by passage through columns containing 5 Å molecular sieves and manganese(II) oxide prior to use on the Schlenk tube line [2]. Nitrogen used for the glove boxes was not prepurified, but an atmosphere thoroughly freed from oxygen and moisture was achieved by continuous circulation through BASF R311 catalyst and 5 Å molecular sieves and was regularly monitored by the use of a toluene solution of $(Cp_2TiCl_2)/Zn$ (which remains green in the absence of these contaminants).

Reaction solvents were predried over sodium wire, with the exception of CH_2Cl_2 which was predried over molecular sieves and CH_3CN which was not predried. They were then dried by refluxing over and distillation from the appropriate drying agent, under a stream of dinitrogen, as follows: 3:1 alloy of sodium and potassium (diethyl ether and pentane),

potassium (THF), sodium (toluene), CaH_2 (CH_2Cl_2, CH_3CN). THF, toluene, diethyl ether and pentane were stored over sodium mirrors. Solvents used for the preparation of pyrazolylborate ligands were not dried or otherwise purified; HMPA, methanol and ethanol (95 %) were similarly used as received.

Y, Sm and Yb metals were purchased from Aldrich as ingots (99.9 %). The triflates of Ce and Nd and the bis{tris(pyrazolyl)borate}triflates of Nd, Eu and Gd were prepared by Dr. G. Maunder [3] and stored in a glovebox.

Ammonium iodide was heated at 120°C for *ca.* 1 hour under vacuum. Diiodoethane was purified by dissolving in diethyl ether and washing with an aqueous solution of sodium thiosulphate and then with water. The solution was then dried over anhydrous $MgSO_4$ and the solvent removed on a rotary evaporator, to give a white crystalline solid which was thoroughly dried overnight under dynamic vacuum. Anthraquinone was sublimed under vacuum prior to use. $(SC_6H_5)_2$, $(S\text{-}4\text{-}Me\text{-}C_6H_4)_2$, $(SCH_2C_6H_5)_2$, $(Se\text{-}4\text{-}Bu^t\text{-}C_6H_4)_2$, $(Se\text{-}4\text{-}MeO\text{-}C_6H_4)_2$, $(SeCH_2C_6H_5)_2$ and $(TeC_6H_5)_2$ were donated by Dr. S. MacWhinney of Brunel University. $[MoCp^{Me}(CO)_3]_2$ and $[MoCp^{t\text{-}Bu}(CO)_3]_2$ were prepared by Omar Zekria. $Mn_2(CO)_{10}$ and $Re_2(CO)_{10}$ were donated by Prof. A. J. Deeming. $Mn_2(CO)_{10}$ was recrystallised from 30/40 petrol or used as received. 3,5-Dimethylpyridine, previously distilled from CaH_2 and stored in the glove box, was redried over KOH. t-Butylamine, 2,4,6-trimethylaniline and 2,6-diisopropylaniline were dried by refluxing over CaH_2 overnight before being distilled under reduced pressure. $KCH(SiMe_3)_2$ and $KCH_2C_6H_5$ were prepared by Dr. G. Maunder. $LiBH_3Ph$ was prepared by Dr. A. Sella. Sodium formate, acetate and benzoate were dried in an oven at 150 - 200°C overnight and then under dynamic vacuum. $NaS_2CNEt_2.3H_2O$ was dried at 100°C under dynamic vacuum. Ammonia gas was not predried. KH (80 % suspension in mineral oil, Aldrich) and NaH (60 % suspension in mineral oil, Aldrich) were washed with several portions of 40/60 petrol, dried under vacuum and stored in a glove box. Li, Na and K metals were cleaned by removing the oxidised surface with a knife in a glove box or under toluene. Hg was not

treated prior to use and Na/Hg amalgam was prepared under a flow of nitrogen. Excess pyrazoles recovered from pyrazolylborate syntheses by distillation or sublimation were reused in subsequent preparations.

The following reagents were purchased from various suppliers and were used without further purification: acetylacetone (acacH), azobenzene, benzotriazole, 1-bromopropane, chloromethyltrimethylsilane, 3,5-dimethylpyrazole, ethyl acetate, ethyl iodide, hydrazine hydrate, hydrazinium sulphate, iodine, $LiAlH_4$, $MgSO_4$ (anhydrous), $HgBr_2$, $HgPh_2$, 1-octyne, phenylacetylene, pinacolone, p-tolylisocyanate, KBH_4, $NaBH_4$, $NaBPh_4$, $NaBF_4$, $Fe(CO)_5$, $Fe_2(CO)_9$, 2,6-quinone.

All NMR solvents were purchased from Aldrich. Benzene-d_6 and toluene-d_8 were dried over a 1:3 alloy of sodium and potassium and then either filtered through glass wool or vacuum transferred to a clean, dry ampoule and stored in a glove box. Chloroform-d was dried and stored over activated 3 Å molecular sieves.

Instrumentation

NMR spectra were run on Bruker AC300 (^1H, ^{13}C) Varian XL200 (^1H) and Varian VXR400 (^1H, ^{13}C, ^{11}B, ^{27}Al and ^{125}Te) spectrometers. Spectra were referenced to peaks produced by residual non-deuterated molecules present in the solvent. IR spectra were obtained using a Nicolet 205 FTIR spectrometer.

All elemental micro-analyses were performed by Mr. Alan Stones of the Analytical Services of the Christopher Ingold Laboratories, UCL. Moderately air-sensitive samples were sealed in Pyrex tubes and then weighed rapidly in air or under an atmosphere of argon. The analysis of more reactive compounds was achieved by sealing the sample directly inside a preweighed aluminium analysis boat in a glove box, reweighed to determine the mass of sample and analysing as normal.

Starting Materials

Preparation of 3,5-dimethyl-4-ethylpyrazole[3]

Acetylacetone (110 g, 1.10 mol) was added dropwise to a suspension of sodium sand (23.0 g, 1.00 mol) in toluene (1000 ml) over a period of 30 minutes. After addition, the mixture was refluxed for 30 minutes until all the sodium had dissolved. After cooling the white solid was filtered in air on a Buchner funnel, washed with petrol (250 ml) and dried under dynamic vacuum. The sodium acetylacetonate was then mixed with ethyl iodide (500 g, 3.20 mol) and HMPA (50 ml) in a pressure vessel and stirred at 90°C for 4 days, during which time the solution turned dark red-brown and a pale yellow precipitate of NaI formed. After cooling, water (600 ml) and toluene (750 ml) were added and the mixture transferred to a separating funnel. The organic phase was washed with water (3 x 300 ml) to remove NaI and HMPA, then solvent was removed on a rotary evaporator. The residue was dissolved in methanol and hydrazine hydrate (50.1 g, 1.00 mol) added to the stirred solution. After initial exothermic reaction the solution was stirred for 30 minutes. After removal of solvent on a rotary evaporator the resulting oil was dissolved in toluene and the solution washed with water. The toluene phase was then dried over $MgSO_4$ and distilled at 66-98°C at 1 mm Hg in a short path distillation device to give 64.5 g (0.52 mol, 52 %) of 3,5-dimethyl-4-ethylpyrazole as pale yellow crystals.

^1H NMR ($CDCl_3$): 1.04 (t, 3H, CH_3), 2.05 (s, 6H, 3,5-Me), 2.20 (q, 2H, CH_2).

Preparation of 3-*tert*-butyl-5-methylpyrazole[4,5]

A three-necked round bottomed flask (5000 ml), fitted with an overhead stirrer, an efficient condenser and a nitrogen bubbler, was charged with ethyl acetate (176 g, 2.0 mol), sodium hydride (80 g of 60 % NaH in mineral oil, 2.0 mol) and diethyl ether (2500 ml). Pinacolone (100 g, 1.0 mol) was then added dropwise to the stirred mixture. Slight warming was necessary to initiate the reaction (as seen by the evolution of hydrogen) and

the mixture was refluxed gently for 14 hours until hydrogen evolution had ceased and the mixture had become off-white. The mixture was then allowed to cool and water carefully added in air, with stirring. The aqueous layer was separated and the ether extracted with water (3 x 200 ml). A solution of hydrazine dihydrochloride $H_2NNH_2.2HCl$ (105 g, 1.0 mol) in water (2500 ml) was half-neutralised by adding sodium carbonate (58 g, 0.5 mol). To the stirred solution of $H_2NNH_2.HCl$ in water were added the combined aqueous extracts and a cream precipitate was formed immediately. Stirring was continued for 30 minutes and the solid filtered on a Buchner funnel to give a cream-coloured powdery solid. This crude product was purified by vacuum sublimation (150°C, 10^{-1} mbar) to give 73.5 g (0.53 mol, 53 %) of the pale yellow crystalline 3-tert-butyl-5-methylpyrazole.

^1H NMR ($CDCl_3$): 1.29 (s, 27H, Bu^t), 2.25 (s, 9H, Me), 5.86 (s, 3H, 4-C-H).

Preparation of Sodium Hydrotris(3,5-dimethylpyrazol-1-yl)borate ($NaTp^{Me,Me}$)6

A mixture of sodium borohydride (1.6 g, 0.043 mol) and 3,5-dimethylpyrazole (25 g, 0.26 mol) was heated in a round bottomed flask fitted with an air condenser and a nitrogen bubbler. The temperature (which was measured by means of a thermometer sitting inside the apparatus) was steadily increased to 210°C until a clear melt was obtained and hydrogen evolution had ceased. Heating was stopped and the melt allowed to cool to 180°C before being poured carefully into 100 ml of stirred 40/60 petrol. After removal of the solvent the excess pyrazole was separated from the product by vacuum sublimation at 100-130°C, (10^{-1} mmHg) to leave 10 g (0.031 mol, 72 %) of sodium hydrotris(3,5-dimethylpyrazol-1-yl)borate as a white powder.

IR (KBr, cm^{-1}): 2453 (BH).

^1H NMR ($CDCl_3$): 2.0 (s, 3H, Me), 2.25 (s, 3H, Me), 5.50 (s, 1H, 4-H).

Preparation of Potassium Hydrotris(3,5-dimethylpyrazol-1-yl)borate ($KTp^{Me,Me}$)6

A mixture of potassium borohydride (6.0 g, 0.11 mol) and 3,5-dimethylpyrazole (66 g, 0.69 mol) was heated in a round bottomed flask fitted with an air condenser and a nitrogen bubbler. The temperature (which was measured by means of a thermometer sitting inside the apparatus) was steadily increased to 230°C until a clear melt was obtained and hydrogen evolution had ceased. Heating was stopped and the melt allowed to cool to 180°C before being poured carefully into 100 ml of stirred 40/60 petrol. After removal of the solvent the excess pyrazole was separated from the product by vacuum sublimation at 100-130°C, (10^{-1} mmHg) to leave 22 g (0.065 mol, 59 %) of potassium hydrotris(3,5-dimethylpyrazol-1-yl)borate as a white powder.

IR (KBr, cm^{-1}): 2453 (BH).

^1H NMR (d_6-acetone): 2.0 (s, 3H, Me), 2.15 (s, 3H, Me), 5.50 (s, 1H, 4-H).

Preparation of Potassium Hydrotris(3,5-dimethyl-4-ethylpyrazol-1-yl)borate ($KTp^{Me,Me\text{-}4\text{-}Et}$)3

3,5-Dimethyl-4-ethylpyrazole (18.2 g, 0.147 mol) and potassium borohydride (1.64 g, 0.03 mol) were placed in a round bottomed flask fitted with an air condenser and a nitrogen bubbler. The temperature (monitored by means of a thermometer sitting inside the apparatus) was steadily increased to 200°C and maintained at this temperature overnight after which time hydrogen evolution had ceased. Most of the excess pyrazole was distilled out of the mixture by attaching a still head directly onto the round bottomed flask. Final traces of pyrazole were removed by vacuum sublimation at 100°C (10^{-1} mmHg) to leave 4.12 g (11.21 mmol, 37 %) of potassium hydrotris(3,5-dimethyl-4-ethylpyrazol-1-yl)borate.

IR (KBr, cm^{-1}): 2441 (BH). ^1H NMR ($CDCl_3$): 0.94 (t, 9H, CH_3), 1.97 (s, 9H, Me), 2.12 (s, 9H, Me), 2.25 (q, 6H, CH_2).

Synthesis of Potassium Hydrotris(3-*tert*-butyl-5-methylpyrazol-1-yl)borate ($KTp^{t\text{-}Bu,Me}$)5

A mixture of potassium borohydride (2.01 g, 0.037 mol) and 3-tert-butyl-5-methylpyrazole (30 g, 0.22 mol) was heated in a round bottomed flask fitted with an air condenser and a nitrogen bubbler. The temperature (which was monitored by means of a thermometer sitting inside the apparatus) was steadily increased to 210°C until a clear melt was obtained and hydrogen evolution had ceased. The temperature was raised to 225°C for 5 minutes to ensure all the KBH_4 had reacted, then heating was stopped and the melt allowed to cool to 180°C before being poured carefully into 200 ml of stirred 40/60 petrol in air. An off-white precipitate formed and after stirring for 30 minutes this was filtered on a Buchner funnel. Excess pyrazole was removed from the product by vacuum sublimation (150-180°C, 10^{-1} mmHg) to yield 13 g (0.029 mol, 78 %) of potassium hydrotris(3-tert-butyl-5-methylpyrazol-1-yl)borate as a white powdery solid.

IR (KBr, cm^{-1}): 2456 (BH).

^1H NMR ($CDCl_3$): 0.68 (s, 9H, Bu^t), 1.60 (s, 3H, 5-Me), 5.20 (s, 1H, 4-H).

Preparation of Samarium Diiodide[7]

To a lump of Sm metal (10.284 g, 0.068 mol) was added a solution of 1,2-diiodoethane (11.1 g, 0.039 mol) in THF (300 ml). The mixture was stirred for 10 days, forming first a yellow precipitate of SmI_3 which gradually redissolved, and eventually a dark blue precipitate of $SmI_2(THF)_n$. The solution was filtered (keeping it above 50°C to prevent crystallisation), solvent removed under reduced pressure, and the dark blue-grey solid dried under dynamic vacuum to afford 22.6 g (0.040 mol, 100 %) of $SmI_2(THF)_{1.95}$.

Elemental Analysis Calculated: C 17.27, H 2.56, N 0.00. Found C 17.95, H 2.56, N 0.00.

Preparation of Ytterbium Diiodide[8]

A piece of ytterbium metal (4.31 g, 0.025 mol) was placed in a three-necked round bottomed flask containing a stir bar and fitted with a take off adaptor and a cardice condenser. The flask was evacuated, cooled to –78°C, and liquid ammonia (150 ml) condensed onto the metal. A blue solution was formed immediately and the contents of the flask were stirred for *ca.* 30 minutes to allow the ytterbium metal to dissolve. Ammonium iodide (7.2 g, 0.05 mol) was added in several portions under a counterflow of nitrogen and a yellow-orange precipitate of $YbI_2(NH_3)_x$ was formed. After addition was complete the flask contents were stirred at –78°C for 2 hours before the ammonia was allowed to warm to reflux and boil off. The yellow solid obtained was heated under dynamic vacuum overnight (200°C, 10^{-2} mmHg) to remove solvated ammonia. 10.41 g (98 %) of YbI_2 was obtained as a yellow free-flowing fine powder.

Elemental analysis: C 0.00 (0.00), H 0.34 (0.00), N 1.95 (0.00)

Preparation of $SmBr_3$

To a piece of Sm metal (3.47 g, 0.023 mol) in 30/40 petrol (100 ml) at –78°C was added neat bromine (5.5 g, 0.035 mol). The red/brown mixture was stirred for 2 h while warming to room temperature, then for 6 days at room temperature. A small amount of yellow precipitate formed initially, but subsequently no more formed, even on scratching the metal surface with a glass rod. The solvent was removed *in vacuo* and the remaining pale yellow solid washed with 30/40 petrol (2 x 10 ml) then dried at room temperature under dynamic vacuum to afford 82 mg (0.21 mmol, 1 %) of pale yellow powder. Addition of a small quantity of $HgBr_2$ to the reaction did not improve the yield.

Preparation of YCl_3

Yttrium metal (8.01 g, 0.09 mol) was dissolved carefully in conc. HCl and ammonium chloride (28.9 g, 0.54 mol) added. The mixture was heated until all HCl had boiled off. Excess ammonium chloride was removed from the resulting grey solid by sublimation

under dynamic vacuum for 12 h at 100°C then 24 h at 250°C followed by a further 12 h at 350°C, to afford 14.5 g (0.074 mol, 83 %) of YCl_3 as a grey powder.

Powder diffraction: 2θ = 14.75, 26.4, 32.8, 36.1, 45.6, 48.3°.

Preparation of YI_3

Yttrium metal (2.5 g, 28 mmol) and mercuric iodide (20 g, 44 mmol) were placed in a glass tube which was then sealed under vacuum. The tube was heated in a tube furnace to 300°C for 5 days. The mixture gave a dark red melt from which drops of mercury sublimed out into the cool end of the tube. After 3 days the reaction mixture had decolourised leaving a grey solid. 8.7 g (19 mmol, 68 %) of YI_3 was obtained as a grey powder.

Powder diffraction: 2θ = 23.7, 25.6, 27.0, 29.1, 35.1, 41.7, 46.0°.

Preparation of $[Sm(Tp^{Me,Me})_2]^3$

$SmI_2(THF)_{1.95}$ (2.01 g, 3.82 mmol) and $NaTp^{Me,Me}$ (2.69 g, 8.40 mmol) were placed in a Schlenk tube, cooled to -78°C and THF (50 ml) added with stirring. The dark green solution was allowed to warm to room temperature, during which time it turned purple, and stirred for two hours. After settling overnight the supernatant liquid was decanted off and the purple product washed with THF (2x100ml). Drying under dynamic vacuum gave 2.31g (3.11 mmol, 81 %) of bis(hydrotris(3,5-dimethylpyrazol-1-yl)borate)samarium as a purple powder.

IR (KBr, cm^{-1}): 2529 (BH).

Preparation of $[Sm(Tp^{Me,Me-4-Et})_2]^3$

$SmI_2(THF)_{1.95}$ (615 mg, 1.19 mmol) and $KTp^{Me,Me,4-Et}$ (967 mg, 2.29 mmol) were mixed in a Schlenk tube and cooled to –78°C before THF (50 ml) was added. The green solution was stirred for 1 h at -78°C, during which time it turned purple, then allowed to warm to room temperature and stirred overnight. The mixture was allowed to settle, then the solution was filtered and the KI residue extracted with THF (3 x 20 ml) until it was

virtually colourless. The volume of the filtrate was reduced to 40 ml while keeping the solution above 50°C to keep the product from crystallising. Slow cooling to –25°C gave a purple microcrystalline product which was dried *in vacuo* at 80°C. Yield 520 mg (0.57 mmol, 48 %)

IR (KBr, cm^{-1}): 2527 (BH). ^1H NMR (C_6D_6): -0.05 (s, 18H, 3-Me), 1.73 (t, 18H, CH_3), 2.73 (q, 12H, CH_2), 18.27 (s, 18H, 5-Me).

Preparation of $[Ce(Tp^{Me,Me})_2OTf.THF]$[3]

$Ce(OTf)_3$ (2.0 g, 3.4 mmol) and $KTp^{Me,Me}$ (2.29 g, 6.8 mmol) were mixed in a Schlenk tube and THF (50 ml) added at room temperature. The reaction mixture was stirred overnight, then solvent removed and the yellow product extracted into toluene (3 x 30 ml). After reducing the volume of solvent to 30 ml, cooling overnight to –30°C afforded a crop of pale yellow crystals. The supernatant was decanted and further concentrated and cooled to give a second crop of crystals. The crystalline solid was dried at 50°C under dynamic vacuum to give a combined yield of 2.09 g (2.37 mmol, 70 %) of pale yellow powder.

Elemental Microanalysis calculated for $C_{35}H_{52}N_{12}B_2CeO_4SF_3$: C 43.99, H 5.48, N 17.59. Found C 44.35, H 5.27, N 18.84. IR (KBr, cm-1): 2560 (BH); 1202 (OTf).

Preparation of $[Yb(Tp^{t\text{-}Bu,Me})I.THF]$[3,9]

YbI_2 (2.0 g, 4.69 mmol) and $KTp^{t\text{-}Bu,Me}$ (2.0 g, 4.437 mmol) were mixed in a Schlenk tube, cooled to –78°C and THF (100 ml) added with stirring. The mixture was stirred for 1 hour at –78°C, then overnight at room temperature. The yellow solution was allowed to settle, then filtered and the pale yellow KI residue extracted with THF (50 ml). Solvent was removed from the combined filtrates under reduced pressure and the resulting yellow solid extracted with diethyl ether (2 x 100 ml). After filtration, solvent was removed under reduced pressure and the yellow solid dried under dynamic vacuum (10^{-2} mm Hg) to yield 3.05 g (3.89 mmol, 88 %) of $[Yb(Tp^{t\text{-}Bu,Me})I.THF]$ as a yellow powder.

Elemental analysis calculated for $C_{29}H_{21}N_6BOYbI$: C 42.28, H 6.08, N 10.56. Found: C 41.43, H 6.08, N 10.68. IR (KBR, cm^{-1}): 2554 (BH). ^1H NMR (C_6D_6): 1.10 (m, THF), 1.35 (s, 27H, 3-Bu^t), 2.25 (s, 9H, 5-Me), 3.24 (m, THF), 5.68 (s, 3H, 4-H).

Preparation of $[Sm(Tp^{t\text{-}Bu,Me})I.(THF)_2.(Et_2O)_{0.5}]$[3,9]

SmI_2 (2.0 g, 3.68 mmol) and $KTp^{t\text{-}Bu,Me}$ (1.77 g, 3.84 mmol) were mixed in a Schlenk tube, cooled to –78°C and THF (100 ml) added with stirring. The mixture was stirred for 1 hour at –78°C, then overnight at room temperature. The dark blue/black solution was allowed to settle, then filtered and the KI residue extracted with THF (50 ml). Solvent was removed from the combined filtrates under reduced pressure and the resulting blue/black solid extracted with diethyl ether (2 x 100 ml). After filtration, solvent was removed under reduced pressure and the blue/black solid dried under dynamic vacuum (10^{-2} mm Hg) to yield 1.77 g (2.03 mmol, 55 %) of $[Sm(Tp^{t\text{-}Bu,Me})I.(THF)_2.(Et_2O)_{0.5}]$ as a blue/black powder.

Elemental analysis calculated for $C_{34}H_{61}N_6BO_{2.5}SmI$: C 46.30, H 6.97, N 9.53. Found: C 47.25, H 7.26, N 10.64. IR (KBr, cm^{-1}): 2554 (BH). ^1H NMR (C_6D_6): 1.10 (m, THF), 1.35 (s, 27H, 3-Bu^t), 2.25 (s, 9H, 5-Me), 3.24 (m, THF), 5.68 (s, 3H, 4-H).

Preparation of $K\{(C_5H_5)Fe(CO)_2\}$

$\{(C_5H_5)Fe(CO)_2\}_2$ (0.92 g, 2.6 mmol) and potassium metal (large excess) were placed in a Schlenk tube and 100 ml THF added. The mixture was stirred overnight, during which time a red crystalline solid formed. The solution and solid were decanted into a clean Schlenk tube and the volume of solvent reduced in vacuo to 40 ml. Cooling of the red slurry to -25°C, followed by filtration, washing with THF (20 ml) and drying *in vacuo* yielded 530 mg (2.45 mmol, 94 %) of red/orange solid.

IR (KBr, cm^{-1}): 1757, 1797, 1875, 1939, 1991.

Preparation of $Na\{(CH_3C_5H_4)Mo(CO)_3\}$

To a Na/Hg amalgam was added $\{(CH_3C_5H_4)Mo(CO)_3\}_2$ (36 mg, 0.069 mmol) in THF (20 ml) with stirring. The pink solution became paler and turned pale yellow over *ca.* 10 minutes. The pale yellow solution was used immediately in the reaction with $[Sm(Tp^{t\text{-}Bu,Me})I.(THF)_2.(Et_2O)_{0.5}]$ or $[Yb(Tp^{t\text{-}Bu,Me})I.THF]$, *vide infra*. No characterisation data were obtained.

Preparation of $Hg(C{\equiv}CPh)_2$.[10]

An alkaline solution of mercuric iodide was first prepared by dissolving $HgCl_2$ (2.71 g, 0.01 mol) in a solution of KI (6.64 g, 0.04 mol) and water (7 ml) and adding 10 % NaOH (10 ml). A solution of phenylacetylene (2.25 g, 0.022 mol) in 96 % ethanol (42 ml, 20 volume equivalents) was added dropwise over 5 minutes to the cooled, diluted HgI_2 solution. Immediate precipitation occurred. The mixture was filtered on a Buchner funnel and the precipitate washed with cold ethanol. The crude product was purified by recrystallisation from ethanol to give 1.3 g (3.23 mmol, 32 %) of shiny white plates.

Elemental analysis calculated for $C_{16}H_{10}Hg$: C 47.70, H 2.50, N 0.00. Found: C 47.24, H 2.36, N 0.00. IR (KBr, cm^{-1}): 2120 (C≡C). ^1H NMR (DMSO): 7.4 - 7.5 (m, Ph-H)

M.p. = 118 - 120°C (literature m.p. = 124.5 - 125°C).

Preparation of $LiNHBu^t$

A solution of H_2NBu^t (4.0 ml, 37.5 mmol) in Et_2O was cooled to –78°C then a solution of 2.5 M $LiBu^n$ in hexanes (15 ml, 37.5 mmol) added over 10 minutes. The mixture was stirred for 2 h while warming to room temperature, during which time a white precipitate formed, then allowed to settle and the yellow supernatant decanted into a Schlenk tube. The white residue was washed with 30/40 petrol (2 x 40 ml) until the petrol solution was colourless, then dried *in vacuo* at room temperature for 30 minutes to afford 835 mg (10.5 mmol, 28 %) of white powder.

^1H NMR (C_6D_6): 1.359 (s, Bu^t).

Preparation of LiNH-2,4,6-$Me_3C_6H_2$

To a solution of 2,4,6-trimethylaniline (5.0 g, 37.5 mmol) in Et_2O at –78°C was added a solution of 2.5 M LiBu in hexanes (15 ml, 37.5 mmol) over 5 minutes. The solution immediately turned cloudy and was stirred for a further hour before being brought to room temperature. The mixture was allowed to settle and the pale yellow solution decanted from the white solid. The precipitate was washed with 30/40 petrol until the washings were colourless, then the fine white powder was dried *in vacuo* at room temperature. 4.68 g (33 mmol, 88%) of LiNH-2,4,6-$Me_3C_6H_2$ was obtained.

Preparation of LiNH-2,6-$Pr^i_2C_6H_3$

The same method was used as for the previous reaction, utilising 0.14 ml (0.75 mmol) 2,6-diisopropylaniline and 0.3 ml $LiBu^n$ (2.5 M, 0.75 mmol). The product was filtered and used immediately in the reaction with $Y(Tp^{Me,Me})Cl_3K.THF$

Preparation of $NaN(SiMe_3)_2$

$NH(SiMe_3)_2$ (0.5 ml, 0.29 mmol) was added to a slurry of NaH (50 mg of 60 % dispersion in oil, 1.25 mmol) in THF. The mixture was refluxed for 4 h, then filtered and used immediately in the reaction with $[Y(Tp^{Me,Me})I_2.THF]$.

Preparation of $KNHBu^t$

To a stirred slurry of KH (0.75 g, 19 mmol) in THF at room temperature was added H_2NBu^t (1.5 ml, 14 mmol). The Schlenk tube was then fitted with a water condenser and a nitrogen bubbler and the mixture refluxed at 90°C overnight, during which time a grey precipitate formed and H_2 was evolved. After cooling to room temperature the mixture was filtered and the grey residue washed with THF (30 ml). Solvent was removed from the filtrate to afford a brown oil. Washing this oil with petrol afforded 612 mg (5.5 mmol, 40 %) of brown powder.

IR (KBr, cm^{-1}): 2926 (NH).

Preparation of $LiCH_2SiMe_3$

Method A

To a solution of chloromethyltrimethylsilane (2.8 ml, 2.45 g, 20 mmol) in Et_2O at –78°C was added a cooled solution of 2.5 M LiBu (8 ml, 20 mmol) in hexanes diluted with Et_2O over 10 minutes. The mixture was stirred for 2 h at –78°C then allowed to warm to –20°C. The solution was kept at –20°C to prevent formation of the thermodynamic product, LiCl, while removing the solvent *in vacuo* to give a yellow oily product. The product was washed with 30/40 petrol (2 x 30 ml) and the washings decanted into a toluene/isopropanol mixture to destroy unreacted LiBu. The pale yellow product was dried under dynamic vacuum. Yield 180 mg (1.9 mmol, 10 %).

Method B

Pieces of lithium wire (high sodium) (2.15 g, 0.3 mol, excess) were placed in an ampoule with Et_2O at 0°C and a solution of chloromethyltrimethylsilane (5 ml, 35.8 mmol) in Et_2O added over 5 minutes. The mixture was stirred under a slight vacuum (to prevent the formation of unreactive surface lithium nitrides) for 5 days then the solvent was removed and 30/40 petrol added. The mixture was slurried across into a Schlenk tube, filtered and the white precipitate washed with 30/40 petrol (2 x 100 ml). The solvent was removed from the combined washings to afford an off-white, slightly oily solid. This product was washed with cold petrol to remove final traces of $ClCH_2SiMe_3$. 650 mg (6.4 mmol, 18 %) of white solid were obtained.

Preparation of KCH_2SiMe_3

To a slurry of $KOBu^t$ (360 mg, 3.2 mmol) in 30/40 petrol at 0°C was added a solution of $LiCH_2SiMe_3$ (300 mg, 3.2 mmol) in 30/40 petrol. The mixture immediately turned pale yellow/cream and was stirred overnight before being allowed to settle. The supernatant

containing $LiOBu^t$ was decanted off and the solid washed with 30/40 petrol (3 x 30 ml) then dried under dynamic vacuum to afford 185 mg (1.5 mmol, 46 %) of KCH_2SiMe_3.

Chapter 2: Preparation of Bis(pyrazolylborate)samarium chalcogenolate complexes

Attempted Preparation of $[Sm(Tp^{Me,Me\text{-}4\text{-}Et})_2O_2C_6H_4]$

$[Sm(Tp^{Me,Me\text{-}4\text{-}Et})_2]$ (100 mg, 0.11 mmol) and $O_2C_6H_4$ (12 mg, 0.11 mmol) were mixed in a Schlenk tube and THF added at room temperature. The solution immediately turned green and was stirred for a further hour before removing solvent *in vacuo*. Attempts at recrystallisation from a number of solvent systems invariably resulted in some decomposition, giving an intimate mixture of the green solid with a yellow material. Data were, therefore, collected on the crude reaction product (green).

^1H NMR (C_6D_6): 12.5 (b, 2H, *o*-H), 7.7 (b, 3H, *m*-H), 5.8 (s, 1H, 4-CH), 3.37 (s, 18H, 5-Me), 2.31 (q, 12H, 4-C$\underline{H}_2$CH$_3$), 1.09 (t, 18H, 4-CH$_2$C$\underline{H}_3$), –0.79 (s, 1H), –0.87 (s, 1H), –1.36 (s, 13H, 3-Me), –1.55 (s, 1H), –1.62 (s, 1H).

Attempted Preparation of $[\{Sm(Tp^{Me,Me\text{-}4\text{-}Et})_2\}_2O_2C_6H_4]$

$[Sm(Tp^{Me,Me\text{-}4\text{-}Et})_2]$ (100 mg, 0.11 mmol) and $O_2C_6H_4$ (6 mg, 0.06 mmol) were mixed in a Schlenk tube and THF added at room temperature. The solution was stirred for 2 h, during which time it turned yellow, then the solvent was removed *in vacuo*. The yellow solid was extracted into toluene and cooled, following concentration to 10 ml, to afford 130 mg of yellow solid.

Elemental analysis calculated for $C_{90}H_{124}N_{24}B_4O_2Sm_2$: C 56.36, H 6.52, N 17.53. Elemental analysis calculated for $C_{48}H_{64}N_{12}B_2O_2Sm$: C 45.45, H 5.34, N 10.60. Found C 38.34, H 4.84, N 11.41. C:H:N ratio closer to 1:1 complex. IR (KBr, cm^{-1}): 2555, 2528 (BH); 1570 (CO). ^1H NMR (C_6D_6): –1.62 (s, 1H), –1.55 (s, 1H), –1.29 (s, 13H, 3-Me),

–0.87 (s, 1H), –0.79 (s, 1H), 1.10 (t, 18H, 4-$CH_2C\underline{H}_3$), 2.34 (q, 12H, 4-$C\underline{H}_2CH_3$), 3.9 (s, 18H, 5-Me), 12.6 (2H, *o*-H).

Preparation of $[\{Sm(Tp^{Me,Me})_2\}_2O_2C_{14}H_8]$, 2.1

$[Sm(Tp^{Me,Me})_2]$ (100 mg, 0.13 mmol) and 9,10-anthraquinone (13 mg, 0.06 mmol) were mixed in a Schlenk tube under N_2 and THF (30 ml) added at –78°C. The purple $[Sm(Tp^{Me,Me})_2]$ dissolved and the mixture turned deep red over 15 minutes. The solution was stirred for 2 h while warming to room temperature then filtered into a clean dry Schlenk tube. The volume of solvent was reduced slightly and *ca.* 10 ml of Et_2O added. Slow cooling to –30°C gave 100 mg (0.058 mmol, 88 %) of fine red crystals. The product was soluble in THF and CH_2Cl_2, sparingly soluble in toluene, Et_2O, DME and petrol and could also be crystallised at low temperature from a mixture of CH_2Cl_2 and toluene.

Elemental analysis calculated for $C_{74}H_{96}N_{24}B_4O_2Sm_2$: C 52.35, H 5.70, N 19.80. Found C 51.11, H 5.61, N 18.94. IR (KBr, cm^{-1}): 2552, 2525 (BH); 1561 - 1684 (br) (CO and overtones from anthraquinone). ^1H NMR (C_6D_6): –8.35 (s, 6H, 3-Me), 0.80 (s, 6H, 3(5)-Me), 2.06 (s, 6H, 3(5)-Me), 2.30 (s, 6H, 5(3)-Me), 3.03 (s, 6H, 5(3)-Me), 3.06 (m, 4H, $C_{14}H_8O_2$), 3.34 (m, 4H, $C_{14}H_8O_2$), 3.4 (s, 6H, 5(3)-Me), 5.57 (s, 2H, 4-CH), 5.79 (s, 2H, 4-CH), 6.00 (s, 2H, 4-CH).

Preparation of $[\{Sm(Tp^{Me,Me\text{-}4\text{-}Et})_2\}_2O_2C_{14}H_8]$

The reaction was carried out analogously to the preparation of **2.1**, utilising 100 mg (0.11 mmol) $[Sm(Tp^{Me,Me\text{-}4\text{-}Et})_2]$ and 11 mg (0.05 mmol) anthraquinone. Recrystallisation from CH_2Cl_2/toluene at –30°C afforded a red oily solid which was washed with 30/40 petrol to give 100 mg (0.05 mmol, 93 %) of red powder.

IR (KBr, cm^{-1}): 2553, 2531 (BH). ^1H NMR (C_6D_6): –7.44 (s, Me), 0.38 (q, 4-$C\underline{H}_2CH_3$), 0.58 (s, Me), 0.77 (t, 4-$CH_2C\underline{H}_3$), 0.85 (t, 4-$CH_2C\underline{H}_3$), 1.85 (t, 4-$CH_2C\underline{H}_3$), 1.95 (q, 4-$C\underline{H}_2CH_3$) 2.20 (q, 4-$C\underline{H}_2CH_3$), 3.08 (s, Me), 3.24 (s, Me), 3.36 (s, Me), 3.40 (s, Me),

3.84 (s, $C_{14}H_8O_2$), 3.94 (s, $C_{14}H_8O_2$), 4.46 (s, Me), 4.63 (s, Me), 8.05 (s, $C_{14}H_8O_2$), 8.13 (s, $C_{14}H_8O_2$).

Preparation of $[Sm(Tp^{Me,Me})_2SPh^{Me}]$, 2.3

$[Sm(Tp^{Me,Me})_2]$ (100 mg, 0.13 mmol) was placed in a Schlenk flask under N_2. Toluene (20 cm^3) was added and the flask was then cooled to –78°C in a dry-ice acetone bath. Di(p-tolyl)disulfide (17 mg, 0.07 mmol) dissolved in toluene (30 cm^3) was added dropwise and the mixture stirred overnight. The suspension turned from deep purple to a clear pale yellow solution as the mixture warmed up. The solution was then concentrated to 15 cm^3 under reduced pressure before placed into a freezer (–10°C) for recrystallization. Yield 60 mg (52%).

Elemental Analysis: Calcd for $C_{37}H_{51}N_{12}B_2SSm$. C 51.07, H 5.91, N 19.33. Found: C 50.92, H 5.93, N 19.04. IR(KBr, cm^{-1}): 2562 (BH). ^1H NMR (C_6D_6, 298 K) : 0.42 (s, 18H, Me); 1.29 (s, 3H, MePh); 1.40 (s, 18H, Me); 5.31 (s, 6H, CH)7.21 (d, 2H, Ph); 8.64 (m, 2H, Ph). ^{13}C NMR ($CDCl_3$, 298 K) : 12.9 (q, 3 or 5Me); 13.5 (q, 5 or 3Me); 21.4 (q, MePh); 105.4 (d, C(4)); 128.6 (d, Ph); 133.2 (d, Ph); 145.0 (s, C(3) or C(5)); 150.4 (s, C(5) or C(3)).

Preparation of $[Sm(Tp^{Me,Me})_2(SBz)]$

To a purple suspension of $[Sm(Tp^{Me,Me})_2]$ (200 mg, 0.2 mmol) in toluene (40 cm^3) cooled to –78°C was added $(SCH_2Ph)_2$ (172 mg, 11mmol). The mixture was stirred at –78°C and then allowed to warm to room temperature and stirred for a further 48 hours during which time it turned yellow. After filtration the solvent was removed under reduced pressure to leave a yellow oil. After dissolving in pentane (15 m;) and cooling to -30°C yellow crystals were obtained. Yield: 69 mg (30 %).

Anal. Calcd for $C_{49}H_{79}N_{12}B_2SSm$: C, 56.79; H, 7.29; N, 16.22. Found: C, 56.21; H, 7.27; N, 15.84. IR (KBr, cm^{-1}): 2540 (sh) (BH). ^1H NMR (C_6D_6, 298K): –1.40 (s, 1H, CH_2Ph); 0.51 (s, 18H, 3-Me); 1.01 (t, 3H, Me); 2.18 (q, 12H, CH_2); 2.31 (s, 18H, 5-

Me); 3.13 (s, 1H, CH_2Ph); 7.50 (t, 1H, *p*-H), 7.69 (m, 2H, CH_2Ph); 7.77 (t, 2H, *m*-H); 9.04 (d, 2H, *o*-H).

Preparation of $[Sm(Tp^{Me,Me-4-Et})_2SC_6H_5]$ (NMR scale)

$[Sm(Tp^{Me,Me-4-Et})_2]$ (13mg, 0.014 mmol) and diphenyl disulfide $(SPh)_2$ (1-2 mg, *ca.* 0.009 mmol) were mixed and 1 ml C_6D_6 added. The solution immediately became orange, turning yellow within 5 minutes, and was transferred to an NMR tube which was sealed *in vacuo*. ^1H NMR (C_6D_6): 0.65 (s, 18H, 3-Me), 0.97 (t, 18H, CH_3), 2.13 (q, 12H, CH_2), 2.30 (s, 18H, 5-Me), 7.48 (m, 2H, *m*-H), 7.59 (t, 1H, *p*-H), 9.35 (d, 2H, *o*-H).

Preparation of $[Sm(Tp^{Me,Me})_2SePh^{4\text{-}t\text{-}Bu}]$, 2.4

The compound was prepared by analogy with **2.3**.

Elemental Analysis: Calcd for $C_{40}H_{57}N_{12}B_2SeSm$: C 50.03, H 5.99, N 17.52. Found: C 47.81, H 6.14, N 15.31. IR (KBr, cm^{-1}): 2541 (BH). ^1H NMR (C_6D_6, 298 K): (0.50 (s, 18H, Me); 1.47 (s, 9H, Bu^t); 2.44 (s, 18H, Me); 5.47 (s, 6H, CH); 7.37 (d, 2H, Ph); 8.76 (m, 2H, Ph). ^{13}C NMR ($CDCl_3$, 298 K): 13.5 (q, 3 or 5Me); 13.6 (q, 5 or 3Me); 31.6 (q, Bu^t); 105.6 (d, C-H); 124.6 (d, Ph); 124.8 (d, Ph); 135.8 (s, 2H); 145.4 (s, C(3) or C(5)); 150.9 (s, C(5) or C(3)).

Preparation of $[Sm(Tp^{Me,Me-4-Et})_2SeBz]$

To a solution of $[Sm(Tp^{Me,Me-4-Et})_2]$ (105 mg, 0.11 mmol) in 50 ml toluene at –78°C was added $(SeCH_2C_6H_5)_2$ (21 mg, 0.055 mmol) in toluene over 5 minutes with stirring. The mixture was stirred at –78°C for 3 h, during which time it turned deep red, then orange. The solution was then allowed to warm to room temperature, turning golden yellow. The solution was filtered and the volume of solvent reduced *in vacuo* to 10 ml. Cooling to -25°C did not yield a crystalline product and no reliable characterisation data were obtained.

Preparation of [Sm($Tp^{Me,Me-4-Et}$)$_2$Se-4-OMe-C_6H_4] (NMR scale)

To [Sm($Tp^{Me,Me-4-Et}$)$_2$] (12 mg, 0.012 mmol) in C_6D_6 was added (Se-4-OMe-C_6H_5)$_2$ (2-3 mg, *ca.* 0.006 mmol) in C_6D_6. The orange mixture was transferred to an NMR tube which was sealed *in vacuo*, during which time the solution turned yellow.

^{1}H NMR (C_6D_6): -3.47 (m), 0.32 (s, 3-Me), 0.93 (t, CH_3), 1.93 (b, CH_2), 2.00 (s, 5-Me), 6.56, 7.54 (Ph-H). Very broad resonances prevented reliable assignment of chemical shifts.

Preparation of [Sm($Tp^{Me,Me-4-Et}$)$_2$Se-4-Bu^t-C_6H_4] (NMR scale)

[Sm($Tp^{Me,Me-4-Et}$)$_2$] (11 mg, 0.012 mmol) and (Se-4-Bu^t-C_6H_5)$_2$ (2-3 mg, *ca.* 0.006 mmol) were mixed and 1 ml of C_6D_6 added. The orange solution was transferred to an NMR tube which was sealed *in vacuo*. Over the course of 5-10 minutes the solution turned yellow.

^{1}H NMR (C_6D_6): 0.68 (s, 3-Me), 0.99 (t, CH_3), 1.63 (s, Bu^t), 2.17 (q, CH_2), 2.29 (d, 5-Me), 7.45 (d, *m*-H), 9.16 (d, *o*-H).

Preparation of [Sm($Tp^{Me,Me}$)$_2$TePh], 2.5

The compound was prepared by analogy with **2.3**, using 100 mg (0.13 mmol) Sm($Tp^{Me,Me}$)$_2$ and 27 mg (0.07 mmol) (TePh)$_2$. Yield 66 mg (0.07 mmol, 54 %) orange crystals.

Elemental Analysis: Calcd for $C_{36}H_{49}N_{12}B_2SmTe$. C 45.48, H 5.15, N 17.68 Found: C 44.67, H 5.22, N 17.04. IR (KBr, cm^{-1}): 2554 (BH). ^{1}H NMR (C_6D_6): 0.695 (s, 18H, 3-Me), 2.130 (s, 18H, 5-Me), 5.465 (s, 6H, 4-CH), 7.462 (t, 2H, *m*-CH), 9.47 7.607 (t, 1H, *p*-CH), (d, 2H, *o*-CH)

Preparation of [Sm($Tp^{Me,Me-4-Et}$)$_2$TePh]

[Sm($Tp^{Me,Me-4-Et}$)$_2$] (100 mg, 0.11 mmol) and (TePh)$_2$ (28 mg, 0.068 mmol) were mixed in a Schlenk tube, cooled to -78°C and 30 ml toluene added. The mixture was stirred at -78°C for two hours, during which time it turned bright orange, then allowed to warm to room

temperature. The solvent was removed *in vacuo* to give a sticky orange/brown solid, which was dissolved in pentane. Slow cooling to -25°C followed by decanting the supernatant and drying *in vacuo* gave 25mg of orange solid.

IR (KBr, cm^{-1}): 2550. UV/Vis (C_6D_6, nm): λ_{max} 510. ^1H NMR (C_6D_6): 0.651 (s, 3-Me), 0.959 (t, CH_3), 2.15 (q, CH_2), 2.22 (s, 5-Me), 7.20 (m, *m*-H), 7.31 (t, *p*-H), 9.06 (d, *o*-H).

Preparation of $[Sm(Tp^{Me,Me})_2][TePh]_3$, 2.7

$[Sm(Tp^{Me,Me})_2]$ (100 mg, 0.13 mmol) and Te_2Ph_2 (83 mg, 0.20 mmol) were stirred in toluene at room temperature. The purple solid gradually dissolved to give a red/orange slightly turbid solution. After warming to 60°C the solution was filtered to give a clear deep red solution. The volume of the solution was reduced slightly and cooled slowly to -20°C to give dark red crystals of **2.7**. Yield: 72 mg (0.05 mmol, 41 %)

Elemental Analysis: Calcd for $C_{48}H_{59}N_{12}B_2SmTe_3$. C 42.13, H 4.35, N 12.29. Found: C 43.21, H 4.44, N 11.94. IR (KBr, cm^{-1}): 2554 (BH). ^1H NMR ($CDCl_3$, 298 K): –0.99 (s, 18H, Me); 3.08 (s, 18H, Me); 5.53 (s, 6H, CH); 7.19 (m, 5H, Ph). ^{13}C NMR ($CDCl_3$, 298 K): 11.3 (q, 3 or 5Me); 14.2 (q, 5 or 3Me); 105.4 (d, C-H); 128.1 (d, Ph); 129.3(s, Ph); 137.6 (d, Ph); 139.0 (d, Ph); 145.5 (s, C(3) or C(5)); 149.4 (s, C(5) or C(3)).

^{125}Te NMR ($CDCl_3$): 416.626.

Preparation of $[Sm(Tp^{Me,Me})_2(S_2CNEt_2)]$, 2.6

To a slurry of $[Sm(Tp^{Me,Me})_2]$ (205 mg, 0.28 mmol) in toluene at –78°C was added a solution of tetraethylthiuram disulfide (38 mg, 0.14 mmol) in toluene. The mixture was stirred overnight, during which time it became pale yellow. The solution was filtered and the toluene removed *in vacuo*. The pale yellow solid was dissolved in Et_2O and the volume reduced to *ca.* 5 ml. Slow cooling to –78°C yielded 143 mg (0.16 mmol, 59 %) of pale yellow crystalline solid.

Elemental microanalysis calculated for $C_{35}H_{54}N_{13}B_2S_2Sm$: C 47.07, H 6.09, N 20.39. Found: C 46.35, H 6.31, N 19.59. IR (KBr, cm^{-1}): 2557, 2525 (BH); 1476 (CN); 1008 (CS). ^1H NMR (C_6D_6): –3.777 (s, 3 or 5-Me), 1.159 (s, 3 or 5-Me), 2.030 (t, CH_2-$C\underline{H}_3$), 2.160 (s, TpMe), 2.349 (s, 3 or 5-Me), 2.809 (b, $C\underline{H}_2$-CH_3), 3.981 (s, 3 or 5-Me), 5.115 (s, 4-CH), 5.602 (s, TpMe), 6.229 (s, 4-CH).

Chapter 3: Reactions of (pyrazolylborate)lanthanide complexes with transition metal carbonyls

Preparation of $[Sm(Tp^{tBu,Me})(THF)Mo(\eta\text{-}C_5H_4CH_3)(CO)_3]_2$, 3.1

A solution of $[Mo(\eta\text{-}C_5H_4CH_3)(CO)_3]_2$ (37 mg, 0.057 mmol) in THF (15 ml) was stirred over excess 1 % Na/Hg amalgam for five minutes until the red colour had disappeared. The resulting yellow solution was filtered directly onto a green/black solution of $[Sm(Tp^{t\text{-}Bu,Me})I.(THF)_2.(Et_2O)_{0.5}]$ (100 mg, 0.115 mmol) in THF (20 ml) at –78°C and the mixture stirred for 12 hours while warming to room temperature. The solvent was removed under reduced pressure from the dark green solution and the green residue extracted into Et_2O (30 ml). The volume of solvent was reduced slightly and slow cooling to –20°C gave large deep blue crystals of **3.1**. Yield: 32 mg (22 %). Analysis calculated for $C_{74}H_{110}N_{12}B_2O_8Mo_2Sm_2$: C 49.1; H 6.13; N, 9.2. Found: C 48.35; H 6.20; N 9.09. ^1H NMR (C_6D_6, 298K) 1.25 (s, 3H, MeCp); 1.32 (s, 27H, Bu^t); 2.19 (s, 9H, 5-Me); 5.69 (s, 6H, pz CH); 4.48 (s, 2H, Cp); 4.63 (s, 2H, Cp). IR (KBr disk, cm^{-1}) 2555 (BH), 1914, 1828, 1630 (br) (CO).

Preparation of $[Yb(Tp^{tBu,Me})(THF)Mo(\eta\text{-}C_5H_4CH_3)(CO)_3]_2$, 3.2

The preparation of **3.2** was carried out analogously to that described above using $[Yb(Tp^{tBu,Me})I(THF)]$ (100 mg, 0.126 mmol) and $[Mo(\eta\text{-}C_5H_4CH_3)(CO)_3]_2$ (34 mg, 0.066 mmol) to give yellow crystals of **3.2**. Yield: 50 mg (46 %). Analysis calculated for $C_{74}H_{110}N_{12}B_2O_8Mo_2Yb_2$: C 45.67; H 6.43; N, 9.83. Found: C 45.45; H 5.57; N 9.65. ^1H

NMR (C_6D_6, 298K) 1.35 (s, 27H, Bu^t); 1.16 (s, 3H, MeCp); 2.16 (s, 9H, 5-Me); 5.62 (s, 3H, pz CH); 4.50 (m, 2H, Cp); 4.4.65 (m, 2H, Cp). IR (KBr disk, cm^{-1}) 2552 (ν_{B-H}), 1920(s, ν_{CO}), 1835 (s, ν_{CO}), 1647 (br, $\nu_{\mu-CO}$).

Preparation of $[Sm(Tp^{tBu,Me})(Me_2\text{-}py)_nMo(\eta\text{-}C_5H_4CH_3)(CO)_3]$,

In the glove box a few drops of 2,6-$Me_2C_5H_3N$ were added to the solid $[Sm(Tp^{tBu,Me})(THF)Mo(\eta\text{-}C_5H_4CH_3)(CO)_3]_2$, with immediate formation of a blue solution which gradually turned yellow on standing.

IR (toluene, cm^{-1}) 1913, 1820, 1672 (CO).

Preparation of $[Yb(Tp^{tBu,Me})(Me_2\text{-}py)_nMo(\eta\text{-}C_5H_4CH_3)(CO)_3]$,

Addition of a few drops of 2,6-$Me_2C_5H_3N$ to $[Yb(Tp^{tBu,Me})(THF)Mo(\eta\text{-}C_5H_4CH_3)(CO)_3]_2$, resulted in formation of a dark red solution. Attempts at recrystallisation in the glove box were unsuccessful.

IR (toluene, cm^{-1}) 1913, 1820, 1672 (CO).

Attempted preparation of $[Sm(Tp^{t\text{-}Bu,Me})\{Fe(C_5H_5)(CO)_2\}]$

To a dark green/black solution of $[Sm(Tp^{t\text{-}Bu,Me})I.THF.2Et_2O]$ (26 mg, 0.03 mmol) in THF at –78°C was added an orange solution of $K[FeCp(CO)_2]$ (8 mg, 0.03 mmol) in THF. On warming to room temperature and stirring overnight a dark green/yellow solution was obtained but the expected precipitate of KI was not observed. The solvent was removed *in vacuo* and the green/brown solid extracted into Et_2O to afford a pale yellow solution in which the product was assumed to have decomposed.

Attempted preparation of $[Yb(Tp^{t\text{-}Bu,Me})\{Fe(C_5H_5)(CO)_2\}]$

$[Yb(Tp^{t\text{-}Bu,Me})I.THF]$ (100 mg, 0.126 mmol) and $K\{(C_5H_5)Fe(CO)_2\}$ (27 mg, 0.126 mmol) were mixed in a Schlenk tube, cooled to –78°C and THF (50ml) added. The yellow/orange mixture was stirred for 2 hours at –78°C and allowed to warm to room temperature while stirring overnight, during which time it turned golden brown and a fine

white precipitate formed. After filtration the solvent was removed under reduced pressure to yield 200 mg of brown solid.

IR (KBr pellet, cm^{-1}): 2500w (BH) 1778, 1782, 1995, 1952 (CO). ^1H NMR: 1.33 (s, 27H, 3-Bu^t), 2.195 (s, 9H, 5-Me), 4.228 (s, 1H, 4-CH), 5.66 (s, C_5H_5?), 5.69 (s, C_5H_5?).

Attempted Preparation of $[Sm(Tp^{tBu,Me})]_2[Fe(CO)_4]$

To a solution of $[Sm(Tp^{t\text{-}Bu,Me})I.(THF)_2.(Et_2O)_{0.5}]$ (200 mg, 0.23 mmol) in THF at –78°C was added a solution of $Na_2Fe(CO)_4.^3/_2$dioxane (41 mg, 0.11 mmol) in THF. The dark green/black solution was stirred overnight while warming to room temperature then solvent was removed and the green/brown solid extracted into Et_2O (2 x 25 ml). The volume of solvent was reduced to 15 ml and the solution cooled slowly to –30°C to give a fine brown precipitate. The supernatant was decanted and the residue dried *in vacuo* to afford a brown powder. This product exhibited no ν_{BH} and few other bands in the infrared spectrum which would indicate the presence of either pyrazole or pyrazolylborate.

IR (KBr, cm^{-1}): 2004 (br) (CO).

Attempted Preparation of $[Yb(Tp^{tBu,Me})]_2[Fe(CO)_4]$,

The reaction was carried out analogously to the previous one, utilising 200 mg (0.25 mmol) of $[Yb(Tp^{t\text{-}Bu,Me})I.THF]$ and 44 mg (0.13 mmol) of $Na_2Fe(CO)_4.^3/_2$dioxane. A bright yellow solution was obtained and infrared spectroscopy carried out on this solution. Cooling a concentrated solution in Et_2O afforded a small quantity of beige powder. Attempts at recrystallisation from DME were similarly unsuccessful.

IR (Et_2O, cm^{-1}): 2551, 2521, 2499 (sh) (BH); 1996, 1922 (br), 1907 (CO).

Preparation of $[Sm(Tp^{Me,Me})_2(\mu\text{-}OC)WCp(CO)_2]$

To a purple slurry of bis(hydrotris(3,5-dimethylpyrazol-1-yl)borate)samarium (250 mg, 0.27 mmol) in toluene (40 ml) at –78°C was added $[W(\eta\text{-}C_5H_5)(CO)_3]_2$ (230 mg, 0.35

mmol) in toluene over 5 minutes. The mixture was stirred for 3 hours at low temperature, warming to room temperature while stirring overnight, during which time it turned yellow. The solution was filtered and the volume of solvent reduced to 30ml under reduced pressure. The golden yellow solution was cooled slowly to –25°C and a yellow crystalline solid was obtained. Yield 200 mg (0.186 mmol, 55 %).

Elemental analysis calculated for $C_{43}H_{57}N_{14}O_3B_2SmW$: C 44.03, H 4.81, N 16.72. Found: C 44.45, H 5.09, N 18.06. IR (toluene solution, cm^{-1}): 2554 (B-H); 1632, 1828, 1918 (CO). IR (KBr pellet, cm^{-1}): 2563 (B-H); 1642-1653, 1814, 1910 (CO). ^1H NMR (C_6D_6): -1.67 (s, 18H, 3-Me), 3.22 (d, 18H, 5-Me) 5.38 (s, 5H, C_5H_5), 6.26 (s, 3H, 4-H).

Attempted Preparation of $[Yb(Tp^{Me,Me})_2(\mu\text{-}OC)MoCp(CO)_2]$

$[Yb(Tp^{Me,Me})_2]$ (100 mg, 0.13 mmol) and $[MoCp^{Me}(CO)_3]_2$ (33 mg, 0.06 mmol) were mixed in a Schlenk tube and THF added at room temperature. No reaction was observed on stirring the mixture for 3 days at room temperature or on heating to 50°C for 12 h.

Attempted Preparation of $[Yb(Tp^{Me,Me})_2Mn(CO)_5]$

To a stirred pink slurry of $[Yb(Tp^{Me,Me})_2]$ (100 mg, 0.13 mmol) in toluene (40 ml) at -78°C was added a yellow solution of $[Mn_2(CO)_{10}]$ (25 mg, 0.065 mmol) in toluene. The mixture was stirred for 30 min at -78°C then allowed to warm to room temperature and stirred for a further 5 days, then heated to 50°C for 12 h. No reaction was observed.

Attempted Preparation of $[Yb(Tp^{Me,Me})_2Fe(\eta\text{-}C_5H_5)(CO)_2]$

To a stirred pink slurry of $[Yb(Tp^{Me,Me})_2]$ (100 mg, 0.13 mmol) in toluene (40 ml) at -78°C was added a red/brown solution of $[Fe(\eta\text{-}C_5H_5)(CO)_2]_2$ (23 mg, 0.065 mmol) in toluene. The mixture was stirred for 30 min at -78°C then allowed to warm to room temperature and stirred for a further 5 days, then heated to 50°C for 12 h. No reaction was observed.

Attempted Preparation of $[Sm(Tp^{Me,Me})_2Fe(\eta\text{-}C_5H_5)(CO)_2]$

Method A $[Sm(Tp^{Me,Me})_2Cl] + K[Fe(\eta\text{-}C_5H_5)(CO)_2]$

To a colourless solution of $[Sm(Tp^{Me,Me})_2Cl]$ (100 mg, 0.13 mmol) in THF at –78°C was added an orange/red THF solution of $K[Fe(\eta\text{-}C_5H_5)(CO)_2]$ (27 mg, 0.13 mmol). The mixture was stirred for 2 h while warming to room temperature and then for 10 h, during which time the colour became slightly darker. Longer reaction times resulted in some formation of purple $[Sm(Tp^{Me,Me})_2]$. The THF was removed under dynamic vacuum and the red/brown solid extracted into Et_2O (2 x 20 ml). The volume of solvent was reduced to *ca.* 10 ml and the red/brown solution cooled slowly to –30°C to afford 21 mg of red/brown crystalline material.

IR (toluene solution, cm^{-1}): 2015, 1998, 1956, 1954, 1947, 1940, 1855, 1783 (CO).

IR (KBr pellet, cm^{-1}): 2540, 2524sh (B-H); 1987, 1944 (sh), 1933, 1803 (w), 1776, 1750 (w) (CO). ^1H NMR (C_6D_6): -0.9 (s, 3(5)-Me), 1.15 (t, Et_2O), 1.9 (s, 5(3)-Me), 3.24 (q, Et_2O), 4.23 (s, C_5H_5), 5.38 (s,4-H).

Method B $[Sm(Tp^{Me,Me})_2] + [Fe(\eta\text{-}C_5H_5)(CO)_2]_2$

$[Sm(Tp^{Me,Me})_2]$ (140 mg, 0.19 mmol) and $[Fe(\eta\text{-}C_5H_5)(CO)_2]_2$ (33 mg, 0.09 mmol) were mixed in a Schlenk tube under N_2, cooled to -78°C and toluene (30 ml) added with stirring. The mixture was stirred overnight while warming to room temperature, during which time a deep red solution formed with a slight precipitate of unreacted $[Sm(Tp^{Me,Me})_2]$. Filtration gave a deep red clear solution. The volume of solvent was reduced to 5 ml and 40/60 petrol added (2 ml). Cooling the solution to -25°C afforded dark red/brown crystalline material (21 mg) and some off-white powder.

IR (toluene solution, cm^{-1}): 2015, 1997, 1953, 1950, 1947, 1782 (CO). IR (KBr pellet, cm^{-1}): 2562 (B-H); 1993 (w), 1952 (sh), 1936, 1772, 1768, 1762, 1757 (CO).

Attempted Preparation of $[Sm(Tp^{Me,Me\text{-}4\text{-}Et})_2Fe(\eta\text{-}C_5H_5)(CO)_2]$,

To a purple solution of $[Sm(Tp^{Me,Me\text{-}4\text{-}Et})_2]$ (100 mg, 0.11 mmol) in toluene at –78°C was added an orange/red solution of $[Fe(\eta\text{-}C_5H_5)(CO)_2]_2$ (19 mg, 0.05 mmol) in toluene. The mixture was stirred overnight whilst warming to room temperature during which time a colour change was observed from purple to orange/red, then filtered. Attempts at recrystallisation from toluene solution afforded 140 mg of a red/brown solid.

IR (KBr pellet, cm^{-1}): 2557 (B-H); 1987, 1976, 1953, 1941, 1776, 1774, 1567 (w) (CO).

Attempted Preparation of $[Sm(Tp^{Me,Me})_2]_2[Fe(CO)_4]$

To a cold (–78°C) solution of $[Sm(Tp^{Me,Me})_2Cl]$ (126 mg, 0.16 mmol) in toluene was added a yellow solution of $Na_2Fe(CO)_4.{}^3/_2$dioxane (28 mg, 0.08 mmol) in toluene. The mixture was stirred overnight while warming to room temperature, then filtered and the volume of solvent reduced to 15 ml. The solution was cooled to –25°C to afford a small amount of colourless crystalline material.

Elemental analysis calculated for $[Sm(Tp^{Me,Me})_2]_2[Fe(CO)_4]$, $C_{64}H_{88}N_{24}B_4O_4FeSm_2$: C 46.38, H 5.35, N 20.28. Found C 35.00, H 3.41, N 12.61. (Requires 10 molecules of NaCl to get close to the found values). IR (Et_2O, cm^{-1}): 2184 (w), 2165 (w), 2116 (w), 2022, 2000, 1994, 1941, 1916 (w), 1871, 1858, 1803, 1736 (CO). IR (KBr, cm^{-1}): 2572, 2523sh (BH); 1999 (w), 1907, 1874, 1747 (w) (CO).

Reaction of $[Sm(Tp^{Me,Me})_2]$ with $[Fe(CO)_5]$

To a purple slurry of $[Sm(Tp^{Me,Me})_2]$ (75 mg, 0.1 mmol) in toluene (30 ml) at –78°C was added dropwise $Fe(CO)_5$ (13.2 µl, 0.1 mmol). The mixture was stirred for 2 hours at -78°C then allowed to warm to room temperature, during which time it turned deep red, then orange and finally yellow/brown. The solution was filtered to give a clear yellow solution and the volume of solvent reduced *in vacuo* to 15 ml. Slow cooling to –25°C yielded 30 mg (0.03 mmol, 32 %) of microcrystalline red/brown solid which readily desolvated on removal from the mother liquor.

Elemental analysis calculated for $C_{38.5}H_{48}N_{12}O_5B_2FeSm$: C 46.86, H 4.90, N 17.03. Also calculated for $C_{72}H_{104}N_{24}B_4O_4FeSm_2$: C48.74, H 5.53, N 19.21; and for $C_{85}H_{112}N_{24}B_4O_{11}Fe_3Sm_2$: C 47.5, H 4.88, N 15.64. Found: C 47.39, H 5.02, N 14.19. IR (toluene solution, cm^{-1}): 2554 (B-H); 1680, 1735, 1915, 1938-1944, 1999 (CO). IR (KBr pellet, cm^{-1}): 2563 (B-H); 1637-1686, 1874-1880, 1945, 1997 (CO).

Reaction of $[Sm(Tp^{Me,Me\text{-}4\text{-}Et})_2]$ with $[Fe(CO)_5]$

The experimental details of this reaction are analogous to those of the above reaction. The reaction of $[Sm(Tp^{Me,Me\text{-}4\text{-}Et})_2]$ (77 mg, 0.084 mmol) with $Fe(CO)_5$ (11.5 μl, 0.087 mmol) afforded a red microcrystalline product which desolvated to give a pink solid (34 mg, 0.031 mmol, 37 %).

Elemental Analysis calculated for $C_{47}H_{68}N_{12}B_2O_5FeSm$: C 50.90, H 6.18, N 15.16. Also calculated for $C_{95}H_{136}N_{24}B_4O_{11}Fe_3Sm_2$: C 49.57, H 5.96, N 14.6; and for $C_{88}H_{136}N_{24}B_4O_4FeSm_2$: C 53.01, H 6.87, N 16.86. Found: C 51.06, H 6.54, N 15.45. IR (toluene solution, cm^{-1}): 2550 (B-H); 1742-1745, 1912, 1939, 1944, 1973, 1993, 1999 (CO). IR (KBr pellet, cm^{-1}): 2554 (B-H); 1864, 1885, 1990, 1997 (CO). ^1H NMR (C_6D_6): -1.7 (s, 3-Me), 0.79 (t, CH_3), 1.99 (q, CH_2), 3.3 (s, 5-Me).

Preparation of $[Sm(Tp^{Me,Me})_2][Mn(CO)_5]$, 3.3

$[Sm(Tp^{Me,Me})_2]$ (103 mg, 0.138 mmol) and $Mn_2(CO)_{10}$ (26 mg, 0.067 mmol) were mixed in a Schlenk tube, cooled to –78°C and toluene (50 ml) added with stirring. The purple mixture was stirred for 2 hours at –78°C, then slowly warmed to room temperature, during which time it turned red, then orange and finally yellow. The solution was filtered and the volume of solvent reduced *in vacuo* to 15 ml. Slow cooling to –25°C gave 42 mg (0.045 mmol, 32 %) of orange/yellow crystals which readily desolvated on removal from the mother liquor.

Elemental analysis calculated for $(Tp^{Me2})_2Sm\text{-}Mn(CO)_5$.toluene $C_{42}H_{50}N_{12}O_5B_2MnSm$: C 48.89, H 5.08, N 16.29. Found: C 48.96, H 4.97, N 17.06. IR (toluene solution): 2554

cm^{-1} (B-H); 1718, 1828, 1918 cm^{-1} (CO). IR (KBr pellet): 2559 cm^{-1} (B-H); 1853-1841, 1897-1918 cm^{-1} (CO).

Preparation of $[Sm(Tp^{Me,Me})_2][BPh_4]$

To a yellow solution of **3.3** in CH_2Cl_2 at room temperature was added $NaBPh_4$ in CH_2Cl_2. The mixture was stirred for 2 days with no discernible colour change, then the solvent was removed and toluene added. The reaction mixture was stirred for a further 2 days during which time the yellow colour disappeared and the solution became almost colourless. The solvent was removed *in vacuo* and the off-white product washed with Et_2O.

IR (KBr, cm^{-1}): 2523 (BH).

Preparation of $[Sm(Tp^{Me,Me\text{-}4\text{-}Et})_2][Mn(CO)_5]$

This reaction was carried out in an analogous fashion to the preparation of **3.3**. The reaction of $[Sm(Tp^{Me,Me\text{-}4\text{-}Et})_2]$ (100 mg, 0.11 mmol) and $Mn_2(CO)_{10}$ (21 mg, 0.055 mmol) afforded 50 mg (0.045 mmol, 41 %) of yellow crystals which crumbled when removed from the mother liquor.

Elemental analysis calculated for $C_{47}H_{68}N_{12}O_5B_2SmMn$: C 50.95, H 6.18, N 15.17. Found: C 48.94, H 6.14, N 14.99. IR (toluene solution, cm^{-1}): 2554 (BH); 1632, 1828, 1918 (CO). IR (KBr pellet, cm^{-1}): 2563 (BH); 1642-1653, 1814, 1910 (CO).

^1H NMR (C_6D_6): –1.39 (s, 18H, 3-Me), 0.81 (t, 18H, CH_3), 2.04 (q, 12H, CH_2), 3.17 (d, 18H, 5-Me).

Preparation of $[\{Sm(Tp^{Me,Me})_2\}_2(\mu\text{-}O_2CH)][Mn(CO)_5]$, 3.4

We were unable to devise a rational route for the preparation of **3.4**. Since the product was obtained on only one occasion there is no characterisation data other than that obtained in the single crystal X-ray diffraction study.

Preparation of of $[Sm(Tp^{Me,Me})_2][Re_4(H)(CO)_{17}]$, 3.5

To a purple slurry of $(Tp^{Me,Me})_2Sm$ (250 mg, 0.33 mmol) in toluene was added a colourless solution of $Re_2(CO)_{10}$ (109 mg, 0.17 mmol) in toluene. The mixture was warmed to 80°C and stirred for 5 hours during which time the solid dissolved and the solution turned orange. After cooling to room temperature, the solution was filtered and the volume of solvent reduced to 15 cm^3. Cooling to -20°C gave orange needles. Yield: 44 mg (19 %). Elemental analysis: Calcd. for $C_{47}H_{44}B_2N_{12}O_{17}Re_4Sm$: C 40.09, H 3.22, N 11.94; Found: C 34.24, H 3.29, N 12.30. IR (KBr pellet, cm^{-1}) 2559 (BH); 2083, 2006, 1964, 1914, 1905, 1881 (CO). ^1H NMR (acetone-d_6, 298 K) –17.22 (s, ReH), 2.20 (s, 3-Me), 2.92 (s, 5-Me), 5.72 (s, 4-CH) ,.

Chapter 4 - Synthesis of new (pyrazolylborate)lanthanide complexes

Attempted preparation of $[Sm(Tp^{Me,Me})_2F]$

$[Sm(Tp^{Me,Me})_2]$ (100 mg, 0.13 mmol) and $NaBF_4$ (15 mg, 0.13 mmol) were mixed in a schlenk and THF added at room temperature. The mixture was stirred until the purple colour disappeared and the solution became colourless. Filtration, followed by concentration of the filtrate and cooling to –30°C gave a white precipitate. The supernatant was decanted and the solid dried under dynamic vacuum to afford 28 mg of white powder. Elemental microanalysis calculated for $C_{30}H_{44}N_{12}B_3SmF_4$: C 43.33, H 5.33, N 20.21. Found C 37.61, H 4.68, N 17.09. IR (KBr, cm^{-1}): 2553, 2521, 2495 (BH).

Preparation of $[Sm(Tp^{Me,Me})_2Br.{}^1/_2THF]$

$SmBr_3$ (210 mg, 0.54 mmol) and KTp^{MeMe} (362 mg, 1.1 mmol) were mixed in a Schlenk tube and THF added at room temperature. The white slurry was stirred for 2 days at room temperature then allowed to settle and filtered. The white KBr residue was washed with THF (2 x 30 ml) and the washings added to the filtrate. The volume of solvent was reduced

to *ca.* 30 ml and the solution cooled to –30°C to afford a white precipitate. The supernatant was decanted and the product dried at 50°C under dynamic vacuum to yield 64 mg (0.077 mmol, 14 %) of white powder (crop 1). The supernatant was concentrated to 10 ml and cooled to afford a second batch of white powder (crop 2) (41 mg) which exhibited different infrared and NMR spectra to crop 1 and gave a different elemental analysis.

Crop 1

Elemental Microanalysis calculated for $C_{32}H_{48}N_{12}B_2O_{0.5}SmBr$: C 44.65, H 5.62, N 19.53. Found: C 44.87, H 5.98, N 19.49. IR (KBr, cm^{-1}) 2565, 2460 (BH). $_1H$ NMR (C_6D_6): 1.432 (m, 6H, THF), 2.228 (s, 10H, 3(5)-Me), 2.252 (s, 11H, 5(3)-Me), 3.59 (m, 4H, THF), 5.789 (s, 3H, 4-CH).

Preparation of $[Sm(Tp^{Me,Me})Br_3]K(THF)_n$, 4.1

To a slurry of $SmBr_3$ (300 mg, 0.77 mmol) in THF at –78°C was added KTp^{MeMe} (517 mg, 1.54 mmol) in THF over 10 minutes, during which time a slight white precipitate formed. The mixture warmed to room temperature on stirring overnight and was then allowed to settle, filtered and the white KBr residue washed with THF (30 ml). The volume of solvent was reduced to 15 ml and cooled slowly to –30°C to afford 91 mg (0.05 mmol, 7 %) of colourless crystals which lost solvent on removal from the mother liquor.
Elemental Microanalysis calculated for $C_{23}H_{38}N_6BO_2Br_3KSm$ C 31.73, H 4.40, N 9.65. Found: C 29.78, H 4.70, N 9.11. IR (KBr, cm^{-1}) 2562 (BH). ^1H NMR ($CDCl_3$): –2.49 (s, 18H, 3-Me), 1.13 (s, 7H, THF), 2.78 (s, 9H, THF), 4.04 (s, 18H, 5-Me), 5.28 (s, 6H, 4-CH).

Preparation of $[Sm(Tp^{Me,Me})_2][I_3]$, 2.8

To a purple slurry of $[Sm(Tp^{Me,Me})_2]$ (100 mg, 0.13 mmol) in toluene at room temperature was added a purple/brown solution of iodine (51 mg, 0.2 mmol) in toluene. An immediate colour change from purple to orange was observed along with formation of an orange

precipitate. The toluene was removed *in vacuo* and the orange solid redissolved in CH_2Cl_2, then Et_2O added to precipitate out the product. The mixture was allowed to settle for 1 h then the yellow solution was decanted and the orange/brown solid dried at room temperature under dynamic vacuum. 104 mg (0.09 mmol, 71 %)) of $[Sm(Tp^{Me,Me})_2][I_3]$ were obtained.

Elemental Microanalysis calculated for $C_{30}H_{44}N_{12}B_2SmI_3$: C 32.02, H 3.94, N 14.93. Found: C 31.73, H 3.83, N 14.59. IR (Nujol, cm^{-1}): 2554 (BH). ^1H NMR ($CDCl_3$): – 2.571 (s, 5-Me), 4.028 (s, 3-Me), 5.206 (s, 4-CH). ^{13}C NMR ($CDCl_3$): 9.3 (3-Me), 15.3 (5-Me), 102.1 (4-C), 144.0 (3(5)-C), 147.6 (5(3)-C).

Preparation of $[Sm(Tp^{Me,Me})_2](O_2CH)$, 4.2

$[Sm(Tp^{Me,Me})_2Cl]$ (229 mg, 0.29 mmol) and $Na(O_2CH)$ (20 mg, 0.29 mmol) were mixed in a Schlenk tube and THF added at room temperature. The colourless solution was stirred overnight, during which time a small amount of white precipitate formed, then the solvent was removed *in vacuo* and the white solid extracted into toluene (40 ml). the volume of solvent was reduced slightly and the solution warmed to 50°C, then cooled slowly to -20°C to afford 63 mg (0.08 mmol, 26 %) of colourless microcrystalline solid.

Elemental microanalysis calculated for $C_{31}H_{45}N_{12}B_2O_2Sm$: C 47.15, N 5.74, N 21.28. Found: C 47.23, H 5.74, N 18.95. IR (KBr, cm^{-1}): 2545, 2522, 2486, 2417 (BH); 1644, 1593 (CO_2). MS (FAB) m/z 746 $\{[Sm(Tp^{Me,Me})_2]^+\}$. ^1H NMR ($CDCl_3$): Resonances over range -8.02 to 13.17 ppm.

Preparation of $[Sm(Tp^{Me,Me})_2](O_2CMe)$, 4.3

This reaction was carried out analogously to that for **4.2**, utilising 200 mg (0.26 mmol) of $[Sm(Tp^{Me,Me})_2Cl]$ and 21 mg (0.26 mmol) of $Na(O_2CMe)$. Cooling a toluene solution afforded 30 mg (0.04 mmol, 14 %) of white powder and 4 fractured crystals.

Elemental analysis calculated for $C_{32}H_{47}N_{12}B_2O_2Sm$: C 47.82, H 5.89, N 20.91. Found C 43.41, H 5.99, N 16.81. IR (KBr pellet, cm^{-1}): 2540, 2524, 2393 (BH); v.weak bands

1627 - 1609 (CO_2); 922 (C-C). ^{1}H NMR (C_6D_6): 1.0 (b, s, 18H, 3-Me), 2.093 (s, 18H, 5-Me), 5.092 (s, 3H, O_2C-C$\underline{H}_3$), 5.557 (s, 6H, 4-CH). MS (FAB) m/z 749 ($[Sm(Tp^{Me,Me})_2]^+$).

Preparation of $[Sm(Tp^{Me,Me})_2](O_2CPh)$, 4.4

To a solution of $[Sm(Tp^{Me,Me})_2Cl]$ (200 mg, 0.26 mmol) in THF at room temperature was added a slurry of NaO_2CPh (37 mg, 0.26 mmol) in THF. The mixture was stirred overnight then solvent removed *in vacuo* and the product extracted into toluene (2 x 30 ml). The volume of solvent was reduced and cooled slowly to give 60 mg (0.07 mmol, 25 %) of fine needle-like crystals.

Elemental analysis calculated for $C_{37}H_{49}B_{12}B_2O_2Sm$: C 51.33, H 5.70, N 19.41. Found C 50.88, H 5.57, N 19.33. IR (KBr pellet, cm^{-1}): 2553, 2527 (BH); 1596 (CO_2). ^{1}H NMR (C_6D_6) :0 - 1.3 (b, 3-Me), 2.22 (s, 18H, 5-Me), 5.5 (s, 6H, 4-CH), 7.75 (t, 1H, *p*-H), 7.90 (t, 2H, *m*-H), 10.65 (d, 2H, *0*-H).

Attempted preparation of $[Sm(Tp^{Me,Me})_2Ph]$

To a purple slurry of $[Sm(Tp^{Me,Me})_2]$ (200 mg, 0.27 mmol) in toluene at –78°C was added a solution of $Hg(Ph)_2$ (48 mg, 0.13 mmol). No reaction was observed on stirring the mixture overnight, then at 80°C for several hours. Altering the solvent system and employing a toluene/THF mixture, neat THF, or THF/DME proved fruitless, with no loss of purple colour or formation of mercury observed.

Preparation of $[Sm(Tp^{Me,Me})_2(C{\equiv}CPh)]$, 4.6

To a purple slurry of $[Sm(Tp^{Me,Me})_2]$ (105 mg, 0.141 mmol) in toluene (30 ml) at –78°C was added $Hg(C{\equiv}CPh)_2$ (30 mg, 0.074 mmol) in toluene over a period of 10 minutes with stirring. The mixture was stirred for 30 minutes at -78°C then allowed to warm to room temperature and stirred for a further 72 hours, during which time the purple colour slowly disappeared and small grey droplets of mercury formed. The mixture was filtered to give a

clear, colourless solution. Removal of solvent under reduced pressure yielded 79 mg (0.093 mmol, 66 %) of pale cream solid. This crude product was recrystallised from 40/60 petrol to give colourless crystals.

^{1}H NMR (C_6D_6): -1.33 (s, 9H, 3-Me), 1.42 (m, THF), 2.19 (s, 9H, Me), 2.28 (s, 9H, Me), 3.07 (s, 9H, 5-Me), 3.58 (m, THF), 5.43 (s, 3H, 4-C-H), 5.54 (s, 3H, 4-C-H), 7.01 (m, *m*- and *p*-H), 7.54 (m, *o*-H). IR (KBr pellet, cm^{-1}): 2551 (BH); 2147 (C≡C).

Attempted Preparation of [Sm(Tp$^{Me,Me-4-Et}$)$_2$(C≡CPh)]

This preparation was carried out analogously to that for **4.6**, utilising 200 mg (0.22 mmol) of [Sm(Tp$^{Me,Me-4-Et}$)$_2$] and 45 mg (0.11 mmol) of Hg(C≡CPh)$_2$. The purple colour disappeared almost immediately as the reaction warmed to room temperature. After removal of toluene the white product was extracted into 30/40 petrol and the volume of solvent reduced to 15 ml. An oily solid was obtained.

IR (KBr, cm^{-1}): 2557, 2529 (BH). 1H NMR (C6D6): –1.05 (s, 3-Me), 0.916 (t, 4-$CH_2C\underline{H}_3$), 2.117 (q, CH_2CH_3), 2.973 (s, 5-Me), 7.37 (d, *m*-CH), 7.67 (t, *p*-CH), 8.97 (d, *o*-CH).

Preparation of [Y(Tp^{Me,Me})$_2$Cl.$^1/_2$THF], 4.7

YCl_3 (200 mg, 1 mmol) and KTp^{Me,Me} (670 mg, 2 mmol) were mixed in a Schlenk tube and THF added at room temperature. The mixture was stirred for 1 h then allowed to settle and filtered. The white residue was washed with THF (35 ml) and the combined filtrates concentrated to 15 ml. Cooling overnight yielded a colourless crystalline material. The supernatant was decanted and the white product dried at 70°C under dynamic vacuum to afford 123 mg (0.15 mmol, 15 %) of white powder.

Elemental analysis calculated for $C_{32}H_{48}N_{12}B_2O_{0.5}IY$: C 50.92, H 6.42, N 22.27. Found: C 50.25, H 6.48, N 23.19. IR (KBr, cm^{-1}): ν_{BH} 2557. ^{1}H NMR ($CDCl_3$): 1.77 (m, 20H, 3-Me and THF), 2.507 (s, 18H, 5-Me), 3.76 (m, 2H, THF), 5.893 (s, 6H, 4-CH).

Attempted Preparation of [$Y(Tp^{Me,Me})_2I.^1/_2THF$]

YI_3 (500 mg, 1 mmol) and $KTp^{Me,Me}$ (716 mg, 2 mmol) were mixed in a Schlenk tube and THF added at room temperature. The mixture was stirred overnight then allowed to settle and filtered. The white residue was washed with THF (35 ml) and the solvent removed *in vacuo*. The white product was dried at 70°C under dynamic vacuum to afford 77 mg (0.1 mmol, 10 %) of white powder.

Elemental analysis calculated for $C_{32}H_{48}N_{12}B_2O_{0.5}YI$: C 45.42, H 5.72, N 19.86. Found: C 45.14, H 6.30, N 18.66. IR (KBr, cm^{-1}): 2486, 2438. ^1H NMR (C_6D_6): 1.716 (s, Me), 1.861 (s, Me), 2.0190 (s, Me), 2.120 (s, Me), 2.227 (s, Me), 2.318 (s, Me), 2.386 (s, Me), 2.429 (s, Me), 2.503 (s, Me), 2.520 (s, Me), 5.662 (s, 4-CH), 5.708 (s, 4-CH), 5.924 (s, 4-CH), 6.014 (s, 4-CH).

Preparation of [$Yb(Tp^{Me,Me})_2Cl.^1/_2THF$], 4.8

The reaction carried out analogously to **4.7** utilising 0.5 g (1.8 mmol) $YbCl_3$ and 1.20 g (3.6 mmol) $KTp^{Me,Me}$ afforded 288 mg (0.33 mmol, 18 %)of white powder.

Elemental analysis calculated for $C_{32}H_{48}N_{12}B_2O_{0.5}ClYb$: C 45.81, H 5.77, N 20.03. Found: C 44.70, H 5.84, N 19.74. IR (KBr, cm^{-1}): 2566 (BH). ^1H NMR ($CDCl_3$): 0.079 (s, 18H, 3-Me), 1.77 (m, 2H, THF), 3.302 (s, 18H, 5-Me), 3.76 (m, 2H, THF), 5.693 (s, 9H, 4-CH).

Preparation of [$Y(Tp^{Me,Me})Cl_3K(THF)$], 4.9

YCl_3 (1.00 g, 5.15 mmol) and $KTp^{Me,Me}$ (1.738 g, 5.17 mmol) were placed in a Schlenk tube under N_2 and THF (50 ml) added at –78°C. The mixture formed a dense white precipitate and was stirred overnight at room temperature, then allowed to settle and filtered. The white residue was washed with THF (2 x 50 ml) and the filtrates combined. The volume of solvent was reduced to 15 ml *in vacuo* and the solution cooled to –30°C to afford colourless crystals. The supernatant was decanted off and the product dried at 70°C for 1 h under dynamic vacuum to yield 1.76 g (3.3 mmol, 65 %) of white powder.

Elemental analysis calculated for $C_{19}H_{30}N_6BCl_3OKY$: C 37.8, H 5.01, N 13.92; found: C 37.67, H 4.96, N 15.11. IR (KBr, cm^{-1}): 2554 (BH). ^1H NMR ($CDCl_3$): 1.942 (b, 11H, THF), 2.389 (s, 9H, 5-Me), 2.525 (s, 9H, 3-Me), 3.914 (b, 10H, THF), 5.764 (s, 3H, 4-CH).

Preparation of [$Y(Tp^{Me,Me})I_2$.THF], 4.10

The reaction was carried out analogously to that for **4.3**, utilising 0.521 g (1.06 mmol) of YI_3 and 0.373 g (1.1 mmol) of $KTp^{Me,Me}$. The product did not crystallise from THF but the crude material (0.60 g, 79 %) appeared to be clean by elemental microanalysis and ^1H NMR.

Elemental analysis calculated for $C_{19}H_{30}N_6BOI_2Y$: C 32.05, H 4.25, N 11.80. Found: C 32.40, H 4.73, N 11.22. IR (KBr, cm^{-1}): ν_{BH} 2549. ^1H NMR ($CDCl_3$): 1.203 (b, 6H, THF), 2.004 (s, 9H, 5-Me), 2.622 (s, 9H, 3-Me), 3.749 (b, 6H, THF), 5.385 (s, 3H, 4-CH).

Preparation of [$Yb(Tp^{Me,Me})Cl_2.{}^1/_2THF$], 4.11

The reaction was carried out analogously to that for **4.9**, utilising 0.5 g (1.8 mmol) of $YbCl_3$ and 0.6 g (1.8 mmol) of $KTp^{Me,Me}$. The crude material was identified by elemental analysis. Yield 874 mg (1.4 mmol, 79 %).

Elemental analysis calculated for $C_{17}H_{26}N_6BO_{0.5}Cl_2Yb$: C 35.38, H 4.54, N 14.56. Found: C 35.32, H 4.82, N 13.34. IR (KBr, cm^{-1}): 2554 (BH).

Attempted Preparation of [$Yb(Tp^{t\text{-}Bu,Me})Cl_2$]

The preparation was carried out analogously to that for **4.9**, but only starting materials were recovered.

Attempted Preparation of [$Y(Tp^{Me,Me})Ph_2$]11

To a slurry of [$Y(Tp^{Me,Me})Cl_2$.THF] (205 mg, 0.39 mmol) in Et_2O at –78°C was added a cooled solution of 1.8 M LiPh in hexanes/Et_2O (0.5 ml, 0.9 mmol) diluted in Et_2O over 5

minutes. The mixture was stirred for 1h at –78°C then filtered, the clear filtrate turning cloudy as it warmed to ambient temperature. Following a second filtration the volume of solvent was reduced to 2 ml. Cooling to –30°C yielded a small quantity of colourless crystals. The supernatant was decanted and the solid washed with 30/40 petrol and dried under dynamic vacuum to afford 11 mg of off-white powder.

A mixture of products was obtained: Elemental analysis calculated for 1:1 mixture with 4 solvent molecules, $Y(Tp^{Me,Me})Ph_2$:$LiTp^{Me,Me}$.$4Et_2O$, $C_{65}H_{74}N_{12}B_2O_4YLi$: C 58.61, H 7.28, N 16.40. Found: C 58.97, H 7.32, N 14.00. IR (KBr, cm^{-1}): 2548, 2522 (BH). ^1H NMR (C_6D_6): 0.846 (t, 21H, Et_2O), 1.727 (s, 9H, Me, $LiTp^{Me,Me}$), 1.759 (s, 9H, 3-Me), 2.211 (s, 9H, 5-Me), 2.315 (s, 9H, Me, $LiTp^{Me,Me}$), 2.96 (q, 14H, Et_2O), 5.600 (s, 3H, 4-CH), 5.744 (s, 3H, 4-CH, $LiTp^{Me,Me}$), 7.19 (m, 8H, *m*-, *p*-CH), 8.35 (d, 6H, *o*-CH).

Attempted Preparation of $[Y(Tp^{Me,Me})\{CH(SiMe_3)_2\}_2]$

To a solution of $[Y(Tp^{Me,Me})Cl_2.THF]$ (200 mg, 0.38 mmol) in toluene at –78°C was added a solution of $LiCH(SiMe_3)_2$ (146 mg, 0.88 mmol) in toluene (20 ml) with 5 ml of THF added to aid dissolution. The solution was stirred while warming to room temperature then for 2 days at ambient temperature, then solvent was removed *in vacuo*. The resulting white solid was extracted into 30/40 petrol (3 x 30 ml) with a little Et_2O added and the solvent removed *in vacuo* to afford 227 mg of a pale yellow crunchy solid.

IR (KBr, cm^{-1}): 2553, 2529 (BH). ^1H NMR (C_6D_6): 0.049 (s, 40H, $SiMe_3$), 1.375 (b, 20H, THF), 1.727 (s, 9H, Me, $LiTp^{Me,Me}$), 2.130 (s, 9H, Me), 2.176 (s, 9H, Me), 2.318 (s, 9H, Me, $LiTp^{Me,Me}$), 2.393 (s, 9H, Me), 2.689 (s, 9H, Me), 3.617 (b, 20H, THF), 5.667 (s, 3H, 4-CH), 5.744 (s, 3H, 4-CH, $LiTp^{Me,Me}$).

Attempted Preparation of $[Yb(Tp^{Me,Me})\{CH(SiMe_3)_2\}_2]$

The reaction carried out analogously to that for $[Y(Tp^{Me,Me})\{CH(SiMe_3)_2\}_2]$ resulted in reduction of ytterbium, as evidenced by the formation of a quantity of bright pink material.

Attempted Preparation of $[Y(Tp^{Me,Me})(CH_2SiMe_3)_2]$

Method A $[Y(Tp^{Me,Me})Cl_2.THF] + 2\ Li[CH_2(SiMe_3)]$[11]

To a stirred solution of $[Y(Tp^{Me,Me})Cl_2.THF]$ (100 mg, 0.19 mmol) in toluene at –78°C was added a cooled solution of $Li[CH_2(SiMe_3)]$ (50 mg, 0.53 mmol) in toluene. The solution was allowed to warm to ambient temperature and stirred overnight, during which time a fine white precipitate formed. The reaction mixture was filtered and solvent removed from the filtrate. The resulting solid was dried under dynamic vacuum to yield 164 mg of white powder.

Elemental analysis calculated for $Tp^*YCl(CH_2TMS)$, $C_{19}H_{32}N_6BSi_2Y$: C 44.86, H 6.54, N 16.52. Found: C 44.90, H 6.14, N 17.29. IR (KBr, cm^{-1}): 2554, 2525 (sh) (BH). ^1H NMR (C_6D_6): 0.29 (s, $SiMe_3$), 2.08 (m, 16H, 2 x Me), 5.406 (s, 3H, 4-CH).

If Et_2O/petrol was used as solvent, $LiTp^{Me,Me}$ was identified as the major product.

Identification of $LiTp^{Me,Me}$

^1H NMR (C_6D_6): 1.728 (s, 9H, 3-(5)Me), 2.317 (s, 9H, 5-(3)Me), 5.745 (s, 3H, 4-CH). IR (KBr, cm^{-1}); 2515 or 2500 (BH).

Method B $[Y(Tp^{Me,Me})Cl_2.THF] + 2\ K[CH_2(SiMe_3)]$

To a white slurry of $[Y(Tp^{Me,Me})Cl_2.THF]$ (100 mg, 0.19 mmol) in Et_2O at –78°C was added a cooled solution of $K[CH_2(SiMe_3)]$ (48 mg, 0.38 mmol) in Et_2O over 5 minutes. the cloudy solution was allowed to warm to room temperature and stirred for 2 days, during which time a very fine white precipitate formed. After settling slightly the mixture was filtered and the volume of the filtrate reduced to 5 ml. Cooling to –30°C yielded an off-white precipitate. The supernatant was decanted and the residue dried under dynamic vacuum to afford 13 mg of off-white powder.

Elemental analysis calculated for $Tp^*Y(CH_2TMS)_2$, $C_{23}H_{44}N_6BSi_2Y$: C 49.30, H 7.91, N 15.00. Found C 49.45, H 6.68, N 19.32. ^1H NMR (C_6D_6): 0.88 (t, 3H, Et_2O), 1.20 (s,

27H, $SiMe_3$), 1.33 (s, 27H, $SiMe_3$), 2.175 (s, 9H, 3-(5)Me), 2.275 (s, 9H, 5(3)-Me), 3.35 (q, 2H, Et_2O), 5.85 (s, 3H, 4-CH), 5.975 (s, 3H, 4-CH).

Method C [$Y(Tp^{Me,Me})I_2.THF$] + 2 K[$CH_2(SiMe_3)$]

This reaction was carried out analogously to Method B, utilising 100 mg (0.14 mmol) [$Y(Tp^{Me,Me})I_2.THF$] and 36 mg (0.28 mmol) K[$CH_2(SiMe_3)$]. 22 mg of off-white powder were obtained. ^1H NMR (C_6D_6): 1.135 (s, 7H, THF), 1.457 (s, 25H, Me + $SiMe_3$), 2.165 (s, 9H, 5-(3)Me), 3.25 (b, 3H, THF), 5.642 (s, 3H, 4-CH).

Attempted Preparation of [$Y(Tp^{Me,Me})(NHBu^t)_2$]

Method A [$Y(Tp^{Me,Me})Cl_2.THF$] + 2 Li[$NHBu^t$]

To a solution of [$Y(Tp^{Me,Me})Cl_2.THF$] (200 mg, 0.38 mmol) in THF cooled to –78°C was added a cooled solution of Li[$NHBu^t$] (69 mg, 0.88 mmol) in THF. The solution became slightly cloudy on addition. The mixture was allowed to warm to room temperature and stirred overnight during which time the turbidity disappeared. The THF was removed *in vacuo* and the white solid extracted into toluene (2 x 30 ml). The volume of solvent was reduced and the solution cooled to afford a white precipitate. The supernatant was decanted and the solid dried under dynamic vacuum to yield 26 mg of white powder.

Elemental analysis calculated for $LiTp^{Me,Me}$: C 59.24, H 7.29, N 27.63; found C 55.22, H 7.07, N 25.30. IR (KBr, cm^{-1}): 2499 (BH). ^1H NMR (C_6D_6): 1.73 (s, 9H, Me), 2.3 (s, 9H, Me), 5.75 (s, 3H, 4-CH).

Method B [$Y(Tp^{Me,Me})I_2.THF$] + 2 K[$NHBu^t$]

The reaction was carried out analogously to Method A, utilising 100 mg (0.14 mmol) [$Y(Tp^{Me,Me})I_2.THF$] and 31 mg (0.28 mmol) K[$NHBu^t$] to afford 33 mg (0.06 mmol, 44 %) of white powder.

^1H NMR (C_6D_6): 1.17 (b, 12H, THF), 2.001 (s, 18H, Bu^t), 2.113 (s, 18H, Bu^t), 2.515 (bs, 9H, 3-(5)Me), 2.66 (bs, 9H, 5-(3)Me), 3.776 (s, 9H, THF), 5.390 (bs, 3H, 4-CH).

Attempted Preparation of [Y($Tp^{Me,Me}$)(NH-2,4,6-$Me_3C_6H_2$)$_2$]

The same procedure was used as in the previous reactions, utilising 200 mg (0.38 mmol) [Y($Tp^{Me,Me}$)Cl_2.THF] and 123 mg (0.88 mmol) Li[NH-2,4,6-$Me_3C_6H_2$)$_2$] to afford 15 mg of off-white powder.

Elemental analysis calculated for $C_{33}H_{46}N_8BY$: C 60.56, H 7.08, N 17.12. Also calculated for $C_{24}H_{34}N_7BYCl$: C 51.87, H 6.17, N 17.64. Found C 39.20, H 4.90, N 17.12. Tp*YCl_2 gives C 39.42, H 4.85, N 18.39. IR (KBr, cm^{-1}): 2550, 2524 (BH). ^1H NMR (C_6D_6): 0.206 (s, 1H), 1.108 (t, 2H, Et_2O), 1.728 (s, 1H, $LiTp^{Me,Me}$), 1.902 (s, 9H, Me), 2.101 (b, 5H, Me), 2.317 (s, 1H, $LiTp^{Me,Me}$), 3.25 (q, 1H, Et_2O), 6.730 (s, 3H, 4-CH).

Attempted Preparation of [Y($Tp^{Me,Me}$)(NH-2,6-$Pr^i_3C_6H_3$)$_2$]

A solution of [Y($Tp^{Me,Me}$)Cl_2.THF] (200 mg, 0.38 mmol) in THF was added to Li[NH-2,6-$Pr^i_3C_6H_3$)$_2$] (137 mg, 0.75 mmol) in THF at –78°C. The solution was stirred overnight, warming to room temperature, then allowed to settle and filtered. Attempts at recrystallisation from THF and toluene were unsuccessful; data were, therefore, collected for the crude product (yield 24 mg) obtained on removal of solvent and washing with Et_2O.

Elemental analysis calculated for $C_{39}H_{58}N_8BY$: C 63.42, H 7.91, N 15.17. Found C 30.05, H 4.08, N 8.60. IR (KBr, cm^{-1}): 2552, 2524 (BH).

Attempted Preparation of [Y($Tp^{Me,Me}$){$N(SiMe_3)_2$}$_2$]

A solution of $NaN(SiMe_3)_2$ (assumed 44 mg, 0.28 mmol) in THF was added to a slurry of [Y($Tp^{Me,Me}$)I_2.THF] (100 mg, 0.14 mmol) in Et_2O (10 ml) and the mixture stirred overnight at ambient temperature. Filtration and removal of solvent from the filtrate *in vacuo* yielded 226 mg of beige/yellow solid.

^1H NMR (C_6D_6): 0.3 (s, 18H, $SiMe_3$), 1.22 (b, 9H, THF), 2.08 (s, 9H, 5-Me), 2.65 (b, 3-Me), 5.5 (s, 3H, 4-CH).

Reaction of $[Ce(Tp^{Me,Me})_2OTf]$ with $LiAlH_4$

$[Ce(Tp^{Me,Me})_2OTf]$ (200 mg, 0.11 mmol) and $LiAlH_4$ (10 mg, 0.12 mmol) were mixed in a Schlenk tube, cooled to –78°C and THF added. The pale yellow mixture was stirred overnight while warming to room temperature. No colour change was observed. THF was removed *in vacuo* and the pale yellow solid extracted into toluene (2 x 25 ml). Solvent was removed and the product dried under dynamic vacuum to afford 134 mg of pale yellow powder. IR (KBr, cm^{-1}): 2552 (BH); 2519 (BH, $LiTp^{Me,Me}$); 1850 (br), 1690 (br) (AlH). ^1H NMR (C_6D_6): –13.33 (s, 18H, Me), 1.73 (s, 6H, Me, $LiTp^{Me,Me}$), 2.32 (s, 6H, $LiTp^{Me,Me}$), 3.52 (s, 4H, AlH_4), 5.75 (s, 2H, 4-CH, $LiTp^{Me,Me}$), 6.02 (s, 6H, 4-CH), 6.62 (s, 18H, Me).

Reaction of $[Sm(Tp^{Me,Me})_2Cl]$ with $LiAlH_4$

(200 mg, 0.25 mmol) and (10 mg, 0.26 mmol) were mixed in a Schlenk tube and Et_2O added at room temperature. The mixture was stirred for 2 days then filtered and solvent removed from the filtrate *in vacuo*. The pale yellow solid was dissolved in warm Et_2O and cooled to –30°C to yield a pale yellow microcrystalline solid. The supernatant was decanted and the solid dried under dynamic vacuum. 106 mg (0.14 mmol, 53 %) of pale yellow powder was obtained. The product fizzed on addition of water to a small portion. On storage in the glove box for several days the product appeared to decompose, turning grey. Elemental analysis calculated for $C_{30}H_{48}N_{12}B_2SmAl$: C 46.45, H 6.24, N 21.67. Found C 39.91, H 6.09, N 15.36. IR (Nujol, cm^{-1}): 2521 (BH). ^1H NMR (C_6D_6): 1.10 (t, 3H, Et_2O), 1.728 (s, 18H, Me, $LiTp^{Me,Me}$), 2.318 (s, 18H, Me, $LiTp^{Me,Me}$), 3.25 (q, 2H, Et_2O), 5.746 (s, 6H, 4-CH, $LiTp^{Me,Me}$).

Reaction of $[Eu(Tp^{Me,Me})_2OTf]$ with $LiAlH_4$

To a pale yellow solution of $[Eu(Tp^{Me,Me})_2OTf]$ (200 mg, 0.25 mmol) in THF at –78°C was added a cooled slurry of $LiAlH_4$ (10 mg, 0.26 mmol) in THF. A rapid colour change from pale yellow to bright orange/yellow was observed and the solution effervesced

slightly. The mixture was stirred overnight at ambient temperature then solvent removed *in vacuo*. The orange product was purified by sublimation onto a liquid N_2-cooled finger under vacuum. 10 mg (0.01 mmol, 5 %) of a fine orange powder was obtained.
Elemental analysis calculated for $C_{30}H_{48}N_{12}B_2EuAl$: C 46.35, H 6.22, N 21.62. Found C 31.66, H 4.31, N 13.13. IR (Nujol, cm^{-1}): 2558, 2531 (BH).

Reaction of $[Y(Tp^{Me,Me})Cl_2]$ with $LiAlH_4$

The same method was employed as for $[Ce(Tp^{Me,Me})_2OTf]$, utilising 100 mg (0.19 mmol) $[Y(Tp^{Me,Me})Cl_2]$ with 14 mg (0.38 mmol) $LiAlH_4$. Et_2O was employed as solvent. After filtration and washing the residue with Et_2O the filtrates were combined and the volume of solvent reduced to 10 ml. Cooling to –30 °C gave a colourless microcrystalline solid. The supernatant was decanted and the product washed with 30/40 petrol (2 x 5 ml) and dried under dynamic vacuum to afford 15 mg (0.03 mmol, 18 %) of white powder.
Elemental analysis calculated for $C_{15}H_{30}N_6BAl_2Y$: C 40.20, H 6.75, N 18.75. Found: C 38.82, H 6.12, N 11.91. IR (Nujol, cm^{-1}): 2552, 2536 (sh), 2528 (sh) (BH). ^1H NMR (C_6D_6): 1.133 (t, 3H, Et_2O), 1.235 (s, 5H, THF), 1.993 (s, 2H, AlH), 2.064 (s, 12H, 5-Me), 2.702 (bs, 10H 3-Me), 2.897 (s, 2H, AlH), 3.25 (q, 2H, Et_2O), 3.695 (s, 5H, THF), 5.399 (s, 3H, 4-CH).

Reaction of $[Yb(Tp^{Me,Me})Cl_2]$ with $LiAlH_4$

The reaction carried out analogously with the previous preparation, utilising 100 mg (0.17 mmol) $[Yb(Tp^{Me,Me})Cl_2.{}^1/_2THF]$ and 13 mg (0.35 mmol) $LiAlH_4$ afforded as crude product 22 mg (0.04 mmol, 24 %) of pale pink solid. The pink colour arises from a small amount of reduction of Yb (III) to Yb (II). Spectroscopic data were collected on the crude product.
Elemental analysis calculated for $C_{15}H_{30}N_6BAl_2Yb$: C 33.85, H 5.68, N 15.79. Found: C 34.35, H 5.16, N 12.32. IR (Nujol, cm^{-1}): 2546, 2528 (BH); 1900 - 1750 (AlH).
^1H NMR (C_6D_6): Signals in range –17.21 to 79.18.

Reaction of $[Ce(Tp^{Me,Me})_2OTf]$ with $NaBH_4$

$[Ce(Tp^{Me,Me})_2OTf]$ (200 mg, 0.11 mmol) and $NaBH_4$ (10 mg, 0.14 mmol) were mixed in a Schlenk tube, cooled to –78°C and THF added. The mixture was stirred for several hours while warming to ambient temperature then solvent removed and the pale yellow/green product extracted into toluene. On cooling a small quantity of yellow/green solid precipitated. 5 ml 30/40 petrol was added to the solution in an attempt to precipitate more solid. The supernatant was decanted and the yellow solid dried under dynamic vacuum to afford a yellow powder (11 mg, 0.015 mmol, 13 %).

Elemental analysis calculated for $[Ce(Tp^{Me,Me})_2BH_4].Na(BH_4).THF$, $C_{34}H_{56}N_{12}B_4CeNa$: C 47.53, H 7.04, N 19.56. Found: C 45.44, H 6.06, N 18.64. IR (Nujol, cm^{-1}): 2525 (BH, $Tp^{Me,Me}$); 2475 (w), 2392 ($B–H_t$), 2304, 2228 (w) ($B–H_b$).

Attempted preparation of $[Y(Tp^{Me,Me})(BH_4)_2.THF]$

Method A Reaction of $[Y(Tp^{Me,Me})Cl_2.THF]$ with $NaBH_4$

The same method was employed as for the previous reaction, utilising 100 mg (0.19 mmol) $[Y(Tp^{Me,Me})Cl_2.THF]$ and 16 mg (0.43 mmol) $NaBH_4$. Cooling a solution in toluene did not yield any crystalline material. Redissolving the product in THF and cooling gave a colourless microcrystalline product. The supernatant was decanted and the crystals washed with 30/40 petrol and dried under dynamic vacuum (50°C, 30 minutes) to afford 18 mg of a white powder.

Elemental analysis calculated for $C_{15}H_{30}N_6B_3Y$: C 43.33, H 7.27, N 20.21. Found: C 41.48, H 6.03, N 12.27.

Method B Reaction of $[Y(Tp^{Me,Me})I_2.{}^1/_2THF]$ with $NaBH_4$

The same method was employed as for the previous reaction, utilising 200 mg (0.28 mmol) $[Y(Tp^{Me,Me})I_2.{}^1/_2THF]$ and 24 mg (0.62 mmol) $NaBH_4$. Cooling a solution in THF did not yield any crystalline material so solvent was removed *in vacuo* and the white solid dried

under dynamic vacuum to afford a white powder (200 mg). (Theoretical 100 % yield 116 mg, 0.28 mmol).

IR (Nujol, cm^{-1}): 2558 (BH, $LiTp^{Me,Me}$), 2452 (BH_t); 2376, 2285, 2228, 2212 (BH_b). ^1H NMR (C_6D_6): 1.02 (t, 3H, Et_2O), 1.348 (s, 11H, THF), 2.077 (s, 17H 5-Me and BH_4), 2.313 (s, 9H, 3-Me), 2.65 (b, 2H, Et_2O), 3.547 (s, 20H, THF), 5.489 (s, 3H, 4-CH). ^{11}B NMR (C_6D_6): –9.5 (d, 96.1 Hz, $Tp^{Me,Me}$ B–H), –24.5 (q, 83.5 Hz, BH_4).

Reaction of [Yb($Tp^{Me,Me}$)Cl_2.THF] with $NaBH_4$

The same method was employed as for the previous reaction, utilising 100 mg (0.17 mmol) [Yb($Tp^{Me,Me}$)Cl_2.THF] and 16 mg (0.43 mmol) $NaBH_4$. Cooling a solution in toluene did not yield any crystalline material so solvent was removed *in vacuo* and the white solid dried under dynamic vacuum to afford a white powder (45 mg, 0.09 mmol, 53 %).

IR (Nujol, cm^{-1}): 2559 (BH, $Tp^{Me,Me}$); 2460 (BH_t); 2361, 2341, 2300 (BH_b).

^1H NMR (C_6D_6): Signals in range –88.12 to 78.83 ppm. ^{11}B {H} NMR (C_6D_6): –7.5 - -10.5 (bs).

Reaction of [Nd($Tp^{Me,Me}$)$_2$OTf] with $LiBH_3Ph$

[Nd($Tp^{Me,Me}$)$_2$OTf] (100 mg, 0.11 mmol) and $LiBH_3Ph$ (11 mg, 0.11 mmol) were mixed in a Schlenk tube, cooled to –78°C and Et_2O added. The solution was stirred for several hours while warming to room temperature, during which time a white precipitate formed, then filtered and solvent removed *in vacuo* to afford 53 mg (0.06 mmol, 58 %) of pale blue/mauve powder.

IR (Nujol, cm^{-1}): 2557 (BH, $Tp^{Me,Me}$); 2360, 2292, 2224 (BH_b). ^1H NMR (C_6D_6): Peaks in range -23.03 to 15.49 ppm, of which the following have been assigned: –8.873 (s, 18H, TpMe), 1.731 (s, 4H, Me, $LiTp^{Me,Me}$), 2.319 (s, 6H, Me, $LiTp^{Me,Me}$), 4.458 (s, 18H, TpMe), 5.748 (s, 2H, 4-CH, $LiTp^{Me,Me}$), 7.63 (d, 2H, *o*-CH), 7.85 (s, 4H, 4-CH), 8.03 (t, 1H, *p*-CH).

The same preparative method was employed for the following reactions:

Reaction of [Sm($Tp^{Me,Me}$)$_2$Cl] with $LiBH_3Ph$

150 mg (0.19 mmol) [Sm($Tp^{Me,Me}$)$_2$Cl] and 19 mg (0.19 mmol) $LiBH_3Ph$ were utilised and 26 mg (0.03 mmol, 16 %) colourless microcrystalline material obtained.

Elemental analysis calculated for $C_{30}H_{52}N_{12}B_3Sm$: C 51.74, H 6.27, N 20.11. Found: C 43.02, H 6.22, N 15.36. IR (Nujol, cm^{-1}): 2553 (BH, SmTp), 2515 (BH, LiTp); 2195 (BH_b). ^1H NMR (C_6D_6): –0.94 (s, 23H, Me), 1.0 - 1.3 (bm and t, 23H, THF and Et_2O), 1.73 (s, 34H, Me, $LiTp^{Me,Me}$), 2.20 (s, 17H, Me), 2.32 (s, 42H, Me, $LiTp^{Me,Me}$), 2.39 (s, 11H, Me), 2.85 (s, 20H, Me), 3.58 - 3.18 (br, m and q, 36H, THF and Et_2O), 5.448 (bs, 10H, 4-CH), 5.745 (s, 12H, 4-CH, $LiTp^{Me,Me}$), 7.41 (m, 3H *m*-CH), 7.59 (m, 1H, *p*-CH), 8.19 (d, 2H, *o*-CH). ^{11}B {H} NMR (C_6D_6): –6.78, –8.79.

Reaction of [Eu($Tp^{Me,Me}$)$_2$OTf] with $LiBH_3Ph$

100 mg (0.11 mmol) [Eu($Tp^{Me,Me}$)$_2$OTf] and 11 mg (0.11 mmol) $LiBH_3Ph$ were utilised and 35 mg (0.04 mmol, 38 %) crude yellow material obtained on removal of solvent from the filtrate.

IR (Nujol, cm^{-1}): 2560 (BH, $EuTp^{Me,Me}$); 2362, 2336, 2199 (w) (BH_b).

^1H NMR (C_6D_6): 1.3 - 1.1 (bm and t, THF and Et_2O), 2.04 (s, 5-Me), 3.25 (q, Et_2O), 3.61 (m, 10H, THF), 5.15 (s, 12H, 4-CH), 9.813 (bs, 3-Me). ^{11}B {H} NMR (C_6D_6): –11.17 (b).

Reaction of [Gd($Tp^{Me,Me}$)$_2$OTf] with $LiBH_3Ph$

100 mg (0.11 mmol) [Gd($Tp^{Me,Me}$)$_2$OTf] and 11 mg (0.11 mmol) $LiBH_3Ph$ were utilised and 30 mg (0.04 mmol, 32 %) crude white material obtained on removal of solvent from the filtrate.

IR (Nujol, cm^{-1}): 2556 (BH $GdTp^{Me,Me}$); 2516 (BH, $LiTp^{Me,Me}$); 2360, 2345, 2299 (BH_b).

^1H NMR (C_6D_6): 1.720 (s, Me, $LiTp^{Me,Me}$), 2.309 (s, Me, $LiTp^{Me,Me}$), 5.740 (s, 4-CH, $LiTp^{Me,Me}$)

Reaction of [Y($Tp^{Me,Me}$)Cl_2.THF] with $LiBH_3Ph$

100 mg (0.11 mmol) [Y($Tp^{Me,Me}$)Cl_2] and 11 mg (0.11 mmol) $LiBH_3Ph$ were utilised and 97 mg (0.17 mmol, 90 %) crude white material obtained. Colourless crystals were obtained by cooling a solution in Et_2O.

Elemental analysis calculated for $C_{27}H_{38}N_6B_3Y$: C 57.10, H 6.74, N 14.80. Found: C 32.07, H 5.83, N 11.38. IR (Nujol, cm^{-1}): 2557 (BH); 2214 (b) (BH_b).

^1H NMR (C_6D_6): 1.108 (m, Et_2O, THF)., 2.122 (s, Me), 2.083 (s, Me), **2**.308 (s, BH_4), 3.290 (s, Et_2O), 3.573 (s, THF), 5.55 (s, 4-CH), 7.27 (t, 1H, *p*-CH), 7.42 (m, 2H, *m*-CH), 7.90 (d, 2H, *o*-CH). ^{11}B NMR (C_6D_6): –8.22 (d, 101.2 Hz, $Tp^{Me,Me}$), –12.27 (t, 68.7 Hz, $BH_2Ph.OEt_2$), –13.76 (q, 68.7 Hz, BH_3Ph).

Reaction of [Yb($Tp^{Me,Me}$)Cl_2.THF] with $LiBH_3Ph$

100 mg (0.17 mmol) [Yb($Tp^{Me,Me}$)Cl_2.THF] and 34 mg (0.35 mmol) $LiBH_3Ph$ were utilised. Cooling an Et_2O solution afforded a colourless microcrystalline solid. 22 mg (0.03 mmol, 20 %) white material were obtained after decanting the supernatant and drying the product under dynamic vacuum.

Elemental analysis calculated for $C_{27}H_{38}N_6B_3Yb$: C 49.73, H 5.87, N 12.89. Found: C 44.41, H 5.75, N 9.78. IR (Nujol, cm^{-1}): 2557 (BH, $YbTp^{Me,Me}$); 2290 (sh), 2220, 2150 (sh) (BH_b). ^1H NMR (C_6D_6): Signals in the range –75.14 to 31.21 ppm, of which the following have been assigned: –2.827 (s, 9H, 3-Me), 0.954 (s, 9H, 5-Me), 4.101 (s, 3H, 4-CH), 13.073 (s, 5H, *m*-CH), 20.22 (s, 3H, *o*-CH). ^{11}B NMR (C_6D_6): –12.53 (t, 70 Hz, $BH_2Ph.OEt_2$), –13.65 (bd, $Tp^{Me,Me}$), –22.66 (q, 81.7 Hz, BH_3Ph).

Chapter 5 - References

1) McNally, S.; Cooper, N. J.;*Experimental Organometallic Chemistry : A Practicum In Synthesis and Characterization.*; American Chemical Society: Washington, D.C., 1987; Vol. 357.

2) Shriver, D. F.; Drezdzon, M. A. *The Manipulation of Air-Sensitive Compounds*; 2nd ed.; Wiley: New York, 1986.

3) Maunder, G. H. *PhD thesis* London, 1995.

4) Swamer, F. W.; Hauser, C. R. *J. Am. Chem. Soc.* **1950**, *72*, 1352-1356.

5) Trofimenko, S.; Calabrese, J. C.; Kochi, J. K.; Wolowiec, S.; Hulbergen, F. B.; Reedijk, J. *Inorg. Chem.* **1992**, *31*, 3943-3950.

6) Trofimenko, S. *J. Amer. Chem. Soc.* **1967**, *89*, 6288-6294.

7) Namy, J. L.; Girard, P.; Kagan, H. B. *Nouv. J. Chim.* **1981**, *5*, 479.

8) Ginsberg, A. P. *Inorg. Synth.* Wiley-Interscience: New York, 1990; Vol. 27; Chapter 4.

9) Maunder, G. H.; Sella, A.; Tocher, D. A. *Chem. Commun.* **1994**, 2689-2690.

10) Makarova, L. G.; Nesmeyanov, A. N. *Organic Compounds of Mercury*, 1967; Vol. 4, p.67.

11) Long, D. P.; Bianconi, P. A. *J. Amer. Chem. Soc.* **1996**, *118*, 12453-12454.

Appendix 1 - Crystallographic Details

Except for **2.6** and **4.5**, samples of the crystals in the mother liquor were sent in sealed tubes to Dr Mark Elsegood at the University of Newcastle. Measurements were made on a Siemens SMART CCD diffractometer fitted with an area detector and a variable temperature unit. The crystals were examined and mounted in degassed oil which was frozen in a stream of cold nitrogen on the diffractometer. Data collection, and solution and refinement of the structures were all carried out using standard SHELX-93 procedures.

For complexes **2.6** and **4.5**, samples of the crystals in the mother liquor were sent in sealed tubes to the EPSRC X-ray facility at the University of Cardiff. Measurements were made on a Siemens SMART CCD diffractometer fitted with an area detector and a variable temperature unit, and data collection, solution and refinement carried out as above.

The following tables list the experimental conditions and results of the refinements for the structures presented in this thesis, together with tables of fractional coordinates, bond lengths and bond angles for each structure.

Table A1.1 Crystal data, structure solution and refinement for **2.1**.

Chemical formula	$C_{76}H_{100}B_4Cl_4N_{24}O_2Sm_2$
Formula weight	1867.54
Temperature	160(2) K
Radiation and wavelength	MoKα, 0.71073 Å
Crystal system, space group	triclinic, $P\bar{1}$
Unit cell dimensions	a = 10.8129(16) Å α = 102.135(4)°
	b = 14.0111(19) Å β = 93.804(4)°
	c = 14.493(2) Å γ = 91.768(4)°
Volume	2139.7(5) Å^3
Z	1
Density (calculated)	1.449 g/cm^3
Absorption coefficient μ	1.543 mm^{-1}
F(000)	952
Reflections for cell refinement	5592 (θ range 1.84 to 28.07°)
Crystal colour	red
Crystal size	0.34 × 0.10 × 0.04 mm
Data collection method	Siemens SMART CCD diffractometer,
	ω rotation with narrow frames
θ range for data collection	1.89 to 25.00°
Index ranges	$-12 \le h \le 13$, $-17 \le k \le 15$, $-17 \le \ell \le 19$
Intensity decay of standards	0%
Reflections collected	11000
Independent reflections	7319 (R_{int} = 0.0748)
Reflections with I>2σ(I)	4629
Absorption correction	semi-empirical from ψ-scans
Max. and min. transmission	0.862 and 0.544
Structure solution	direct methods
Refinement method	full-matrix least-squares on F^2
Weighting parameters a, b	0.1078, 0.0000
Data / restraints / parameters	7319 / 120 / 517
Goodness-of-fit on F^2	0.995
Final R indices [I>2σ(I)]	R1 = 0.0905, wR2 = 0.1918
R indices (all data)	R1 = 0.1488, wR2 = 0.2225
Largest and mean shift/esd	0.001 and 0.000
Largest diff. peak and hole	2.563 and −2.744 eÅ^{-3}

Table A1.2 Atomic coordinates (x 104) and equivalent isotropic displacement parameters (Å2 x 103) for **2.1**. U(eq) is defined as one third of the trace of the orthogonalised Uij tensor.

	x	y	z	U(eq)
Sm(1)	7561.1(6)	7256.0(4)	3042.4(5)	19.3(2)
O(1)	8631(8)	8364(5)	4043(6)	27(2)
C(1)	9301(12)	9148(8)	4507(9)	21(3)
C(2)	10407(11)	9072(8)	5015(9)	20(3)
C(3)	11143(12)	9905(8)	5501(9)	23(3)
C(4)	12273(11)	9761(8)	5989(8)	21(3)
C(5)	12661(12)	8866(9)	6031(10)	32(3)
C(6)	11941(13)	8022(9)	5548(10)	31(3)
C(7)	10879(11)	8124(8)	5049(9)	25(3)
N(1)	6722(9)	6815(7)	1281(8)	25(3)
N(2)	6146(10)	7521(7)	881(8)	28(3)
C(8)	6620(12)	6001(8)	597(9)	25(3)
C(9)	5950(13)	6170(9)	-214(10)	34(3)
C(10)	5700(13)	7132(9)	5(9)	31(3)
C(11)	7096(13)	5048(9)	727(11)	39(4)
C(12)	4947(16)	7670(11)	-602(11)	54(5)
N(3)	5677(9)	8221(7)	3020(8)	26(2)
N(4)	5359(9)	8694(6)	2303(7)	20(2)
C(13)	4853(11)	8440(9)	3667(10)	27(3)
C(14)	4010(13)	9084(9)	3378(11)	37(4)
C(15)	4366(13)	9214(9)	2515(10)	30(3)
C(16)	4887(13)	8008(12)	4505(11)	44(4)
C(17)	3743(14)	9806(11)	1888(11)	47(4)
N(5)	8351(9)	8532(7)	2102(7)	20(2)
N(6)	7445(10)	9019(7)	1685(8)	26(3)
C(18)	9384(13)	9091(10)	2190(10)	36(4)
C(19)	9153(14)	9935(9)	1845(10)	36(4)
C(20)	7963(13)	9872(10)	1554(10)	33(3)
C(21)	10592(11)	8807(9)	2604(10)	31(3)
C(22)	7180(15)	10599(10)	1165(12)	51(5)
B(1)	6082(15)	8619(11)	1444(11)	30(4)
N(7)	8852(9)	5795(7)	2687(7)	21(2)
N(8)	8462(9)	4949(6)	2936(7)	20(2)
C(23)	9689(12)	5557(8)	2075(10)	27(3)
C(24)	9883(12)	4550(8)	1919(9)	26(3)
C(25)	9071(12)	4188(8)	2471(8)	22(2)
C(26)	10321(14)	6276(10)	1608(11)	41(4)
C(27)	8840(14)	3144(8)	2559(11)	37(4)
N(9)	5909(10)	5812(7)	2868(8)	30(2)
N(10)	6225(10)	5059(7)	3311(8)	27(2)
C(28)	4703(12)	5682(9)	2609(10)	31(3)
C(29)	4218(13)	4851(10)	2867(11)	37(3)
C(30)	5180(13)	4483(10)	3310(10)	34(3)
C(31)	3987(12)	6324(10)	2095(11)	39(4)
C(32)	5189(15)	3602(13)	3733(14)	67(6)
N(11)	7661(9)	6664(6)	4646(7)	24(2)
N(12)	7860(10)	5681(7)	4592(7)	24(2)

C(33)	7894(12)	7110(8)	5554(9)	28(3)
C(34)	8288(13)	6443(9)	6083(10)	32(3)
C(35)	8247(11)	5565(8)	5453(9)	19(2)
C(36)	7720(13)	8176(8)	5943(10)	30(3)
C(37)	8559(14)	4579(9)	5648(10)	35(3)
B(2)	7533(15)	4915(10)	3686(11)	29(4)
C(38)	11172(18)	2087(15)	201(13)	73(6)
Cl(1)	9576(5)	2142(4)	102(3)	68.0(13)
Cl(2)	11758(5)	1977(4)	1318(4)	78.7(15)

Table A1.3 Bond lengths (Å) and angles (°) for **2.1.**

Sm(1)-O(1)	2.138(8)	Sm(1)-N(3)	2.482(10)
Sm(1)-N(7)	2.497(9)	Sm(1)-N(1)	2.592(11)
Sm(1)-N(9)	2.617(10)	Sm(1)-N(5)	2.621(9)
Sm(1)-N(11)	2.624(10)	O(1)-C(1)	1.326(14)
C(1)-C(2)	1.381(17)	C(1)-C(3a)	1.428(16)
C(2)-C(3)	1.418(16)	C(2)-C(7)	1.447(15)
C(3)-C(4)	1.412(17)	C(3)-C(1a)	1.428(16)
C(4)-C(5)	1.347(16)	C(5)-C(6)	1.420(18)
C(6)-C(7)	1.344(18)	N(1)-C(8)	1.340(15)
N(1)-N(2)	1.391(13)	N(2)-C(10)	1.324(16)
N(2)-B(1)	1.588(17)	C(8)-C(9)	1.406(18)
C(8)-C(11)	1.490(16)	C(9)-C(10)	1.359(17)
C(10)-C(12)	1.491(18)	N(3)-C(13)	1.333(16)
N(3)-N(4)	1.375(13)	N(4)-C(15)	1.332(16)
N(4)-B(1)	1.501(19)	C(13)-C(14)	1.407(17)
C(13)-C(16)	1.465(18)	C(14)-C(15)	1.379(19)
C(15)-C(17)	1.497(18)	N(5)-C(18)	1.328(16)
N(5)-N(6)	1.388(13)	N(6)-C(20)	1.359(15)
N(6)-B(1)	1.551(18)	C(18)-C(19)	1.400(18)
C(18)-C(21)	1.500(19)	C(19)-C(20)	1.321(19)
C(20)-C(22)	1.518(18)	N(7)-C(23)	1.311(15)
N(7)-N(8)	1.371(12)	N(8)-C(25)	1.351(14)
N(8)-B(2)	1.535(19)	C(23)-C(24)	1.405(16)
C(23)-C(26)	1.498(17)	C(24)-C(25)	1.381(17)
C(25)-C(27)	1.509(15)	N(9)-C(28)	1.329(16)
N(9)-N(10)	1.386(13)	N(10)-C(30)	1.368(16)
N(10)-B(2)	1.516(18)	C(28)-C(29)	1.394(17)
C(28)-C(31)	1.486(17)	C(29)-C(30)	1.357(19)
C(30)-C(32)	1.490(18)	N(11)-C(33)	1.336(16)
N(11)-N(12)	1.388(12)	N(12)-C(35)	1.335(16)
N(12)-B(2)	1.524(17)	C(33)-C(34)	1.388(17)
C(33)-C(36)	1.503(15)	C(34)-C(35)	1.367(17)
C(35)-C(37)	1.510(16)	C(38)-Cl(1)	1.73(2)
C(38)-Cl(2)	1.74(2)		

O(1)-Sm(1)-N(3)	95.0(3)	O(1)-Sm(1)-N(7)	107.5(3)
N(3)-Sm(1)-N(7)	157.3(3)	O(1)-Sm(1)-N(1)	141.6(3)
N(3)-Sm(1)-N(1)	76.8(3)	N(7)-Sm(1)-N(1)	87.1(3)
O(1)-Sm(1)-N(9)	144.0(3)	N(3)-Sm(1)-N(9)	82.2(3)
N(7)-Sm(1)-N(9)	77.7(3)	N(1)-Sm(1)-N(9)	73.0(3)
O(1)-Sm(1)-N(5)	73.4(3)	N(3)-Sm(1)-N(5)	81.0(3)
N(7)-Sm(1)-N(5)	108.0(3)	N(1)-Sm(1)-N(5)	68.3(3)
N(9)-Sm(1)-N(5)	140.3(3)	O(1)-Sm(1)-N(11)	74.1(3)
N(3)-Sm(1)-N(11)	106.3(3)	N(7)-Sm(1)-N(11)	77.7(3)
N(1)-Sm(1)-N(11)	144.3(3)	N(9)-Sm(1)-N(11)	72.4(3)
N(5)-Sm(1)-N(11)	147.1(3)	C(1)-O(1)-Sm(1)	167.6(8)
O(1)-C(1)-C(2)	121.7(10)	O(1)-C(1)-C(3a)	119.3(11)
C(2)-C(1)-C(3a)	119.0(10)	C(1)-C(2)-C(3)	122.3(10)
C(1)-C(2)-C(7)	120.5(10)	C(3)-C(2)-C(7)	117.2(11)
C(4)-C(3)-C(2)	118.6(10)	C(4)-C(3)-C(1a)	122.7(11)
C(2)-C(3)-C(1a)	118.7(11)	C(5)-C(4)-C(3)	122.5(12)

C(4)-C(5)-C(6)	119.8(13)	C(7)-C(6)-C(5)	119.6(12)
C(6)-C(7)-C(2)	122.2(11)	C(8)-N(1)-N(2)	104.9(10)
C(8)-N(1)-Sm(1)	135.6(8)	N(2)-N(1)-Sm(1)	119.3(7)
C(10)-N(2)-N(1)	109.9(9)	C(10)-N(2)-B(1)	128.0(10)
N(1)-N(2)-B(1)	122.1(10)	N(1)-C(8)-C(9)	110.6(11)
N(1)-C(8)-C(11)	123.2(11)	C(9)-C(8)-C(11)	126.1(12)
C(10)-C(9)-C(8)	104.7(12)	N(2)-C(10)-C(9)	109.7(11)
N(2)-C(10)-C(12)	123.8(12)	C(9)-C(10)-C(12)	126.2(13)
C(13)-N(3)-N(4)	107.4(9)	C(13)-N(3)-Sm(1)	129.8(8)
N(4)-N(3)-Sm(1)	122.7(7)	C(15)-N(4)-N(3)	109.5(10)
C(15)-N(4)-B(1)	127.9(11)	N(3)-N(4)-B(1)	122.7(10)
N(3)-C(13)-C(14)	109.0(12)	N(3)-C(13)-C(16)	121.3(11)
C(14)-C(13)-C(16)	129.6(13)	C(15)-C(14)-C(13)	105.5(12)
N(4)-C(15)-C(14)	108.6(12)	N(4)-C(15)-C(17)	124.3(12)
C(14)-C(15)-C(17)	127.0(12)	C(18)-N(5)-N(6)	105.8(10)
C(18)-N(5)-Sm(1)	132.9(9)	N(6)-N(5)-Sm(1)	116.3(7)
C(20)-N(6)-N(5)	108.4(10)	C(20)-N(6)-B(1)	128.2(11)
N(5)-N(6)-B(1)	123.4(9)	N(5)-C(18)-C(19)	110.1(13)
N(5)-C(18)-C(21)	122.2(12)	C(19)-C(18)-C(21)	127.8(13)
C(20)-C(19)-C(18)	106.4(12)	C(19)-C(20)-N(6)	109.3(12)
C(19)-C(20)-C(22)	129.8(12)	N(6)-C(20)-C(22)	120.8(12)
N(4)-B(1)-N(6)	112.9(11)	N(4)-B(1)-N(2)	112.1(11)
N(6)-B(1)-N(2)	106.2(10)	C(23)-N(7)-N(8)	106.8(9)
C(23)-N(7)-Sm(1)	131.5(8)	N(8)-N(7)-Sm(1)	118.9(7)
C(25)-N(8)-N(7)	110.0(9)	C(25)-N(8)-B(2)	126.3(10)
N(7)-N(8)-B(2)	123.6(9)	N(7)-C(23)-C(24)	110.6(11)
N(7)-C(23)-C(26)	123.5(11)	C(24)-C(23)-C(26)	125.9(12)
C(25)-C(24)-C(23)	105.1(11)	N(8)-C(25)-C(24)	107.5(10)
N(8)-C(25)-C(27)	123.9(11)	C(24)-C(25)-C(27)	128.6(11)
C(28)-N(9)-N(10)	106.7(9)	C(28)-N(9)-Sm(1)	135.1(8)
N(10)-N(9)-Sm(1)	116.6(7)	C(30)-N(10)-N(9)	108.2(10)
C(30)-N(10)-B(2)	128.0(11)	N(9)-N(10)-B(2)	123.8(9)
N(9)-C(28)-C(29)	110.4(11)	N(9)-C(28)-C(31)	124.4(11)
C(29)-C(28)-C(31)	125.1(12)	C(30)-C(29)-C(28)	105.9(12)
C(29)-C(30)-N(10)	108.7(11)	C(29)-C(30)-C(32)	128.9(13)
N(10)-C(30)-C(32)	122.3(12)	C(33)-N(11)-N(12)	106.6(9)
C(33)-N(11)-Sm(1)	134.3(7)	N(12)-N(11)-Sm(1)	116.4(7)
C(35)-N(12)-N(11)	108.2(10)	C(35)-N(12)-B(2)	129.6(10)
N(11)-N(12)-B(2)	121.9(10)	N(11)-C(33)-C(34)	110.2(11)
N(11)-C(33)-C(36)	124.6(12)	C(34)-C(33)-C(36)	125.3(12)
C(35)-C(34)-C(33)	105.1(12)	N(12)-C(35)-C(34)	109.9(11)
N(12)-C(35)-C(37)	122.2(11)	C(34)-C(35)-C(37)	127.9(12)
N(10)-B(2)-N(12)	108.9(11)	N(10)-B(2)-N(8)	111.1(11)
N(12)-B(2)-N(8)	112.2(11)	Cl(1)-C(38)-Cl(2)	113.2(10)

Symmetry transformations used to generate equivalent atoms:

a: -x+2,-y+2,-z+1

Table A1.4 Crystal data, structure solution and refinement for **2.3**.

Chemical formula	$C_{37}H_{51}B_2N_{12}SSm$
Formula weight	867.93
Temperature	160(2) K
Radiation and wavelength	MoKα, 0.71073 Å
Crystal system, space group	monoclinic, $P2_1/n$
Unit cell dimensions	a = 15.0154(9) Å α = 90°
	b = 13.1853(8) Å β = 108.628(2)°
	c = 21.1254(13) Å γ = 90°
Volume	3963.4(4) Å^3
Z	4
Density (calculated)	1.455 g/cm^3
Absorption coefficient μ	1.578 mm^{-1}
F(000)	1780
Reflections for cell refinement	12561 (θ range 2.52 to 28.70°)
Crystal colour	yellow
Crystal size	0.18 × 0.15 × 0.12 mm
Data collection method	Siemens SMART CCD diffractometer,
	ω rotation with narrow frames
θ range for data collection	1.85 to 28.88°
Index ranges	$-19 \leq h \leq 18$, $-17 \leq k \leq 17$, $-14 \leq \ell \leq 27$
Intensity decay	0%
Reflections collected	24634
Independent reflections	9430 (R_{int} = 0.0452)
Reflections with I>2σ(I)	6867
Absorption correction	semi-empirical from ψ-scans
Max. and min. transmission	0.647 and 0.568
Structure solution	direct methods
Refinement method	full-matrix least-squares on F^2
Weighting parameters a, b	0.0344, 0.0000
Data / restraints / parameters	9430 / 0 / 491
Final R indices [I>2σ(I)]	R1 = 0.0350, wR2 = 0.0687
R indices (all data)	R1 = 0.0644, wR2 = 0.0769
Goodness-of-fit on F^2	0.990
Largest and mean shift/esd	0.003 and 0.000
Largest diff. peak and hole	1.106 and −1.025 eÅ^{-3}

Table A1.5 Atomic coordinates (x 10^4) and equivalent isotropic displacement parameters ($Å^2$ x 10^3) for **2.3.** U(eq) is defined as one third of the trace of the orthogonalised U_{ij} tensor.

	x	y	z	U(eq)
Sm(1)	8089.95(11)	7696.46(12)	696.66(8)	17.13(5)
N(1)	6759.7(17)	8476.3(19)	988.2(13)	20.7(6)
N(2)	6906.6(17)	8561.1(19)	1666.6(13)	20.3(6)
C(1)	5841(2)	8638(2)	683.5(17)	24.9(8)
C(2)	5391(2)	8798(2)	1156.8(18)	28.6(8)
C(3)	6075(2)	8745(2)	1764.2(18)	25.7(8)
C(4)	5414(2)	8660(3)	-60.1(17)	31.4(8)
C(5)	5971(3)	8833(3)	2450.0(18)	38.9(10)
N(3)	8779.6(18)	9265.1(19)	1380.5(13)	20.1(6)
N(4)	8491.3(17)	9456.3(19)	1929.7(13)	19.7(6)
C(6)	9306(2)	10060(2)	1325.7(17)	23.0(7)
C(7)	9357(2)	10761(2)	1829.0(16)	25.9(8)
C(8)	8833(2)	10363(2)	2199.1(17)	24.0(7)
C(9)	9720(2)	10143(3)	766.4(17)	31.8(8)
C(10)	8636(3)	10805(3)	2796.0(17)	32.9(9)
N(5)	8918.9(18)	7263(2)	1937.4(14)	24.6(6)
N(6)	8457.5(18)	7676(2)	2346.7(13)	23.2(6)
C(11)	9505(2)	6557(2)	2304.3(18)	30.4(8)
C(12)	9405(3)	6504(3)	2937.3(19)	38.1(10)
C(13)	8748(3)	7207(3)	2950.9(17)	31.7(8)
C(14)	10203(2)	5996(3)	2064(2)	45.8(11)
C(15)	8378(3)	7470(3)	3508.9(18)	46.6(11)
B(1)	7908(3)	8685(3)	2182.1(19)	23.0(8)
N(7)	7566.4(17)	9133.4(19)	-213.6(13)	20.3(6)
N(8)	7634.8(17)	8910.8(19)	-835.8(13)	20.2(6)
C(16)	7380(2)	10132(2)	-221.5(17)	22.0(7)
C(17)	7347(2)	10549(2)	-832.7(17)	25.6(8)
C(18)	7516(2)	9763(2)	-1209.6(16)	23.2(7)
C(19)	7222(2)	10695(2)	351.9(17)	28.7(8)
C(20)	7607(2)	9800(3)	-1895.4(17)	33.4(9)
N(9)	6892.1(17)	7017.8(19)	-311.5(14)	21.3(6)
N(10)	6999.5(18)	7126.6(19)	-936.7(13)	21.7(6)
C(21)	6136(2)	6420(2)	-396.0(18)	26.2(8)
C(22)	5766(2)	6140(3)	-1059.1(19)	32.2(9)
C(23)	6317(2)	6579(2)	-1390.5(17)	27.8(8)
C(24)	5805(2)	6145(3)	174.8(19)	34.8(9)
C(25)	6233(3)	6486(3)	-2113.2(18)	41.4(10)
N(11)	9153.5(17)	7683(2)	22.7(13)	22.7(6)
N(12)	8774.5(18)	7466.2(18)	-646.2(13)	22.5(6)
C(26)	10067(2)	7422(2)	205.3(18)	26.8(8)
C(27)	10273(2)	7024(3)	-341.4(19)	31.3(9)
C(28)	9448(2)	7054(2)	-866.7(18)	26.1(8)
C(29)	10691(3)	7616(3)	896(2)	43.1(10)

C(30)	9260(3)	6710(3)	-1570.0(19)	38.7(10)
B(2)	7759(3)	7816(3)	-1044.2(19)	23.4(8)
S(1)	8195.8(7)	5572.3(7)	884.3(4)	31.6(2)
C(31)	7781(2)	4856(2)	137.7(17)	24.1(7)
C(32)	8092(2)	5027(2)	-409.4(17)	26.2(8)
C(33)	7719(2)	4490(2)	-997.6(17)	26.2(8)
C(34)	7040(2)	3741(2)	-1062.5(17)	28.7(8)
C(35)	6770(2)	3537(3)	-508.4(18)	29.8(8)
C(36)	7133(2)	4075(2)	82.0(18)	29.5(8)
C(37)	6607(3)	3200(3)	-1725.0(18)	40.8(10)

Table A1.6 Bond lengths (Å) and angles (°) for **2.3**.

Sm(1)-N(11)	2.456(2)	Sm(1)-N(9)	2.475(3)
Sm(1)-N(1)	2.492(2)	Sm(1)-N(3)	2.546(2)
Sm(1)-N(5)	2.581(3)	Sm(1)-N(7)	2.634(3)
Sm(1)-S(1)	2.8260(9)	N(1)-C(1)	1.340(4)
N(1)-N(2)	1.383(3)	N(2)-C(3)	1.350(4)
N(2)-B(1)	1.558(4)	C(1)-C(2)	1.390(4)
C(1)-C(4)	1.495(5)	C(2)-C(3)	1.366(5)
C(3)-C(5)	1.511(5)	N(3)-C(6)	1.340(4)
N(3)-N(4)	1.385(3)	N(4)-C(8)	1.352(4)
N(4)-B(1)	1.544(4)	C(6)-C(7)	1.393(4)
C(6)-C(9)	1.504(4)	C(7)-C(8)	1.378(4)
C(8)-C(10)	1.502(5)	N(5)-C(11)	1.344(4)
N(5)-N(6)	1.381(4)	N(6)-C(13)	1.359(4)
N(6)-B(1)	1.545(5)	C(11)-C(12)	1.394(5)
C(11)-C(14)	1.497(5)	C(12)-C(13)	1.361(5)
C(13)-C(15)	1.496(5)	N(7)-C(16)	1.345(4)
N(7)-N(8)	1.382(3)	N(8)-C(18)	1.352(4)
N(8)-B(2)	1.538(4)	C(16)-C(17)	1.389(5)
C(16)-C(19)	1.503(4)	C(17)-C(18)	1.379(4)
C(18)-C(20)	1.498(5)	N(9)-C(21)	1.347(4)
N(9)-N(10)	1.388(4)	N(10)-C(23)	1.365(4)
N(10)-B(2)	1.532(5)	C(21)-C(22)	1.382(5)
C(21)-C(24)	1.488(5)	C(22)-C(23)	1.370(5)
C(23)-C(25)	1.496(5)	N(11)-C(26)	1.345(4)
N(11)-N(12)	1.374(4)	N(12)-C(28)	1.355(4)
N(12)-B(2)	1.557(4)	C(26)-C(27)	1.391(5)
C(26)-C(29)	1.482(5)	C(27)-C(28)	1.375(5)
C(28)-C(30)	1.491(5)	S(1)-C(31)	1.772(3)
C(31)-C(36)	1.396(4)	C(31)-C(32)	1.396(4)
C(32)-C(33)	1.384(4)	C(33)-C(34)	1.395(5)
C(34)-C(35)	1.382(5)	C(34)-C(37)	1.519(5)
C(35)-C(36)	1.386(5)		

N(11)-Sm(1)-N(9)	85.80(9)	N(11)-Sm(1)-N(1)	150.13(8)
N(9)-Sm(1)-N(1)	86.69(8)	N(11)-Sm(1)-N(3)	96.48(8)
N(9)-Sm(1)-N(3)	146.53(8)	N(1)-Sm(1)-N(3)	74.78(8)
N(11)-Sm(1)-N(5)	113.28(8)	N(9)-Sm(1)-N(5)	140.91(8)
N(1)-Sm(1)-N(5)	90.28(8)	N(3)-Sm(1)-N(5)	68.08(8)
N(11)-Sm(1)-N(7)	71.32(8)	N(9)-Sm(1)-N(7)	70.51(8)
N(1)-Sm(1)-N(7)	78.92(8)	N(3)-Sm(1)-N(7)	78.60(8)
N(5)-Sm(1)-N(7)	146.63(8)	N(11)-Sm(1)-S(1)	93.23(6)
N(9)-Sm(1)-S(1)	75.83(6)	N(1)-Sm(1)-S(1)	112.82(6)
N(3)-Sm(1)-S(1)	136.98(6)	N(5)-Sm(1)-S(1)	69.58(6)
N(7)-Sm(1)-S(1)	143.66(6)	C(1)-N(1)-N(2)	106.5(3)
C(1)-N(1)-Sm(1)	136.9(2)	N(2)-N(1)-Sm(1)	114.47(18)
C(3)-N(2)-N(1)	108.9(3)	C(3)-N(2)-B(1)	127.4(3)
N(1)-N(2)-B(1)	122.1(2)	N(1)-C(1)-C(2)	109.9(3)
N(1)-C(1)-C(4)	122.5(3)	C(2)-C(1)-C(4)	127.5(3)
C(3)-C(2)-C(1)	106.0(3)	N(2)-C(3)-C(2)	108.7(3)
N(2)-C(3)-C(5)	123.0(3)	C(2)-C(3)-C(5)	128.3(3)
C(6)-N(3)-N(4)	106.3(2)	C(6)-N(3)-Sm(1)	136.9(2)

N(4)-N(3)-Sm(1)	116.36(17)	C(8)-N(4)-N(3)	109.6(2)
C(8)-N(4)-B(1)	128.1(3)	N(3)-N(4)-B(1)	122.2(2)
N(3)-C(6)-C(7)	110.1(3)	N(3)-C(6)-C(9)	121.9(3)
C(7)-C(6)-C(9)	128.0(3)	C(8)-C(7)-C(6)	106.2(3)
N(4)-C(8)-C(7)	107.8(3)	N(4)-C(8)-C(10)	123.1(3)
C(7)-C(8)-C(10)	129.0(3)	C(11)-N(5)-N(6)	106.2(3)
C(11)-N(5)-Sm(1)	138.9(2)	N(6)-N(5)-Sm(1)	111.90(17)
C(13)-N(6)-N(5)	109.5(3)	C(13)-N(6)-B(1)	126.3(3)
N(5)-N(6)-B(1)	122.5(3)	N(5)-C(11)-C(12)	109.6(3)
N(5)-C(11)-C(14)	123.2(3)	C(12)-C(11)-C(14)	127.0(3)
C(13)-C(12)-C(11)	106.7(3)	N(6)-C(13)-C(12)	107.9(3)
N(6)-C(13)-C(15)	123.1(3)	C(12)-C(13)-C(15)	129.0(3)
N(4)-B(1)-N(6)	108.9(3)	N(4)-B(1)-N(2)	110.8(3)
N(6)-B(1)-N(2)	113.2(3)	C(16)-N(7)-N(8)	105.9(2)
C(16)-N(7)-Sm(1)	136.5(2)	N(8)-N(7)-Sm(1)	116.48(17)
C(18)-N(8)-N(7)	110.1(2)	C(18)-N(8)-B(2)	128.2(3)
N(7)-N(8)-B(2)	121.6(2)	N(7)-C(16)-C(17)	110.1(3)
N(7)-C(16)-C(19)	124.0(3)	C(17)-C(16)-C(19)	125.9(3)
C(18)-C(17)-C(16)	106.3(3)	N(8)-C(18)-C(17)	107.5(3)
N(8)-C(18)-C(20)	123.8(3)	C(17)-C(18)-C(20)	128.6(3)
C(21)-N(9)-N(10)	106.5(3)	C(21)-N(9)-Sm(1)	132.5(2)
N(10)-N(9)-Sm(1)	120.54(18)	C(23)-N(10)-N(9)	108.9(3)
C(23)-N(10)-B(2)	129.6(3)	N(9)-N(10)-B(2)	121.4(3)
N(9)-C(21)-C(22)	109.8(3)	N(9)-C(21)-C(24)	121.4(3)
C(22)-C(21)-C(24)	128.8(3)	C(23)-C(22)-C(21)	107.0(3)
N(10)-C(23)-C(22)	107.8(3)	N(10)-C(23)-C(25)	124.0(3)
C(22)-C(23)-C(25)	128.3(3)	C(26)-N(11)-N(12)	106.9(3)
C(26)-N(11)-Sm(1)	128.9(2)	N(12)-N(11)-Sm(1)	117.73(18)
C(28)-N(12)-N(11)	109.1(3)	C(28)-N(12)-B(2)	130.0(3)
N(11)-N(12)-B(2)	120.4(2)	N(11)-C(26)-C(27)	109.6(3)
N(11)-C(26)-C(29)	120.3(3)	C(27)-C(26)-C(29)	130.0(3)
C(28)-C(27)-C(26)	106.1(3)	N(12)-C(28)-C(27)	108.3(3)
N(12)-C(28)-C(30)	122.6(3)	C(27)-C(28)-C(30)	129.1(3)
N(10)-B(2)-N(8)	110.5(3)	N(10)-B(2)-N(12)	113.0(3)
N(8)-B(2)-N(12)	108.1(3)	C(31)-S(1)-Sm(1)	114.56(11)
C(36)-C(31)-C(32)	117.3(3)	C(36)-C(31)-S(1)	120.4(3)
C(32)-C(31)-S(1)	122.3(3)	C(33)-C(32)-C(31)	120.9(3)
C(32)-C(33)-C(34)	121.6(3)	C(35)-C(34)-C(33)	117.2(3)
C(35)-C(34)-C(37)	122.3(3)	C(33)-C(34)-C(37)	120.4(3)
C(34)-C(35)-C(36)	121.7(3)	C(35)-C(36)-C(31)	121.1(3)

Table A1.7 Crystal data, structure solution and refinement for **2.4**.

Chemical formula	$C_{40}H_{57}B_2N_{12}SeSm$
Formula weight	956.91
Temperature	160(2) K
Radiation and wavelength	MoKα, 0.71073 Å
Crystal system, space group	triclinic, $P\bar{1}$
Unit cell dimensions	a = 10.1801(6) Å α = 88.313(2)°
	b = 10.2622(6) Å β = 86.268(2)°
	c = 23.4367(14) Å γ = 62.503(2)°
Volume	2167.2(2) Å^3
Z	2
Density (calculated)	1.466 g/cm^3
Absorption coefficient μ	2.238 mm^{-1}
F(000)	974
Reflections for cell refinement	10726 (θ range 2.24 to 28.78°)
Crystal colour	yellow
Crystal size	0.31 × 0.14 × 0.10 mm
Data collection method	Siemens SMART CCD diffractometer,
	ω rotation with narrow frames
θ range for data collection	2.24 to 28.80°
Index ranges	$-13 \le h \le 13$, $-13 \le k \le 13$, $-28 \le \ell \le 30$
Intensity decay	0%
Reflections collected	16032
Independent reflections	9712 (R_{int} = 0.0227)
Reflections with I>2σ(I)	8047
Absorption correction	semi-empirical from ψ-scans
Max. and min. transmission	0.746 and 0.623
Structure solution	direct methods
Refinement method	full-matrix least-squares on F^2
Weighting parameters a, b	0.0337, 0.0000
Data / restraints / parameters	9712 / 0 / 520
Final R indices [I>2σ(I)]	R1 = 0.0305, wR2 = 0.0640
R indices (all data)	R1 = 0.0430, wR2 = 0.0675
Goodness-of-fit on F^2	0.985
Largest and mean shift/esd	0.007 and 0.000
Largest diff. peak and hole	1.236 and -0.957 eÅ^{-3}

Table A1.8 Atomic coordinates (x 10^4) and equivalent isotropic displacement parameters ($Å^2$ x 10^3) for **2.4**. U(eq) is defined as one third of the trace of the orthogonalised U_{ij} tensor.

	x	y	z	U(eq)
Sm(1)	-2.09(15)	8169.03(15)	2986.52(6)	14.85(5)
N(1)	-892(3)	7779(2)	4133.8(10)	20.2(5)
N(2)	560(2)	6698(2)	4006.3(9)	16.2(5)
C(1)	-1652(3)	7070(3)	4305.4(12)	23.5(6)
C(2)	-730(3)	5543(3)	4303.8(12)	25.6(7)
C(3)	637(3)	5334(3)	4111.1(12)	22.6(6)
C(4)	-3286(3)	7885(4)	4445.0(15)	36.8(8)
C(5)	2056(4)	3956(3)	4008.1(17)	40.7(9)
N(3)	2701(2)	6539(2)	3091.5(9)	16.5(5)
N(4)	3093(2)	6285(2)	3652.3(9)	15.5(5)
C(6)	3981(3)	5963(3)	2767.0(12)	19.5(6)
C(7)	5182(3)	5325(3)	3113.0(13)	22.4(6)
C(8)	4587(3)	5557(3)	3665.8(12)	19.8(6)
C(9)	4030(3)	6117(3)	2133.0(12)	24.4(7)
C(10)	5366(3)	5108(3)	4214.6(13)	29.6(7)
N(5)	492(3)	9551(2)	3729.0(9)	17.8(5)
N(6)	1319(2)	8672(2)	4161.0(9)	16.6(5)
C(11)	212(3)	10932(3)	3846.3(12)	19.5(6)
C(12)	843(3)	10943(3)	4357.5(12)	21.7(6)
C(13)	1544(3)	9514(3)	4539.4(12)	18.2(6)
C(14)	-655(4)	12185(3)	3459.0(13)	29.3(7)
C(15)	2429(3)	8904(3)	5057.1(12)	24.2(7)
B(1)	1887(3)	7002(3)	4142.0(13)	16.8(7)
N(7)	356(2)	7382(2)	1971.5(9)	18.2(5)
N(8)	-69(3)	8380(2)	1528.2(9)	18.8(5)
C(16)	856(3)	6054(3)	1732.9(12)	20.6(6)
C(17)	761(3)	6180(3)	1143.9(13)	27.2(7)
C(18)	184(3)	7657(3)	1027.9(12)	25.4(7)
C(19)	1447(3)	4682(3)	2085.6(14)	27.8(7)
C(20)	-131(4)	8427(4)	458.9(13)	40.9(9)
N(9)	-2043(3)	10388(2)	2598.5(10)	20.5(5)
N(10)	-2047(3)	10703(2)	2023.6(10)	20.3(5)
C(21)	-3437(3)	11170(3)	2815.5(13)	23.4(7)
C(22)	-4347(3)	11984(3)	2383.8(13)	26.8(7)
C(23)	-3434(3)	11659(3)	1889.6(13)	24.2(7)
C(24)	-3835(3)	11084(4)	3436.6(13)	33.0(8)
C(25)	-3837(4)	12189(4)	1294.1(13)	35.2(8)
N(11)	1215(3)	9579(2)	2418.6(9)	19.2(5)
N(12)	636(3)	10232(2)	1901.3(10)	19.8(5)
C(26)	2346(3)	9877(3)	2489.6(12)	21.0(6)
C(27)	2506(3)	10696(3)	2029.4(13)	24.4(7)
C(28)	1416(3)	10901(3)	1666.6(12)	22.5(6)
C(29)	3305(3)	9406(3)	2991.3(13)	26.1(7)
C(30)	1089(4)	11697(4)	1106.4(14)	35.2(8)
B(2)	-600(4)	10033(3)	1635.9(14)	21.4(7)

Se(1)	-1941.3(3)	6750.4(4)	2978.42(13)	26.24(8)
C(31)	-2499(3)	6780(3)	2210.2(12)	21.9(6)
C(32)	-3298(3)	8091(3)	1925.0(13)	25.1(7)
C(33)	-3749(3)	8105(3)	1380.4(13)	26.2(7)
C(34)	-3424(3)	6817(3)	1090.4(12)	24.2(7)
C(35)	-2628(3)	5517(3)	1375.6(13)	24.9(7)
C(36)	-2174(3)	5482(3)	1924.9(13)	24.3(7)
C(37)	-4002(4)	6884(4)	494.3(13)	34.8(8)
C(38)	-5670(4)	7609(5)	535.7(17)	64.4(13)
C(39)	-3461(7)	7750(6)	92.4(17)	86.5(19)
C(40)	-3421(5)	5358(5)	230.9(16)	62.6(13)

Table A1.9 Bond lengths (Å) and angles (°) for **2.4**.

Sm(1)-N(9)	2.467(2)	Sm(1)-N(7)	2.484(2)
Sm(1)-N(5)	2.492(2)	Sm(1)-N(3)	2.499(2)
Sm(1)-N(11)	2.594(2)	Sm(1)-N(2)	2.736(2)
Sm(1)-N(1)	2.858(2)	Sm(1)-Se(1)	2.9457(3)
N(1)-C(1)	1.324(4)	N(1)-N(2)	1.397(3)
N(2)-C(3)	1.380(3)	N(2)-B(1)	1.574(4)
C(1)-C(2)	1.407(4)	C(1)-C(4)	1.495(4)
C(2)-C(3)	1.355(4)	C(3)-C(5)	1.494(4)
N(3)-C(6)	1.346(3)	N(3)-N(4)	1.381(3)
N(4)-C(8)	1.352(3)	N(4)-B(1)	1.548(4)
C(6)-C(7)	1.393(4)	C(6)-C(9)	1.490(4)
C(7)-C(8)	1.373(4)	C(8)-C(10)	1.502(4)
N(5)-C(11)	1.343(3)	N(5)-N(6)	1.380(3)
N(6)-C(13)	1.356(3)	N(6)-B(1)	1.536(4)
C(11)-C(12)	1.399(4)	C(11)-C(14)	1.498(4)
C(12)-C(13)	1.370(4)	C(13)-C(15)	1.501(4)
N(7)-C(16)	1.341(3)	N(7)-N(8)	1.379(3)
N(8)-C(18)	1.352(4)	N(8)-B(2)	1.548(4)
C(16)-C(17)	1.388(4)	C(16)-C(19)	1.497(4)
C(17)-C(18)	1.375(4)	C(18)-C(20)	1.505(4)
N(9)-C(21)	1.340(4)	N(9)-N(10)	1.376(3)
N(10)-C(23)	1.347(3)	N(10)-B(2)	1.548(4)
C(21)-C(22)	1.391(4)	C(21)-C(24)	1.497(4)
C(22)-C(23)	1.383(4)	C(23)-C(25)	1.495(4)
N(11)-C(26)	1.341(4)	N(11)-N(12)	1.395(3)
N(12)-C(28)	1.352(4)	N(12)-B(2)	1.536(4)
C(26)-C(27)	1.395(4)	C(26)-C(29)	1.500(4)
C(27)-C(28)	1.377(4)	C(28)-C(30)	1.498(4)
Se(1)-C(31)	1.918(3)	C(31)-C(32)	1.387(4)
C(31)-C(36)	1.396(4)	C(32)-C(33)	1.382(4)
C(33)-C(34)	1.392(4)	C(34)-C(35)	1.380(4)
C(34)-C(37)	1.538(4)	C(35)-C(36)	1.390(4)
C(37)-C(38)	1.504(5)	C(37)-C(39)	1.522(5)
C(37)-C(40)	1.529(5)		
N(9)-Sm(1)-N(7)	81.68(7)	N(9)-Sm(1)-N(5)	93.88(7)
N(7)-Sm(1)-N(5)	147.59(8)	N(9)-Sm(1)-N(3)	150.94(8)
N(7)-Sm(1)-N(3)	88.59(7)	N(5)-Sm(1)-N(3)	79.85(7)
N(9)-Sm(1)-N(11)	73.43(7)	N(7)-Sm(1)-N(11)	72.49(7)
N(5)-Sm(1)-N(11)	75.47(7)	N(3)-Sm(1)-N(11)	77.53(7)
N(9)-Sm(1)-N(2)	136.63(7)	N(7)-Sm(1)-N(2)	133.84(7)
N(5)-Sm(1)-N(2)	68.53(7)	N(3)-Sm(1)-N(2)	67.32(7)
N(11)-Sm(1)-N(2)	132.93(7)	N(9)-Sm(1)-N(1)	107.86(7)
N(7)-Sm(1)-N(1)	147.18(7)	N(5)-Sm(1)-N(1)	64.67(7)
N(3)-Sm(1)-N(1)	95.13(7)	N(11)-Sm(1)-N(1)	140.14(7)
N(2)-Sm(1)-N(1)	28.83(6)	N(9)-Sm(1)-Se(1)	87.77(6)
N(7)-Sm(1)-Se(1)	78.99(5)	N(5)-Sm(1)-Se(1)	133.16(5)
N(3)-Sm(1)-Se(1)	117.26(5)	N(11)-Sm(1)-Se(1)	147.63(5)
N(2)-Sm(1)-Se(1)	78.52(5)	N(1)-Sm(1)-Se(1)	70.32(5)
C(1)-N(1)-N(2)	106.0(2)	C(1)-N(1)-Sm(1)	127.43(18)
N(2)-N(1)-Sm(1)	70.76(13)	C(3)-N(2)-N(1)	108.9(2)
C(3)-N(2)-B(1)	120.5(2)	N(1)-N(2)-B(1)	119.1(2)

C(3)-N(2)-Sm(1)	126.23(17)	N(1)-N(2)-Sm(1)	80.42(13)
B(1)-N(2)-Sm(1)	95.76(15)	N(1)-C(1)-C(2)	110.9(3)
N(1)-C(1)-C(4)	120.8(3)	C(2)-C(1)-C(4)	128.3(3)
C(3)-C(2)-C(1)	106.3(3)	C(2)-C(3)-N(2)	107.8(3)
C(2)-C(3)-C(5)	130.9(3)	N(2)-C(3)-C(5)	121.3(3)
C(6)-N(3)-N(4)	106.1(2)	C(6)-N(3)-Sm(1)	139.24(18)
N(4)-N(3)-Sm(1)	113.83(16)	C(8)-N(4)-N(3)	109.6(2)
C(8)-N(4)-B(1)	130.3(2)	N(3)-N(4)-B(1)	119.5(2)
N(3)-C(6)-C(7)	110.1(2)	N(3)-C(6)-C(9)	122.5(2)
C(7)-C(6)-C(9)	127.3(3)	C(8)-C(7)-C(6)	105.9(3)
N(4)-C(8)-C(7)	108.3(2)	N(4)-C(8)-C(10)	122.6(3)
C(7)-C(8)-C(10)	129.1(3)	C(11)-N(5)-N(6)	106.9(2)
C(11)-N(5)-Sm(1)	139.54(18)	N(6)-N(5)-Sm(1)	113.54(15)
C(13)-N(6)-N(5)	109.3(2)	C(13)-N(6)-B(1)	130.4(2)
N(5)-N(6)-B(1)	120.2(2)	N(5)-C(11)-C(12)	109.3(2)
N(5)-C(11)-C(14)	121.5(2)	C(12)-C(11)-C(14)	129.2(3)
C(13)-C(12)-C(11)	106.5(2)	N(6)-C(13)-C(12)	108.0(2)
N(6)-C(13)-C(15)	123.3(2)	C(12)-C(13)-C(15)	128.6(2)
N(6)-B(1)-N(4)	111.4(2)	N(6)-B(1)-N(2)	108.4(2)
N(4)-B(1)-N(2)	106.4(2)	C(16)-N(7)-N(8)	106.2(2)
C(16)-N(7)-Sm(1)	131.65(18)	N(8)-N(7)-Sm(1)	122.01(16)
C(18)-N(8)-N(7)	109.4(2)	C(18)-N(8)-B(2)	129.3(2)
N(7)-N(8)-B(2)	121.0(2)	N(7)-C(16)-C(17)	110.4(3)
N(7)-C(16)-C(19)	121.5(3)	C(17)-C(16)-C(19)	128.1(3)
C(18)-C(17)-C(16)	105.8(3)	N(8)-C(18)-C(17)	108.2(3)
N(8)-C(18)-C(20)	122.8(3)	C(17)-C(18)-C(20)	128.9(3)
C(21)-N(9)-N(10)	106.9(2)	C(21)-N(9)-Sm(1)	129.01(19)
N(10)-N(9)-Sm(1)	120.80(16)	C(23)-N(10)-N(9)	109.4(2)
C(23)-N(10)-B(2)	129.3(2)	N(9)-N(10)-B(2)	121.3(2)
N(9)-C(21)-C(22)	109.8(3)	N(9)-C(21)-C(24)	121.1(3)
C(22)-C(21)-C(24)	129.1(3)	C(23)-C(22)-C(21)	105.8(3)
N(10)-C(23)-C(22)	108.1(2)	N(10)-C(23)-C(25)	123.2(3)
C(22)-C(23)-C(25)	128.7(3)	C(26)-N(11)-N(12)	105.7(2)
C(26)-N(11)-Sm(1)	135.92(18)	N(12)-N(11)-Sm(1)	118.36(16)
C(28)-N(12)-N(11)	109.9(2)	C(28)-N(12)-B(2)	127.6(2)
N(11)-N(12)-B(2)	122.2(2)	N(11)-C(26)-C(27)	110.3(2)
N(11)-C(26)-C(29)	125.2(3)	C(27)-C(26)-C(29)	124.5(3)
C(28)-C(27)-C(26)	106.3(3)	N(12)-C(28)-C(27)	107.7(2)
N(12)-C(28)-C(30)	123.5(3)	C(27)-C(28)-C(30)	128.8(3)
N(12)-B(2)-N(8)	109.4(2)	N(12)-B(2)-N(10)	111.1(2)
N(8)-B(2)-N(10)	111.0(2)	C(31)-Se(1)-Sm(1)	108.29(9)
C(32)-C(31)-C(36)	117.3(3)	C(32)-C(31)-Se(1)	121.5(2)
C(36)-C(31)-Se(1)	121.2(2)	C(33)-C(32)-C(31)	121.2(3)
C(32)-C(33)-C(34)	122.1(3)	C(35)-C(34)-C(33)	116.5(3)
C(35)-C(34)-C(37)	123.0(3)	C(33)-C(34)-C(37)	120.4(3)
C(34)-C(35)-C(36)	122.2(3)	C(35)-C(36)-C(31)	120.8(3)
C(38)-C(37)-C(39)	110.0(4)	C(38)-C(37)-C(40)	108.9(3)
C(39)-C(37)-C(40)	106.8(4)	C(38)-C(37)-C(34)	109.7(3)
C(39)-C(37)-C(34)	109.4(3)	C(40)-C(37)-C(34)	112.1(3)

Table A1.10 Crystal data, structure solution and refinement for **2.5**.

Chemical formula	$C_{43}H_{57}B_2N_{12}SmTe$
Formula weight	1041.58
Temperature	160(2) K
Radiation and wavelength	MoKα, 0.71073 Å
Crystal system, space group	Monoclinic, $P2_1/c$
Unit cell dimensions	a = 18.7440(10) Å α = 90°
	b = 10.3892(6) Å β = 94.854(2)°
	c = 23.8351(13) Å γ = 90°
Volume	4624.9(4) Å^3
Z	4
Density (calculated)	1.496 g/cm^3
Absorption coefficient μ	1.932 mm^{-1}
F(000)	2092
Reflections for cell refinement	15608 (θ range 2.11 to 28.80°)
Crystal colour	orange
Crystal size	0.23 × 0.20 × 0.15 mm
Data collection method	Siemens SMART CCD diffractometer,
	ω rotation with narrow frames
θ range for data collection	1.71 to 28.82°
Index ranges	$-25 \le h \le 24$, $-13 \le k \le 9$, $-31 \le \ell \le 29$
Intensity decay	0%
Reflections collected	27754
Independent reflections	10922 (R_{int} = 0.0526)
Reflections with I>2σ(I)	7792
Absorption correction	semi-empirical from ψ-scans
Max. and min. transmission	0.647 and 0.537
Structure solution	direct methods
Refinement method	full-matrix least-squares on F^2
Weighting parameters a, b	0.0259, 5.1863
Data / restraints / parameters	10922 / 0 / 546
Final R indices [I>2σ(I)]	R1 = 0.0479, wR2 = 0.0825
R indices (all data)	R1 = 0.0823, wR2 = 0.0932
Goodness-of-fit on F^2	1.062
Extinction coefficient	0.00014(4)
Largest and mean shift/esd	0.011 and 0.000
Largest diff. peak and hole	1.342 and -1.214 eÅ^{-3}

Table A1.11 Atomic coordinates (x 10^4) and equivalent isotropic displacement parameters ($Å^2$ x 10^3) for **2.5**. U(eq) is defined as one third of the trace of the orthogonalised U_{ij} tensor.

	x	y	z	U(eq)
Sm(1)	3126.86(11)	7704.2(2)	4005.68(9)	13.82(7)
N(1)	4087.6(18)	8680(3)	3478.0(15)	17.6(8)
N(2)	4758.6(18)	8123(3)	3556.0(14)	15.7(8)
C(1)	4138(2)	9643(4)	3107.9(18)	20.0(10)
C(2)	4839(2)	9719(4)	2952.6(18)	21.3(10)
C(3)	5212(2)	8745(4)	3234.4(18)	21.1(10)
C(4)	3502(2)	10421(4)	2895(2)	28.0(11)
C(5)	5983(2)	8379(5)	3221(2)	26.4(11)
N(3)	4268.9(18)	8270(3)	4680.3(14)	17.3(8)
N(4)	4765.1(17)	7332(3)	4562.3(14)	15.8(7)
C(6)	4458(2)	8643(4)	5212.4(18)	18.5(9)
C(7)	5037(2)	7932(4)	5440.2(18)	21.9(10)
C(8)	5225(2)	7114(4)	5025.6(18)	20.4(10)
C(9)	4131(2)	9752(4)	5498(2)	25.6(11)
C(10)	5810(2)	6141(5)	5034(2)	27.8(11)
N(5)	3760.9(18)	5730(3)	3675.0(15)	16.9(8)
N(6)	4506.1(18)	5753(3)	3746.9(14)	16.8(8)
C(11)	3593(2)	4608(4)	3411.1(17)	17.9(9)
C(12)	4202(2)	3908(4)	3331.3(19)	22.9(10)
C(13)	4774(2)	4650(4)	3547.1(18)	20.4(10)
C(14)	2838(2)	4264(4)	3197.3(19)	23.9(11)
C(15)	5559(2)	4350(5)	3570(2)	30.6(12)
B(1)	4922(3)	6966(5)	3956(2)	19.6(11)
N(7)	2629.4(18)	7558(3)	2948.0(15)	18.0(8)
N(8)	1917.9(19)	7880(3)	2813.6(15)	19.8(8)
C(16)	2903(2)	7309(4)	2457.7(18)	23.2(10)
C(17)	2375(3)	7456(5)	2009(2)	31.4(12)
C(18)	1764(3)	7814(5)	2247.1(19)	27.0(11)
C(19)	3659(2)	6900(5)	2395.5(19)	26.3(11)
C(20)	1030(3)	8103(6)	1969(2)	46.9(16)
N(9)	2303.5(18)	9527(3)	3834.5(15)	19.5(8)
N(10)	1612.5(19)	9355(3)	3598.0(15)	19.5(8)
C(21)	2336(2)	10720(4)	4049.2(19)	23.0(10)
C(22)	1673(3)	11326(5)	3955(2)	36.8(13)
C(23)	1227(3)	10440(5)	3672(2)	33.4(13)
C(24)	3027(3)	11220(5)	4334(2)	35.1(13)
C(25)	450(3)	10571(6)	3477(3)	53.9(18)
N(11)	1980.1(18)	6472(3)	3955.6(15)	18.1(8)
N(12)	1373.3(19)	6934(3)	3648.8(15)	18.9(8)
C(26)	1787(2)	5365(4)	4190.8(19)	20.8(10)
C(27)	1075(2)	5105(5)	4033.1(19)	24.2(11)
C(28)	824(2)	6113(4)	3698.3(19)	23.9(10)
C(29)	2303(2)	4586(5)	4563(2)	29.2(12)
C(30)	81(3)	6350(5)	3433(2)	38.5(14)
B(2)	1391(3)	8123(5)	3264(2)	22.9(12)

Te(1)	2682.94(18)	7784.0(4)	5266.91(13)	36.80(11)
C(31)	1558(3)	7521(5)	5193(2)	31.7(13)
C(32)	1255(3)	6447(5)	5420(2)	34.4(13)
C(33)	518(3)	6258(6)	5371(2)	40.1(14)
C(34)	80(3)	7146(6)	5096(3)	49.7(16)
C(35)	360(3)	8247(6)	4874(3)	51.8(16)
C(36)	1096(3)	8432(6)	4923(2)	44.3(15)
C(37)	1544(5)	3279(18)	1983(7)	134(5)
C(38)	1763(5)	1935(11)	2113(7)	116(5)
C(39)	2080(7)	1396(14)	1696(7)	128(5)
C(40)	2206(7)	2050(2)	1160(8)	168(7)
C(41)	1990(8)	3282(17)	1078(9)	159(6)
C(42)	1671(7)	3810(16)	1525(6)	126(6)
C(43)	1222(5)	3792(14)	2411(6)	179(7)

Table A1.12 Bond lengths (Å) and angles (°) for **2.5**.

Sm(1)-N(9)	2.455(4)	Sm(1)-N(11)	2.496(3)
Sm(1)-N(1)	2.497(4)	Sm(1)-N(5)	2.530(3)
Sm(1)-N(7)	2.617(3)	Sm(1)-N(3)	2.633(3)
Sm(1)-Te(1)	3.1874(4)	N(1)-C(1)	1.342(5)
N(1)-N(2)	1.383(5)	N(2)-C(3)	1.356(5)
N(2)-B(1)	1.548(6)	C(1)-C(2)	1.397(6)
C(1)-C(4)	1.494(6)	C(2)-C(3)	1.372(6)
C(3)-C(5)	1.497(6)	N(3)-C(6)	1.345(5)
N(3)-N(4)	1.393(5)	N(4)-C(8)	1.361(5)
N(4)-B(1)	1.546(6)	C(6)-C(7)	1.386(6)
C(6)-C(9)	1.496(6)	C(7)-C(8)	1.372(6)
C(8)-C(10)	1.490(6)	N(5)-C(11)	1.349(5)
N(5)-N(6)	1.393(5)	N(6)-C(13)	1.354(5)
N(6)-B(1)	1.542(6)	C(11)-C(12)	1.381(6)
C(11)-C(14)	1.506(6)	C(12)-C(13)	1.383(6)
C(13)-C(15)	1.501(6)	N(7)-C(16)	1.341(5)
N(7)-N(8)	1.386(5)	N(8)-C(18)	1.358(5)
N(8)-B(2)	1.539(6)	C(16)-C(17)	1.403(6)
C(16)-C(19)	1.499(6)	C(17)-C(18)	1.372(7)
C(18)-C(20)	1.505(6)	N(9)-C(21)	1.341(5)
N(9)-N(10)	1.380(5)	N(10)-C(23)	1.358(6)
N(10)-B(2)	1.546(6)	C(21)-C(22)	1.394(6)
C(21)-C(24)	1.502(6)	C(22)-C(23)	1.381(7)
C(23)-C(25)	1.497(7)	N(11)-C(26)	1.342(5)
N(11)-N(12)	1.385(5)	N(12)-C(28)	1.350(5)
N(12)-B(2)	1.541(6)	C(26)-C(27)	1.382(6)
C(26)-C(29)	1.494(6)	C(27)-C(28)	1.376(6)
C(28)-C(30)	1.501(6)	Te(1)-C(31)	2.119(5)
C(31)-C(32)	1.383(7)	C(31)-C(36)	1.401(7)
C(32)-C(33)	1.389(7)	C(33)-C(34)	1.365(8)
C(34)-C(35)	1.382(8)	C(35)-C(36)	1.388(8)
C(37)-C(42)	1.261(17)	C(37)-C(43)	1.341(14)
C(37)-C(38)	1.481(19)	C(38)-C(39)	1.324(16)
C(39)-C(40)	1.485(19)	C(40)-C(41)	1.35(2)
C(41)-C(42)	1.380(18)		

N(9)-Sm(1)-N(11)	82.01(12)	N(9)-Sm(1)-N(1)	94.19(12)
N(11)-Sm(1)-N(1)	147.03(11)	N(9)-Sm(1)-N(5)	151.51(12)
N(11)-Sm(1)-N(5)	89.69(11)	N(1)-Sm(1)-N(5)	78.14(11)
N(9)-Sm(1)-N(7)	73.55(11)	N(11)-Sm(1)-N(7)	71.89(11)
N(1)-Sm(1)-N(7)	75.62(11)	N(5)-Sm(1)-N(7)	77.96(11)
N(9)-Sm(1)-N(3)	113.35(11)	N(11)-Sm(1)-N(3)	142.77(11)
N(1)-Sm(1)-N(3)	68.48(11)	N(5)-Sm(1)-N(3)	89.56(11)
N(7)-Sm(1)-N(3)	143.72(11)	N(9)-Sm(1)-Te(1)	85.76(9)
N(11)-Sm(1)-Te(1)	76.47(8)	N(1)-Sm(1)-Te(1)	136.16(8)
N(5)-Sm(1)-Te(1)	118.82(8)	N(7)-Sm(1)-Te(1)	144.08(8)
N(3)-Sm(1)-Te(1)	71.45(8)	C(1)-N(1)-N(2)	106.6(3)
C(1)-N(1)-Sm(1)	136.7(3)	N(2)-N(1)-Sm(1)	116.7(2)
C(3)-N(2)-N(1)	109.3(3)	C(3)-N(2)-B(1)	128.1(4)
N(1)-N(2)-B(1)	122.5(3)	N(1)-C(1)-C(2)	109.7(4)
N(1)-C(1)-C(4)	121.8(4)	C(2)-C(1)-C(4)	128.4(4)
C(3)-C(2)-C(1)	106.3(4)	N(2)-C(3)-C(2)	108.1(4)

N(2)-C(3)-C(5)	122.9(4)	C(2)-C(3)-C(5)	129.0(4)
C(6)-N(3)-N(4)	105.4(3)	C(6)-N(3)-Sm(1)	140.9(3)
N(4)-N(3)-Sm(1)	104.0(2)	C(8)-N(4)-N(3)	109.9(3)
C(8)-N(4)-B(1)	124.0(4)	N(3)-N(4)-B(1)	122.9(3)
N(3)-C(6)-C(7)	110.6(4)	N(3)-C(6)-C(9)	124.5(4)
C(7)-C(6)-C(9)	124.8(4)	C(8)-C(7)-C(6)	106.8(4)
N(4)-C(8)-C(7)	107.3(4)	N(4)-C(8)-C(10)	122.6(4)
C(7)-C(8)-C(10)	130.1(4)	C(11)-N(5)-N(6)	105.4(3)
C(11)-N(5)-Sm(1)	138.4(3)	N(6)-N(5)-Sm(1)	116.1(2)
C(13)-N(6)-N(5)	109.8(3)	C(13)-N(6)-B(1)	127.9(4)
N(5)-N(6)-B(1)	121.9(3)	N(5)-C(11)-C(12)	110.8(4)
N(5)-C(11)-C(14)	122.6(4)	C(12)-C(11)-C(14)	126.4(4)
C(11)-C(12)-C(13)	106.2(4)	N(6)-C(13)-C(12)	107.7(4)
N(6)-C(13)-C(15)	123.6(4)	C(12)-C(13)-C(15)	128.6(4)
N(6)-B(1)-N(4)	111.8(4)	N(6)-B(1)-N(2)	111.5(4)
N(4)-B(1)-N(2)	110.0(4)	C(16)-N(7)-N(8)	106.1(3)
C(16)-N(7)-Sm(1)	136.0(3)	N(8)-N(7)-Sm(1)	117.8(2)
C(18)-N(8)-N(7)	109.7(4)	C(18)-N(8)-B(2)	127.3(4)
N(7)-N(8)-B(2)	122.7(3)	N(7)-C(16)-C(17)	110.2(4)
N(7)-C(16)-C(19)	125.2(4)	C(17)-C(16)-C(19)	124.6(4)
C(18)-C(17)-C(16)	105.9(4)	N(8)-C(18)-C(17)	108.1(4)
N(8)-C(18)-C(20)	122.5(5)	C(17)-C(18)-C(20)	129.4(4)
C(21)-N(9)-N(10)	106.7(3)	C(21)-N(9)-Sm(1)	129.9(3)
N(10)-N(9)-Sm(1)	121.6(3)	C(23)-N(10)-N(9)	109.3(4)
C(23)-N(10)-B(2)	129.2(4)	N(9)-N(10)-B(2)	121.3(4)
N(9)-C(21)-C(22)	110.2(4)	N(9)-C(21)-C(24)	120.1(4)
C(22)-C(21)-C(24)	129.7(4)	C(23)-C(22)-C(21)	105.8(4)
N(10)-C(23)-C(22)	108.1(4)	N(10)-C(23)-C(25)	123.3(5)
C(22)-C(23)-C(25)	128.6(5)	C(26)-N(11)-N(12)	106.2(3)
C(26)-N(11)-Sm(1)	132.9(3)	N(12)-N(11)-Sm(1)	120.8(3)
C(28)-N(12)-N(11)	109.4(4)	C(28)-N(12)-B(2)	127.9(4)
N(11)-N(12)-B(2)	122.3(3)	N(11)-C(26)-C(27)	110.0(4)
N(11)-C(26)-C(29)	121.9(4)	C(27)-C(26)-C(29)	128.1(4)
C(28)-C(27)-C(26)	106.5(4)	N(12)-C(28)-C(27)	107.8(4)
N(12)-C(28)-C(30)	123.1(4)	C(27)-C(28)-C(30)	129.1(4)
N(8)-B(2)-N(12)	109.4(4)	N(8)-B(2)-N(10)	109.6(4)
N(12)-B(2)-N(10)	112.0(4)	C(31)-Te(1)-Sm(1)	104.83(13)
C(32)-C(31)-C(36)	117.8(5)	C(32)-C(31)-Te(1)	120.7(4)
C(36)-C(31)-Te(1)	121.5(4)	C(31)-C(32)-C(33)	121.3(5)
C(34)-C(33)-C(32)	119.9(5)	C(33)-C(34)-C(35)	120.7(6)
C(34)-C(35)-C(36)	119.3(6)	C(35)-C(36)-C(31)	121.0(5)
C(42)-C(37)-C(43)	128(2)	C(42)-C(37)-C(38)	121.6(14)
C(43)-C(37)-C(38)	110.4(19)	C(39)-C(38)-C(37)	112.0(15)
C(38)-C(39)-C(40)	124.5(17)	C(41)-C(40)-C(39)	119.4(17)
C(40)-C(41)-C(42)	114(2)	C(37)-C(42)-C(41)	128.3(19)

Table A1.13 Crystal data, structure solution and refinement for **2.6**.

Empirical formula	C35 H54 B2 N13 S2 Sm
Formula weight	893.00
Temperature	293(2) K
Wavelength	0.71073 A
Crystal system	$P\bar{1}$.
Space group	triclinic
Unit cell dimensions	a = 11.459(2) A alpha = 84.19(3) deg. b = 12.787(3) A beta = 82.14(3) deg. c = 15.062(3) A gamma = 71.92(3) deg.
Volume	2074.2(7) A^3
Z	2
Density (calculated)	1.430 Mg/m^3
Absorption coefficient	1.559 mm^-1
F(000)	918
Crystal size	? x ? x ? mm
Theta range for data collection	1.88 to 24.98 deg.
Index ranges	-12<=h<=13, -14<=k<=14, 0<=l<=16
Reflections collected	5663
Independent reflections	5663 [R(int) = 0.0000]
Refinement method	Full-matrix least-squares on F^2
Data / restraints / parameters	5645 / 0 / 478
Goodness-of-fit on F^2	1.014
Final R indices [I>2sigma(I)]	R1 = 0.0451, wR2 = 0.1181
R indices (all data)	R1 = 0.0514, wR2 = 0.1381
Largest diff. peak and hole	1.360 and -0.868 e.A^-3

Table A1.14 Atomic coordinates (x 10^4) and equivalent isotropic displacement parameters ($Å^2$ x 10^3) for **2.6**. U(eq) is defined as one third of the trace of the orthogonalised U_{ij} tensor.

	x	y	z	U(eq)
Sm(1)	1257(1)	1897(1)	2552(1)	14(1)
B(1)	2525(7)	-292(6)	1016(5)	17(2)
B(2)	2032(7)	2645(6)	4610(5)	17(2)
N(11)	1501(5)	1788(4)	737(3)	17(1)
N(12)	1761(5)	735(4)	483(3)	14(1)
N(21)	1037(5)	24(4)	2460(3)	17(1)
N(22)	1684(5)	-665(4)	1796(3)	18(1)
N(31)	3486(5)	781(4)	1896(3)	17(1)
N(32)	3616(5)	-56(4)	1341(3)	15(1)
N(41)	2517(5)	806(5)	3894(3)	19(1)
N(42)	2587(5)	1425(5)	4591(3)	17(1)
N(51)	-23(5)	2580(5)	4159(3)	18(1)
N(52)	632(5)	2975(4)	4698(3)	16(1)
N(61)	2293(5)	3232(5)	2944(3)	18(1)
N(62)	2582(5)	3268(5)	3794(3)	18(1)
C(11)	530(8)	3680(6)	27(5)	38(2)
C(12)	995(7)	2440(6)	41(4)	25(2)
C(13)	945(7)	1830(6)	-641(4)	21(2)
C(14)	1446(6)	727(6)	-353(4)	18(2)
C(15)	1533(7)	-272(6)	-805(4)	26(2)
C(21)	-398(7)	-88(6)	3840(4)	32(2)
C(22)	406(6)	-562(5)	3021(4)	18(2)
C(23)	665(7)	-1601(6)	2726(4)	23(2)
C(24)	1481(7)	-1657(6)	1957(4)	22(2)
C(25)	2071(8)	-2613(6)	1387(5)	38(2)
C(31)	4934(7)	1458(6)	2631(5)	25(2)
C(32)	4650(7)	697(6)	2059(4)	22(2)
C(33)	5515(7)	-186(6)	1621(4)	23(2)
C(34)	4837(6)	-644(5)	1167(4)	19(2)
C(35)	5308(7)	-1602(6)	578(4)	29(2)
C(41)	3335(7)	-1179(6)	3536(4)	23(2)
C(42)	3114(6)	-244(5)	4113(4)	18(2)
C(43)	3575(7)	-326(6)	4950(4)	20(2)
C(44)	3213(6)	717(6)	5232(4)	19(2)
C(45)	3392(8)	1124(7)	6096(5)	33(2)
C(51)	-2251(7)	2671(7)	4194(5)	32(2)
C(52)	-1204(6)	2887(6)	4538(4)	19(2)
C(53)	-1319(7)	3462(6)	5300(4)	24(2)
C(54)	-150(7)	3510(5)	5388(4)	18(2)
C(55)	204(7)	4059(6)	6081(4)	27(2)
C(61)	2720(8)	4080(7)	1424(4)	34(2)
C(62)	2795(7)	3949(6)	2415(4)	22(2)
C(63)	3391(7)	4430(6)	2928(5)	28(2)
C(64)	3246(7)	3960(6)	3798(5)	24(2)
C(65)	3767(8)	4141(7)	4611(5)	34(2)
S(1)	-312(2)	4137(1)	2293(1)	22(1)
S(2)	-1145(2)	2259(2)	1995(1)	25(1)
N(1)	-2564(5)	4353(5)	1869(3)	24(1)
C(1)	-1443(7)	3647(6)	2032(4)	21(2)
C(2)	-2831(8)	5537(7)	1855(5)	40(2)
C(3)	-3430(10)	5996(9)	2764(7)	68(3)
C(4)	-3545(7)	3932(8)	1684(5)	40(2)
C(5)	-3520(10)	3781(11)	707(6)	77(4)

Table A1.15 Bond lengths (Å) and angles (°) for **2.6**.

Sm(1)-N(21)	2.503(5)
Sm(1)-N(61)	2.516(6)
Sm(1)-N(31)	2.621(6)
Sm(1)-N(41)	2.665(5)
Sm(1)-N(11)	2.722(5)
Sm(1)-N(51)	2.728(5)
Sm(1)-S(2)	2.873(2)
Sm(1)-S(1)	2.891(2)
B(1)-N(32)	1.524(10)
B(1)-N(22)	1.549(8)
B(1)-N(12)	1.550(9)
B(2)-N(42)	1.492(10)
B(2)-N(52)	1.517(10)
B(2)-N(62)	1.564(9)
N(11)-C(12)	1.349(8)
N(11)-N(12)	1.368(7)
N(12)-C(14)	1.358(8)
N(21)-C(22)	1.356(8)
N(21)-N(22)	1.377(7)
N(22)-C(24)	1.352(8)
N(31)-C(32)	1.359(9)
N(31)-N(32)	1.384(7)
N(32)-C(34)	1.371(8)
N(41)-C(42)	1.334(8)
N(41)-N(42)	1.401(7)
N(42)-C(44)	1.369(8)
N(51)-C(52)	1.347(9)
N(51)-N(52)	1.401(7)
N(52)-C(54)	1.363(8)
N(61)-C(62)	1.364(8)
N(61)-N(62)	1.373(7)
N(62)-C(64)	1.335(9)
C(11)-C(12)	1.506(10)
C(12)-C(13)	1.368(10)
C(13)-C(14)	1.396(9)
C(14)-C(15)	1.477(9)
C(21)-C(22)	1.494(9)
C(22)-C(23)	1.374(10)
C(23)-C(24)	1.378(10)
C(24)-C(25)	1.493(10)
C(31)-C(32)	1.497(10)
C(32)-C(33)	1.403(10)
C(33)-C(34)	1.386(10)
C(34)-C(35)	1.503(10)
C(41)-C(42)	1.487(9)
C(42)-C(43)	1.415(10)
C(43)-C(44)	1.362(10)
C(44)-C(45)	1.510(10)
C(51)-C(52)	1.480(10)
C(52)-C(53)	1.395(9)
C(53)-C(54)	1.385(10)
C(54)-C(55)	1.479(9)
C(61)-C(62)	1.497(10)
C(62)-C(63)	1.394(10)
C(63)-C(64)	1.396(10)
C(64)-C(65)	1.501(10)
S(1)-C(1)	1.710(7)
S(2)-C(1)	1.704(7)
N(1)-C(1)	1.359(9)
N(1)-C(2)	1.448(10)

N(1)-C(4)	1.457(10)
C(2)-C(3)	1.531(11)
C(4)-C(5)	1.499(12)

N(21)-Sm(1)-N(61)	154.7(2)
N(21)-Sm(1)-N(31)	78.0(2)
N(61)-Sm(1)-N(31)	84.5(2)
N(21)-Sm(1)-N(41)	79.9(2)
N(61)-Sm(1)-N(41)	77.2(2)
N(31)-Sm(1)-N(41)	70.8(2)
N(21)-Sm(1)-N(11)	79.9(2)
N(61)-Sm(1)-N(11)	109.9(2)
N(31)-Sm(1)-N(11)	66.9(2)
N(41)-Sm(1)-N(11)	136.0(2)
N(21)-Sm(1)-N(51)	104.3(2)
N(61)-Sm(1)-N(51)	77.6(2)
N(31)-Sm(1)-N(51)	139.5(2)
N(41)-Sm(1)-N(51)	69.9(2)
N(11)-Sm(1)-N(51)	153.5(2)
N(21)-Sm(1)-S(2)	73.97(13)
N(61)-Sm(1)-S(2)	130.93(13)
N(31)-Sm(1)-S(2)	132.90(13)
N(41)-Sm(1)-S(2)	137.35(12)
N(11)-Sm(1)-S(2)	71.39(13)
N(51)-Sm(1)-S(2)	84.52(13)
N(21)-Sm(1)-S(1)	135.24(13)
N(61)-Sm(1)-S(1)	69.68(13)
N(31)-Sm(1)-S(1)	134.92(12)
N(41)-Sm(1)-S(1)	132.98(13)
N(11)-Sm(1)-S(1)	87.39(12)
N(51)-Sm(1)-S(1)	71.11(12)
S(2)-Sm(1)-S(1)	61.31(6)
N(32)-B(1)-N(22)	112.4(5)
N(32)-B(1)-N(12)	110.3(5)
N(22)-B(1)-N(12)	110.2(6)
N(42)-B(2)-N(52)	111.4(6)
N(42)-B(2)-N(62)	111.9(6)
N(52)-B(2)-N(62)	112.6(6)
C(12)-N(11)-N(12)	104.9(5)
C(12)-N(11)-Sm(1)	136.0(4)
N(12)-N(11)-Sm(1)	112.8(3)
C(14)-N(12)-N(11)	111.4(5)
C(14)-N(12)-B(1)	124.5(5)
N(11)-N(12)-B(1)	123.2(5)
C(22)-N(21)-N(22)	105.8(5)
C(22)-N(21)-Sm(1)	131.5(4)
N(22)-N(21)-Sm(1)	122.5(4)
C(24)-N(22)-N(21)	110.0(5)
C(24)-N(22)-B(1)	128.2(6)
N(21)-N(22)-B(1)	121.7(5)
C(32)-N(31)-N(32)	105.5(5)
C(32)-N(31)-Sm(1)	135.2(4)
N(32)-N(31)-Sm(1)	118.5(4)
C(34)-N(32)-N(31)	110.3(6)
C(34)-N(32)-B(1)	126.3(6)
N(31)-N(32)-B(1)	123.3(5)
C(42)-N(41)-N(42)	106.9(5)
C(42)-N(41)-Sm(1)	136.1(4)
N(42)-N(41)-Sm(1)	117.0(4)
C(44)-N(42)-N(41)	108.3(5)
C(44)-N(42)-B(2)	127.5(6)
N(41)-N(42)-B(2)	124.2(5)
C(52)-N(51)-N(52)	105.6(5)
C(52)-N(51)-Sm(1)	138.3(4)

N(52)-N(51)-Sm(1)	114.1(4)
C(54)-N(52)-N(51)	109.9(5)
C(54)-N(52)-B(2)	126.0(6)
N(51)-N(52)-B(2)	123.0(5)
C(62)-N(61)-N(62)	105.7(5)
C(62)-N(61)-Sm(1)	131.0(4)
N(62)-N(61)-Sm(1)	122.9(4)
C(64)-N(62)-N(61)	110.8(5)
C(64)-N(62)-B(2)	128.5(6)
N(61)-N(62)-B(2)	120.4(5)
N(11)-C(12)-C(13)	111.3(6)
N(11)-C(12)-C(11)	124.1(6)
C(13)-C(12)-C(11)	124.7(6)
C(12)-C(13)-C(14)	106.4(6)
N(12)-C(14)-C(13)	106.0(6)
N(12)-C(14)-C(15)	125.2(6)
C(13)-C(14)-C(15)	128.6(6)
N(21)-C(22)-C(23)	109.9(6)
N(21)-C(22)-C(21)	121.6(6)
C(23)-C(22)-C(21)	128.5(6)
C(22)-C(23)-C(24)	106.8(6)
N(22)-C(24)-C(23)	107.4(6)
N(22)-C(24)-C(25)	124.3(6)
C(23)-C(24)-C(25)	128.4(7)
N(31)-C(32)-C(33)	110.7(6)
N(31)-C(32)-C(31)	123.2(6)
C(33)-C(32)-C(31)	126.1(7)
C(34)-C(33)-C(32)	105.8(6)
N(32)-C(34)-C(33)	107.7(6)
N(32)-C(34)-C(35)	124.3(7)
C(33)-C(34)-C(35)	128.0(7)
N(41)-C(42)-C(43)	109.9(6)
N(41)-C(42)-C(41)	125.1(6)
C(43)-C(42)-C(41)	124.9(6)
C(44)-C(43)-C(42)	106.1(6)
C(43)-C(44)-N(42)	108.9(6)
C(43)-C(44)-C(45)	129.7(6)
N(42)-C(44)-C(45)	121.4(6)
N(51)-C(52)-C(53)	110.6(6)
N(51)-C(52)-C(51)	125.5(6)
C(53)-C(52)-C(51)	123.9(6)
C(54)-C(53)-C(52)	106.5(6)
N(52)-C(54)-C(53)	107.4(6)
N(52)-C(54)-C(55)	125.4(7)
C(53)-C(54)-C(55)	127.2(6)
N(61)-C(62)-C(63)	110.1(6)
N(61)-C(62)-C(61)	120.6(6)
C(63)-C(62)-C(61)	129.2(6)
C(62)-C(63)-C(64)	105.2(6)
N(62)-C(64)-C(63)	108.2(6)
N(62)-C(64)-C(65)	124.1(6)
C(63)-C(64)-C(65)	127.6(7)
C(1)-S(1)-Sm(1)	89.5(2)
C(1)-S(2)-Sm(1)	90.2(3)
C(1)-N(1)-C(2)	122.3(7)
C(1)-N(1)-C(4)	120.3(6)
C(2)-N(1)-C(4)	117.4(6)
N(1)-C(1)-S(2)	120.8(6)
N(1)-C(1)-S(1)	120.3(6)
S(2)-C(1)-S(1)	118.8(4)
N(1)-C(2)-C(3)	112.4(7)
N(1)-C(4)-C(5)	113.0(7)

Table A1.16 Crystal data, structure solution and refinement for **3.1**.

Chemical formula	$C_{82}H_{130}B_2Mo_2N_{12}O_{10}Sm_2$
Formula weight	1958.18
Temperature	160(2) K
Radiation and wavelength	MoKα, 0.71073 Å
Crystal system, space group	triclinic, $P\bar{1}$
Unit cell dimensions	a = 13.6825(5) Å α = 63.455(2)°
	b = 13.7204(5) Å β = 67.914(2)°
	c = 15.1643(6) Å γ = 88.812(2)°
Volume	2322.26(15) Å^3
Z	1
Density (calculated)	1.400 g/cm^3
Absorption coefficient μ	1.567 mm^{-1}
F(000)	1004
Reflections for cell refinement	13261 (θ range 1.64 to 28.32°)
Crystal colour	dark blue
Crystal size	0.65 x 0.46 x 0.44 mm
Data collection method	Siemens SMART CCD diffractometer,
	ω rotation with narrow frames
θ range for data collection	1.71 to 28.43°
Index ranges	$-17 \le h \le 17$, $-18 \le k \le 17$, $-16 \le \ell \le 19$
Intensity decay	0%
Reflections collected	17258
Independent reflections	10241 (R_{int} = 0.0201)
Reflections with I>2σ(I)	9234
Absorption correction	semi-empirical from ψ-scans
Max. and min. transmission	0.604 and 0.491
Structure solution	Patterson synthesis
Refinement method	full-matrix least-squares on F^2
Weighting parameters a, b	0.0261, 1.1740
Data / restraints / parameters	10241 / 0 / 512
Final R indices [I>2σ(I)]	R1 = 0.0252, wR2 = 0.0613
R indices (all data)	R1 = 0.0305, wR2 = 0.0641
Goodness-of-fit on F^2	1.046
Extinction coefficient	0.00045(16)
Largest and mean shift/esd	0.004 and 0.000
Largest diff. peak and hole	1.233 and -0.902 eÅ^{-3}

Table A1.17 Atomic coordinates (x 10^4) and equivalent isotropic displacement parameters ($Å^2$ x 10^3) for **3.1**. U(eq) is defined as one third of the trace of the orthogonalised U_{ij} tensor.

	x	y	z	U(eq)
Mo(1)	6123.15(16)	13237.73(16)	-956.08(17)	24.05(6)
C(1)	4872(2)	12183(2)	145(2)	27.5(5)
O(1)	4099.2(15)	11481.2(15)	793.6(15)	36.2(4)
C(2)	6835(2)	12612(2)	27(3)	38.7(6)
O(2)	7256(2)	12252(2)	614(2)	64.8(7)
C(3)	6399(2)	12067(2)	-1309(2)	27.6(5)
O(3)	6510.3(17)	11331.4(16)	-1521.6(16)	40.9(5)
C(4)	6606(2)	14661(2)	-2764(2)	36.7(6)
C(5)	5538(2)	14665(2)	-2154(2)	37.8(6)
C(6)	5520(3)	14969(2)	-1377(2)	43.6(7)
C(7)	6563(3)	15146(2)	-1495(3)	43.3(7)
C(8)	7244(2)	14964(2)	-2346(2)	37.9(6)
C(9)	6988(4)	14466(3)	-3721(3)	64.2(11)
Sm(1)	3361.00(9)	9731.87(9)	2585.72(9)	19.91(5)
N(1)	1712.6(16)	8125.0(16)	3942.5(17)	25.6(4)
N(2)	1781.6(16)	7377.8(16)	4886.8(17)	25.3(4)
C(10)	843(2)	7705(2)	3929(2)	32.7(6)
C(11)	353(2)	6695(2)	4865(3)	42.4(7)
C(12)	959(2)	6506(2)	5450(2)	37.2(6)
C(13)	458(2)	8256(3)	3035(3)	41.3(7)
C(14)	1140(3)	9363(3)	2134(3)	52.8(8)
C(15)	461(3)	7484(3)	2553(3)	68.0(11)
C(16)	-690(3)	8434(4)	3528(4)	75.3(13)
C(17)	783(3)	5553(2)	6522(3)	52.2(9)
N(3)	4366.0(15)	8204.9(15)	3453.1(16)	23.7(4)
N(4)	3788.6(16)	7431.5(15)	4519.3(16)	23.5(4)
C(18)	5332(2)	7925(2)	3141(2)	27.5(5)
C(19)	5375(2)	6965(2)	4003(2)	33.8(6)
C(20)	4400(2)	6674(2)	4850(2)	29.6(5)
C(21)	6220.3(19)	8590(2)	2030(2)	30.8(6)
C(22)	7189(3)	8978(3)	2143(3)	58.9(10)
C(23)	5891(2)	9608(2)	1311(2)	42.8(7)
C(24)	6550(2)	7855(3)	1486(3)	43.4(7)
C(25)	4020(3)	5714(2)	5965(2)	41.6(7)
N(5)	3273.1(15)	9632.6(15)	4359.3(16)	22.1(4)
N(6)	2737.9(15)	8636.4(15)	5271.9(16)	21.2(4)
C(26)	3320.2(18)	10363.1(18)	4708.8(19)	21.8(5)
C(27)	2792(2)	9857(2)	5832(2)	27.5(5)
C(28)	2451.0(19)	8767(2)	6165(2)	25.5(5)
C(29)	3977.9(19)	11522.9(19)	3955(2)	25.9(5)
C(30)	4404(3)	11791(2)	2779(2)	41.6(7)
C(31)	3315(2)	12377(2)	4123(3)	42.0(7)
C(32)	4929(2)	11575(2)	4247(3)	46.0(8)
C(33)	1924(2)	7842(2)	7294(2)	38.0(6)
B(1)	2677(2)	7532(2)	5232(2)	24.4(5)
O(4)	2016.6(14)	11078.6(14)	2800.4(15)	32.0(4)

C(34)	1120(2)	10791(2)	3814(2)	35.2(6)
C(35)	357(3)	11554(3)	3544(3)	61.3(10)
C(36)	1062(3)	12560(3)	2541(3)	56.6(9)
C(37)	1952(2)	12117(2)	1963(3)	44.7(7)
O(5)	1077(2)	13401(2)	-222(2)	76.6(8)
C(38)	273(4)	13029(4)	-420(4)	98.8(17)
C(39)	0(4)	11808(4)	188(4)	82.7(13)
C(40)	1502(5)	14500(4)	-850(4)	99.6(17)
C(41)	2345(5)	14832(5)	-590(5)	116(2)

Table A1.18 Bond lengths (Å) and angles (°) for **3.1**.

Mo(1)-C(3)	1.897(3)	Mo(1)-C(1)	1.899(3)
Mo(1)-C(2)	1.955(3)	Mo(1)-C(5)	2.372(3)
Mo(1)-C(8)	2.379(3)	Mo(1)-C(7)	2.381(3)
Mo(1)-C(4)	2.382(3)	Mo(1)-C(6)	2.386(3)
C(1)-O(1)	1.194(3)	O(1)-Sm(1)	2.5244(18)
C(2)-O(2)	1.160(3)	C(3)-O(3)	1.181(3)
O(3)-Sm(1a)	2.5773(18)	C(4)-C(5)	1.407(4)
C(4)-C(8)	1.416(4)	C(4)-C(9)	1.490(4)
C(5)-C(6)	1.407(4)	C(6)-C(7)	1.382(5)
C(7)-C(8)	1.404(4)	Sm(1)-O(3a)	2.5773(18)
Sm(1)-N(5)	2.588(2)	Sm(1)-N(3)	2.6054(19)
Sm(1)-N(1)	2.616(2)	Sm(1)-O(4)	2.6173(17)
N(1)-C(10)	1.344(3)	N(1)-N(2)	1.377(3)
N(2)-C(12)	1.359(3)	N(2)-B(1)	1.553(3)
C(10)-C(11)	1.396(4)	C(10)-C(13)	1.513(4)
C(11)-C(12)	1.370(4)	C(12)-C(17)	1.494(4)
C(13)-C(14)	1.513(5)	C(13)-C(15)	1.532(4)
C(13)-C(16)	1.533(4)	N(3)-C(18)	1.338(3)
N(3)-N(4)	1.380(3)	N(4)-C(20)	1.358(3)
N(4)-B(1)	1.545(3)	C(18)-C(19)	1.401(4)
C(18)-C(21)	1.509(4)	C(19)-C(20)	1.366(4)
C(20)-C(25)	1.497(4)	C(21)-C(23)	1.525(4)
C(21)-C(24)	1.532(4)	C(21)-C(22)	1.532(4)
N(5)-C(26)	1.339(3)	N(5)-N(6)	1.381(3)
N(6)-C(28)	1.355(3)	N(6)-B(1)	1.549(3)
C(26)-C(27)	1.395(3)	C(26)-C(29)	1.519(3)
C(27)-C(28)	1.373(3)	C(28)-C(33)	1.493(4)
C(29)-C(30)	1.516(4)	C(29)-C(31)	1.520(3)
C(29)-C(32)	1.536(3)	O(4)-C(34)	1.443(3)
O(4)-C(37)	1.453(3)	C(34)-C(35)	1.499(4)
C(35)-C(36)	1.491(5)	C(36)-C(37)	1.505(4)
O(5)-C(40)	1.362(5)	O(5)-C(38)	1.404(5)
C(38)-C(39)	1.477(6)	C(40)-C(41)	1.490(6)
C(3)-Mo(1)-C(1)	81.06(10)	C(3)-Mo(1)-C(2)	89.09(11)
C(1)-Mo(1)-C(2)	88.29(11)	C(3)-Mo(1)-C(5)	112.11(11)
C(1)-Mo(1)-C(5)	105.97(10)	C(2)-Mo(1)-C(5)	155.74(10)
C(3)-Mo(1)-C(8)	113.36(10)	C(1)-Mo(1)-C(8)	160.23(10)
C(2)-Mo(1)-C(8)	104.77(11)	C(5)-Mo(1)-C(8)	56.89(10)
C(3)-Mo(1)-C(7)	147.67(11)	C(1)-Mo(1)-C(7)	130.05(11)
C(2)-Mo(1)-C(7)	99.16(11)	C(5)-Mo(1)-C(7)	56.63(10)
C(8)-Mo(1)-C(7)	34.31(10)	C(3)-Mo(1)-C(4)	95.65(10)
C(1)-Mo(1)-C(4)	135.26(11)	C(2)-Mo(1)-C(4)	136.42(11)
C(5)-Mo(1)-C(4)	34.43(10)	C(8)-Mo(1)-C(4)	34.60(10)
C(7)-Mo(1)-C(4)	57.29(10)	C(3)-Mo(1)-C(6)	146.47(11)
C(1)-Mo(1)-C(6)	103.70(11)	C(2)-Mo(1)-C(6)	123.89(11)
C(5)-Mo(1)-C(6)	34.40(11)	C(8)-Mo(1)-C(6)	56.73(10)
C(7)-Mo(1)-C(6)	33.71(11)	C(4)-Mo(1)-C(6)	57.34(10)
O(1)-C(1)-Mo(1)	175.3(2)	C(1)-O(1)-Sm(1)	144.27(17)
O(2)-C(2)-Mo(1)	179.1(3)	O(3)-C(3)-Mo(1)	176.2(2)
C(3)-O(3)-Sm(1a)	158.71(19)	C(5)-C(4)-C(8)	106.6(3)
C(5)-C(4)-C(9)	126.1(3)	C(8)-C(4)-C(9)	127.1(3)
C(5)-C(4)-Mo(1)	72.39(15)	C(8)-C(4)-Mo(1)	72.60(15)

C(9)-C(4)-Mo(1)	124.0(2)	C(6)-C(5)-C(4)	108.8(3)
C(6)-C(5)-Mo(1)	73.34(16)	C(4)-C(5)-Mo(1)	73.18(15)
C(7)-C(6)-C(5)	107.9(3)	C(7)-C(6)-Mo(1)	72.96(16)
C(5)-C(6)-Mo(1)	72.26(15)	C(6)-C(7)-C(8)	108.7(3)
C(6)-C(7)-Mo(1)	73.33(16)	C(8)-C(7)-Mo(1)	72.78(15)
C(7)-C(8)-C(4)	108.1(3)	C(7)-C(8)-Mo(1)	72.91(15)
C(4)-C(8)-Mo(1)	72.80(15)	O(1)-Sm(1)-O(3a)	87.46(6)
O(1)-Sm(1)-N(5)	123.14(6)	O(3a)-Sm(1)-N(5)	146.53(6)
O(1)-Sm(1)-N(3)	129.01(6)	O(3a)-Sm(1)-N(3)	81.15(6)
N(5)-Sm(1)-N(3)	69.22(6)	O(1)-Sm(1)-N(1)	144.10(6)
O(3a)-Sm(1)-N(1)	78.77(6)	N(5)-Sm(1)-N(1)	81.78(6)
N(3)-Sm(1)-N(1)	81.69(6)	O(1)-Sm(1)-O(4)	74.66(6)
O(3a)-Sm(1)-O(4)	125.21(6)	N(5)-Sm(1)-O(4)	80.03(6)
N(3)-Sm(1)-O(4)	148.27(6)	N(1)-Sm(1)-O(4)	86.47(6)
C(10)-N(1)-N(2)	106.6(2)	C(10)-N(1)-Sm(1)	137.22(18)
N(2)-N(1)-Sm(1)	115.35(13)	C(12)-N(2)-N(1)	109.7(2)
C(12)-N(2)-B(1)	126.2(2)	N(1)-N(2)-B(1)	124.04(18)
N(1)-C(10)-C(11)	109.5(2)	N(1)-C(10)-C(13)	124.7(2)
C(11)-C(10)-C(13)	125.8(2)	C(12)-C(11)-C(10)	106.7(2)
N(2)-C(12)-C(11)	107.6(2)	N(2)-C(12)-C(17)	123.7(3)
C(11)-C(12)-C(17)	128.7(2)	C(10)-C(13)-C(14)	113.7(2)
C(10)-C(13)-C(15)	108.5(3)	C(14)-C(13)-C(15)	108.5(3)
C(10)-C(13)-C(16)	108.3(3)	C(14)-C(13)-C(16)	108.5(3)
C(15)-C(13)-C(16)	109.3(3)	C(18)-N(3)-N(4)	106.81(19)
C(18)-N(3)-Sm(1)	137.21(17)	N(4)-N(3)-Sm(1)	115.97(13)
C(20)-N(4)-N(3)	109.4(2)	C(20)-N(4)-B(1)	126.7(2)
N(3)-N(4)-B(1)	123.46(18)	N(3)-C(18)-C(19)	109.3(2)
N(3)-C(18)-C(21)	123.4(2)	C(19)-C(18)-C(21)	127.3(2)
C(20)-C(19)-C(18)	106.6(2)	N(4)-C(20)-C(19)	107.8(2)
N(4)-C(20)-C(25)	123.6(2)	C(19)-C(20)-C(25)	128.6(2)
C(18)-C(21)-C(23)	112.5(2)	C(18)-C(21)-C(24)	109.2(2)
C(23)-C(21)-C(24)	108.9(2)	C(18)-C(21)-C(22)	109.1(2)
C(23)-C(21)-C(22)	108.3(3)	C(24)-C(21)-C(22)	108.8(2)
C(26)-N(5)-N(6)	106.23(18)	C(26)-N(5)-Sm(1)	135.99(15)
N(6)-N(5)-Sm(1)	114.31(13)	C(28)-N(6)-N(5)	109.71(18)
C(28)-N(6)-B(1)	127.1(2)	N(5)-N(6)-B(1)	122.42(19)
N(5)-C(26)-C(27)	110.1(2)	N(5)-C(26)-C(29)	122.2(2)
C(27)-C(26)-C(29)	127.4(2)	C(28)-C(27)-C(26)	106.2(2)
N(6)-C(28)-C(27)	107.8(2)	N(6)-C(28)-C(33)	123.9(2)
C(27)-C(28)-C(33)	128.2(2)	C(30)-C(29)-C(26)	112.0(2)
C(30)-C(29)-C(31)	109.6(2)	C(26)-C(29)-C(31)	110.5(2)
C(30)-C(29)-C(32)	108.9(2)	C(26)-C(29)-C(32)	107.3(2)
C(31)-C(29)-C(32)	108.5(2)	N(4)-B(1)-N(6)	110.41(19)
N(4)-B(1)-N(2)	113.0(2)	N(6)-B(1)-N(2)	111.89(19)
C(34)-O(4)-C(37)	109.6(2)	C(34)-O(4)-Sm(1)	121.85(14)
C(37)-O(4)-Sm(1)	128.14(16)	O(4)-C(34)-C(35)	106.0(2)
C(36)-C(35)-C(34)	103.9(3)	C(35)-C(36)-C(37)	104.2(2)
O(4)-C(37)-C(36)	105.6(2)	C(40)-O(5)-C(38)	115.4(4)
O(5)-C(38)-C(39)	110.0(4)	O(5)-C(40)-C(41)	112.2(4)

Symmetry transformations used to generate equivalent atoms:

a: -x+1,-y+2,-z

Table A1.19 Crystal data, structure solution and refinement for **3.2**.

Chemical formula	$C_{41}H_{65}BMoN_6O_5Yb$
Formula weight	1001.78
Temperature	160(2) K
Radiation and wavelength	MoKα, 0.71073 Å
Crystal system, space group	triclinic, $P\bar{1}$
Unit cell dimensions	a = 13.6797(7) Å α = 63.213(2)°
	b = 13.7364(8) Å β = 67.115(2)°
	c = 15.1241(8) Å γ = 89.525(2)°
Volume	2288.6(2) $Å^3$
Z	2
Density (calculated)	1.454 g/cm^3
Absorption coefficient μ	2.351 mm^{-1}
F(000)	1020
Reflections for cell refinement	10980 (θ range 2.10 to 28.58°)
Crystal colour	yellow
Crystal size	0.25 × 0.13 × 0.04 mm
Data collection method	Siemens SMART CCD diffractometer,
	ω rotation with narrow frames
θ range for data collection	1.65 to 28.60°
Index ranges	$-17 \le h \le 18$, $-17 \le k \le 15$, $-20 \le \ell \le 19$
Intensity decay of standards	0%
Reflections collected	15610
Independent reflections	9993 (R_{int} = 0.0277)
Reflections with I>2σ(I)	8411
Absorption correction	semi-empirical from ψ-scans
Max. and min. transmission	0.740 and 0.556
Structure solution	direct methods
Refinement method	full-matrix least-squares on F^2
Weighting parameters a, b	0.0190, 0.3151
Data / restraints / parameters	9993 / 0 / 512
Goodness-of-fit on F^2	1.066
Final R indices [I>2σ(I)]	R1 = 0.0368, wR2 = 0.0646
R indices (all data)	R1 = 0.0516, wR2 = 0.0698
Extinction coefficient	0.00118(11)
Largest and mean shift/esd	0.002 and 0.000
Largest diff. peak and hole	0.706 and -0.698 $eÅ^{-3}$

Table A1.20 Atomic coordinates (x 10^4) and equivalent isotropic displacement parameters ($Å^2$ x 10^3) for **3.2**. U(eq) is defined as one third of the trace of the orthogonalised U_{ij} tensor.

	x	y	z	U(eq)
Mo(1)	6130.4(3)	13169.2(3)	-982.1(3)	20.62(8)
C(1)	4906(3)	12038(3)	187(3)	23.7(8)
O(1)	4156(2)	11284(2)	881(2)	29.1(7)
C(2)	6918(4)	12587(4)	-72(4)	33.7(10)
O(2)	7393(3)	12270(3)	456(3)	55.7(10)
C(3)	6405(3)	12034(3)	-1389(3)	23.3(8)
O(3)	6518(2)	11312(2)	-1623(2)	32.8(7)
C(4)	6609(4)	14657(3)	-2795(3)	32.9(10)
C(5)	5518(4)	14582(3)	-2148(3)	34.2(11)
C(6)	5459(4)	14848(3)	-1334(4)	37.3(11)
C(7)	6503(4)	15081(3)	-1456(3)	34.4(10)
C(8)	7230(3)	14968(3)	-2357(3)	31.1(10)
C(9)	7062(5)	14517(4)	-3797(4)	64.2(17)
Yb(1)	3351.43(13)	9671.50(14)	2658.46(13)	17.63(6)
N(1)	1697(2)	8162(3)	3928(2)	21.3(7)
N(2)	1729(2)	7398(2)	4894(2)	22.0(7)
C(10)	822(3)	7743(3)	3913(3)	28.2(9)
C(11)	296(3)	6728(4)	4862(4)	36.5(11)
C(12)	884(3)	6529(3)	5467(3)	29.7(10)
C(13)	455(3)	8300(4)	3008(4)	34.0(10)
C(14)	1173(4)	9410(4)	2073(4)	46.9(13)
C(15)	429(5)	7517(5)	2538(4)	62.0(16)
C(16)	-692(4)	8493(6)	3504(4)	65.8(18)
C(17)	672(4)	5549(4)	6561(4)	51.0(14)
N(3)	4350(2)	8241(2)	3431(2)	19.9(7)
N(4)	3737(2)	7439(2)	4522(2)	19.4(7)
C(18)	5315(3)	7953(3)	3115(3)	22.6(8)
C(19)	5331(3)	6980(3)	3986(3)	29.1(9)
C(20)	4335(3)	6678(3)	4856(3)	26.2(9)
C(21)	6239(3)	8635(3)	1986(3)	26.1(9)
C(22)	7201(4)	9029(5)	2122(4)	49.8(14)
C(23)	5927(3)	9664(4)	1259(3)	35.2(10)
C(24)	6581(4)	7911(4)	1431(4)	38.0(11)
C(25)	3930(4)	5709(3)	5975(3)	34.6(10)
N(5)	3285(2)	9657(2)	4325(2)	18.8(7)
N(6)	2704(2)	8654(2)	5269(2)	19.4(7)
C(26)	3354(3)	10393(3)	4664(3)	19.1(8)
C(27)	2801(3)	9886(3)	5806(3)	26.1(9)
C(28)	2415(3)	8798(3)	6159(3)	21.9(8)
C(29)	4053(3)	11547(3)	3894(3)	22.5(8)
C(30)	4533(4)	11815(4)	2698(3)	42.8(12)
C(31)	3416(4)	12420(4)	4019(4)	40.4(11)
C(32)	4986(4)	11606(4)	4206(4)	47.7(13)
C(33)	1847(4)	7863(4)	7315(3)	38.1(11)
B(1)	2619(4)	7547(4)	5242(4)	22.2(9)
O(4)	2123(2)	11019(2)	2781(2)	28.1(6)

C(34)	1196(3)	10764(3)	3800(3)	29.0(9)
C(35)	465(4)	11525(4)	3503(4)	56.2(15)
C(36)	1196(4)	12514(4)	2457(4)	51.0(14)
C(37)	2110(4)	12067(4)	1911(3)	37.6(11)
O(5)	1079(3)	13422(3)	-220(3)	68.7(12)
C(38)	281(5)	13034(5)	-410(5)	79(2)
C(39)	43(5)	11804(5)	150(5)	72.8(18)
C(40)	1488(5)	14561(6)	-845(5)	84(2)
C(41)	2342(6)	14908(6)	-605(6)	103(3)

Table A1.21 Bond lengths (Å) and angles (°) for **3.2**.

Mo(1)-C(1)	1.900(4)	Mo(1)-C(3)	1.905(4)
Mo(1)-C(2)	1.960(5)	Mo(1)-C(5)	2.370(4)
Mo(1)-C(6)	2.384(4)	Mo(1)-C(8)	2.385(4)
Mo(1)-C(4)	2.387(4)	Mo(1)-C(7)	2.390(4)
C(1)-O(1)	1.195(4)	O(1)-Yb(1)	2.390(3)
C(2)-O(2)	1.155(5)	C(3)-O(3)	1.184(5)
O(3)-Yb(1')	2.449(3)	C(4)-C(5)	1.405(6)
C(4)-C(8)	1.429(6)	C(4)-C(9)	1.499(6)
C(5)-C(6)	1.408(6)	C(6)-C(7)	1.388(6)
C(7)-C(8)	1.416(6)	Yb(1)-O(3')	2.449(3)
Yb(1)-N(5)	2.478(3)	Yb(1)-N(1)	2.494(3)
Yb(1)-N(3)	2.494(3)	Yb(1)-O(4)	2.510(3)
N(1)-C(10)	1.344(5)	N(1)-N(2)	1.381(4)
N(2)-C(12)	1.350(5)	N(2)-B(1)	1.549(5)
C(10)-C(11)	1.390(6)	C(10)-C(13)	1.516(6)
C(11)-C(12)	1.379(6)	C(12)-C(17)	1.503(6)
C(13)-C(14)	1.513(6)	C(13)-C(16)	1.534(6)
C(13)-C(15)	1.540(6)	N(3)-C(18)	1.341(5)
N(3)-N(4)	1.393(4)	N(4)-C(20)	1.359(5)
N(4)-B(1)	1.547(5)	C(18)-C(19)	1.399(5)
C(18)-C(21)	1.513(5)	C(19)-C(20)	1.372(5)
C(20)-C(25)	1.482(5)	C(21)-C(23)	1.531(6)
C(21)-C(24)	1.533(6)	C(21)-C(22)	1.546(5)
N(5)-C(26)	1.341(4)	N(5)-N(6)	1.389(4)
N(6)-C(28)	1.354(5)	N(6)-B(1)	1.546(5)
C(26)-C(27)	1.396(5)	C(26)-C(29)	1.509(5)
C(27)-C(28)	1.368(5)	C(28)-C(33)	1.499(5)
C(29)-C(31)	1.514(5)	C(29)-C(30)	1.522(5)
C(29)-C(32)	1.537(5)	O(4)-C(34)	1.452(4)
O(4)-C(37)	1.455(5)	C(34)-C(35)	1.484(6)
C(35)-C(36)	1.484(6)	C(36)-C(37)	1.504(6)
O(5)-C(40)	1.387(7)	O(5)-C(38)	1.397(6)
C(38)-C(39)	1.477(8)	C(40)-C(41)	1.490(8)
C(1)-Mo(1)-C(3)	80.94(16)	C(1)-Mo(1)-C(2)	88.28(16)
C(3)-Mo(1)-C(2)	90.20(17)	C(1)-Mo(1)-C(5)	107.99(15)
C(3)-Mo(1)-C(5)	110.73(16)	C(2)-Mo(1)-C(5)	154.91(16)
C(1)-Mo(1)-C(6)	103.78(16)	C(3)-Mo(1)-C(6)	144.99(16)
C(2)-Mo(1)-C(6)	124.28(17)	C(5)-Mo(1)-C(6)	34.45(15)
C(1)-Mo(1)-C(8)	160.62(16)	C(3)-Mo(1)-C(8)	114.84(15)
C(2)-Mo(1)-C(8)	102.21(16)	C(5)-Mo(1)-C(8)	57.08(14)
C(6)-Mo(1)-C(8)	56.85(15)	C(1)-Mo(1)-C(4)	138.03(16)
C(3)-Mo(1)-C(4)	95.74(15)	C(2)-Mo(1)-C(4)	133.69(17)
C(5)-Mo(1)-C(4)	34.34(15)	C(6)-Mo(1)-C(4)	57.33(15)
C(8)-Mo(1)-C(4)	34.85(14)	C(1)-Mo(1)-C(7)	128.58(16)
C(3)-Mo(1)-C(7)	149.28(15)	C(2)-Mo(1)-C(7)	98.08(16)
C(5)-Mo(1)-C(7)	56.87(15)	C(6)-Mo(1)-C(7)	33.80(15)
C(8)-Mo(1)-C(7)	34.49(14)	C(4)-Mo(1)-C(7)	57.58(14)
O(1)-C(1)-Mo(1)	175.2(3)	C(1)-O(1)-Yb(1)	149.1(3)
O(2)-C(2)-Mo(1)	178.3(4)	O(3)-C(3)-Mo(1)	176.4(3)
C(3)-O(3)-Yb(1')	159.4(3)	C(5)-C(4)-C(8)	106.6(4)

C(5)-C(4)-C(9)	127.6(4)	C(8)-C(4)-C(9)	125.7(5)
C(5)-C(4)-Mo(1)	72.1(2)	C(8)-C(4)-Mo(1)	72.5(2)
C(9)-C(4)-Mo(1)	123.4(3)	C(4)-C(5)-C(6)	108.9(4)
C(4)-C(5)-Mo(1)	73.5(2)	C(6)-C(5)-Mo(1)	73.3(2)
C(7)-C(6)-C(5)	108.4(4)	C(7)-C(6)-Mo(1)	73.3(3)
C(5)-C(6)-Mo(1)	72.2(3)	C(6)-C(7)-C(8)	108.1(4)
C(6)-C(7)-Mo(1)	72.9(2)	C(8)-C(7)-Mo(1)	72.6(2)
C(7)-C(8)-C(4)	108.0(4)	C(7)-C(8)-Mo(1)	72.9(2)
C(4)-C(8)-Mo(1)	72.7(2)	O(1)-Yb(1)-O(3')	83.91(9)
O(1)-Yb(1)-N(5)	122.78(9)	O(3')-Yb(1)-N(5)	149.48(10)
O(1)-Yb(1)-N(1)	141.88(10)	O(3')-Yb(1)-N(1)	78.47(9)
N(5)-Yb(1)-N(1)	86.02(10)	O(1)-Yb(1)-N(3)	124.32(10)
O(3')-Yb(1)-N(3)	80.79(10)	N(5)-Yb(1)-N(3)	71.95(10)
N(1)-Yb(1)-N(3)	85.94(10)	O(1)-Yb(1)-O(4)	75.38(9)
O(3')-Yb(1)-O(4)	124.19(9)	N(5)-Yb(1)-O(4)	80.45(9)
N(1)-Yb(1)-O(4)	87.03(9)	N(3)-Yb(1)-O(4)	151.91(9)
C(10)-N(1)-N(2)	106.3(3)	C(10)-N(1)-Yb(1)	139.2(3)
N(2)-N(1)-Yb(1)	113.5(2)	C(12)-N(2)-N(1)	110.0(3)
C(12)-N(2)-B(1)	126.3(3)	N(1)-N(2)-B(1)	123.6(3)
N(1)-C(10)-C(11)	109.7(4)	N(1)-C(10)-C(13)	125.3(4)
C(11)-C(10)-C(13)	125.1(4)	C(12)-C(11)-C(10)	106.6(4)
N(2)-C(12)-C(11)	107.4(4)	N(2)-C(12)-C(17)	124.0(4)
C(11)-C(12)-C(17)	128.6(4)	C(14)-C(13)-C(10)	114.0(3)
C(14)-C(13)-C(16)	108.1(4)	C(10)-C(13)-C(16)	108.5(4)
C(14)-C(13)-C(15)	108.4(4)	C(10)-C(13)-C(15)	108.7(4)
C(16)-C(13)-C(15)	109.2(4)	C(18)-N(3)-N(4)	106.2(3)
C(18)-N(3)-Yb(1)	139.9(3)	N(4)-N(3)-Yb(1)	113.8(2)
C(20)-N(4)-N(3)	109.5(3)	C(20)-N(4)-B(1)	127.3(3)
N(3)-N(4)-B(1)	122.6(3)	N(3)-C(18)-C(19)	109.9(3)
N(3)-C(18)-C(21)	123.2(3)	C(19)-C(18)-C(21)	126.8(3)
C(20)-C(19)-C(18)	106.5(3)	N(4)-C(20)-C(19)	107.8(3)
N(4)-C(20)-C(25)	123.7(4)	C(19)-C(20)-C(25)	128.5(4)
C(18)-C(21)-C(23)	111.9(3)	C(18)-C(21)-C(24)	109.5(3)
C(23)-C(21)-C(24)	109.3(3)	C(18)-C(21)-C(22)	108.3(3)
C(23)-C(21)-C(22)	108.3(4)	C(24)-C(21)-C(22)	109.6(4)
C(26)-N(5)-N(6)	106.2(3)	C(26)-N(5)-Yb(1)	138.3(2)
N(6)-N(5)-Yb(1)	112.0(2)	C(28)-N(6)-N(5)	109.3(3)
C(28)-N(6)-B(1)	127.9(3)	N(5)-N(6)-B(1)	121.9(3)
N(5)-C(26)-C(27)	110.0(3)	N(5)-C(26)-C(29)	122.5(3)
C(27)-C(26)-C(29)	127.1(3)	C(28)-C(27)-C(26)	106.2(3)
N(6)-C(28)-C(27)	108.3(3)	N(6)-C(28)-C(33)	123.1(3)
C(27)-C(28)-C(33)	128.4(4)	C(26)-C(29)-C(31)	110.9(3)
C(26)-C(29)-C(30)	112.4(3)	C(31)-C(29)-C(30)	109.1(4)
C(26)-C(29)-C(32)	107.7(3)	C(31)-C(29)-C(32)	107.9(4)
C(30)-C(29)-C(32)	108.6(4)	N(6)-B(1)-N(4)	110.7(3)
N(6)-B(1)-N(2)	112.0(3)	N(4)-B(1)-N(2)	112.6(3)
C(34)-O(4)-C(37)	108.7(3)	C(34)-O(4)-Yb(1)	121.7(2)
C(37)-O(4)-Yb(1)	129.3(2)	O(4)-C(34)-C(35)	106.8(3)
C(34)-C(35)-C(36)	104.4(4)	C(35)-C(36)-C(37)	104.9(4)
O(4)-C(37)-C(36)	106.2(3)	C(40)-O(5)-C(38)	115.3(4)
O(5)-C(38)-C(39)	110.4(5)	O(5)-C(40)-C(41)	112.1(5)

Symmetry transformations used to generate equivalent atoms:

': -x+1,-y+2,-z

Table A1.22 Crystal data, structure solution and refinement for **3.3**.

Chemical formula	$C_{42}H_{52}B_2MnN_{12}O_5Sm$
Formula weight	1031.87
Temperature	160(2) K
Radiation and wavelength	MoKα, 0.71073 Å
Crystal system, space group	triclinic, $P\bar{1}$
Unit cell dimensions	a = 10.6613(16) Å α = 97.437(4)°
	b = 11.5186(17) Å β = 98.612(3)°
	c = 20.715(3) Å γ = 105.281(4)°
Volume	2387.9(6) Å^3
Z	2
Density (calculated)	1.435 g/cm^3
Absorption coefficient μ	1.537 mm^{-1}
F(000)	1050
Reflections for cell refinement	5554 (θ range 1.86 to 25.48°)
Crystal colour	pale yellow
Crystal size	0.42 × 0.24 × 0.14 mm
Data collection method	Siemens SMART CCD diffractometer,
	ω rotation with narrow frames
θ range for data collection	2.02 to 25.00°
Index ranges	$-12 \le h \le 12$, $-13 \le k \le 12$, $-24 \le \ell \le 24$
Intensity decay	0%
Reflections collected	14347
Independent reflections	8309 (R_{int} = 0.0623)
Reflections with I>2σ(I)	5010
Absorption correction	semi-empirical from ψ-scans
Max. and min. transmission	0.862 and 0.527
Structure solution	solved by placing Sm atom at 0.5 0.5 0.5
Refinement method	full-matrix least-squares on F^2
Weighting parameters a, b	0.1400, 0.0000
Data / restraints / parameters	8309 / 927 / 779
Final R indices [I>2σ(I)]	R1 = 0.0881, wR2 = 0.2113
R indices (all data)	R1 = 0.1380, wR2 = 0.2401
Goodness-of-fit on F^2	0.993
Largest and mean shift/esd	0.012 and 0.002
Largest diff. peak and hole	2.808 and −2.061 eÅ^{-3}

Table A1.23 Atomic coordinates (x 10^4) and equivalent isotropic displacement parameters ($Å^2$ x 10^3) for **3.3**. U(eq) is defined as one third of the trace of the orthogonalised U_{ij} tensor.

	x	y	z	U(eq)
Sm(1)	5000	5000	5000	25.9(2)
N(1)	5790(10)	7135(8)	4940(5)	55(3)
N(2)	5643(10)	7459(9)	4313(5)	59(3)
C(1)	6067(14)	8144(11)	5374(8)	72(4)
C(2)	6151(16)	9117(12)	5044(10)	100(6)
C(3)	5865(16)	8649(14)	4382(9)	88(5)
C(4)	6282(15)	8114(13)	6105(7)	91(5)
C(5)	5790(2)	9370(14)	3812(10)	138(9)
N(3)	3417(9)	5139(10)	4060(4)	55(3)
N(4)	3926(10)	5691(10)	3563(4)	61(3)
C(6)	2176(11)	4415(16)	3809(6)	77(5)
C(7)	1890(16)	4430(3)	3136(7)	161(12)
C(8)	2969(15)	5240(2)	2996(7)	124(8)
C(9)	1324(13)	3693(17)	4215(7)	101(6)
C(10)	3232(18)	5670(3)	2359(8)	204(15)
N(5)	6296(8)	4954(7)	4133(3)	31.4(19)
N(6)	6357(8)	5767(7)	3707(4)	36(2)
C(11)	7240(10)	4392(9)	4022(5)	41(3)
C(12)	7844(10)	4837(9)	3508(5)	42(3)
C(13)	7271(10)	5683(9)	3340(5)	38(2)
C(14)	7449(14)	3411(12)	4414(6)	69(4)
C(15)	7510(13)	6423(11)	2795(6)	64(4)
B(1)	5355(14)	6532(12)	3686(7)	50(4)
Sm(2)	9900(2)	5305.6(18)	9973.1(11)	53.5(6)
N(7)	9762(18)	6620(2)	9173(9)	60(2)
N(8)	8815(16)	7230(2)	9126(8)	57(2)
C(16)	10590(2)	7010(3)	8763(11)	58(2)
C(17)	10140(2)	7890(3)	8440(10)	59(3)
C(18)	9022(19)	7910(3)	8695(10)	59(2)
C(19)	11670(2)	6440(3)	8644(12)	60(4)
C(20)	8166(19)	8660(3)	8517(10)	65(5)
N(9)	7563(15)	4699(18)	9544(9)	67(2)
N(10)	6932(14)	5569(17)	9449(8)	64(2)
C(21)	6612(18)	3586(18)	9353(11)	71(2)
C(22)	5408(17)	3760(2)	9143(16)	71(3)
C(23)	5640(15)	5018(19)	9215(9)	66(3)
C(24)	6990(3)	2440(2)	9340(2)	78(4)
C(25)	4660(17)	5700(2)	9052(10)	71(4)
N(11)	9209(18)	6797(18)	10642(7)	60(2)
N(12)	8442(16)	7381(18)	10301(7)	58(2)
C(26)	9670(2)	7460(2)	11271(8)	60(3)
C(27)	9118(18)	8390(2)	11337(8)	60(3)
C(28)	8338(19)	8320(2)	10724(8)	60(3)
C(29)	10580(4)	7050(3)	11750(14)	65(5)
C(30)	7570(2)	9170(2)	10521(10)	70(5)

B(2)	7720(2)	6850(3)	9531(11)	60(2)
N(7A)	9960(16)	5840(2)	9158(8)	68(2)
N(8A)	8867(17)	6250(2)	9022(9)	71(2)
C(16A)	10798(18)	6270(3)	8740(10)	69(3)
C(17A)	10229(18)	6930(3)	8354(11)	73(3)
C(18A)	8923(18)	6650(3)	8447(10)	71(2)
C(19A)	12060(2)	5940(3)	8772(13)	76(5)
C(20A)	7800(2)	6970(3)	8079(12)	86(5)
N(9A)	7799(16)	3722(18)	9510(9)	74(2)
N(10A)	7075(16)	4494(19)	9338(10)	72(2)
C(21A)	6930(2)	2570(2)	9430(2)	75(3)
C(22A)	5694(18)	2600(2)	9176(11)	79(3)
C(23A)	5794(18)	3830(2)	9165(17)	76(3)
C(24A)	7430(2)	1510(2)	9540(14)	91(5)
C(25A)	4740(2)	4410(3)	8976(13)	87(4)
N(11A)	9181(18)	6181(19)	10526(8)	61(2)
N(12A)	8230(16)	6490(2)	10128(7)	65(2)
C(26A)	9440(2)	6900(2)	11138(8)	60(3)
C(27A)	8660(2)	7660(2)	11127(9)	64(2)
C(28A)	7970(2)	7430(2)	10472(10)	65(2)
C(29A)	10440(4)	6720(3)	11666(14)	63(5)
C(30A)	6880(2)	7920(3)	10197(12)	80(5)
B(2A)	7580(3)	5600(4)	9386(13)	67.1(18)
Mn(1)	5741.6(16)	952.4(16)	2148.4(9)	47.9(5)
C(31)	6232(11)	-440(12)	2075(6)	58(3)
O(1)	6581(11)	-1309(9)	2073(5)	88(3)
C(32)	5293(12)	2366(14)	2348(7)	74(4)
O(2)	4982(11)	3242(11)	2491(6)	114(4)
C(33)	4228(13)	133(13)	2360(7)	71(4)
O(3)	3262(9)	-463(11)	2483(6)	103(4)
C(34)	5584(12)	1025(12)	1284(7)	60(3)
O(4)	5425(11)	1019(9)	723(5)	92(3)
C(35)	7324(10)	1695(10)	2684(5)	40(3)
O(5)	8344(8)	2111(8)	3016(4)	61(2)
C(36)	750(2)	9080(2)	3399(9)	106(6)
C(37)	10(2)	9822(18)	3455(13)	131(9)
C(38)	-770(3)	9630(3)	3944(18)	181(15)
C(39)	-700(3)	8820(3)	4349(15)	175(15)
C(40)	51(17)	8140(2)	4293(11)	122(8)
C(41)	874(17)	8207(16)	3816(11)	106(7)
C(42)	1670(2)	7480(2)	3762(15)	200(13)

Table A1.24 Bond lengths (Å) and angles (°) for **3.3**.

Sm(1)-N(1)	2.406(9)	Sm(1)-N(1')	2.406(9)
Sm(1)-N(5')	2.427(7)	Sm(1)-N(5)	2.427(7)
Sm(1)-N(3')	2.430(9)	Sm(1)-N(3)	2.430(9)
N(1)-C(1)	1.310(14)	N(1)-N(2)	1.396(13)
N(2)-C(3)	1.313(16)	N(2)-B(1)	1.506(17)
C(1)-C(2)	1.376(19)	C(1)-C(4)	1.50(2)
C(2)-C(3)	1.37(2)	C(3)-C(5)	1.53(2)
N(3)-C(6)	1.347(15)	N(3)-N(4)	1.384(13)
N(4)-C(8)	1.376(18)	N(4)-B(1)	1.538(18)
C(6)-C(7)	1.386(17)	C(6)-C(9)	1.495(19)
C(7)-C(8)	1.37(3)	C(8)-C(10)	1.51(2)
N(5)-C(11)	1.364(12)	N(5)-N(6)	1.365(10)
N(6)-C(13)	1.337(12)	N(6)-B(1)	1.553(13)
C(11)-C(12)	1.409(14)	C(11)-C(14)	1.519(14)
C(12)-C(13)	1.335(13)	C(13)-C(15)	1.511(14)
Sm(2)-Sm(2'')	0.804(3)	Sm(2)-N(11A)	1.813(16)
Sm(2)-N(7A)	1.873(15)	Sm(2)-N(7A'')	2.373(17)
Sm(2)-N(11A'')	2.385(16)	Sm(2)-N(9)	2.396(15)
Sm(2)-N(7)	2.40(2)	Sm(2)-N(11)	2.402(16)
Sm(2)-N(9A'')	2.424(16)	Sm(2)-N(9A)	2.452(16)
Sm(2)-N(12A)	2.543(17)	Sm(2)-N(8A)	2.608(17)
N(7)-C(16)	1.35(3)	N(7)-N(8)	1.38(3)
N(8)-C(18)	1.27(3)	N(8)-B(2)	1.55(3)
C(16)-C(17)	1.42(4)	C(16)-C(19)	1.51(3)
C(17)-C(18)	1.38(3)	C(18)-C(20)	1.45(3)
N(9)-N(10)	1.365(18)	N(9)-C(21)	1.375(1S)
N(9)-Sm(2'')	2.741(16)	N(10)-C(23)	1.340(17)
N(10)-B(2)	1.46(4)	C(21)-C(22)	1.37(2)
C(21)-C(24)	1.47(2)	C(22)-C(23)	1.39(2)
C(23)-C(25)	1.491(19)	N(11)-N(12)	1.364(16)
N(11)-C(26)	1.369(17)	N(12)-C(28)	1.344(18)
N(12)-B(2)	1.63(3)	C(26)-C(27)	1.352(19)
C(26)-C(29)	1.483(18)	C(27)-C(28)	1.393(18)
C(28)-C(30)	1.488(19)	N(7A)-N(8A)	1.372(17)
N(7A)-C(16A)	1.380(17)	N(7A)-Sm(2'')	2.373(17)
N(8A)-C(18A)	1.338(17)	N(8A)-B(2A)	1.71(3)
C(16A)-C(17A)	1.36(2)	C(16A)-C(19A)	1.478(19)
C(17A)-C(18A)	1.392(19)	C(18A)-C(20A)	1.475(19)
N(9A)-N(10A)	1.369(18)	N(9A)-C(21A)	1.373(19)
N(9A)-Sm(2'')	2.424(15)	N(10A)-B(2A)	1.23(4)
N(10A)-C(23A)	1.346(18)	C(21A)-C(22A)	1.35(2)
C(21A)-C(24A)	1.49(2)	C(22A)-C(23A)	1.39(2)
C(23A)-C(25A)	1.48(2)	N(11A)-N(12A)	1.360(16)
N(11A)-C(26A)	1.369(17)	N(11A)-Sm(2'')	2.385(16)
N(12A)-C(28A)	1.331(19)	N(12A)-B(2A)	1.67(3)
C(26A)-C(27A)	1.355(19)	C(26A)-C(29A)	1.484(17)
C(27A)-C(28A)	1.400(19)	C(28A)-C(30A)	1.496(19)
Mn(1)-C(34)	1.789(14)	Mn(1)-C(33)	1.790(14)
Mn(1)-C(35)	1.801(11)	Mn(1)-C(31)	1.809(14)
Mn(1)-C(32)	1.829(15)	C(31)-O(1)	1.156(14)
C(32)-O(2)	1.160(15)	C(33)-O(3)	1.161(15)
C(34)-O(4)	1.148(14)	C(35)-O(5)	1.141(12)
C(36)-C(37)	1.32(3)	C(36)-C(41)	1.42(3)
C(37)-C(38)	1.41(3)	C(38)-C(39)	1.35(4)
C(39)-C(40)	1.27(4)	C(40)-C(41)	1.41(3)
C(41)-C(42)	1.35(3)		
N(1)-Sm(1)-N(1')	179.998(1)	N(1)-Sm(1)-N(5')	101.8(3)

N(1')-Sm(1)-N(5')	78.2(3)	N(1)-Sm(1)-N(5)	78.2(3)
N(1')-Sm(1)-N(5)	101.8(3)	N(5')-Sm(1)-N(5)	179.999(2)
N(1)-Sm(1)-N(3')	100.9(4)	N(1')-Sm(1)-N(3')	79.1(4)
N(5')-Sm(1)-N(3')	79.8(3)	N(5)-Sm(1)-N(3')	100.2(3)
N(1)-Sm(1)-N(3)	79.1(4)	N(1')-Sm(1)-N(3)	100.9(4)
N(5')-Sm(1)-N(3)	100.2(3)	N(5)-Sm(1)-N(3)	79.8(3)
N(3')-Sm(1)-N(3)	179.999(2)	C(1)-N(1)-N(2)	106.9(10)
C(1)-N(1)-Sm(1)	133.6(8)	N(2)-N(1)-Sm(1)	117.4(7)
C(3)-N(2)-N(1)	108.9(11)	C(3)-N(2)-B(1)	128.9(11)
N(1)-N(2)-B(1)	122.1(9)	N(1)-C(1)-C(2)	109.2(14)
N(1)-C(1)-C(4)	120.4(12)	C(2)-C(1)-C(4)	130.3(13)
C(3)-C(2)-C(1)	106.9(12)	N(2)-C(3)-C(2)	108.1(13)
N(2)-C(3)-C(5)	125.4(16)	C(2)-C(3)-C(5)	126.6(15)
C(6)-N(3)-N(4)	108.9(9)	C(6)-N(3)-Sm(1)	129.4(9)
N(4)-N(3)-Sm(1)	117.1(7)	C(8)-N(4)-N(3)	106.2(11)
C(8)-N(4)-B(1)	132.1(11)	N(3)-N(4)-B(1)	121.4(9)
N(3)-C(6)-C(7)	108.9(14)	N(3)-C(6)-C(9)	123.1(11)
C(7)-C(6)-C(9)	128.0(14)	C(8)-C(7)-C(6)	106.3(15)
N(4)-C(8)-C(7)	109.6(11)	N(4)-C(8)-C(10)	119.1(17)
C(7)-C(8)-C(10)	131.3(16)	C(11)-N(5)-N(6)	105.0(7)
C(11)-N(5)-Sm(1)	133.0(6)	N(6)-N(5)-Sm(1)	120.9(5)
C(13)-N(6)-N(5)	110.0(7)	C(13)-N(6)-B(1)	131.5(8)
N(5)-N(6)-B(1)	118.4(7)	N(5)-C(11)-C(12)	109.7(8)
N(5)-C(11)-C(14)	119.6(9)	C(12)-C(11)-C(14)	130.6(9)
C(13)-C(12)-C(11)	105.0(8)	C(12)-C(13)-N(6)	110.3(8)
C(12)-C(13)-C(15)	127.5(9)	N(6)-C(13)-C(15)	122.1(9)
N(2)-B(1)-N(4)	110.7(9)	N(2)-B(1)-N(6)	111.4(10)
N(4)-B(1)-N(6)	110.6(9)	Sm(2'')-Sm(2)-N(11A)	127.1(8)
Sm(2'')-Sm(2)-N(7A)	119.4(8)	N(11A)-Sm(2)-N(7A)	113.1(9)
Sm(2'')-Sm(2)-N(7A'')	43.5(6)	N(11A)-Sm(2)-N(7A'')	84.0(8)
N(7A)-Sm(2)-N(7A'')	162.8(2)	Sm(2'')-Sm(2)-N(11A'')	37.3(6)
N(11A)-Sm(2)-N(11A'')	164.4(2)	N(7A)-Sm(2)-N(11A'')	82.4(8)
N(7A'')-Sm(2)-N(11A'')	80.5(7)	Sm(2'')-Sm(2)-N(9)	107.0(6)
N(11A)-Sm(2)-N(9)	73.2(7)	N(7A)-Sm(2)-N(9)	82.0(7)
N(7A'')-Sm(2)-N(9)	102.0(7)	N(11A'')-Sm(2)-N(9)	108.5(7)
Sm(2'')-Sm(2)-N(7)	141.6(6)	N(11A)-Sm(2)-N(7)	91.2(8)
N(7A)-Sm(2)-N(7)	22.3(8)	N(7A'')-Sm(2)-N(7)	174.7(7)
N(11A'')-Sm(2)-N(7)	104.3(7)	N(9)-Sm(2)-N(7)	78.6(7)
Sm(2'')-Sm(2)-N(11)	135.5(6)	N(11A)-Sm(2)-N(11)	10.9(11)
N(7A)-Sm(2)-N(11)	105.2(9)	N(7A'')-Sm(2)-N(11)	92.0(7)
N(11A'')-Sm(2)-N(11)	170.5(6)	N(9)-Sm(2)-N(11)	78.6(6)
N(7)-Sm(2)-N(11)	82.9(7)	Sm(2'')-Sm(2)-N(9A'')	82.5(6)
N(11A)-Sm(2)-N(9A'')	97.3(8)	N(7A)-Sm(2)-N(9A'')	97.7(7)
N(7A'')-Sm(2)-N(9A'')	81.4(7)	N(11A'')-Sm(2)-N(9A'')	82.0(7)
N(9)-Sm(2)-N(9A'')	169.3(6)	N(7)-Sm(2)-N(9A'')	97.0(7)
N(11)-Sm(2)-N(9A'')	91.2(7)	Sm(2'')-Sm(2)-N(9A)	78.5(6)
N(11A)-Sm(2)-N(9A)	94.2(8)	N(7A)-Sm(2)-N(9A)	91.6(8)
N(7A'')-Sm(2)-N(9A)	84.8(7)	N(11A'')-Sm(2)-N(9A)	83.0(7)
N(9)-Sm(2)-N(9A)	28.9(6)	N(7)-Sm(2)-N(9A)	97.8(7)
N(11)-Sm(2)-N(9A)	102.3(7)	N(9A'')-Sm(2)-N(9A)	161.03(13)
Sm(2'')-Sm(2)-N(12A)	145.4(6)	N(11A)-Sm(2)-N(12A)	31.0(5)
N(7A)-Sm(2)-N(12A)	86.8(7)	N(7A'')-Sm(2)-N(12A)	108.8(6)
N(11A'')-Sm(2)-N(12A)	158.3(5)	N(9)-Sm(2)-N(12A)	51.0(6)
N(7)-Sm(2)-N(12A)	67.4(6)	N(11)-Sm(2)-N(12A)	30.6(5)
N(9A'')-Sm(2)-N(12A)	118.3(7)	N(9A)-Sm(2)-N(12A)	78.6(7)
Sm(2'')-Sm(2)-N(8A)	139.6(7)	N(11A)-Sm(2)-N(8A)	87.0(7)
N(7A)-Sm(2)-N(8A)	30.4(5)	N(7A'')-Sm(2)-N(8A)	159.8(5)
N(11A'')-Sm(2)-N(8A)	107.3(6)	N(9)-Sm(2)-N(8A)	58.0(7)
N(7)-Sm(2)-N(8A)	20.7(6)	N(11)-Sm(2)-N(8A)	81.7(6)
N(9A'')-Sm(2)-N(8A)	117.7(7)	N(9A)-Sm(2)-N(8A)	77.9(7)
N(12A)-Sm(2)-N(8A)	57.7(6)	C(16)-N(7)-N(8)	108(2)
C(16)-N(7)-Sm(2)	130.5(17)	N(8)-N(7)-Sm(2)	121.5(12)

C(18)-N(8)-N(7)	108.3(17)	C(18)-N(8)-B(2)	136(2)
N(7)-N(8)-B(2)	116(2)	N(7)-C(16)-C(17)	109(2)
N(7)-C(16)-C(19)	121(2)	C(17)-C(16)-C(19)	130(2)
C(18)-C(17)-C(16)	102(2)	N(8)-C(18)-C(17)	113(2)
N(8)-C(18)-C(20)	121.8(19)	C(17)-C(18)-C(20)	125(2)
N(10)-N(9)-C(21)	106.5(13)	N(10)-N(9)-Sm(2)	119.7(12)
C(21)-N(9)-Sm(2)	133.8(13)	N(10)-N(9)-Sm(2'')	135.9(11)
C(21)-N(9)-Sm(2'')	117.5(12)	Sm(2)-N(9)-Sm(2'')	16.29(15)
C(23)-N(10)-N(9)	109.0(15)	C(23)-N(10)-B(2)	131.2(19)
N(9)-N(10)-B(2)	119.3(17)	C(22)-C(21)-N(9)	109.7(15)
C(22)-C(21)-C(24)	129.7(19)	N(9)-C(21)-C(24)	120.4(19)
C(21)-C(22)-C(23)	105.6(15)	N(10)-C(23)-C(22)	109.2(15)
N(10)-C(23)-C(25)	123.1(17)	C(22)-C(23)-C(25)	127.7(16)
N(12)-N(11)-C(26)	107.7(14)	N(12)-N(11)-Sm(2)	115.4(10)
C(26)-N(11)-Sm(2)	134.1(11)	C(28)-N(12)-N(11)	108.2(13)
C(28)-N(12)-B(2)	130.0(18)	N(11)-N(12)-B(2)	121.5(18)
C(27)-C(26)-N(11)	108.7(13)	C(27)-C(26)-C(29)	131.7(17)
N(11)-C(26)-C(29)	119.5(17)	C(26)-C(27)-C(28)	106.8(14)
N(12)-C(28)-C(27)	108.3(14)	N(12)-C(28)-C(30)	123.0(15)
C(27)-C(28)-C(30)	128.5(16)	N(10)-B(2)-N(8)	121(2)
N(10)-B(2)-N(12)	111(2)	N(8)-B(2)-N(12)	104.9(17)
N(8A)-N(7A)-C(16A)	107.3(14)	N(8A)-N(7A)-Sm(2)	105.9(10)
C(16A)-N(7A)-Sm(2)	143.7(13)	N(8A)-N(7A)-Sm(2'')	118.7(10)
C(16A)-N(7A)-Sm(2'')	134.0(12)	Sm(2)-N(7A)-Sm(2'')	17.2(2)
C(18A)-N(8A)-N(7A)	106.0(14)	C(18A)-N(8A)-B(2A)	133.0(17)
N(7A)-N(8A)-B(2A)	114.6(19)	C(18A)-N(8A)-Sm(2)	149.7(12)
N(7A)-N(8A)-Sm(2)	43.7(7)	B(2A)-N(8A)-Sm(2)	74.6(13)
C(17A)-C(16A)-N(7A)	108.5(14)	C(17A)-C(16A)-C(19A)	132.5(17)
N(7A)-C(16A)-C(19A)	119.0(17)	C(16A)-C(17A)-C(18A)	104.6(15)
N(8A)-C(18A)-C(17A)	108.7(14)	N(8A)-C(18A)-C(20A)	122.0(16)
C(17A)-C(18A)-C(20A)	128.1(17)	N(10A)-N(9A)-C(21A)	107.4(14)
N(10A)-N(9A)-Sm(2'')	115.8(12)	C(21A)-N(9A)-Sm(2'')	136.0(14)
N(10A)-N(9A)-Sm(2)	96.8(11)	C(21A)-N(9A)-Sm(2)	154.3(15)
Sm(2'')-N(9A)-Sm(2)	18.97(14)	B(2A)-N(10A)-C(23A)	130(2)
B(2A)-N(10A)-N(9A)	122(2)	C(23A)-N(10A)-N(9A)	107.5(15)
B(2A)-N(10A)-Sm(2)	67.0(17)	C(23A)-N(10A)-Sm(2)	161.1(16)
N(9A)-N(10A)-Sm(2)	55.7(9)	C(22A)-C(21A)-N(9A)	109.7(15)
C(22A)-C(21A)-C(24A)	129.8(19)	N(9A)-C(21A)-C(24A)	120.2(19)
C(21A)-C(22A)-C(23A)	105.5(15)	N(10A)-C(23A)-C(22A)	109.6(16)
N(10A)-C(23A)-C(25A)	121.0(18)	C(22A)-C(23A)-C(25A)	129.4(17)
N(12A)-N(11A)-C(26A)	108.3(13)	N(12A)-N(11A)-Sm(2)	105.7(11)
C(26A)-N(11A)-Sm(2)	142.8(13)	N(12A)-N(11A)-Sm(2'')	117.0(11)
C(26A)-N(11A)-Sm(2'')	134.6(11)	Sm(2)-N(11A)-Sm(2'')	15.6(2)
C(28A)-N(12A)-N(11A)	107.6(13)	C(28A)-N(12A)-B(2A)	135.0(19)
N(11A)-N(12A)-B(2A)	117(2)	C(28A)-N(12A)-Sm(2)	146.8(12)
N(11A)-N(12A)-Sm(2)	43.3(8)	B(2A)-N(12A)-Sm(2)	77.1(14)
C(27A)-C(26A)-N(11A)	108.7(13)	C(27A)-C(26A)-C(29A)	132.9(18)
N(11A)-C(26A)-C(29A)	118.3(17)	C(27A)-C(26A)-Sm(2)	127.6(11)
N(11A)-C(26A)-Sm(2)	21.3(8)	C(29A)-C(26A)-Sm(2)	98.9(14)
C(26A)-C(27A)-C(28A)	105.5(15)	N(12A)-C(28A)-C(27A)	109.5(15)
N(12A)-C(28A)-C(30A)	121.1(17)	C(27A)-C(28A)-C(30A)	128.1(17)
N(10A)-B(2A)-N(12A)	121(3)	N(10A)-B(2A)-N(8A)	125(3)
N(12A)-B(2A)-N(8A)	94.6(19)	N(10A)-B(2A)-Sm(2)	88(2)
N(12A)-B(2A)-Sm(2)	66.0(11)	N(8A)-B(2A)-Sm(2)	67.9(11)
C(34)-Mn(1)-C(33)	112.9(6)	C(34)-Mn(1)-C(35)	118.4(5)
C(33)-Mn(1)-C(35)	128.7(6)	C(34)-Mn(1)-C(31)	94.7(6)
C(33)-Mn(1)-C(31)	89.1(6)	C(35)-Mn(1)-C(31)	87.6(5)
C(34)-Mn(1)-C(32)	93.2(6)	C(33)-Mn(1)-C(32)	88.6(6)
C(35)-Mn(1)-C(32)	87.9(5)	C(31)-Mn(1)-C(32)	172.0(6)
O(1)-C(31)-Mn(1)	175.4(12)	O(2)-C(32)-Mn(1)	177.4(15)
O(3)-C(33)-Mn(1)	175.8(13)	O(4)-C(34)-Mn(1)	176.3(12)
O(5)-C(35)-Mn(1)	176.5(9)	C(37)-C(36)-C(41)	125(2)

C(36)-C(37)-C(38)	114(2)	C(39)-C(38)-C(37)	123(3)
C(40)-C(39)-C(38)	121(3)	C(39)-C(40)-C(41)	122(3)
C(42)-C(41)-C(40)	122(3)	C(42)-C(41)-C(36)	124(3)
C(40)-C(41)-C(36)	114.2(18)		

Symmetry transformations used to generate equivalent atoms:

': -x+1,-y+1,-z+1 '': -x+2,-y+1,-z+2

Table A1.25 Crystal data, structure solution and refinement for **3.4**.

Chemical formula	$C_{94}H_{121}B_4MnN_{24}O_7Sm_2$
Formula weight	2098.03
Temperature	160(2) K
Radiation and wavelength	MoKα, 0.71073 Å
Crystal system, space group	orthorhombic, $Pna2_1$
Unit cell dimensions	a = 21.1214(12) Å α = 90°
	b = 17.4688(9) Å β = 90°
	c = 27.3426(15) Å γ = 90°
Volume	10088.5(10) $Å^3$
Z	4
Density (calculated)	1.381 g/cm^3
Absorption coefficient μ	1.336 mm^{-1}
F(000)	4312
Reflections for cell refinement	43107 (θ range 1.68 to 28.37°)
Crystal colour	pale yellow
Crystal size	0.51 × 0.50 × 0.27 mm
Data collection method	Siemens SMART CCD diffractometer,
	ω rotation with narrow frames
θ range for data collection	1.38 to 28.41°
Index ranges	$-27 \le h \le 24$, $-21 \le k \le 23$, $-36 \le \ell \le 29$
Intensity decay of standards	0%
Reflections collected	61153
Independent reflections	20411 (R_{int} = 0.0413)
Reflections with I>2σ(I)	17043
Absorption correction	semi-empirical from ψ-scans
Max. and min. transmission	0.694 and 0.579
Structure solution	Patterson synthesis
Refinement method	full-matrix least-squares on F^2
Weighting parameters a, b	0.0326, 2.1605
Data / restraints / parameters	20411 / 2 / 1161
Goodness-of-fit on F^2	1.069
Final R indices [I>2σ(I)]	R1 = 0.0361, wR2 = 0.0718
R indices (all data)	R1 = 0.0514, wR2 = 0.0781
Absolute structure parameter	0.819(7)
Largest and mean shift/esd	0.040 and 0.001
Largest diff. peak and hole	0.899 and -1.081 $eÅ^{-3}$

Table A1.26 Atomic coordinates (x 10^4) and equivalent isotropic displacement parameters ($Å^2$ x 10^3) for **3.4**. U(eq) is defined as one third of the trace of the orthogonalised U_{ij} tensor.

	x	y	z	U(eq)
Sm(1)	2942.95(10)	6295.15(11)	2504.63(7)	21.37(5)
Sm(2)	2044.59(9)	10079.28(10)	2645.01(7)	20.41(5)
B(1)	2507(3)	5102(3)	1532(2)	31.0(13)
N(1)	2619.2(18)	6558(2)	1614.2(13)	27.0(8)
N(2)	2369.4(17)	5931(2)	1368.9(13)	26.1(8)
C(1)	2475(2)	7168(3)	1332.3(16)	28.6(10)
C(2)	2133(2)	6938(3)	926.1(17)	34.0(11)
C(3)	2066(2)	6154(3)	957.6(16)	31.5(10)
C(4)	2709(3)	7968(2)	1426.5(17)	36.5(11)
C(5)	1741(3)	5612(3)	618.3(17)	42.7(12)
N(3)	3546.3(18)	5381(2)	1982.0(13)	26.9(8)
N(4)	3216.3(18)	4986.7(19)	1628.1(14)	28.7(8)
C(6)	4151(2)	5113(2)	1975.1(19)	28.9(10)
C(7)	4197(3)	4560(3)	1607.4(18)	38.5(12)
C(8)	3613(2)	4488(2)	1401.4(17)	34.0(11)
C(9)	4653(2)	5348(3)	2311.6(19)	37.4(11)
C(10)	3403(3)	3971(3)	995(2)	51.2(14)
N(5)	2150.3(17)	5245(2)	2428.7(14)	31.0(9)
N(6)	2096.0(19)	4879(2)	1981.6(15)	31.7(9)
C(11)	1760(2)	4864(3)	2736.1(18)	36.7(11)
C(12)	1453(2)	4273(3)	2481(2)	41.9(12)
C(13)	1678(2)	4294(3)	2020(2)	42.7(12)
C(14)	1740(3)	5028(3)	3273(2)	58.1(17)
C(15)	1511(4)	3775(3)	1593(3)	75(2)
B(2)	3744(3)	6477(3)	3652.5(18)	27.3(11)
N(7)	3451.2(17)	5334(2)	3115.8(13)	26.5(8)
N(8)	3773.1(17)	5625(2)	3510.8(13)	26.8(8)
C(16)	3558(2)	4575(2)	3117.0(17)	30.0(10)
C(17)	3952(2)	4387(3)	3506.3(18)	35.9(11)
C(18)	4080(2)	5056(3)	3749.5(17)	31.1(10)
C(19)	3291(3)	4025(2)	2756(2)	48.7(14)
C(20)	4453(2)	5184(3)	4209.5(18)	42.1(12)
N(9)	2620.3(18)	6675(2)	3352.0(13)	28.3(8)
N(10)	3060.0(18)	6725(2)	3721.6(13)	31.1(9)
C(21)	2073(2)	6937(3)	3528.4(17)	36.7(11)
C(22)	2143(3)	7139(4)	4008.8(19)	55.6(16)
C(23)	2770(3)	7011(4)	4126(2)	56.5(16)
C(24)	1492(2)	6982(3)	3222(2)	50.6(14)
C(25)	3117(4)	7117(6)	4592(2)	112(4)
N(11)	3932.2(16)	6885.2(18)	2763.6(12)	27.3(8)
N(12)	4075.0(17)	6969.7(19)	3252.9(12)	26.3(8)
C(26)	4334.3(18)	7335(2)	2517.2(17)	27.0(8)
C(27)	4735(2)	7712(3)	2840.6(17)	32.4(10)
C(28)	4547(2)	7474(2)	3305.8(16)	30.2(10)
C(29)	4322(2)	7350(3)	1970.5(17)	34.6(11)
C(30)	4808(3)	7717(3)	3788.5(18)	44.8(13)
B(3)	2730(3)	10214(3)	3843.4(19)	27.4(11)
N(13)	3134.9(18)	9876.7(19)	2996.4(14)	29.2(8)
N(14)	3248.9(19)	9932.2(19)	3494.3(15)	29.7(9)
C(31)	3674(2)	9632(3)	2800.0(18)	34.8(11)
C(32)	4130(2)	9532(3)	3158(2)	46.2(13)

C(33)	3848(2)	9729(3)	3590(2)	40.8(12)
C(34)	3731(3)	9489(3)	2268(2)	50.0(14)
C(35)	4124(3)	9750(4)	4097(2)	65.2(18)
N(15)	2295.3(18)	11204.4(19)	3231.2(13)	26.0(8)
N(16)	2534.6(17)	11037(2)	3692.3(13)	24.8(8)
C(36)	2222(2)	11967(2)	3222.9(17)	29.1(10)
C(37)	2412(2)	12281(3)	3661.1(18)	34.7(11)
C(38)	2614(2)	11684(3)	3952.3(17)	31.9(10)
C(39)	1974(2)	12406(2)	2781.8(19)	38.1(13)
C(40)	2869(3)	11705(3)	4458.9(18)	43.9(13)
N(17)	1729.6(18)	9643.7(19)	3457.7(12)	26.2(8)
N(18)	2138.3(18)	9687(2)	3848.5(13)	29.0(8)
C(41)	1245(2)	9202(2)	3592.2(17)	31.0(10)
C(42)	1340(3)	8961(3)	4073.8(18)	41.5(12)
C(43)	1902(3)	9269(3)	4221.2(17)	40.9(13)
C(44)	701(2)	9070(3)	3257.5(18)	37.5(12)
C(45)	2233(3)	9198(4)	4702(2)	65.0(19)
B(4)	1243(3)	10960(3)	1662(2)	32.1(12)
N(19)	1340.2(16)	9568.8(19)	1948.2(13)	24.8(8)
N(20)	1184.5(18)	10090.0(19)	1586.5(14)	26.7(9)
C(46)	1133(2)	8890(2)	1779.1(16)	27.1(9)
C(47)	869(2)	8963(3)	1319.3(18)	33.8(11)
C(48)	904(2)	9732(3)	1207.1(15)	29.0(10)
C(49)	1161(2)	8166(2)	2075.9(17)	32.6(10)
C(50)	699(3)	10125(3)	746.5(18)	45.3(13)
N(21)	2368.9(18)	11041(2)	2023.0(13)	27.0(8)
N(22)	1940.9(18)	11226(2)	1658.1(13)	29.1(8)
C(51)	2891(2)	11465(3)	1937.7(19)	35.1(11)
C(52)	2810(3)	11898(3)	1516.7(18)	39.3(12)
C(53)	2217(3)	11738(3)	1349.9(17)	36.9(12)
C(54)	3452(2)	11477(3)	2278.6(19)	46.7(13)
C(55)	1887(3)	12032(3)	901.1(19)	52.6(15)
N(23)	1068.2(15)	10901.8(16)	2591.5(13)	26.8(7)
N(24)	906.0(18)	11201.5(19)	2139.2(14)	28.9(8)
C(56)	684(2)	11258(2)	2915.7(18)	29.5(10)
C(57)	284(2)	11763(2)	2681(2)	39.4(11)
C(58)	438(2)	11723(2)	2196.6(19)	35.2(11)
C(59)	718(2)	11114(3)	3453.0(19)	39.6(12)
C(60)	166(3)	12188(3)	1778(2)	50.9(14)
O(1)	2633.5(13)	7583.5(15)	2482.0(12)	30.4(6)
O(2)	2322.1(13)	8788.7(14)	2544.9(12)	30.2(6)
C(61)	2609(2)	8206(2)	2690.9(17)	34.4(10)
Mn(1)	4615.1(4)	11979.0(4)	248.7(3)	39.22(18)
C(62)	4453(2)	11346(3)	-266.2(19)	41.0(12)
O(62)	4341.3(18)	10950(2)	-587.3(13)	51.8(10)
C(63)	4862(4)	12950(4)	130(2)	71(2)
O(63)	5002(3)	13581(3)	40.0(17)	103(2)
C(64)	3797(3)	12280(3)	249.8(18)	42.7(12)
O(64)	3277(2)	12471(2)	255.4(15)	59.7(11)
C(65)	4508(3)	11642(3)	868(2)	42.7(12)
O(65)	4429(2)	11431(2)	1263.8(13)	58.5(11)
C(66)	5435(3)	11662(4)	263(2)	60.4(16)
O(66)	5954(2)	11449(3)	280(2)	91.5(16)
C(67)	5377(3)	8993(3)	1383(3)	59.0(16)
C(68)	5396(3)	8370(4)	1089(3)	66.5(18)
C(69)	5129(4)	8374(4)	621(3)	89(2)
C(70)	4860(4)	9045(5)	448(3)	90(2)
C(71)	4854(4)	9667(5)	733(3)	88(2)
C(72)	5087(3)	9656(4)	1199(3)	60.9(16)
C(73)	5667(4)	8999(4)	1871(2)	79(2)
C(74)	2749(3)	9856(3)	464(2)	43.0(13)
C(75)	3069(3)	10207(4)	89(2)	60.7(17)

O(1)-C(61)-O(2)	126.3(4)	C(63)-Mn(1)-C(64)	90.1(3)
C(63)-Mn(1)-C(65)	120.8(3)	C(64)-Mn(1)-C(65)	88.5(2)
C(63)-Mn(1)-C(66)	90.9(3)	C(64)-Mn(1)-C(66)	178.4(3)
C(65)-Mn(1)-C(66)	90.0(3)	C(63)-Mn(1)-C(62)	119.0(3)
C(64)-Mn(1)-C(62)	89.9(2)	C(65)-Mn(1)-C(62)	120.2(2)
C(66)-Mn(1)-C(62)	90.6(3)	O(62)-C(62)-Mn(1)	179.0(5)
O(63)-C(63)-Mn(1)	177.3(7)	O(64)-C(64)-Mn(1)	179.3(5)
O(65)-C(65)-Mn(1)	178.9(5)	O(66)-C(66)-Mn(1)	178.5(6)
C(68)-C(67)-C(72)	117.7(7)	C(68)-C(67)-C(73)	122.2(7)
C(72)-C(67)-C(73)	120.1(6)	C(67)-C(68)-C(69)	121.9(7)
C(70)-C(69)-C(68)	118.8(7)	C(71)-C(70)-C(69)	119.4(8)
C(70)-C(71)-C(72)	122.0(8)	C(71)-C(72)-C(67)	120.1(7)
C(75)-C(74)-C(79)	118.5(6)	C(75)-C(74)-C(80)	120.3(5)
C(79)-C(74)-C(80)	121.1(5)	C(76)-C(75)-C(74)	120.7(6)
C(77)-C(76)-C(75)	121.5(7)	C(76)-C(77)-C(78)	119.0(7)
C(77)-C(78)-C(79)	120.3(6)	C(74)-C(79)-C(78)	119.9(6)
C(86)-C(81)-C(82)	118.5(5)	C(86)-C(81)-C(87)	121.7(5)
C(82)-C(81)-C(87)	119.9(5)	C(83)-C(82)-C(81)	120.2(6)
C(84)-C(83)-C(82)	121.0(6)	C(83)-C(84)-C(85)	119.7(6)
C(86)-C(85)-C(84)	118.7(5)	C(81)-C(86)-C(85)	121.9(5)
C(89)-C(88)-C(93)	120.0	C(89)-C(88)-C(94)	125.0
C(93)-C(88)-C(94)	115.0	C(88)-C(89)-C(90)	120.0
C(89)-C(90)-C(91)	120.0	C(90)-C(91)-C(92)	120.0
C(93)-C(92)-C(91)	120.0	C(92)-C(93)-C(88)	120.0

Table A1.27 Bond lengths (Å) and angles (°) for **3.4**.

Sm(1)-O(1)	2.344(3)	Sm(1)-N(11)	2.435(3)
Sm(1)-N(5)	2.492(4)	Sm(1)-N(3)	2.493(4)
Sm(1)-N(9)	2.504(4)	Sm(1)-N(1)	2.570(4)
Sm(1)-N(7)	2.601(3)	Sm(2)-O(2)	2.345(2)
Sm(2)-N(17)	2.441(3)	Sm(2)-N(21)	2.486(3)
Sm(2)-N(23)	2.518(3)	Sm(2)-N(13)	2.520(4)
Sm(2)-N(19)	2.577(3)	Sm(2)-N(15)	2.591(3)
B(1)-N(4)	1.535(7)	B(1)-N(2)	1.542(6)
B(1)-N(6)	1.554(7)	N(1)-C(1)	1.350(5)
N(1)-N(2)	1.389(5)	N(2)-C(3)	1.352(5)
C(1)-C(2)	1.385(6)	C(1)-C(4)	1.504(6)
C(2)-C(3)	1.380(7)	C(3)-C(5)	1.493(6)
N(3)-C(6)	1.360(6)	N(3)-N(4)	1.377(5)
N(4)-C(8)	1.359(5)	C(6)-C(7)	1.398(7)
C(6)-C(9)	1.463(7)	C(7)-C(8)	1.362(7)
C(8)-C(10)	1.500(7)	N(5)-C(11)	1.352(6)
N(5)-N(6)	1.384(5)	N(6)-C(13)	1.355(6)
C(11)-C(12)	1.405(7)	C(11)-C(14)	1.496(7)
C(12)-C(13)	1.348(8)	C(13)-C(15)	1.520(8)
B(2)-N(10)	1.520(6)	B(2)-N(8)	1.540(6)
B(2)-N(12)	1.556(6)	N(7)-C(16)	1.345(5)
N(7)-N(8)	1.374(5)	N(8)-C(18)	1.354(5)
C(16)-C(17)	1.391(6)	C(16)-C(19)	1.489(6)
C(17)-C(18)	1.371(7)	C(18)-C(20)	1.502(6)
N(9)-C(21)	1.334(6)	N(9)-N(10)	1.375(5)
N(10)-C(23)	1.359(6)	C(21)-C(22)	1.368(7)
C(21)-C(24)	1.487(7)	C(22)-C(23)	1.382(8)
C(23)-C(25)	1.482(9)	N(11)-C(26)	1.339(5)
N(11)-N(12)	1.379(5)	N(12)-C(28)	1.339(5)
C(26)-C(27)	1.390(6)	C(26)-C(29)	1.495(6)
C(27)-C(28)	1.395(7)	C(28)-C(30)	1.492(6)
B(3)-N(14)	1.535(7)	B(3)-N(18)	1.551(6)
B(3)-N(16)	1.553(6)	N(13)-C(31)	1.330(6)
N(13)-N(14)	1.386(5)	N(14)-C(33)	1.341(6)
C(31)-C(32)	1.384(7)	C(31)-C(34)	1.479(7)
C(32)-C(33)	1.367(8)	C(33)-C(35)	1.504(7)
N(15)-C(36)	1.341(5)	N(15)-N(16)	1.389(5)
N(16)-C(38)	1.345(5)	C(36)-C(37)	1.378(6)
C(36)-C(39)	1.522(6)	C(37)-C(38)	1.381(6)
C(38)-C(40)	1.487(6)	N(17)-C(41)	1.334(6)
N(17)-N(18)	1.376(5)	N(18)-C(43)	1.350(6)
C(41)-C(42)	1.397(6)	C(41)-C(44)	1.487(7)
C(42)-C(43)	1.365(7)	C(43)-C(45)	1.494(7)
B(4)-N(20)	1.539(6)	B(4)-N(24)	1.545(7)
B(4)-N(22)	1.546(7)	N(19)-C(46)	1.346(5)
N(19)-N(20)	1.384(5)	N(20)-C(48)	1.348(5)
C(46)-C(47)	1.381(6)	C(46)-C(49)	1.503(6)
C(47)-C(48)	1.381(6)	C(48)-C(50)	1.498(6)
N(21)-C(51)	1.349(6)	N(21)-N(22)	1.385(5)
N(22)-C(53)	1.360(6)	C(51)-C(52)	1.388(7)
C(51)-C(54)	1.508(7)	C(52)-C(53)	1.362(7)
C(53)-C(55)	1.502(7)	N(23)-C(56)	1.353(5)
N(23)-N(24)	1.386(5)	N(24)-C(58)	1.354(6)
C(56)-C(57)	1.379(6)	C(56)-C(59)	1.492(7)
C(57)-C(58)	1.366(7)	C(58)-C(60)	1.517(7)
O(1)-C(61)	1.230(5)	O(2)-C(61)	1.250(5)
Mn(1)-C(63)	1.804(6)	Mn(1)-C(64)	1.805(6)
Mn(1)-C(65)	1.808(6)	Mn(1)-C(66)	1.818(7)

Mn(1)-C(62)	1.823(5)	C(62)-O(62)	1.141(6)
C(63)-O(63)	1.166(7)	C(64)-O(64)	1.150(6)
C(65)-O(65)	1.155(6)	C(66)-O(66)	1.159(7)
C(67)-C(68)	1.353(9)	C(67)-C(72)	1.403(8)
C(67)-C(73)	1.470(9)	C(68)-C(69)	1.395(10)
C(69)-C(70)	1.385(10)	C(70)-C(71)	1.339(11)
C(71)-C(72)	1.366(10)	C(74)-C(75)	1.373(7)
C(74)-C(79)	1.383(8)	C(74)-C(80)	1.502(8)
C(75)-C(76)	1.360(10)	C(76)-C(77)	1.358(10)
C(77)-C(78)	1.368(10)	C(78)-C(79)	1.391(10)
C(81)-C(86)	1.364(7)	C(81)-C(82)	1.379(7)
C(81)-C(87)	1.524(7)	C(82)-C(83)	1.370(8)
C(83)-C(84)	1.361(9)	C(84)-C(85)	1.383(8)
C(85)-C(86)	1.378(8)	C(88)-C(89)	1.3900
C(88)-C(93)	1.3900	C(88)-C(94)	1.4645
C(89)-C(90)	1.3900	C(90)-C(91)	1.3900
C(91)-C(92)	1.3900	C(92)-C(93)	1.3900

O(1)-Sm(1)-N(11)	80.83(10)	O(1)-Sm(1)-N(5)	121.15(11)
N(11)-Sm(1)-N(5)	155.80(11)	O(1)-Sm(1)-N(3)	137.92(11)
N(11)-Sm(1)-N(3)	89.96(12)	N(5)-Sm(1)-N(3)	79.87(12)
O(1)-Sm(1)-N(9)	72.21(11)	N(11)-Sm(1)-N(9)	81.52(12)
N(5)-Sm(1)-N(9)	95.11(12)	N(3)-Sm(1)-N(9)	147.02(12)
O(1)-Sm(1)-N(1)	74.30(11)	N(11)-Sm(1)-N(1)	115.35(12)
N(5)-Sm(1)-N(1)	82.75(12)	N(3)-Sm(1)-N(1)	72.98(12)
N(9)-Sm(1)-N(1)	139.17(11)	O(1)-Sm(1)-N(7)	138.75(11)
N(11)-Sm(1)-N(7)	74.47(11)	N(5)-Sm(1)-N(7)	81.69(12)
N(3)-Sm(1)-N(7)	75.16(11)	N(9)-Sm(1)-N(7)	71.87(11)
N(1)-Sm(1)-N(7)	146.48(11)	O(2)-Sm(2)-N(17)	82.80(12)
O(2)-Sm(2)-N(21)	120.04(12)	N(17)-Sm(2)-N(21)	155.26(12)
O(2)-Sm(2)-N(23)	138.29(10)	N(17)-Sm(2)-N(23)	90.43(12)
N(21)-Sm(2)-N(23)	78.49(11)	O(2)-Sm(2)-N(13)	71.41(10)
N(17)-Sm(2)-N(13)	81.85(12)	N(21)-Sm(2)-N(13)	95.96(12)
N(23)-Sm(2)-N(13)	148.29(11)	O(2)-Sm(2)-N(19)	74.06(10)
N(17)-Sm(2)-N(19)	114.07(12)	N(21)-Sm(2)-N(19)	83.52(11)
N(23)-Sm(2)-N(19)	71.44(11)	N(13)-Sm(2)-N(19)	139.54(11)
O(2)-Sm(2)-N(15)	138.62(11)	N(17)-Sm(2)-N(15)	74.28(11)
N(21)-Sm(2)-N(15)	81.63(11)	N(23)-Sm(2)-N(15)	76.73(11)
N(13)-Sm(2)-N(15)	71.58(11)	N(19)-Sm(2)-N(15)	146.93(11)
N(4)-B(1)-N(2)	110.9(4)	N(4)-B(1)-N(6)	112.2(4)
N(2)-B(1)-N(6)	111.0(4)	C(1)-N(1)-N(2)	105.2(3)
C(1)-N(1)-Sm(1)	137.9(3)	N(2)-N(1)-Sm(1)	114.7(2)
C(3)-N(2)-N(1)	110.7(3)	C(3)-N(2)-B(1)	126.9(4)
N(1)-N(2)-B(1)	122.0(4)	N(1)-C(1)-C(2)	110.3(4)
N(1)-C(1)-C(4)	124.2(4)	C(2)-C(1)-C(4)	125.3(4)
C(3)-C(2)-C(1)	106.9(4)	N(2)-C(3)-C(2)	106.9(4)
N(2)-C(3)-C(5)	123.5(4)	C(2)-C(3)-C(5)	129.6(4)
C(6)-N(3)-N(4)	107.1(4)	C(6)-N(3)-Sm(1)	135.1(3)
N(4)-N(3)-Sm(1)	117.7(3)	C(8)-N(4)-N(3)	109.2(4)
C(8)-N(4)-B(1)	127.5(4)	N(3)-N(4)-B(1)	123.3(3)
N(3)-C(6)-C(7)	108.3(4)	N(3)-C(6)-C(9)	125.1(4)
C(7)-C(6)-C(9)	126.6(4)	C(8)-C(7)-C(6)	107.3(4)
N(4)-C(8)-C(7)	108.1(4)	N(4)-C(8)-C(10)	122.8(5)
C(7)-C(8)-C(10)	129.1(5)	C(11)-N(5)-N(6)	105.7(3)
C(11)-N(5)-Sm(1)	136.1(3)	N(6)-N(5)-Sm(1)	118.0(3)
C(13)-N(6)-N(5)	109.5(4)	C(13)-N(6)-B(1)	127.9(4)
N(5)-N(6)-B(1)	122.5(3)	N(5)-C(11)-C(12)	109.6(4)
N(5)-C(11)-C(14)	122.1(4)	C(12)-C(11)-C(14)	128.0(4)
C(13)-C(12)-C(11)	106.3(4)	C(12)-C(13)-N(6)	108.9(5)
C(12)-C(13)-C(15)	128.3(5)	N(6)-C(13)-C(15)	122.8(5)
N(10)-B(2)-N(8)	110.1(4)	N(10)-B(2)-N(12)	110.9(4)
N(8)-B(2)-N(12)	109.9(4)	C(16)-N(7)-N(8)	106.2(3)

C(16)-N(7)-Sm(1)	135.0(3)	N(8)-N(7)-Sm(1)	118.1(2)
C(18)-N(8)-N(7)	110.1(3)	C(18)-N(8)-B(2)	127.4(4)
N(7)-N(8)-B(2)	122.4(3)	N(7)-C(16)-C(17)	109.6(4)
N(7)-C(16)-C(19)	124.8(4)	C(17)-C(16)-C(19)	125.6(4)
C(18)-C(17)-C(16)	106.7(4)	N(8)-C(18)-C(17)	107.4(4)
N(8)-C(18)-C(20)	123.0(4)	C(17)-C(18)-C(20)	129.5(4)
C(21)-N(9)-N(10)	107.3(4)	C(21)-N(9)-Sm(1)	131.4(3)
N(10)-N(9)-Sm(1)	120.9(3)	C(23)-N(10)-N(9)	108.5(4)
C(23)-N(10)-B(2)	129.3(4)	N(9)-N(10)-B(2)	122.2(3)
N(9)-C(21)-C(22)	110.0(4)	N(9)-C(21)-C(24)	121.9(4)
C(22)-C(21)-C(24)	128.1(5)	C(21)-C(22)-C(23)	106.5(5)
N(10)-C(23)-C(22)	107.6(5)	N(10)-C(23)-C(25)	121.6(5)
C(22)-C(23)-C(25)	130.8(5)	C(26)-N(11)-N(12)	106.6(3)
C(26)-N(11)-Sm(1)	130.3(3)	N(12)-N(11)-Sm(1)	121.0(3)
C(28)-N(12)-N(11)	109.8(3)	C(28)-N(12)-B(2)	128.5(4)
N(11)-N(12)-B(2)	121.6(3)	N(11)-C(26)-C(27)	110.1(4)
N(11)-C(26)-C(29)	120.2(4)	C(27)-C(26)-C(29)	129.6(4)
C(26)-C(27)-C(28)	105.4(4)	N(12)-C(28)-C(27)	108.0(4)
N(12)-C(28)-C(30)	123.9(4)	C(27)-C(28)-C(30)	128.1(4)
N(14)-B(3)-N(18)	113.0(4)	N(14)-B(3)-N(16)	108.7(4)
N(18)-B(3)-N(16)	109.8(4)	C(31)-N(13)-N(14)	105.7(4)
C(31)-N(13)-Sm(2)	132.4(3)	N(14)-N(13)-Sm(2)	121.6(3)
C(33)-N(14)-N(13)	109.7(4)	C(33)-N(14)-B(3)	129.6(4)
N(13)-N(14)-B(3)	120.6(4)	N(13)-C(31)-C(32)	110.5(4)
N(13)-C(31)-C(34)	121.4(5)	C(32)-C(31)-C(34)	128.1(5)
C(33)-C(32)-C(31)	106.1(4)	N(14)-C(33)-C(32)	108.0(5)
N(14)-C(33)-C(35)	122.7(5)	C(32)-C(33)-C(35)	129.4(5)
C(36)-N(15)-N(16)	105.4(3)	C(36)-N(15)-Sm(2)	136.0(3)
N(16)-N(15)-Sm(2)	118.5(2)	C(38)-N(16)-N(15)	110.4(4)
C(38)-N(16)-B(3)	127.2(4)	N(15)-N(16)-B(3)	122.2(3)
N(15)-C(36)-C(37)	110.3(4)	N(15)-C(36)-C(39)	123.6(4)
C(37)-C(36)-C(39)	126.1(4)	C(36)-C(37)-C(38)	106.9(4)
N(16)-C(38)-C(37)	106.9(4)	N(16)-C(38)-C(40)	124.0(4)
C(37)-C(38)-C(40)	129.0(4)	C(41)-N(17)-N(18)	107.4(3)
C(41)-N(17)-Sm(2)	129.8(3)	N(18)-N(17)-Sm(2)	121.2(3)
C(43)-N(18)-N(17)	108.9(4)	C(43)-N(18)-B(3)	128.7(4)
N(17)-N(18)-B(3)	122.1(3)	N(17)-C(41)-C(42)	108.9(4)
N(17)-C(41)-C(44)	120.9(4)	C(42)-C(41)-C(44)	130.1(4)
C(43)-C(42)-C(41)	106.5(4)	N(18)-C(43)-C(42)	108.2(4)
N(18)-C(43)-C(45)	122.4(5)	C(42)-C(43)-C(45)	129.4(5)
N(20)-B(4)-N(24)	110.2(4)	N(20)-B(4)-N(22)	111.9(4)
N(24)-B(4)-N(22)	111.3(4)	C(46)-N(19)-N(20)	104.9(3)
C(46)-N(19)-Sm(2)	138.3(3)	N(20)-N(19)-Sm(2)	116.0(2)
C(48)-N(20)-N(19)	110.5(3)	C(48)-N(20)-B(4)	126.6(4)
N(19)-N(20)-B(4)	122.3(4)	N(19)-C(46)-C(47)	111.2(4)
N(19)-C(46)-C(49)	122.9(4)	C(47)-C(46)-C(49)	125.8(4)
C(48)-C(47)-C(46)	105.7(4)	N(20)-C(48)-C(47)	107.6(4)
N(20)-C(48)-C(50)	124.2(4)	C(47)-C(48)-C(50)	128.1(4)
C(51)-N(21)-N(22)	106.3(3)	C(51)-N(21)-Sm(2)	135.6(3)
N(22)-N(21)-Sm(2)	118.1(3)	C(53)-N(22)-N(21)	108.7(4)
C(53)-N(22)-B(4)	127.6(4)	N(21)-N(22)-B(4)	123.2(3)
N(21)-C(51)-C(52)	110.0(4)	N(21)-C(51)-C(54)	122.9(4)
C(52)-C(51)-C(54)	127.0(4)	C(53)-C(52)-C(51)	106.2(4)
N(22)-C(53)-C(52)	108.8(4)	N(22)-C(53)-C(55)	122.1(5)
C(52)-C(53)-C(55)	129.1(5)	C(56)-N(23)-N(24)	105.2(3)
C(56)-N(23)-Sm(2)	135.7(3)	N(24)-N(23)-Sm(2)	118.0(2)
C(58)-N(24)-N(23)	109.3(4)	C(58)-N(24)-B(4)	128.2(4)
N(23)-N(24)-B(4)	122.5(3)	N(23)-C(56)-C(57)	110.9(4)
N(23)-C(56)-C(59)	122.6(4)	C(57)-C(56)-C(59)	126.5(4)
C(58)-C(57)-C(56)	105.8(4)	N(24)-C(58)-C(57)	108.7(4)
N(24)-C(58)-C(60)	123.4(5)	C(57)-C(58)-C(60)	127.9(5)
C(61)-O(1)-Sm(1)	148.1(3)	C(61)-O(2)-Sm(2)	150.0(3)

O(1)-C(61)-O(2)	126.3(4)	C(63)-Mn(1)-C(64)	90.1(3)
C(63)-Mn(1)-C(65)	120.8(3)	C(64)-Mn(1)-C(65)	88.5(2)
C(63)-Mn(1)-C(66)	90.9(3)	C(64)-Mn(1)-C(66)	178.4(3)
C(65)-Mn(1)-C(66)	90.0(3)	C(63)-Mn(1)-C(62)	119.0(3)
C(64)-Mn(1)-C(62)	89.9(2)	C(65)-Mn(1)-C(62)	120.2(2)
C(66)-Mn(1)-C(62)	90.6(3)	O(62)-C(62)-Mn(1)	179.0(5)
O(63)-C(63)-Mn(1)	177.3(7)	O(64)-C(64)-Mn(1)	179.3(5)
O(65)-C(65)-Mn(1)	178.9(5)	O(66)-C(66)-Mn(1)	178.5(6)
C(68)-C(67)-C(72)	117.7(7)	C(68)-C(67)-C(73)	122.2(7)
C(72)-C(67)-C(73)	120.1(6)	C(67)-C(68)-C(69)	121.9(7)
C(70)-C(69)-C(68)	118.8(7)	C(71)-C(70)-C(69)	119.4(8)
C(70)-C(71)-C(72)	122.0(8)	C(71)-C(72)-C(67)	120.1(7)
C(75)-C(74)-C(79)	118.5(6)	C(75)-C(74)-C(80)	120.3(5)
C(79)-C(74)-C(80)	121.1(5)	C(76)-C(75)-C(74)	120.7(6)
C(77)-C(76)-C(75)	121.5(7)	C(76)-C(77)-C(78)	119.0(7)
C(77)-C(78)-C(79)	120.3(6)	C(74)-C(79)-C(78)	119.9(6)
C(86)-C(81)-C(82)	118.5(5)	C(86)-C(81)-C(87)	121.7(5)
C(82)-C(81)-C(87)	119.9(5)	C(83)-C(82)-C(81)	120.2(6)
C(84)-C(83)-C(82)	121.0(6)	C(83)-C(84)-C(85)	119.7(6)
C(86)-C(85)-C(84)	118.7(5)	C(81)-C(86)-C(85)	121.9(5)
C(89)-C(88)-C(93)	120.0	C(89)-C(88)-C(94)	125.0
C(93)-C(88)-C(94)	115.0	C(88)-C(89)-C(90)	120.0
C(89)-C(90)-C(91)	120.0	C(90)-C(91)-C(92)	120.0
C(93)-C(92)-C(91)	120.0	C(92)-C(93)-C(88)	120.0

Table A1.28 Crystal data, structure solution and refinement for **3.5**.

Crystal Data: $C_{47}H_{44}B_2N_{12}O_{17}Re_4Sm$, yellow crystal of dimensions 0.24 × 0.20 × 0.04 mm, M = 1965.71, triclinic space groupP1, a = 10.4574(7), b = 11.4168(8), c = 26.1519(19) Å, α = 88.088(2)°, β = 78.298(2)°, γ = 78.804(2)°, U = 2999.1(4)Å^3, Z = 2, F(000) = 1836, D_c = 2.177 g cm^{-1}, μ(Mo-Kα) = 9.081 mm^{-1}, 2θmax = 50.00°, T = 160K.

Data collection, structure solution and refinement: 18308 reflections (10312 unique with R_{int} = 0.0418) were collected on a Bruker AXS SMART CCD area detector diffractometer with narrow frames (0.3° in ω) and three dimensional profile fitting using graphite monochromated Mo-Ka radiation (λ = 0.71073 Å). Data were corrected semi-empirically for absorption based on symmetry equivalent and repeated reflections. Cell parameters were refined by locally written software from the observed w angles of 14076 reflections in the range $1.82 < \theta < 28.36°$ with $I > 10\sigma(I)$. The structure was solved by direct methods and refined by full-matrix least-squares on F^2 values. All non-H atoms were refined anisotropically, H atoms were constrained. Final $wR^2 = \{\Sigma[w(F_o^2 - F_c^2)^2]/\Sigma[w(F_o^2)^2]\} = 0.1118$ {where $w^{-1} = \sigma^2(F_o^2) + (\alpha P)^2 + \beta P$ and $P = (F_o^2 + 2F_c^2)/3$} for 763 refined parameters, conventional $R = 0.0453$ [for F values of 7686 data with $F^2 > 4\sigma(F^2)$]. The largest features in the final difference synthesis were within ±2.65 eÅ^{-3}, close to the metal atoms. Programs: SHELXTL[a] for structure solution and refinement and molecular graphics, Bruker AXS SMART (control), and SAINT (integration) and local programs.[b]

a. Sheldrick, G.M. SHELXTL user manual, version 5; Bruker AXS Inc.: Madison, WI, 1994.
b. SMART and SAINT software for CCD diffractometers; Bruker AXS Inc.: Madison, WI, 1994.

Table A1.29 Atomic coordinates (x 10^4) and equivalent isotropic displacement parameters ($Å^2$ x 10^3) for **3.5**. U(eq) is defined as one third of the trace of the orthogonalised U_{ij} tensor.

	x	y	z	U(eq)
Sm(1)	0	5000	0	37.8(2)
N(1)	1343(9)	4446(8)	676(4)	36(2)
N(2)	2432(8)	3513(7)	575(4)	27(2)
C(1)	1107(11)	4624(10)	1198(5)	38(3)
C(2)	1949(12)	3851(9)	1426(5)	37(3)
C(3)	2811(10)	3132(9)	1031(4)	27(2)
C(4)	5(14)	5629(12)	1440(6)	65(4)
C(5)	3911(12)	2127(10)	1070(5)	41(3)
N(3)	737(9)	2851(8)	-158(4)	36(2)
N(4)	2036(8)	2302(7)	-147(4)	30(2)
C(6)	130(11)	2010(10)	-295(5)	42(3)
C(7)	1043(13)	927(10)	-376(5)	42(3)
C(8)	2205(11)	1142(9)	-276(5)	34(3)
C(9)	-1292(13)	2266(12)	-335(7)	65(5)
C(10)	3479(11)	262(10)	-269(5)	42(3)
N(5)	2235(9)	4850(8)	-506(4)	42(3)
N(6)	3287(8)	4025(8)	-377(4)	30(2)
C(11)	2787(12)	5590(11)	-857(5)	47(3)
C(12)	4144(12)	5284(11)	-932(5)	42(3)
C(13)	4421(10)	4289(10)	-628(4)	30(3)
C(14)	1945(13)	6592(13)	-1088(6)	69(5)
C(15)	5741(10)	3623(11)	-548(5)	45(3)

B(1)	3022(12)	3001(11)	17(5)	32(3)
Sm(2)	5000	5000	5000	26.12(19)
N(7)	7233(8)	4336(7)	5162(3)	25(2)
N(8)	7768(8)	5015(7)	5461(4)	26(2)
C(16)	8124(12)	3299(9)	5061(4)	31(3)
C(17)	9210(12)	3326(11)	5283(5)	44(3)
C(18)	8944(10)	4393(10)	5541(5)	33(3)
C(19)	7879(13)	2337(10)	4740(5)	51(4)
C(20)	9773(12)	4852(12)	5868(5)	51(4)
N(9)	5906(8)	6818(7)	4899(3)	25(2)
N(10)	6613(8)	7107(7)	5258(3)	22.9(19)
C(21)	5688(10)	7796(9)	4601(4)	30(3)
C(22)	6255(11)	8684(9)	4765(4)	31(3)
C(23)	6795(10)	8233(8)	5189(4)	24(2)
C(24)	4945(11)	7791(11)	4173(4)	37(3)
C(25)	7462(13)	8850(10)	5518(5)	42(3)
N(11)	4729(8)	5586(7)	5921(3)	26(2)
N(12)	5712(8)	6062(7)	6086(3)	22.8(19)
C(26)	3783(11)	5561(9)	6352(4)	28(3)
C(27)	4132(11)	5985(9)	6778(4)	28(3)
C(28)	5359(11)	6296(9)	6604(4)	27(2)
C(29)	2557(11)	5100(11)	6318(5)	39(3)
C(30)	6179(14)	6827(12)	6907(5)	48(3)
B(2)	6986(11)	6230(10)	5688(5)	23(3)
Re(1)	-1206.9(4)	10152.6(3)	3345.53(17)	25.45(13)
Re(2)	-906.3(4)	10653.1(4)	2172.36(17)	26.03(13)
Re(3)	1432.0(4)	9187.3(4)	2605.60(17)	23.57(12)
Re(4)	4236.2(4)	7719.5(4)	2463.05(18)	26.65(13)
C(31)	-1908(11)	8702(11)	3253(4)	35(3)

O(31)	-2359(9)	7872(8)	3216(4)	57(3)
C(32)	-800(10)	9601(9)	3995(5)	37(3)
O(32)	-578(8)	9333(7)	4427(3)	45(2)
C(33)	-2914(12)	10930(9)	3710(4)	34(3)
O(33)	-3974(8)	11349(7)	3941(3)	48(2)
C(34)	-346(11)	11523(10)	3407(4)	30(3)
O(34)	193(9)	12280(7)	3465(3)	45(2)
C(35)	-1255(11)	9052(11)	2040(4)	34(3)
O(35)	-1482(9)	8152(8)	1953(4)	57(3)
C(36)	-2587(13)	11364(11)	2008(5)	40(3)
O(36)	-3614(9)	11710(9)	1912(4)	63(3)
C(37)	22(11)	10788(10)	1469(5)	35(3)
O(37)	564(9)	10923(7)	1037(3)	46(2)
C(38)	-549(11)	12239(10)	2331(4)	30(3)
O(38)	-432(9)	13191(7)	2407(3)	46(2)
C(39)	789(11)	7663(11)	2752(5)	37(3)
O(39)	494(9)	6750(7)	2837(4)	58(3)
C(40)	1769(13)	8793(11)	1863(4)	46(3)
O(40)	2062(11)	8532(10)	1429(4)	91(4)
C(41)	1793(10)	9284(9)	3305(4)	25(2)
O(41)	2118(8)	9299(7)	3712(3)	41(2)
C(42)	2086(11)	10713(11)	2452(5)	37(3)
O(42)	2515(8)	11550(7)	2359(4)	47(2)
C(43)	3534(12)	6568(10)	2101(5)	43(3)
O(43)	3130(9)	5884(9)	1905(4)	65(3)
C(44)	4697(14)	8617(12)	1799(6)	58(4)
O(44)	4921(12)	9130(10)	1433(4)	94(4)
C(45)	5974(12)	6714(10)	2381(5)	37(3)
O(45)	7006(8)	6085(7)	2322(4)	60(3)

C(46)	3551(10)	6931(8)	3140(5)	26(2)
O(46)	3135(8)	6489(7)	3499(3)	40(2)
C(47)	4695(11)	9035(11)	2828(5)	42(3)
O(47)	4926(9)	9803(8)	3040(4)	54(3)

Table A1.30 Bond lengths (Å) and angles (°) for **3.5**.

Sm(1)-N(5a)	2.418(9)
Sm(1)-N(5)	2.418(9)
Sm(1)-N(3)	2.447(9)
Sm(1)-N(3a)	2.447(9)
Sm(1)-N(1a)	2.467(10)
Sm(1)-N(1)	2.467(10)
N(1)-C(1)	1.352(15)
N(1)-N(2)	1.388(11)
N(2)-C(3)	1.365(13)
N(2)-B(1)	1.550(15)
C(1)-C(2)	1.337(16)
C(1)-C(4)	1.512(15)
C(2)-C(3)	1.395(15)
C(3)-C(5)	1.476(14)
N(3)-C(6)	1.343(14)
N(3)-N(4)	1.387(11)
N(4)-C(8)	1.347(13)
N(4)-B(1)	1.551(16)
C(6)-C(7)	1.401(16)
C(6)-C(9)	1.484(16)
C(7)-C(8)	1.361(16)
C(8)-C(10)	1.509(14)

N(5)-C(11)	1.347(15)
N(5)-N(6)	1.392(12)
N(6)-C(13)	1.319(13)
N(6)-B(1)	1.559(15)
C(11)-C(12)	1.369(16)
C(11)-C(14)	1.492(16)
C(12)-C(13)	1.383(16)
C(13)-C(15)	1.492(15)
Sm(2)-N(9a')	2.429(8)
Sm(2)-N(9)	2.429(8)
Sm(2)-N(7a')	2.429(8)
Sm(2)-N(7)	2.429(8)
Sm(2)-N(11a')	2.468(9)
Sm(2)-N(11)	2.468(9)
N(7)-C(16)	1.353(13)
N(7)-N(8)	1.382(11)
N(8)-C(18)	1.348(13)
N(8)-B(2)	1.537(14)
C(16)-C(17)	1.382(17)
C(16)-C(19)	1.496(16)
C(17)-C(18)	1.366(17)
C(18)-C(20)	1.505(17)
N(9)-C(21)	1.349(12)
N(9)-N(10)	1.390(11)
N(10)-C(23)	1.337(12)
N(10)-B(2)	1.541(13)
C(21)-C(22)	1.388(15)
C(21)-C(24)	1.488(15)
C(22)-C(23)	1.385(15)

C(23)-C(25)	1.484(15)
N(11)-C(26)	1.344(13)
N(11)-N(12)	1.396(11)
N(12)-C(28)	1.352(13)
N(12)-B(2)	1.555(14)
C(26)-C(27)	1.369(15)
C(26)-C(29)	1.497(14)
C(27)-C(28)	1.381(14)
C(28)-C(30)	1.496(15)
Re(1)-C(32)	1.892(14)
Re(1)-C(33)	1.907(11)
Re(1)-C(34)	1.976(13)
Re(1)-C(31)	1.978(13)
Re(1)-Re(3)	3.0610(6)
Re(1)-Re(2)	3.0659(6)
Re(2)-C(36)	1.914(12)
Re(2)-C(37)	1.915(13)
Re(2)-C(35)	1.986(12)
Re(2)-C(38)	1.991(12)
Re(2)-Re(3)	3.0776(6)
Re(3)-C(41)	1.952(11)
Re(3)-C(40)	1.953(12)
Re(3)-C(39)	1.983(13)
Re(3)-C(42)	1.992(12)
Re(3)-Re(4)	3.0392(6)
Re(4)-C(45)	1.927(12)
Re(4)-C(43)	1.975(14)
Re(4)-C(47)	1.990(15)
Re(4)-C(44)	2.007(15)

Re(4)-C(46)	2.021(12)
C(31)-O(31)	1.153(13)
C(32)-O(32)	1.216(15)
C(33)-O(33)	1.168(13)
C(34)-O(34)	1.149(13)
C(35)-O(35)	1.139(13)
C(36)-O(36)	1.144(14)
C(37)-O(37)	1.175(14)
C(38)-O(38)	1.145(12)
C(39)-O(39)	1.145(13)
C(40)-O(40)	1.149(14)
C(41)-O(41)	1.182(12)
C(42)-O(42)	1.131(13)
C(43)-O(43)	1.138(15)
C(44)-O(44)	1.115(16)
C(45)-O(45)	1.158(13)
C(46)-O(46)	1.102(12)
C(47)-O(47)	1.141(14)

N(5a)-Sm(1)-N(5)	180.0(6)
N(5a)-Sm(1)-N(3)	103.0(3)
N(5)-Sm(1)-N(3)	77.0(3)
N(5a)-Sm(1)-N(3a)	77.0(3)
N(5)-Sm(1)-N(3a)	103.0(3)
N(3)-Sm(1)-N(3a)	180.000(1)
N(5a)-Sm(1)-N(1a)	78.4(3)
N(5)-Sm(1)-N(1a)	101.6(3)
N(3)-Sm(1)-N(1a)	101.1(3)

N(3a)-Sm(1)-N(1a)78.9(3)

N(5a)-Sm(1)-N(1)101.6(3)

N(5)-Sm(1)-N(1) 78.4(3)

N(3)-Sm(1)-N(1) 78.9(3)

N(3a)-Sm(1)-N(1)101.1(3)

N(1a)-Sm(1)-N(1)180.0(5)

C(1)-N(1)-N(2) 105.0(9)

C(1)-N(1)-Sm(1)133.8(7)

N(2)-N(1)-Sm(1)118.8(7)

C(3)-N(2)-N(1) 109.6(9)

C(3)-N(2)-B(1) 128.3(9)

N(1)-N(2)-B(1) 122.0(9)

C(2)-C(1)-N(1) 111.9(10)

C(2)-C(1)-C(4) 129.2(13)

N(1)-C(1)-C(4) 118.9(11)

C(1)-C(2)-C(3) 107.0(11)

N(2)-C(3)-C(2) 106.5(10)

N(2)-C(3)-C(5) 124.2(10)

C(2)-C(3)-C(5) 129.3(11)

C(6)-N(3)-N(4) 106.9(9)

C(6)-N(3)-Sm(1)132.3(7)

N(4)-N(3)-Sm(1)120.6(6)

C(8)-N(4)-N(3) 108.8(9)

C(8)-N(4)-B(1) 130.0(8)

N(3)-N(4)-B(1) 121.1(8)

N(3)-C(6)-C(7) 109.0(10)

N(3)-C(6)-C(9) 122.3(11)

C(7)-C(6)-C(9) 128.8(11)

C(8)-C(7)-C(6) 106.5(10)

N(4)-C(8)-C(7) 108.8(9)

N(4)-C(8)-C(10)122.8(10)

C(7)-C(8)-C(10)128.3(10)

C(11)-N(5)-N(6) 106.2(9)

C(11)-N(5)-Sm(1)131.6(7)

N(6)-N(5)-Sm(1)120.9(6)

C(13)-N(6)-N(5) 109.2(8)

C(13)-N(6)-B(1) 130.1(9)

N(5)-N(6)-B(1) 120.7(8)

N(5)-C(11)-C(12)109.5(11)

N(5)-C(11)-C(14)121.1(11)

C(12)-C(11)-C(14)129.3(12)

C(11)-C(12)-C(13)106.4(10)

N(6)-C(13)-C(12)108.6(9)

N(6)-C(13)-C(15)122.6(10)

C(12)-C(13)-C(15)128.7(10)

N(2)-B(1)-N(4) 108.8(9)

N(2)-B(1)-N(6) 110.6(9)

N(4)-B(1)-N(6)110.7(10)

N(9a')-Sm(2)-N(9)180.000(1)

N(9a')-Sm(2)-N(7a')77.1(3)

N(9)-Sm(2)-N(7a')102.9(3)

N(9a')-Sm(2)-N(7)102.9(3)

N(9)-Sm(2)-N(7) 77.1(3)

N(7a')-Sm(2)-N(7)180.0(4)

N(9a')-Sm(2)-N(11a')79.1(3)

N(9)-Sm(2)-N(11a')100.9(3)

N(7a')-Sm(2)-N(11a')77.8(3)

N(7)-Sm(2)-N(11a')102.2(3)

N(9a')-Sm(2)-N(11)100.9(3)

N(9)-Sm(2)-N(11)79.1(3)

N(7a')-Sm(2)-N(11)102.2(3)

N(7)-Sm(2)-N(11)77.8(3)

N(11a')-Sm(2)-N(11)180.00(12)

C(16)-N(7)-N(8) 105.9(8)

C(16)-N(7)-Sm(2)132.7(7)

N(8)-N(7)-Sm(2)121.0(6)

C(18)-N(8)-N(7) 109.3(8)

C(18)-N(8)-B(2) 129.3(9)

N(7)-N(8)-B(2) 121.2(8)

N(7)-C(16)-C(17)109.9(10)

N(7)-C(16)-C(19)121.0(11)

C(17)-C(16)-C(19)129.0(11)

C(18)-C(17)-C(16)106.2(10)

N(8)-C(18)-C(17)108.6(10)

N(8)-C(18)-C(20)123.3(11)

C(17)-C(18)-C(20)128.1(10)

C(21)-N(9)-N(10)106.0(8)

C(21)-N(9)-Sm(2)132.6(7)

N(10)-N(9)-Sm(2)120.2(6)

C(23)-N(10)-N(9)110.2(8)

C(23)-N(10)-B(2)128.1(9)

N(9)-N(10)-B(2)121.5(8)

N(9)-C(21)-C(22)109.5(10)

N(9)-C(21)-C(24)120.1(10)

C(22)-C(21)-C(24)130.4(10)

C(23)-C(22)-C(21)106.7(9)

N(10)-C(23)-C(22)107.6(9)

N(10)-C(23)-C(25)124.5(10)

C(22)-C(23)-C(25)127.9(9)

C(26)-N(11)-N(12)105.1(9)

C(26)-N(11)-Sm(2)134.5(7)

N(12)-N(11)-Sm(2)120.5(6)

C(28)-N(12)-N(11)110.0(8)

C(28)-N(12)-B(2)130.0(9)

N(11)-N(12)-B(2)120.0(8)

N(11)-C(26)-C(27)111.0(10)

N(11)-C(26)-C(29)119.7(10)

C(27)-C(26)-C(29)129.3(10)

C(26)-C(27)-C(28)106.7(10)

N(12)-C(28)-C(27)107.2(9)

N(12)-C(28)-C(30)124.0(10)

C(27)-C(28)-C(30)128.8(10)

N(8)-B(2)-N(10)111.9(9)

N(8)-B(2)-N(12)110.2(8)

N(10)-B(2)-N(12)110.1(8)

C(32)-Re(1)-C(33)88.6(4)

C(32)-Re(1)-C(34)88.5(5)

C(33)-Re(1)-C(34)94.3(4)

C(32)-Re(1)-C(31)91.4(5)

C(33)-Re(1)-C(31)90.9(5)

C(34)-Re(1)-C(31)174.8(4)

C(32)-Re(1)-Re(3)100.8(3)

C(33)-Re(1)-Re(3)170.2(3)

C(34)-Re(1)-Re(3)83.1(3)

C(31)-Re(1)-Re(3)91.8(3)

C(32)-Re(1)-Re(2)161.1(3)

C(33)-Re(1)-Re(2)110.3(3)

C(34)-Re(1)-Re(2)88.3(3)

C(31)-Re(1)-Re(2)90.1(3)

Re(3)-Re(1)-Re(2)60.307(14)

C(36)-Re(2)-C(37)92.6(5)

C(36)-Re(2)-C(35)89.3(5)

C(37)-Re(2)-C(35)92.6(5)

C(36)-Re(2)-C(38)91.8(5)

C(37)-Re(2)-C(38)89.1(5)

C(35)-Re(2)-C(38)177.9(4)

C(36)-Re(2)-Re(1)110.6(4)

C(37)-Re(2)-Re(1)156.5(3)

C(35)-Re(2)-Re(1)91.3(3)

C(38)-Re(2)-Re(1)86.7(3)

C(36)-Re(2)-Re(3)167.5(4)

C(37)-Re(2)-Re(3)97.7(3)

C(35)-Re(2)-Re(3)83.2(3)

C(38)-Re(2)-Re(3)95.3(3)

Re(1)-Re(2)-Re(3)59.767(14)

C(41)-Re(3)-C(40)158.4(5)

C(41)-Re(3)-C(39)93.1(5)

C(40)-Re(3)-C(39)87.9(5)

C(41)-Re(3)-C(42)87.3(5)

C(40)-Re(3)-C(42)91.6(5)

C(39)-Re(3)-C(42)179.5(5)

C(41)-Re(3)-Re(4)79.0(3)

C(40)-Re(3)-Re(4)79.6(4)

C(39)-Re(3)-Re(4)87.1(3)

C(42)-Re(3)-Re(4)92.7(3)

C(41)-Re(3)-Re(1)72.1(3)

C(40)-Re(3)-Re(1)129.3(4)

C(39)-Re(3)-Re(1)81.6(3)

C(42)-Re(3)-Re(1)98.9(3)

Re(4)-Re(3)-Re(1)148.098(19)

C(41)-Re(3)-Re(2)127.3(3)

C(40)-Re(3)-Re(2)73.5(4)

C(39)-Re(3)-Re(2)99.9(3)

C(42)-Re(3)-Re(2)80.2(3)

Re(4)-Re(3)-Re(2)151.897(19)

Re(1)-Re(3)-Re(2)59.926(14)

C(45)-Re(4)-C(43)92.9(5)

C(45)-Re(4)-C(47)95.3(5)

C(43)-Re(4)-C(47)171.8(4)

C(45)-Re(4)-C(44)94.1(5)

C(43)-Re(4)-C(44)91.7(6)

C(47)-Re(4)-C(44)86.8(6)

C(45)-Re(4)-C(46)92.7(4)

C(43)-Re(4)-C(46)87.5(5)

C(47)-Re(4)-C(46)92.9(5)

C(44)-Re(4)-C(46)173.2(5)

C(45)-Re(4)-Re(3)176.9(3)

C(43)-Re(4)-Re(3)84.8(3)

C(47)-Re(4)-Re(3)87.1(3)

C(44)-Re(4)-Re(3)88.0(4)

C(46)-Re(4)-Re(3)85.2(3)

O(31)-C(31)-Re(1)177.2(10)

O(32)-C(32)-Re(1)175.1(9)

O(33)-C(33)-Re(1)176.5(10)

O(34)-C(34)-Re(1)175.7(10)

O(35)-C(35)-Re(2)177.7(10)

O(36)-C(36)-Re(2)175.2(11)

O(37)-C(37)-Re(2)177.1(10)

O(38)-C(38)-Re(2)174.5(9)

O(39)-C(39)-Re(3)176.0(10)

O(40)-C(40)-Re(3)175.1(12)

O(41)-C(41)-Re(3)174.5(8)

O(42)-C(42)-Re(3)176.9(10)

O(43)-C(43)-Re(4)178.1(12)

O(44)-C(44)-Re(4)178.3(14)

O(45)-C(45)-Re(4)177.9(12)

O(46)-C(46)-Re(4)176.9(10)

O(47)-C(47)-Re(4)178.3(11)

Symmetry transformations used to generate equivalent atoms:

a: -x,-y+1,-z a': -x+1,-y+1,-z+1

Appendix 2 - NMR spectra for chapter 2.

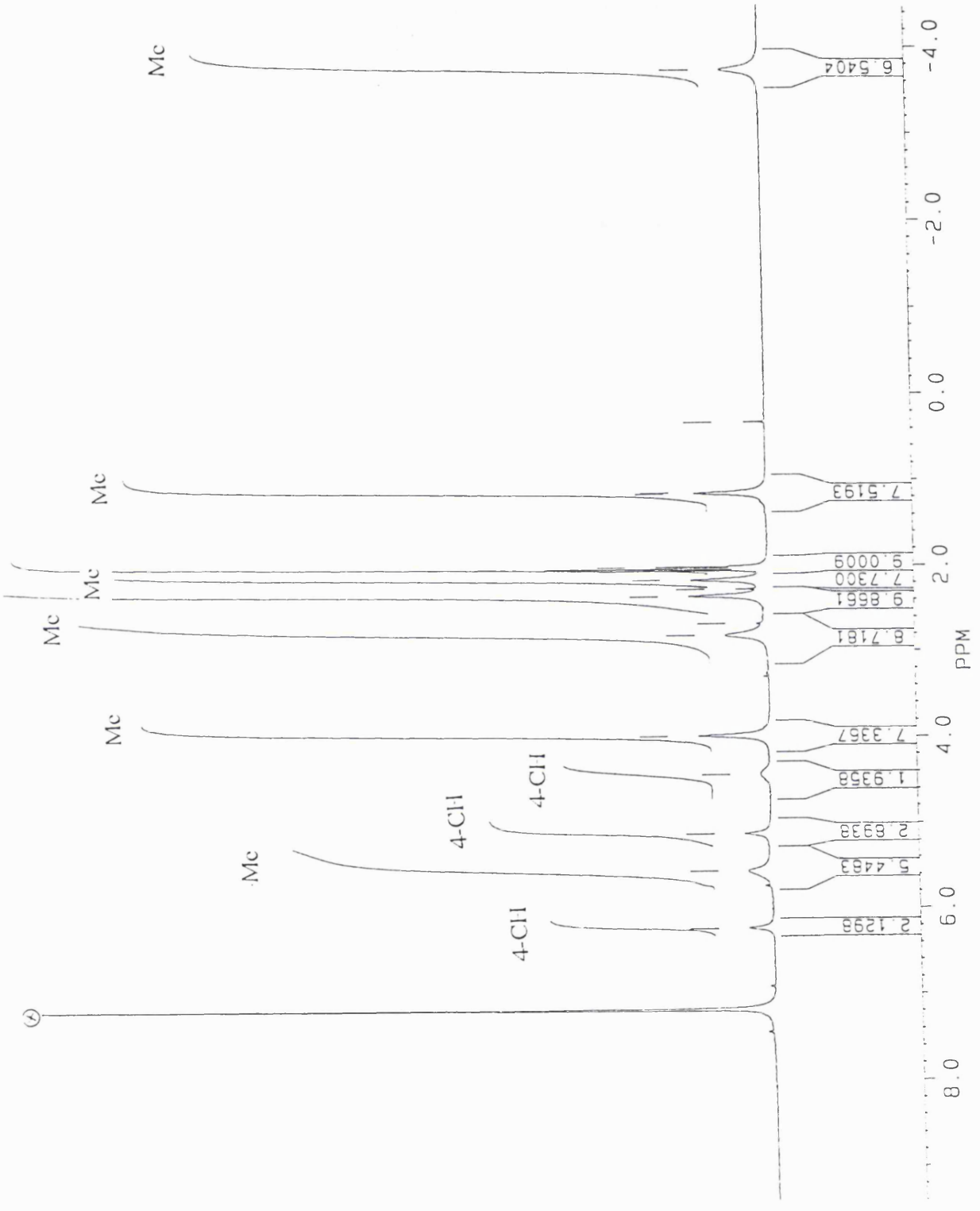

Appendix 2.1 ^{1}H NMR spectrum of $[SmTp^{Me,Me}]_2S_2CNEt_2]$

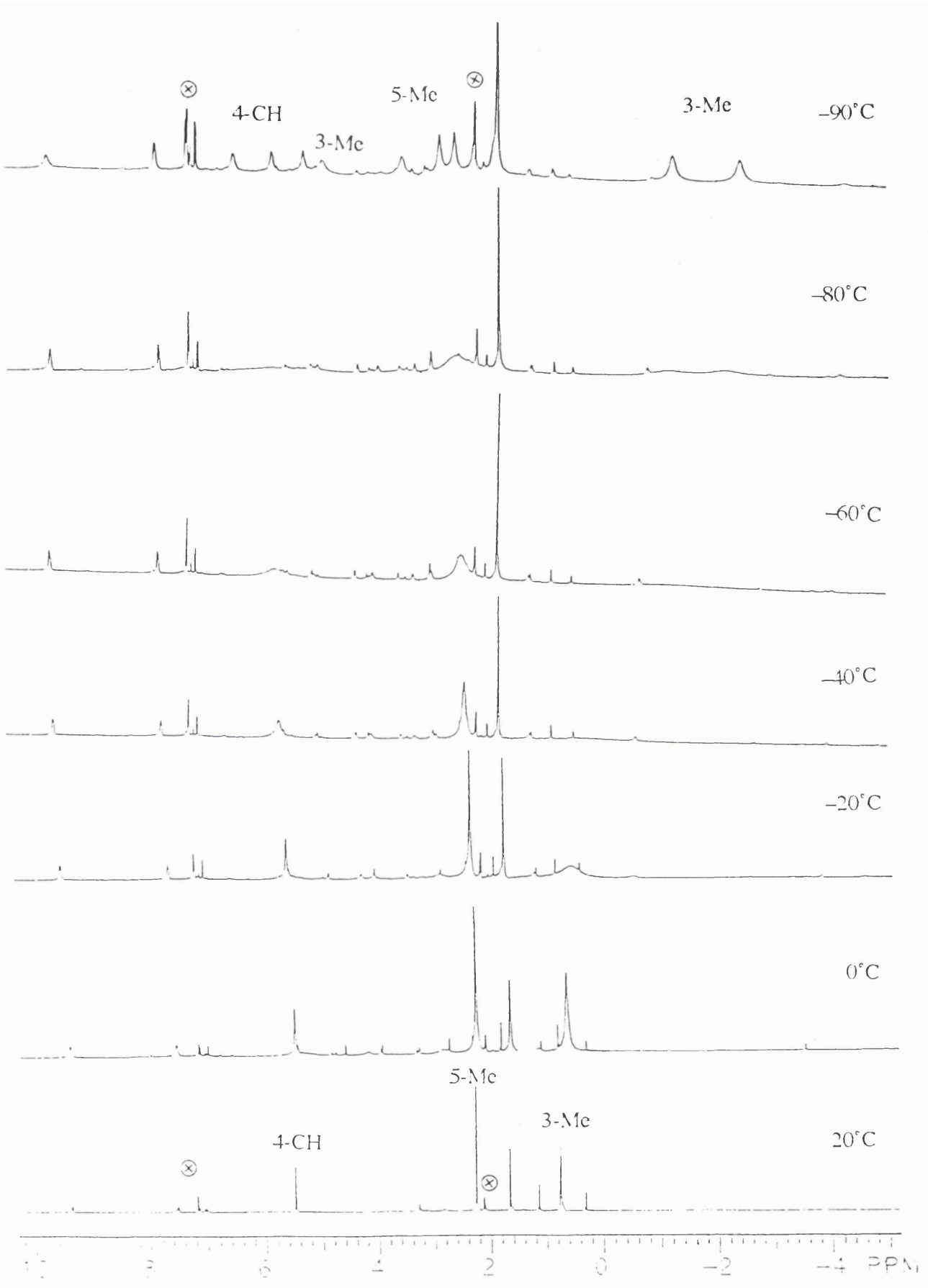

Appendix 2.2 Variable temperature ^{1}H NMR spectrum of [Sm(Tp^{Me,Me})$_2$ScPh^{tBu}]

Appendix 3 - NMR and IR spectra for chapter 4.

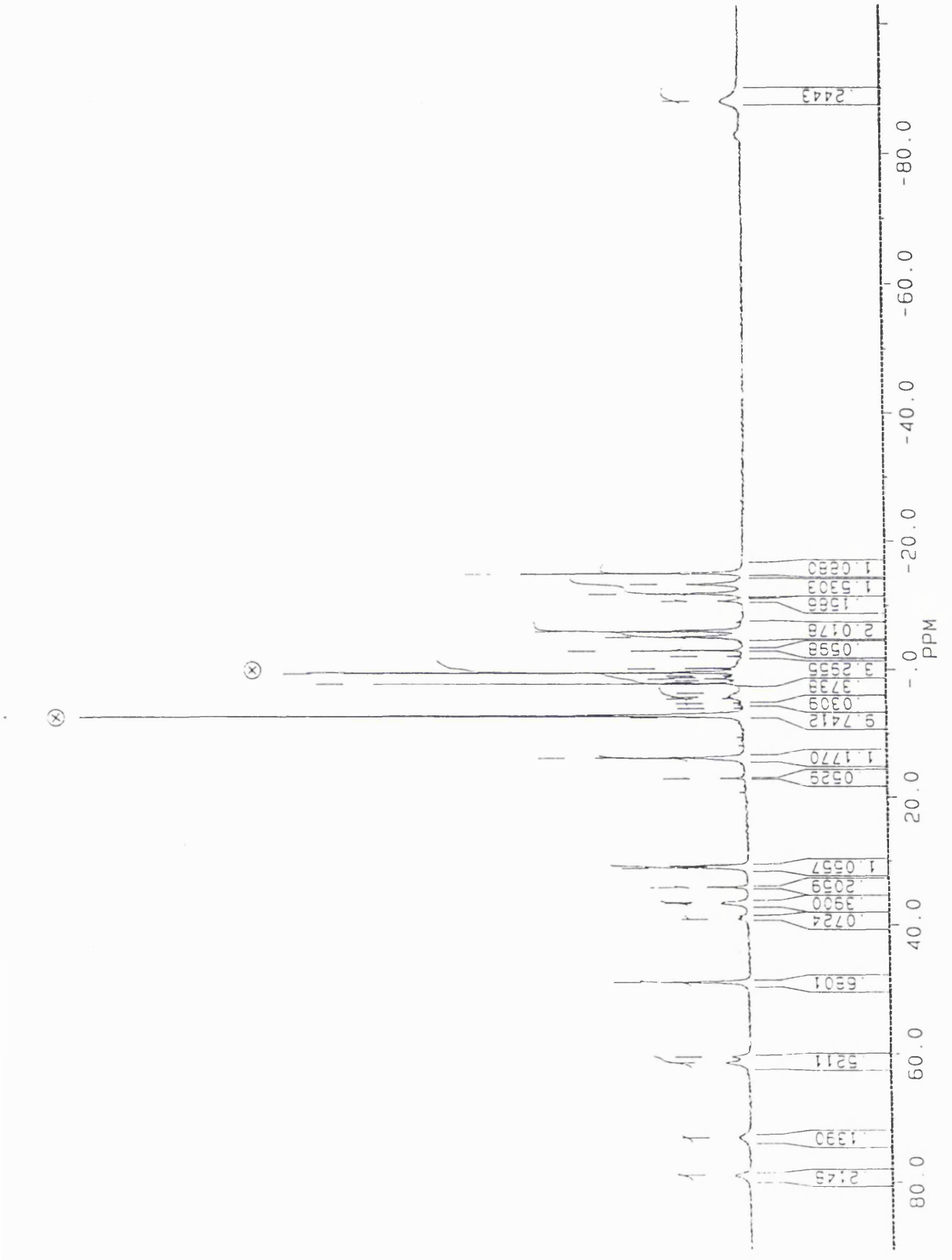

Appendix 3.1 ^{1}H NMR spectrum of reaction product of 4.11 + $NaBH_4$.